Groundwater-surface water interaction in urban lowland catchments

Water quality dynamics in the city of Amsterdam

Liang Yu

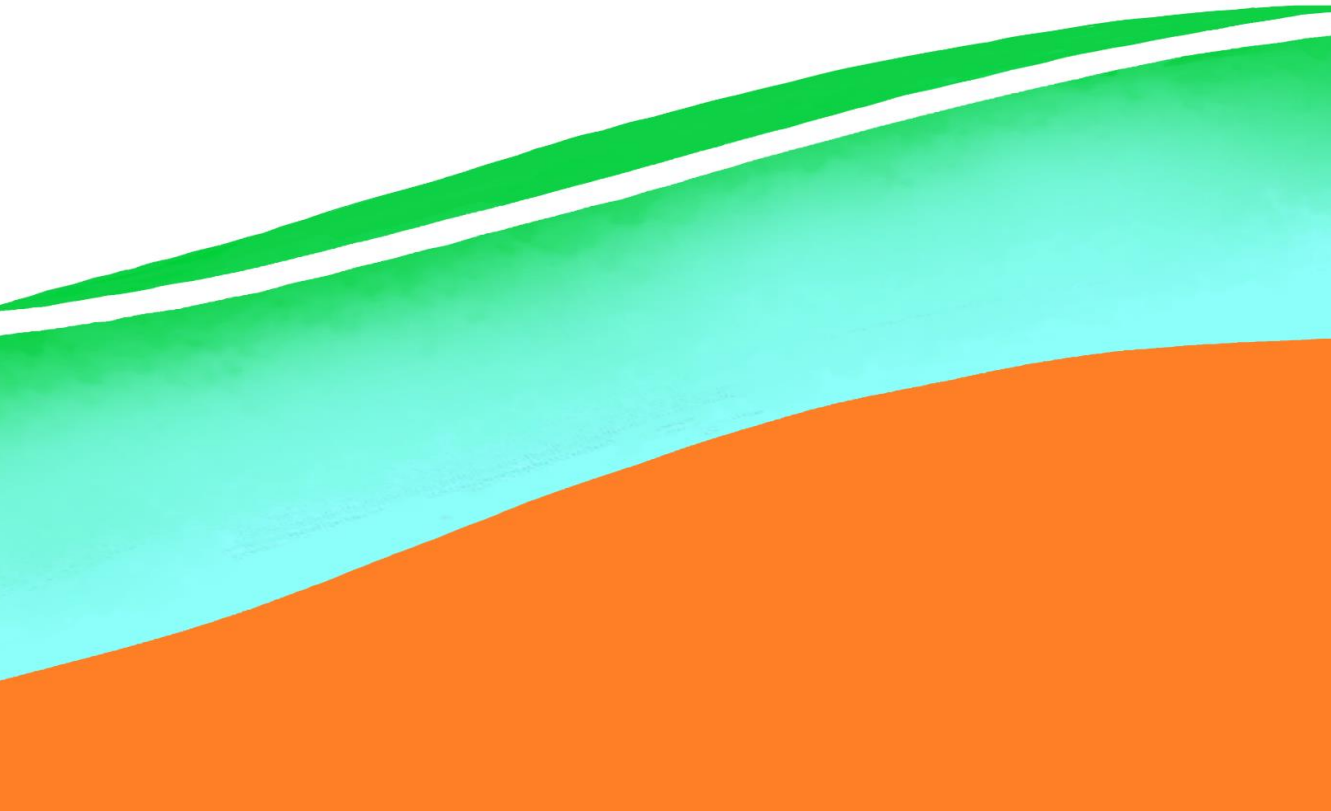

Groundwater-surface water interaction in urban lowland catchments

Water quality dynamics in the city of Amsterdam

Liang Yu

于良

2020

Cover page design: Liang Yu

Groundwater-surface water interaction in urban lowland catchments - Water quality dynamics in the city of Amsterdam

Author: Liang Yu

This research was major funded by the China Scholarship Council under the agreement number: 201309110088. It was also financially supported by Waternet, TNO, Vrije Universiteit Amsterdam, Deltares, and TU Delft. The research was performed at Vrije Universiteit Amsterdam, Waternet, TNO, and Deltares.

Published in: 2020
Printed by: PROEFSCHRIFTMAKEN

VRIJE UNIVERSITEIT

Groundwater-surface water interaction in urban lowland catchments

Water quality dynamics in the city of Amsterdam

ACADEMISCH PROEFSCHRIFT

ter verkrijging van de graad Doctor of Philosophy
aan de Vrije Universiteit Amsterdam,
op gezag van de rector magnificus
prof.dr. V. Subramaniam,
in het openbaar te verdedigen
ten overstaan van de promotiecommissie
van de Faculteit der Bètawetenschappen
op woensdag 13 januari 2021 om 11.45 uur
in de aula van de universiteit,
De Boelelaan 1105

door

Liang Yu

geboren te Jilin, China

promotoren: prof.dr. A. J. Dolman
prof.dr. J. J. Middelburg

copromotoren: dr. H. P. Broers
dr. J. C. Rozemeijer

reading committee: prof.dr. E.J. Moors
prof.dr. J.C.J.H. Aerts
prof.dr. B. Schmalz
prof.dr. B. Kronvang
dr. B. Van der Grift

Contents

Summary **1**

Samenvatting **5**

1. Introduction **9**

1.1 Water quality in low lying coastal cities 9
1.2 Water quality management in Europe – 20 years under the European Water Framework Directive 10
1.3 Water quality management in The Netherlands 11
1.4 Water management and water quality in Amsterdam 13
1.5 Research questions 15
1.6 Thesis structure 15

2. Groundwater impacts on surface water quality and nutrient loads in lowland polder catchments: monitoring the greater Amsterdam area **19**

2.1 Introduction 21
2.2 Methods 22
2.2.1 Study area 22
2.2.2 Data processing 27
2.3 Results 31
2.3.1 Spatial pattern and statistical analysis of groundwater quality 31
2.3.2 Spatial patterns and statistical analysis of surface water quality 36
2.3.3 Groundwater and surface water quality comparison 39
2.3.4 Surface water solute redistribution 41
2.4 Discussion 41
2.4.1 Key hydro chemical processes 42
2.4.2 Groundwater contribution to surface water composition 45
2.4.3 Other sources of nutrients 45
2.4.4 Uncertainties 46
2.4.5 Perspectives 46
2.5 Conclusion 47
Supplementary Information 48

3. Urban hydrogeology: transport routes and mixing of water and solutes in a groundwater influenced urban lowland catchment 57

3.1 Introduction 58
3.2 Methods 59
3.2.1 Data collection 62
3.2.2 Data processing 65
3.3 Results & Discussion 67
3.3.1 Runoff, ditch water, drain water, and groundwater flow routes survey 67
3.3.2 Spatial and temporal variations in the urban catchment 70
3.3.3 Temporal variations at the polder's main outlet 76
3.3.4 The effects of urbanization on polder hydrogeochemistry 78
3.4 Conclusions 79
Supplementary Information 81

4. Drivers of nitrogen and phosphorus dynamics in a groundwater-fed urban catchment revealed by high frequency monitoring 91

4.1 Introduction 93
4.2 Methods 94
4.2.1 Study site 94
4.2.2 Monitoring network setup 95
4.2.3 Data processing and analysis 98
4.3 Results 100
4.3.1 Annual pattern of meteorological, hydrological, and water quality time series 100
4.3.2 Model of water quality time series based on water balance 102
4.3.3 Water quality responses to single events analysis 102
4.4 Discussion 107
4.4.1 Hydrological mixing between groundwater and rainfall 107
4.4.2 Primary production and nutrients 108
4.4.3 P binding and turbidity 110
4.4.4 Process synthesis 111
4.4.5 Event scale N and P dynamics 112
4.4.6 Implications for urban water management in low lying catchments 114
4.5 Conclusions 114
Supplementary Information 116

5. Synthesis **125**

5.1 Summary 125
5.2 Main conclusions 128
5.3 Implications 128
5.3.1 Implications for urban water management in low lying areas 128
5.3.2 Implications for urban water quality monitoring 131
5.4 Recommendations for future research 132
5.4.1 Collect information of the subsurface in surface water quality management in coastal cities 132
5.4.2 A comprehensive study on the sediment-water interface --- benthic zone and nutrients dynamics 132
5.4.3 Study on the limiting factors for ecological status 133
5.4.4 Upscaling from catchment scale to regional scale ---- Integrated model for artificial urban water systems 135
5.5 Final messages 135

Acknowledgements **137**

References **141**

Summary

Urban water eutrophication is a worldwide issue causing significant societal, economic and environmental losses. Nutrient loads reduction has been set as a target for abating eutrophication in natural and artificial water bodies. However, effective water quality management in the urban systems is seriously hampered by a lack of knowledge of the water quality dynamics and its related processes. The central objective of this thesis is to contribute to the understanding of the spatial and temporal patterns of surface water quality in urban coastal low-lying catchments. The research area described in this thesis was in the west of The Netherlands where lands consist of low-lying polders, a form of artificial catchments which are actively pumped to maintain water levels. The spatial and temporal patterns of water quality in this region were studied at different scales from a multidisciplinary perspective. A series of field experiments and statistical analyses were conducted, revealing the importance of groundwater for the surface water quality, especially for nitrogen and phosphorus.

The research was conducted from a local (a single polder) to a regional spatial scale (the greater Amsterdam region) and from short (events) to long (seasonal to years) time scales. I statistically analysed long-term monitoring data at the regional scale in Chapter 2 based on 144 polders, averaging over 7 years for surface water, and mostly over 33 years for groundwater, filtering out the key factors determining the spatial patterns of the surface water quality. In Chapter 3, the analysis was based on a 10-year monthly average dataset and an over one-year weekly monitoring dataset at the catchment scale of the Geuzenveld urban polder. The temporal patterns of water quality and the potential related processes were discussed qualitatively and statistically. Chapter 4 describes a set of additional high-resolution water quality time series (hourly average) that was collected at the catchment outlet, further exploring the temporal patterns of nutrients and their related biohydrogeochemical processes at seasonal and event scales.

This thesis concludes that, in low-lying urban catchments in near shore river deltas, groundwater is likely to outcompete other traditionally considered urban factors as an important source of nutrients. The water quality dynamics in such region is determined by the interaction between groundwater and surface water through space and time.

Concentrations of major elements in the surface water in and around Amsterdam appear to be highly correlated to the concentrations in the underlying groundwater. Subsurface organic matter acts as the most important source of nutrients in groundwater and affects surface water composition by groundwater seepage (Chapter 2). Organic matter is in ample presence in the subsurface around the world, especially in delta settings (Dai et al., 2019). The Dutch subsurface is known to contain abundant reactive organic matter, such as peat formed during the Holocene marine transgression, or organic detritus incorporated in fluvial and marine sediments (Griffioen et al., 2013). Human activities, such as the excavation of peat and the extended pumping for dry land, caused a drop in groundwater levels and resulted in peat oxidation, which is a process that potentially releases nutrients into the pore water. Moreover, groundwater sulfate in the relict brackish waters that resulted from periods with sea water intrusion provided an electron acceptor needed for microbial decomposition of organic matter in the subsurface. Our study suggests that the processes of sulfate reduction induced organic matter oxidation

released nutrients into the groundwater. This nutrient-rich groundwater then seeps into the surface water system, eventually leading to the exceedance of the environmental quality standards for nutrients. Alterations to the groundwater flow paths, such as the installation of groundwater drainage system and regional re-distribution of the seepage water, further accelerate the flow of groundwater into open water bodies, thus enhancing the nutrient inputs and changing the surface water quality dynamics.

The mixing between the anoxic, high mineralized, nutrient- and iron-rich anoxic groundwater and oxic and less mineralized runoff is the key hydrological process that determines the water quality dynamics in the urban study catchment. It was notably illustrated by the temporal pattern of relatively conservative parameters such as EC and Cl, in both a long-term monthly discrete monitoring (Chapter 3) and a short-term high frequency monitoring campaign (Chapter 4). In the urban polder setting, the installation of rain and groundwater drainage systems leads to flow shortcuts where rain water and groundwater bypass large parts of the shallow subsurface and soil system. It transfers the mixing zone from the upper soil layer to the open water systems, such as ditches, ponds and shallow reservoirs. Thus, it makes the mixing between groundwater and surface water into a fast process.

On top of the physical mixing process, biogeochemical processes, such as primary production and iron redox transformations were also strongly suggested by the continuous and discrete sampling data to be the drivers of N and P dynamics in the shallow ditches. As a preferable form of nitrogen by plants and microbes, NH_4 concentrations in our study area were drastically lowered by primary producers (presumably both phytoplankton and benthic algae) during the growing season, which was deduced from the monthly distribution of chlorophyll-a (high in summer) and silica (lower in spring and summer). But it sustained almost year-round fluxes being pumped towards downstream catchments with either organic-N or NH_4 as the dominant form. Primary production produces O_2, which subsequently influenced the redox status in the sediments and in the water column, which directly regulated the pattern of P in the ditches. In the shallow water courses, the sediment-water interface is of importance where O_2 is released from primary production fixating P in ironhydroxides in growing seasons and releasing P when temperature drops and benthic algae die off in the late autumn and winter. I concluded that the iron redox chemistry is the dominant process controlling the P dynamics in the shallow groundwater fed ditches and suggested that the high turbidity levels which occurred in the late autumn and winter were the result of iron hydroxides formation in the water column. The turbidity time series and Fe grab sampling data suggested a shift of the anoxic/oxic interface where the formation of iron hydroxides moves from the sediment in summer towards the water column in autumn and winter. The novel high-frequency monitoring technology proved to be crucial to capture the temporal patterns and helped to frame a conceptual model that may be explored by water managers for creating more effective eutrophication mitigation strategies.

According to the results obtained from Chapter 1-4, suggestions to future water management were given in Chapter 5 aiming for reducing nutrients loads to surface water and for improving the ecological status. I proposed that effective mitigation measures for nutrient discharge to downstream should be based on the dynamics of N and P over the year, as exemplified by this study. Potential measures for managing drain water, surface water outlet, and runoff to remove the nutrients directly or increase their retention were discussed. Regulation of the hydrogeometry of the water courses as a potential measure to improve the ecological status is also discussed in this chapter. I also suggest to regard the discrete and continuous monitoring as complementary methods in water quality management according to their pros and cons.

Recommendations for future research were given at the end, including: thorough investigation of the ecosystem, studying the physicochemical characteristics of the hyporheic zone and the microbial community structure; integration of subsurface conditions into surface water quality management in coastal cities; comprehensively study on the sediment-water interface - benthic zone and nutrients dynamics; explore on the limiting factors for ecological status, such as nutrient sources, physical dimension of water courses; and upscale from catchment scale to regional scale basing on integrated model for artificial urban water systems.

Samenvatting

Stedelijke watereutrofiëring is een wereldwijd probleem dat aanzienlijke maatschappelijke, economische en ecologische schade veroorzaakt. Vermindering van de nutriëntenbelasting is vastgesteld als een doelstelling voor het verminderen van eutrofiëring in natuurlijke en kunstmatige waterlichamen. Effectief waterkwaliteitsbeheer in de stedelijke systemen wordt echter ernstig belemmerd door een gebrek aan kennis van de waterkwaliteitsdynamiek en de daarmee samenhangende processen. Het centrale doel van dit proefschrift is om bij te dragen aan het begrip van de ruimtelijke en temporele patronen van de oppervlaktewaterkwaliteit in laaggelegen stroomgebieden in stedelijke kustgebieden. Het in dit proefschrift beschreven onderzoeksgebied lag in het westen van Nederland, waar het land voornamelijk bestaat uit laaggelegen polders. Dit zijn kunstmatige stroomgebieden die actief worden opgepompt om het waterpeil op peil te houden. De ruimtelijke en temporele patronen van waterkwaliteit in deze regio werden op verschillende schaalniveaus bestudeerd vanuit een multidisciplinair perspectief. Er is een reeks veldexperimenten en statistische analyses uitgevoerd, op basis waarvan het belang van grondwater voor de oppervlaktewaterkwaliteit in beeld is gebracht, met name voor stikstof en fosfor.

Het onderzoek is uitgevoerd van een lokale (een enkele polder) naar een regionale ruimtelijke schaal (de regio groot Amsterdam) en van een korte (evenementen) tot een lange (seizoengebonden tot jaren) tijdschaal. In Hoofdstuk 2 heb ik statistische analyses uitgevoerd met langetermijnmonitoringgegevens op regionale schaal (144 polders, gemiddeld over 7 jaar voor oppervlaktewater, meestal over 33 jaar voor grondwater) om de sleutelfactoren die het ruimtelijke patroon van de oppervlaktewaterkwaliteit bepalen eruit te filteren. In Hoofdstuk 3 was de analyse gebaseerd op een 10-jarige dataset en meer dan een jaar aan wekelijkse data op stroomgebiedschaal. Het temporele patroon van de waterkwaliteit en de mogelijke gerelateerde processen zijn besproken. Een reeks hoge-resolutie waterkwaliteitstijdreeksen (uurgemiddelde) werd verzameld op stroomgebiedschaal voor verder onderzoek naar het temporele patroon van nutriënten en hun gerelateerde biohydrogeochemische processen in Hoofdstuk 4.

Dit proefschrift concludeert dat, in laaggelegen stedelijke stroomgebieden in rivierdelta's langs de oever, het grondwater waarschijnlijk een belangrijkere bron van nutriënten is dan andere, traditioneel-beschouwde, stedelijke factoren. En de waterkwaliteitsdynamiek in zo'n regio wordt bepaald door de interactie tussen grondwater en oppervlaktewater door ruimte en tijd.

Concentraties van belangrijke elementen in het oppervlaktewater in en rond Amsterdam lijken sterk samen te hangen met de concentraties in het onderliggende grondwater. De ondergrondse organische stof fungeert als de belangrijkste bron van nutriënten in het grondwater en beïnvloedt de samenstelling van het oppervlaktewater door kwel van het grondwater (hoofdstuk 2). Organische stof is ruimschoots aanwezig in de ondergrond over de hele wereld, vooral in deltas (Dai et al., 2019). De Nederlandse ondergrond bevat overvloedig reactief organisch materiaal, zoals veen gevormd tijdens de transgressie op zee in het Holoceen, of organisch afval dat is verwerkt in rivier- en mariene sedimenten (Griffioen et al., 2013). Menselijke activiteiten, zoals het afgraven van veen en het langdurig oppompen naar droog land, veroorzaakten een daling van het grondwaterpeil. Verder resulteerde dit in veenoxidatie, een

proces waarbij mogelijk nutriënten in het poriënwater terechtkomen. Bovendien zorgde grondwatersulfaat in hetbrakke water, dat het gevolg was van perioden met indringing van zeewater, voor een elektronenacceptor die nodig was voor microbiële afbraak van organisch materiaal in de ondergrond. Onze studie suggereert dat de oxidatie van organische stof als gevlog van sulfaatreductie voedingsstoffen in het grondwater vrijgeven. Dit voedselrijke grondwater sijpelt vervolgens in het oppervlaktewatersysteem en leidt uiteindelijk tot overschrijding van de milieukwaliteitsnormen voor nutriënten. Veranderingen in de grondwaterstroompaden, zoals de aanleg van een grondwaterafvoersysteem en regionale herverdeling van het kwelwater, versnellen de doorstroming van grondwater naar open waterlichamen. Dit vergroot de nutriëntentoevoer en verandert de kwaliteit van het oppervlaktewater.

De vermenging van het anoxische, hooggemineraliseerde, nutriënten- en ijzerrijke anoxische grondwater en oxische en minder gemineraliseerde afvoerwater is het belangrijkste hydrologische proces dat de waterkwaliteitsdynamiek in het stedelijke studiegebied bepaalt. Het werd met name geïllustreerd door het temporele patroon van relatief conservatieve parameters zoals EC en Cl, zowel in een maandelijkse discrete monitoringcampagne op lange termijn (Hoofdstuk 3) als in een korte termijn hoogfrequente monitoringcampagne (Hoofdstuk 4). In de stedelijke polderomgeving leidt de aanleg van regen- en grondwaterafvoersystemen tot afsnijroutes waar regenwater en grondwater grote delen van de ondiepe ondergrond en het bodemsysteem omzeilen. Dit verplaatst de mengzone van de bovenste bodemlaag naar de open watersystemen, zoals sloten, vijvers en ondiepe reservoirs. Zo wordt de menging tussen grond- en oppervlaktewater een versneld proces.

Naast het fysieke mengproces werden biogeochemische processen, zoals primaire productie en ijzerredoxtransformaties, ook sterk gesuggereerd als de drijvende krachten achter de N- en P-dynamiek in de ondiepe sloten, volgens de continue en discrete bemonsteringsgegevens. Als een geprefereerde vorm van stikstof door planten en microben, werden NH_4 concentraties in ons studiegebied drastisch verlaagd door primaire producenten (vermoedelijk zowel fytoplankton als benthische algen) tijdens het groeiseizoen, wat werd afgeleid uit de maandelijkse verdeling van chlorofyll-a (hoog in zomer) en silica (lager in lente en zomer). Maar het hield bijna het hele jaar door fluxen aan die naar stroomafwaartse stroomgebieden werden gepompt met organische N of NH_4 als de dominante vorm. Bij de primaire productie wordt O_2 geproduceerd, dat vervolgens de redoxstatus in de sedimenten en in de waterkolom beïnvloedt en het patroon van P in de sloten direct reguleert. In de ondiepe watelopen is het sediment-water grensvlak van belang waar O_2 vrijkomt uit de primaire productie, waarbij P wordt gefixeerd in ijzerhydroxiden in groeiseizoenen en P vrijkomt als de temperatuur daalt en benthische algen afsterven in de late herfst en winter. Ik concludeerde dat de ijzer redox-chemie het dominante proces is dat de P-dynamiek in de ondiepe grondwater-gevoede sloten regelt en suggereerde dat de hoge troebelheidniveaus die optraden in de late herfst en winter het gevolg waren van de vorming van ijzerhydroxiden in de waterkolom. De troebelheidstijdreeksen en Fe grab bemonsteringsgegevens suggereerden een verschuiving van het anoxische/oxische grensvlak waar de vorming van ijzerhydroxiden in de zomer van het sediment naar de waterkolom in de herfst en winter beweegt. De nieuwe hoogfrequente monitoringtechnologie bleek cruciaal te zijn om de temporele patronen vast te leggen en hielp bij het opstellen van een conceptueel model dat door waterbeheerders kan worden onderzocht om effectievere strategieën voor het verminderen van eutrofiëring te ontwikkelen.

Gebasseerd op de resultaten uit hoofdstuk 1-4 zijn in Hoofdstuk 5 suggesties gedaan voor toekomstig waterbeheer om de nutriëntenbelasting naar het oppervlaktewater te verminderen en de ecologische staat te verbeteren. Ik stelde voor dat effectieve mitigerende maatregelen voor de afvoer van nutriënten naar stroomafwaarts gebaseerd zouden moeten zijn op de dynamiek van N en P gedurende het jaar, zoals geïllustreerd door deze studie. Mogelijke maatregelen voor het beheer van drainwater, uitstroom van oppervlaktewater en afstromend water om de nutriënten direct af te voeren of hun retentie te vergroten, werden besproken. De regeling van de hydrogeometrie van de waterlopen als mogelijke maatregel om de ecologische toestand te verbeteren komt in dit hoofdstuk ook aan de orde. Ik stel ook voor om discrete en continue monitoring te beschouwen als complementaire methoden in het waterkwaliteitsbeheer, op basis van hun voor- en nadelen.

Ten slotte werden aanbevelingen gedaan voor toekomstig onderzoek, waaronder: grondig onderzoek van het ecosysteem, de fysisch-chemische kenmerken van de hyporheische zone en de microbiële gemeenschapsstructuur; de toestand van de ondergrond integreren in het beheer van de oppervlaktewaterkwaliteit in kuststeden; een uitgebreide studie van de sediment-water interface--- benthische zone en nutriënten dynamiek; onderzoek naar de beperkende factoren voor de ecologische toestand, zoals bronnen van nutriënten, fysieke afmetingen van waterlopen; en opschaling van stroomgebiedsschaal naar regionale schaal op basis van een geïntegreerd model voor kunstmatige stedelijke watersystemen.

Chapter 1

Introduction

1.1 Water quality in low lying coastal cities

As an area of high economic value (over 30% of the total EU GPD), coastal areas (50 km of the coast) are holding one third of the EU population*, mostly residing in cities. Worldwide, low-lying deltas account for 2% of the world's land but are estimated to accommodate 1400 million people by 2060 (Neumann et al., 2015). However, due to intensive human activities, the natural system has been intensively altered. Coastal cities are not only facing natural stressors such as sea water intrusion, land erosion, land subsidence, natural disasters, etc, but also facing multiple direct human induced pressures resulting from urbanization, such as increasing demand for good quality water, the over use of groundwater resources, urban flooding, water logging, and the most notorious problem ---- water quality degradation. For example, in the coastal city Jakarta in Indonesia, both surface water and groundwater are severely polluted by industrial and municipal effluents due to lack of sewerage (Luo et al., 2019). The capital even has to move away for a better environment. Cities like Ho Chi Minh (Vietnam), La Plata (Argentina) (Armendáriz et al., 2017), and New Orleans are all struggling with water quality deterioration, such as toxic algae blooms. Coastal cities often occupy key positions in the land-sea continuum. Their contaminated water eventually ends up in the estuaries, resulting in deterioration of the receiving sea water (Neal and Robson, 2000; Chen et al., 2017).

Nutrients exported from coastal cities have resulted in severely eutrophicated conditions in coastal water bodies. Eutrophication is a natural process of explosive growth of organisms induced by the overabundance of nutrients. Anthropogenic activities have intensified eutrophication by adding excess nutrients thus changing the time of the water systems degradation span from geological time scale to much shorter time scales (Le Moal et al., 2019). It is causing severe environmental issues, damaging economy and raising societal concerns, such as harmful algae blooms that threatens human health, loss of biodiversity, hypoxia, problems with uses of water resources (drinking water reservoirs, industrial, recreational water use (shoreline activities, bathing, navigation), fisheries). It becomes one of the most notorious worldwide issues, such as in the Gulf of Mexico, Baltic sea, the Laurentian Great Lakes, the

* https://ec.europa.eu/environment/iczm/state_coast.htm

Chesapeake Bay, and large number of coastal areas in China (Boesch et al., 2001; Gustafsson et al., 2012; Wang et al., 2018), etc.

Research of Jenny et al. (2016) shows that, instead of agricultural activity, the wide spread occurrence of (historical) hypoxia in European lakes is related to socioeconomic changes. Since CE 1850 urbanization and land cultivation intensified which associated with urban point pollution source. In the Netherlands, many former lakes and coastal strips were cultivated. Gradually some of these evolved into urban landscapes as the cities are continuously expending. As an example, Gouda has recently expanded southwestward into the deepest polder in The Netherlands (Westergouwe) (OECD, 2014). In these delta areas, seepage might bring up significant amounts of salt water from past sea water intrusion or marine water stored in the aquifer which get released by land cultivation (Delsman et al., 2014).

The nutrients causing eutrophication and algae blooms are usually nitrogen (N) and phosphorus (P) which are two ubiquitous elements in the environment. Natural sources of nutrients come from fixation of gas N_2 from the atmosphere by plants and microbes and decomposition of dead organisms. Anthropogenic sources that result in nutrients enrichment are (1) point sources, including municipal and industrial wastewater effluent and also including effluents from municipal and waste water treatment plants and misconnections (Borst et al., 2013; Strokal et al., 2015; Revitt and Ellis, 2016; McGrane et al., 2017). Although these sources have been eliminated in most developed countries, they are still a major source in many other countries. (2) non-point sources, such as application of fertilizer, pet waste, duck feeding, atmospheric deposition, decomposition of peat due to excavation, and precedent anthropogenic activity legacy such as the accumulated nutrients in previous farm land, are playing an important role (Jenny et al., 2016; Hobbie et al., 2017; Vadas et al., 2018). Internal eutrophication (Smolders et al., 2006) has been introduced as a concept to represent the processes of remobilizing nutrients in the water bodies in the Netherlands. Apart from anthropogenic sources from the coastal cities, nutrients delivered by submarine groundwater discharge may also be an important source to the sea (Charette and Buesseler, 2004).

Water bodies in the low lying delta regions, have a high chance to be groundwater fed. Therefore, the composition of groundwater quality might to some extend affect surface water quality. Especially in delta regions, where groundwaters can be rich in nutrients due to both natural decomposition processes of organic rich subsurface layers or municipal and agricultural pollution (Vada et al., 2007; Robinson, 2015;). However, the role of groundwater for surface water quality has received minor attention in literature.

1.2 Water quality management in Europe – 20 years under the European Water Framework Directive

The EU Water Framework Directive (WFD) has been into force since 2000, aiming to establish a guideline for its member states to realize a good status for all waters*, covering water bodies of inland, transitional, coastal, and groundwaters†. The member states act to achieve the objectives set by the

* https://ec.europa.eu/environment/water/water-framework/index_en.html
† https://eur-lex.europa.eu/legal-content/EN/TXT/?uri=CELEX:32000L0060

WFD following a 6-year based management cycle. 2021 and 2027 are the deadlines of the next two cycles (European Commission, 2012).

Since the Water Framework Directive has been implemented in EU member states, only 10% of water bodies have improved until 2015 (Koschorreck et al., 2019), and the quality of most waters has been classified to be from moderate to bad status (Destouni et al., 2017). The cause for failure of achieving the targets varies from country to country, such as (1) far-to-reach targets resulting in challenging implementation process, (2) strict time tables does not endure time lags before some measures start to have significant effects (Bouraoui and Grizzetti, 2011), (3) unrealistic nutrient criteria (Poikane et al., 2019), (4) extra stressors such as climate change, (5) neglecting extra sources and/or internal sources of nutrients, and (6) groundwater contribution (Destouni and Jarsjö, 2018). Reported by Koschorreck (Koschorreck et al., 2019), the WFD focuses on large surface water areas neglecting small artificial and heavily modified water bodies[‡] which represent a large proportion of total surface water area in Europe. These water bodies have not received as much of attention compared to natural water bodies but might be important nutrients sources. Small water bodies, such as headwater streams, are only recommended to be included in the River Basin Management Plans (RBMP) when they obstruct the achievement of the objectives in WFD (EC, 2003).

1.3 Water quality management in The Netherlands

The Netherlands is a low-lying country (about 25% of its land below the mean sea level) along the North Sea, in which large amount of water bodies are artificial and heavily modified to accommodate residential and agriculture activity. These artificial catchments are called “polders”, mostly are constructed out of former lakes and seas. The scheme of a polder catchment is shown in Figure 1.1.

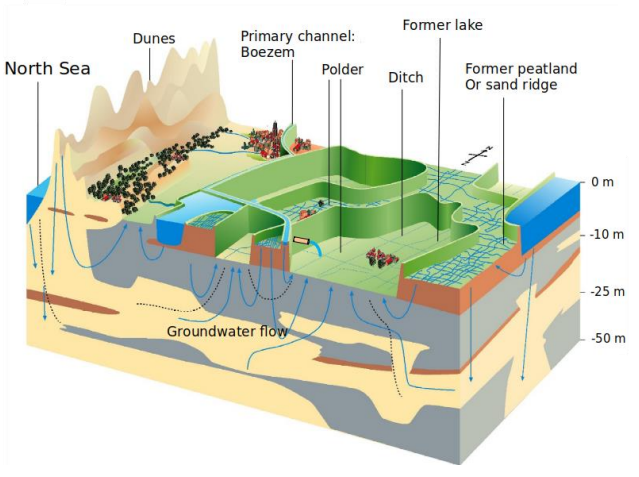

Figure 1.1 Polder water system in the Netherlands (Griffioen et al., 2003).

A polder typically consists of land strips separated by man-made surface water courses which are called “ditches”. The ditch water level is monitored by sensors at the outlet (pumping station), and regulated

[‡] https://eur-lex.europa.eu/legal-content/EN/TXT/?uri=CELEX:32000L0060

by following specific pumping schemes to prevent droughts and floods in the polder. Each polder has a specific water level range. When the water level exceeds the upper limit, the excess water in the ditches is pumped out to an elevated secondary channel and/or let into neighboring polders with lower elevations. Inlet water from the secondary channel is let into the polders by gravity flow when the water level is lower than the lower limit. All the excess headwater from the polder ditches ends up in the primary channel called "boezem". Until 1850, water was pumped to these boezems using windmills which were replaced by steam engines and electrical pumping stations later. The boezem typically is a large natural or artificial water course, that transfer the collected headwaters to the receiving water bodies, such as lakes, rivers, and estuaries, then discharged into the North Sea.

In the Netherlands, management of water quality is the responsibility of local water authorities, enforced by provincial municipalities and the EU Water Framework Directive (EU, 2000). Water authorities and provinces set detailed development and application of policies, standards and measures, to meet the target of good ecological status set by WFD. Under the restriction of WFD, several legislations have been rigorously enforced: Manure legislation (1987), Urban Waste Water Treatment Directive (1991), and Nitrates Directive (1991). Significant improvement of nutrient concentration was observed since the application of these legislations. To assess the physical, chemical, biological and microbiological status, routine monitoring campaigns are necessary and required by the WFD. This monitoring is conducted by water managers with set time intervals. In The Netherlands, surface water quality monitoring normally is done once a month. These discrete samples are mainly taken at the pumping station to represent the status of the entire catchment. The ecological status in most water bodies is investigated once a year. The frequency might increase or decrease depending on the investigated parameters and needs. Meanwhile, groundwater quality monitoring activity has been performed in The Netherlands since 1984, when the National Groundwater Quality Monitoring Network started full operation, in a density of 1 well every 100 km^2 and a yearly sampling frequency. The network consists of 380 wells with 2 m screen lengths at 2 m depth interval, covering both shallow (5-15 m below surface level) and deep (15-30 m below surface level) groundwater. However, even under the strict application of the legislations and routine assessment, in 2012, it still showed that up to 76% of water in agricultural area did not meet the environmental quality standards (Rozemeijer et al., 2014). About 60% of the fresh surface waters were eutrophic by 2016, excluding water bodies with good ecological status but high nutrients concentrations which accounted for 80% in marine waters (RIVM, 2017). The shallow groundwater (<30 m depth) under agricultural land was more polluted by nitrate than the deeper (>30 m) groundwater. And more pollution was found in sand region of the Netherlands.

The lack of knowledge of the pollutants biogeochemical cycles, and their spatial and temporal patterns, path ways, and the interaction between groundwater and surface water, are an obstacle preventing the achievement of good water quality (Wenger et al., 2009; Destouni and Jarsjö, 2018; Rozemeijer, 2010). Along with the development of knowledge and technology, researchers and water managers start to notice the inadequacy of the traditional discrete sampling. For example, Rozemeijer et al. (2014) reported that nutrient loads estimation by traditional monitoring method (monthly) is very uncertain due to changes in concentrations during discharge events, which was shown after engaging high frequency monitoring technology in an agricultural catchment. New monitoring technologies such as continuous monitoring sensors, robotic monitoring platforms, acoustic monitoring technology and

remote sensing, are gaining more attention and have proven their ability for understanding pollutants temporal dynamics. Different from surface water, groundwater monitoring requires more complicated sampling procedures than grabbing a sample from a ditch. A lower monitoring frequency is also justified due to the stability of groundwater quality over time. Quantification of nutrients from groundwater mostly is done by modeling. But, still, the low spatial and temporal monitoring resolutions, the lack of permanent groundwater quality monitoring wells in urban areas, have obscured our understanding of the interaction between groundwater and surface water quality in such landscape setting.

1.4 Water management and water quality in Amsterdam

Amsterdam locates in the west part of The Netherlands with Amstel River flowing through it from the south to the north. It has grown from a small fishing village into a densely populated city (5200 persons/km^2)*. The Amsterdam area consists of the city of Amsterdam and its surrounding polders, which are mostly excavated peat lands or lakes that were once drained to allow for agricultural use. Many of the polders in the city of Amsterdam were agricultural land before being urbanized. The change of land use types leads to the change of water bodies functions: from natural and traditional usage (agriculture, transport, domestic and industrial use) to serving for ecological, aesthetic and recreational purposes.

Water bodies in the greater Amsterdam area are either artificial or are heavily modified. The water management of Amsterdam is performed by the local water board: Waterschap Amstel, Gooi en Vecht Gemeente Amsterdam (Waternet). Due to the shallow groundwater table, intensive groundwater drainage systems and rain harvesting systems have been installed to create suitable condition for residence, construction, and agriculture. However, the Amsterdam region suffers from poor quality of deep groundwater that seeps up into the deep polders. This water is mostly nutrient rich and/or brackish. Several measures have been taken such as the utilization of these water resources for drinking water production, used for inlet water to release drought of neighboring catchments after de-phosporisation (e.g. Botshol receiving water from Groot Mijdrecht) and installation of new water treatment plants further reduce the loads of nutrients to the downstream. For instance, since the application of the new wastewater treatment plant RWZI Amsterdam-West from 2005 (water treatment plant), the export of P to downstream (North Sea) has been significantly reduced (Fig.1.3). The sources of the load of P into Amsterdam and from Amsterdam into the North Sea are illustrated in Fig.1.3. The outflow of P was still larger than inflow after the operation of RI West treatment plant, indicating the additional source of P from within the city of Amsterdam.

To assess the status, monitor the trend of water quality, and to understand the diversity among polders, routine monthly monitoring focusing on the polder outlet pumping systems have been conducted by Waternet water authority. As introduced in the previous section, the WFD mainly focuses on large surface water overlooking small water bodies, such as ditches which occupy a large proportion of surface water area in The Netherlands. Since 2020, the current water quality targets of WFD are extended by water boards towards smaller scale water bodies, which were not required to be reported

* https://en.wikipedia.org/wiki/Amsterdam

to the WFD before. The goal of this is to achieve substantial ecological improvement by 2027. Water quality in the artificial urban canals and ditches become the focus of water management in the next years. Therefore, filling in the knowledge gaps of nutrients dynamics and related biogeochemical processes is highly necessary to achieve an effective management strategy and fulfill the target of a better ecological status. Koschorreck et al. (2019) stated in their paper that, the artificial and small water courses "can provide useful and usable systems to test and monitor processes that take place in less manipulable natural systems and thus serve as experimental setups on which to design and test innovative management options and monitoring frameworks". Amsterdam area makes a perfect study field. Research in this area will help to gain more insights of nutrients dynamics and the interaction between groundwater and surface water in coastal cities, as well in other regions with eutrophicated water bodies.

Figure 1.2 Eutrophication in the city of Amsterdam: (a) duck weed, (b) blue green algae in Amstel river, (c) blue green algae in a low-lying polder

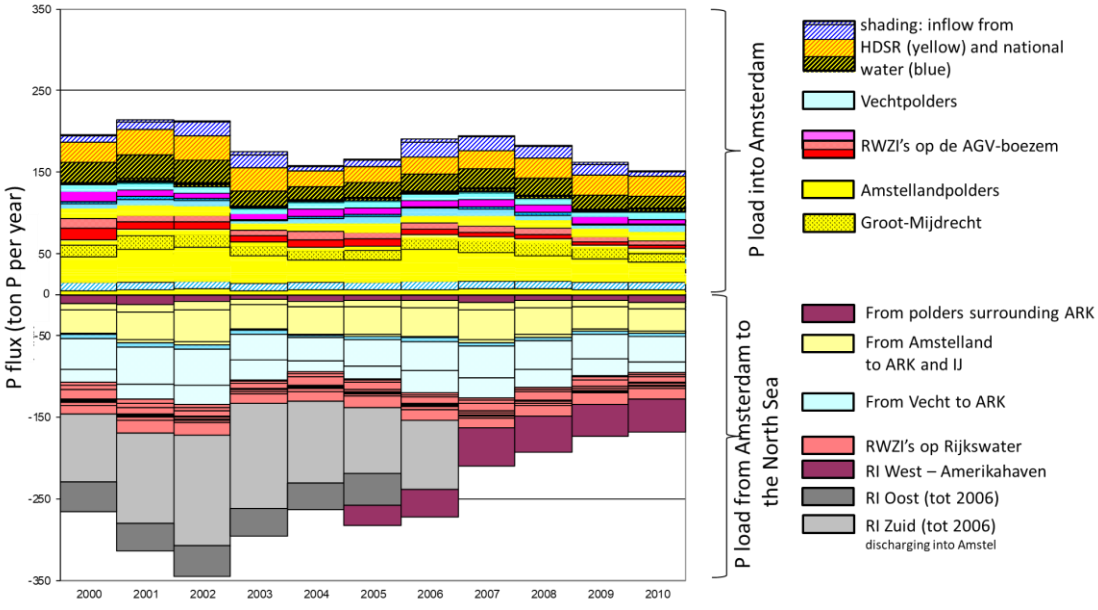

Figure 1.3 P flux (ton P per year) from upstream to Amsterdam and from Amsterdam to the North Sea. "RI" is "RWZI" (made by Waternet Amsterdam Water Authority).

1.5 Research questions

An effective water quality management strategy requires thorough understanding of the water systems from an integrated perspective (Bouwman et al., 2013; Paerl et al., 2016). It has been promoted frequently by researchers and managers to integrate the knowledge of hydrology, geology, chemistry and biology/ecology, and even broader to social sciences. The central objective of this thesis is to contribute to the understanding of the surface water quality in urban coastal low-lying catchments, focusing on the Amsterdam area as a data-rich example. Unraveling the flow routes, forms, and dynamics of solutes in concern, especially nutrients, will eventually contribute to a more effective surface water quality management that improves urban water quality and reduces nutrients loads to downstream water bodies. This objective leads to the following research questions:

Question 1 (Q1): What is the impact of groundwater on the surface water quality in the polder catchments of the greater Amsterdam city area?

Question 2 (Q2): What are the flow routes and mixing processes that control surface water quality in the groundwater influenced urban catchment?

Question 3 (Q3): What are the mechanisms controlling the dynamics of N and P in urban delta catchments affected by groundwater? (i.e. hydrogeological and biogeochemical processes that are controlling solutes dynamics along their pathways)

1.6 Thesis structure

To answer these research questions, we conducted our research on local (a single polder) to regional spatial scale (the greater Amsterdam region) and in short (events) and long (seasonal to years) time scales: (1) Chapter 2 - long term monitoring analysis at a regional scale (144 polders, average over 7 years for surface water, mostly over 33 years for groundwater), (2) Chapter 3 - long term and short term monitoring at the catchment scale (in one specific urban polder, monthly average over 10 years) and (3) Chapter 4 – short term (1 year) high-resolution monitoring of the water quality at the catchment scale (hourly average). The structure of the thesis is shown in Figure 1.4.

Chapter 2: Groundwater impacts on surface water quality and nutrient loads in lowland polder catchments: monitoring the greater Amsterdam area

Chapter 2 aims to answer research question (1) at the regional-yearly average data scale (Fig.1.4). In this chapter, to identify the inducing factors of the release of nutrients into surface water bodies, factors such as surface water quality, groundwater quality, and elevation, paved area, surface water area, agricultural N and P input, seepage rate, and soil types (humus, calcite and clay) were included in a statistical analysis. The spatial distribution of solutes: TP, TN, NH_4, NO_3, HCO_3, SO_4, SO_4/Cl, Ca and Cl in both groundwater and surface water were analysed addressing the important relation between these two water types with respect to quality.

Chapter 3: Urban hydrogeology: transport routes and mixing of water and solutes in a groundwater influenced urban lowland catchment

In this chapter, research question (2) is answered at the catchment-monthly data scale (Fig.1.4) using results from systematic discrete sample monitoring. The influences of urban settings in a groundwater fed catchment, such as the installation of groundwater drains, the fast flow path of rain runoff to the surface water system, and the pumping activity regulating water level in the polder, were revealed in the spatial survey of the water quality of runoff, drain water, ditch water and deep and shallow groundwater. The temporal patterns of solutes of the discharge were explored based on the antecedent precipitation and evapotranspiration index.

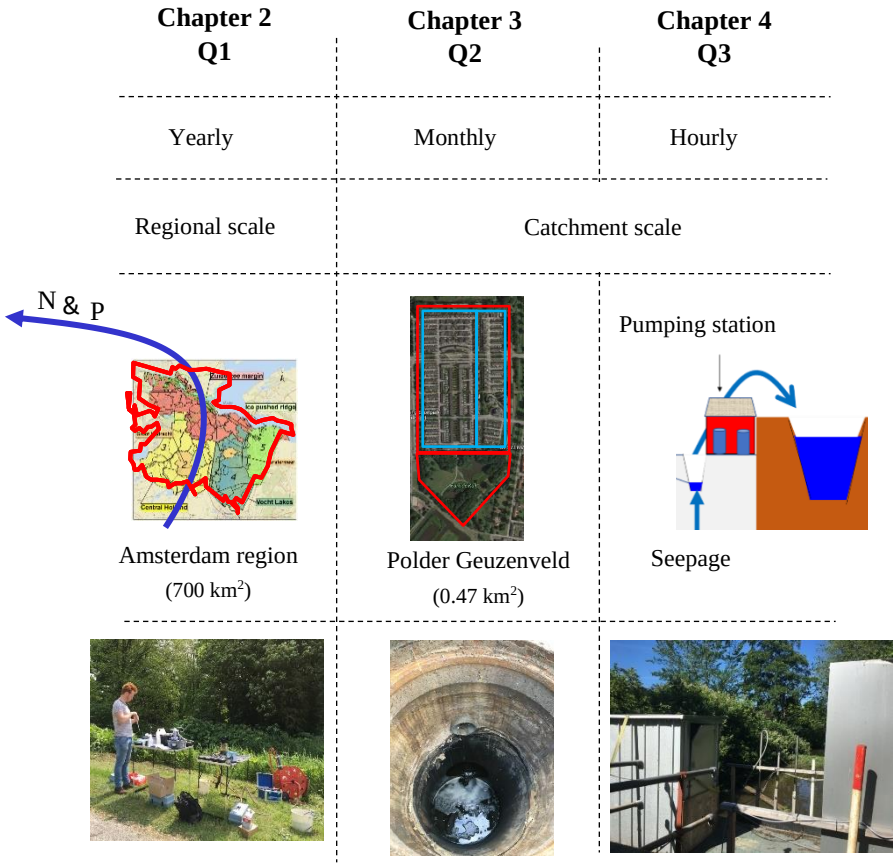

Figure 1.4 Thesis structure, chapters showed in different spatial and temporal scale and related research questions in each chapter

Chapter 4: Assessing the controlling mechanisms of Nitrogen and Phosphorus dynamics in a groundwater-fed urban catchment through high frequency monitoring

This chapter focuses on the research question (3) at the catchment-hourly data scale (Fig.1.4). Water quality of the polder discharge was monitored using high frequency monitoring technology at the pumping station. The temporal patterns of EC, NH_4, TP and Turbidity response to rainfall and pumping events were demonstrated in an annual, rain event and single pumping event scale. Combining with a

weekly/biweekly grab sampling campaign in the same period, the dynamics of nitrogen and phosphorus in urban groundwater-fed catchment were analyzed from an interdisciplinary perspective, which led to a possible foundation for creating optimized cost-effective strategies to reduce and control the urban water eutrophication phenomenon.

Chapter 5: Synthesis

The synthesis summaries the impacts of groundwater on surface water quality, the groundwater and surface water interaction in space and time, and the driving mechanisms for the temporal dynamics of nutrients. Implications of this thesis are on the aspects of integrated urban management, lowland urban water system design, and urban water quality monitoring strategies, so to cope with the inevitable further urbanization in low-lying deltas. In this vision, future research should further assess the specific effects of groundwater drainage systems, and should further study on ecosystem functioning using integrated data and modeling approaches, which are addressed at the end.

Chapter 2

Groundwater impacts on surface water quality and nutrient loads in lowland polder catchments: monitoring the greater Amsterdam area*

Abstract: The Amsterdam area, a highly manipulated delta area formed by polders and reclaimed lakes, struggles with high nutrient levels in its surface water system. The polders receive spatially and temporally variable amounts of water and nutrients via surface runoff, groundwater seepage, sewer leakage, and via water inlet from upstream polders. Diffuse anthropogenic sources, such as manure and fertilizer use and atmospheric deposition, add to the water quality problems in the polders. The major nutrient sources and pathways have not yet been clarified due to the complex hydrological system in such lowland catchments with both urban and agricultural areas. In this study, the spatial variability of the groundwater seepage impact was identified by exploiting the dense groundwater and surface water monitoring networks in Amsterdam and its surrounding polders. Twenty-five variables (concentrations of Total-N, Total-P, NH_4, NO_3, HCO_3, SO_4, Ca, and Cl in surface water and groundwater, N and P agricultural inputs, seepage rate, elevation, land-use, and soil type) for 144 polders were analysed statistically and interpreted in relation to sources, transport mechanisms, and pathways. The results imply that groundwater is a large source of nutrients in the greater Amsterdam mixed urban/agricultural catchments. The groundwater nutrient concentrations exceeded the surface water Environmental Quality Standards (EQSs) in 93 % of the polders for TP and in 91 % for TN. Groundwater outflow into the polders thus adds to nutrient levels in the surface water. High correlations (R^2 up to 0.88) between solutes in groundwater and surface water, together with the close similarities in their spatial patterns, confirmed the large impact of groundwater on surface water chemistry, especially in the polders that have high seepage rates. Our analysis indicates that the elevated nutrient and bicarbonate concentrations in the groundwater seepage originate from the decomposition of organic matter in subsurface sediments coupled to sulfate reduction and possibly methanogenesis. The large loads of nutrient rich groundwater seepage into the deepest polders indirectly affect surface water quality in the surrounding area, because excess water from the deep polders is pumped out and used to supply water to the surrounding

* Based on: Liang Yu, Joachim Rozemeijer, Boris M. van Breukelen, Maarten Ouboter, Corné van der Vlugt, Hans Peter Broers. Groundwater impacts on surface water quality and nutrient loads in lowland polder catchments: monitoring the greater Amsterdam area. *Hydrology and Earth System Sciences*, 22: 478-508, 2018.

infiltrating polders in dry periods. The study shows the importance of the connection between groundwater and surface water nutrient chemistry in the greater Amsterdam area. We expect that taking account of groundwater-surface water interaction is also important in other subsiding and urbanising deltas around the world, where water is managed intensively in order to enable agricultural productivity and achieve water sustainable cities.

2.1 Introduction

The hydrology of many lowland delta areas is highly manipulated by human activities such as ditching, draining, and embanking, to enable agriculture and habitation. Lowland deltas account for 2 % of the world's land, but accommodated around 600 million people in 2000, and about 1400 million by 2060 as was estimated by Neumann et al. (2015). The reclamation of swamps and lakes and the drainage of peat areas to enable urbanisation and agriculture severely changed the hydrological, chemical, and ecological environment of these areas (Ellis et al., 2005; Yan et al., 2017). Lowland delta areas are vulnerable for water quality deterioration by processes like salinization and eutrophication, which can be amplified by climate change (Wu et al., 2015) and land subsidence (Minderhoud et al., 2017).

The Netherlands is a densely populated country where surface water salinization and eutrophication are common problems. It is a typical highly urbanized country, with 2/3 of its land lying below mean sea level. In The Netherlands, small regulated catchments called polders have been developed over centuries by diking in and draining lakes and swamps (Huisman, 1998). Over 10 million people are living in the coastal area, mainly in the Western part where a Holocene layer of peat and clay covers Pleistocene fluvioglacial sands. Especially the deepest polders receive large amounts of groundwater seepage. The surface water levels within the polder catchments are artificially controlled by pumping water out into the regional water systems (called Boezem), which further accelerates groundwater seepage. Some of the deep polders exhibit upconing of deep saline groundwater into the surface water. The salt loading towards these polders is expected to increase, mainly due to the further lowering of surface water levels in response to subsidence (e.g. Oude Essink et al., 2010; Delsman et al., 2014). Draining the peat polders has also led to subsidence and repetitive lowering of surface water and groundwater levels. As a consequence, nutrients are released due to peat oxidation (Hellmann and Vermaat, 2012). Another nutrient source is the large scale agricultural application of manure and fertilizer. Although manure legislation was already enforced in 1986, surface water quality in the area still does not meet the EU Water Framework Directive standards for chemical and ecological water quality (Rozemeijer et al., 2014). The local water authority, called Waternet, is commissioned to improve water quality in a cost-effective mitigation program. The assessment of load contributions from different pollution sources is essential to set realistic region-specific water quality targets and to select appropriate mitigation options.

Influences of groundwater on surface water quality have recently gained more attention by hydrologists (e.g. Rozemeijer and Broers, 2007; De Louw et al., 2010; Garrett et al., 2012; Delsman et al., 2015). Rozemeijer et al. (2010) found that groundwater seepage has large impacts on surface water quality in a lowland agricultural catchment. A study by Holman et al. (2008) in the United Kingdom and the Republic of Ireland also suggested that the groundwater contribution to surface water nutrient concentrations is more important than previously thought. Furthermore, Meinikmann et al. (2015) found that lacustrine groundwater discharge contributed for more than 50% of the overall external P load in their study lake. Vermonden et al. (2009) concluded that upward seepage from Meuse-Waal canal delivered NO_3 and Cl to urban surface water system. The impact of other landscape characteristics on surface water quality, such as soil type and land use, has also been explored. For example, Van Beek et al. (2007) found that nutrient rich peat layers will remain a potential source of nutrients in surface water in many peat polders in the western part of The Netherlands. Mourad et al. (2009) found that the spatial patterns of nitrate and phosphate concentrations in the Ahja River catchment in Estonia were

related to spatial differences in urban and agricultural land use proportions. Vermaat et al. (2010) studied 13 peat polders in the Netherlands and reported that agricultural land use largely determined the variability in nutrient concentrations and loads. Phosphorus was observed in higher concentrations in urban areas than in rural areas by Meinikmann et al. (2015) In some studies, point sources like effluent from sewage treatment plants dominated the phosphorus loads (e.g. Wade et al., 2012), but the Netherlands is known to have early invested in centralised sewage treatment works, thus avoiding the many individual spills that are present is some bordering countries (EU, 2017).

Previous water quality research in polder areas have mainly focused on the impact of land use types and topography. The impact of groundwater and flow routes on spatial water quality patterns in polders has not been systematically studied. Such insight is highly needed, as a cost-effective protection and regulation of water resources requires an integrated assessment of water and contaminant flow routes in the water system as a whole. In general however, water and contaminant flow routes in urban settings are more complex than in rural areas, due to the highly variable surface permeability and human emissions of pollutants.

This study aimed at identifying the impact of groundwater on surface water quality in the polder catchments of the greater Amsterdam city area, which is the management area of Waternet, the organisation which manages dikes, regulates water levels and pumping regimes and is responsible for the clean surface water, drinking water supply and waste water treatment. To achieve this, we analysed regional surface water and groundwater quality monitoring data in combination with ten landscape characteristic variables for 144 polders: N and P agricultural inputs, surface elevation, paved area percentage, surface water percentage, seepage rate, and soil type represented by calcite, humus, and clay percentages. Our statistical analyses yielded insight into the impact of groundwater on the surface water chemistry of the urban and rural polders of Amsterdam. The presented approach contributes to realistic and effective water quality regulation in the Waternet management area and can also be applied to other deltas in the world with adequate groundwater and surface water monitoring data.

2.2 Methods

2.2.1 Study area

This study focuses on the polder catchment landscape around the city of Amsterdam in The Netherlands. The whole study area spans 700 km^2, from downtown Amsterdam situated in the northwest to the border of the province of Utrecht in the southeast (Fig.2.1). Amsterdam is a low-lying highly paved city located in the western part of the Netherlands, developed around the levees of the tidal outlet of the Amstel River about 700 years ago (Vos, 2015). Nowadays, the water system in Amsterdam is connected to the large fresh water body of the Lake IJ (Fig.2.1). Besides Lake IJ, other important large water bodies are the Amstel and Vecht rivers and the Amsterdam-Rhine canal. This regional water system, also called the 'Boezem', connects the Amsterdam-area water system to the Rhine River (upstream) and the Lake IJssel and the North Sea (downstream). In the 19th and 20th centuries, the city expanded, and many new neighbourhoods and suburbs were built. Polders and reclaimed lakes form the main landscape in the southward extensions of the city. Some of these polders are at several meters below Mean Sea Level (MSL) and are influenced by groundwater seepage.

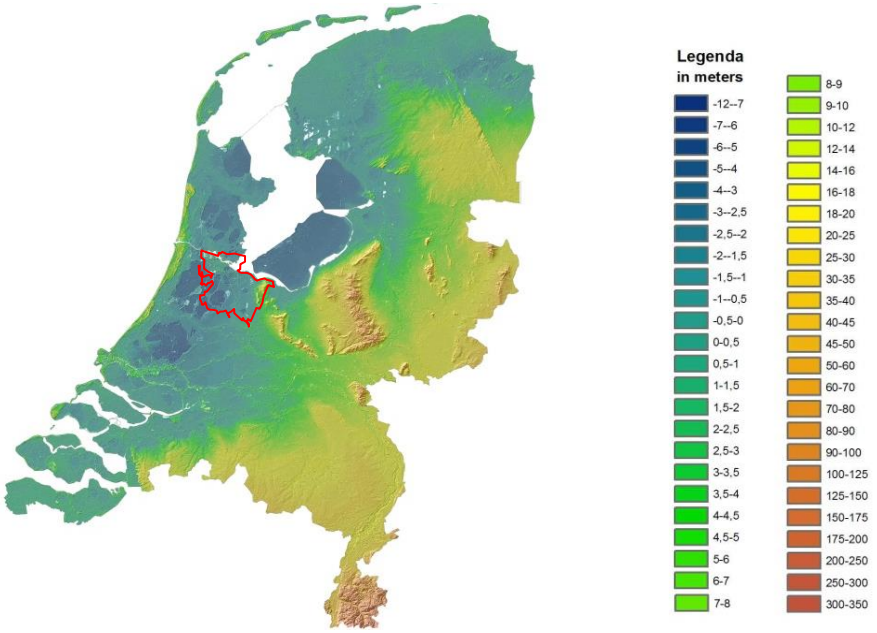

Figure 2.1 Location of the research area (red) projected on the elevation map of The Netherlands (elevations in meters above mean sea level (MSL))

2.2.1.1 Landscape history and hydrology

Landscape history

Our study area is located in the western part of The Netherlands where large rivers and the sea have intensively interacted for millions of years. The main topographic feature is a Pleistocene sandy ice pushed ridge with elevations ranging from 0 to 30 m, which is located on the east part of the study area (Fig.2.1, Fig. S1). To the west, the ridge is bordered by the broad periglacial Pleistocene river plains of the Rhine delta. During the Holocene, these sandy river plains were covered with peat and clay, which are currently found at the surface throughout the western part of the Netherlands, on top of Pleistocene sands. The average thickness of the Holocene peat and clay cover is 20 m, although it increases to over 50 m in former tidal inlet channels (Hijma, 2009).

In 1000 AD, about 5000 years after first settlers appeared in these low lands, the inhabitants started mining peat, digging ditches, constructing dikes, reclaiming former swamps and lakes, and pumping water out into a large scale drainage system (called Boezem). Special hydrological catchments called ‘polders’ were formed, connected by the ‘Boezem’ main waterways around them. Fig. S2.1 and and Table S2.1 in the Supplementary Information show the entire system of polder catchments (indicated by numbers for reference) and boezems studied in this paper. Prominent on these maps are two deep polders Horstermeer (#79) and Groot Mijdrecht (# 80), two former lakes that were formed after peat excavations. Drainage for lake reclamation and groundwater extraction (Schot, 1992a) caused further subsidence and increased seepage of paleo-marine brackish groundwater from deep aquifers (Delsman et al., 2014).

The long history of marine influence stopped after closing off the estuaries and the inland sea in the 20th century (Huisman, 1998). In 1932, the construction of the Closure Dike (Afsluitdijk) created the fresh water Lake IJssel out of the former salt water Zuiderzee ('Southern Sea') to protect the surroundings from floods and to enable land reclamation. The former marine impact is still reflected by the presence of brackish groundwater in the shallow subsurface (Schot, 1992 b).

The construction of the Amsterdam Rhine Canal separated the study area into two parts (Fig. S1): the Central Holland in the west and the Vecht lakes area in the east. In the Central Holland polders, relatively thick peat layers and pyrite rich clays are still present in the shallow subsoil, as described by Van Wallenburg (1975). The Vecht lakes area is characterized by large open water areas and a number of wetland nature reserves. The rest of the Vecht lakes area is mainly grassland used for dairy farming. Soils in this area are generally wet and rich in organic matter and clay (Schot, 1992 b).

Mainly during the 20th century, the urban areas have been growing from the historic city-centres on river and tidal channel levees into the surrounding low-lying polders. To facilitate the construction of buildings, a 1-5 meter-layer of sand was often supplied on top of the original sediments. The thickness of this suppletion sand layer is extremely variable even at a small scale. The sand suppletions are either calcite-poor without shell fragments or calcite rich with shell fragments that indicate their (peri-) marine origin. The spatial distribution and sources of the sand suppletions probably influence groundwater and surface water chemistry, but are poorly registered.

Polder hydrology

Within the polders, the water levels are artificially maintained between fixed boundary levels to optimize conditions for their urban or agricultural land use. Boezem water levels always exceed the polder surface water levels. In the case of water deficiency, water is let into the polder ditches from the boezem through pipes by gravity flow (Fig.2.2a). Pumping stations are situated at the boezems to regulate the water levels in the polders in times of precipitation excess. In the case of a water surplus, pumping stations start pumping water out of the polder into the boezem-system (Fig.2.2b).

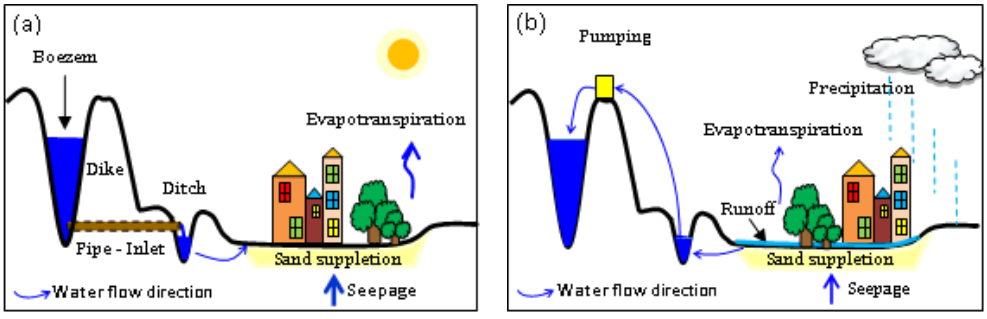

Figure 2.2 Conceptual model of water fluxes in a polder system in times of water deficiency (a) and surplus (b).

The regional flow directions in wet and dry periods in the study area are depicted in Fig.2.3. The Amsterdam-Rhine canal, the Amstel River, and the Vecht River are the main water courses discharging

surface water from the south to the north in periods of water surplus (Fig.2.3). In periods of water deficiency, however, the flow directions are reversed in some parts of the system.

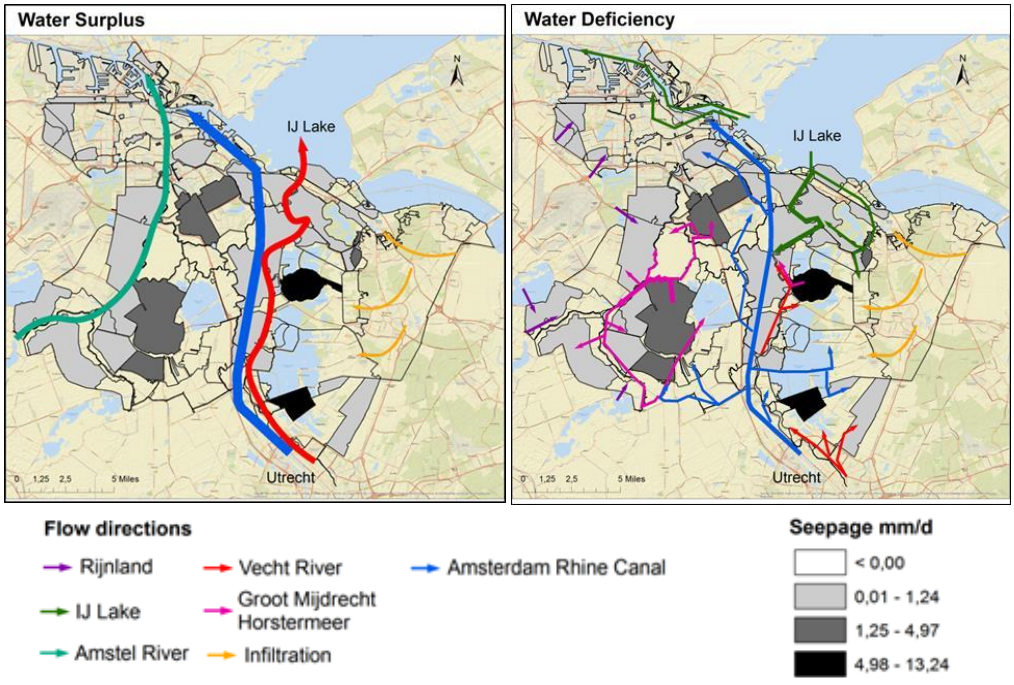

Figure 2.3 Flow directions of surface water in water surplus and water deficiency period

There are six main sources of inlet water to compensate for water shortage in dry periods (Fig.2.3): (1) Amsterdam Rhine Canal (ARC): water of the ARC originates from the Rhine and is supplied as inlet water for the southeast polders and polders in the southeast of Amsterdam city; (2) Amstel River: the historic canals of the city of Amsterdam are mainly flushed by water from the Amstel River. Via the canals, this water discharges to the downstream part of the ARC and further into the North Sea; (3) Groot Mijdrecht and Horstermeer: the brackish surplus of seepage water from the deep polder Groot Mijdrecht (~1000 mg Cl L^{-1} on average) and Horstermeer (~500 mg Cl L^{-1}) is pumped into the Boezem system and is redistributed towards surrounding polders (pink lines in Fig.2.3); (4) Rijnland Water Authority district: polders in the far west of the study area receive inlet from the neighboring Water Authority district Rijnland. The water quality of this source is unknown. (5) and (6) Vecht River and Lake IJ: polders along the Vecht River receive inlet water that partly originates from the Rhine and partly from Lake IJ. Polders close to Lake IJ receive large amounts of water directly from the lake. The Lake IJ water is also used to flush canals in the city of Amsterdam.

2.2.1.2 Characterisation of regions

Based on the geology and paleohydrological history as introduced in section 2.2.1.1, 5 regions were identified (see Fig.2.4).

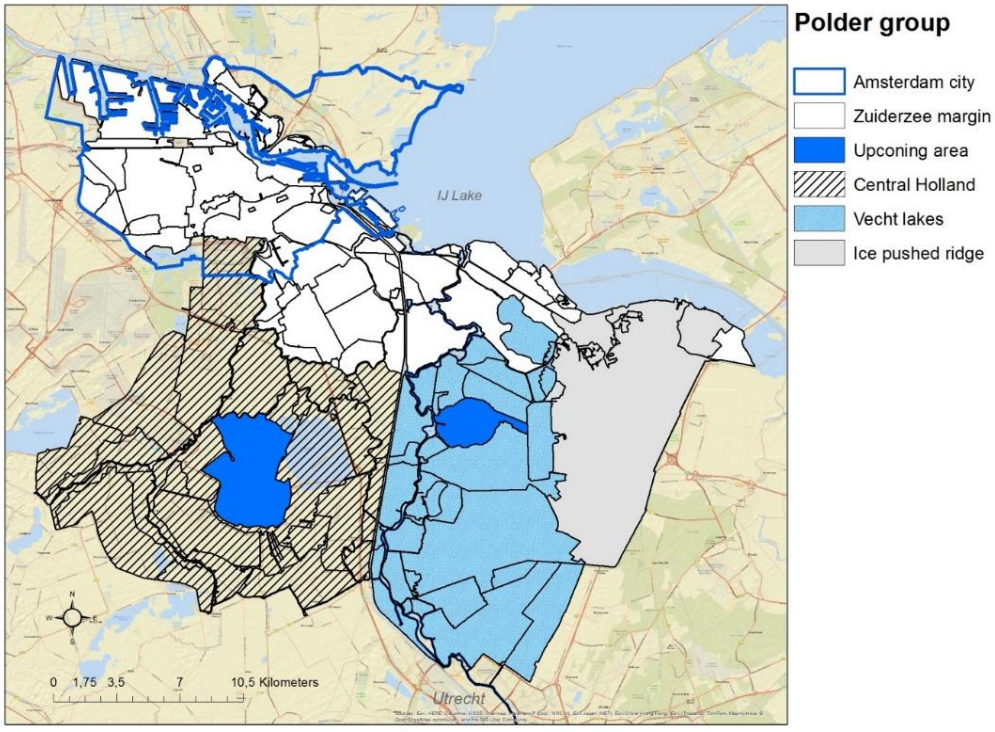

Figure 2.4 Regions of the study area: (1) Zuiderzee margin, (2) Upconing area (deep brackish seepage polders Groot Mijdrecht and Horstermeer), (3) Central Holland, (4) Vecht lakes and 5) Ice pushed ridge. The Amsterdam city area is circled by the blue line.

The 5 regions are: (1) the Zuiderzee margin region, with shallow brackish groundwater, lies directly adjacent to the former salt water Zuiderzee, which was dammed in the 1930s and transformed into the fresh water Lake IJssel (connected to Lake IJ), which is now the biggest fresh water reservoir of The Netherlands; (2) the deep polders Groot-Mijdrecht and Horstermeer, which are reclaimed lakes with clayey lake sediments at the surface. These polders are characterized by upconing of salt groundwater from deeper layers (Oude Essink et al., 2005; Delsman et al., 2014) and intensive arable farming; (3) the Central Holland region, where the polders are characterized by a relatively thick sequence of marine clays and intercalated peats; (4) the Vecht lakes region at the western margin of the ice pushed ridge, characterized by shallow peat soils over a sandy subsoil and large shallow lakes and wetlands resulting from peat excavations (van Loon, 2010) with mostly dairy farming; and (5) the Ice pushed ridge in the eastern part of the study area, which is characterized by permeable sandy soils, recharge of freshly infiltrated water, and the mere absence of draining water courses.

Our a priori expectation was that the groundwater quality of these 5 regions is significantly different, because of their specific paleohydrological situations and present day groundwater flow patterns. We therefore used the regions to evaluate the groundwater quality patterns and to give structure to our comparisons between groundwater and surface water concentrations and loads.

2.2.2 Data processing

The database that was compiled and used for this study covers 144 individual polders and includes monthly surface water quality data, spatiotemporally averaged groundwater quality data (TN, NO_3, NH_4, SO_4, TP, Ca, HCO_3, and Cl), daily pumping station discharge time series, and polder averages of the following statistic variables: N and P agricultural inputs, polder seepage rates, elevations, surface water and paved area percentages, and calcite, clay, and humus percentages of the upper soil layer. More information about the data processing and the database can be found in the Supplementary Information.

2.2.2.1 Groundwater data

A total of 802 observation wells of groundwater quality are available from the period 1910-2013 (mostly after 1980), largely drawn from the National Groundwater Database DINO (TNO, DINOLoket). We selected analyses from the upper 50 m of the subsurface, which corresponds with the thickness of the first main Pleistocene aquifer in the area and the Holocene cover layer. For our analyses, in order to use as much of the available groundwater data as possible to cover the entire region and all the polders, we averaged concentrations at individual monitoring screens of each monitoring well for all sampling dates available. The large majority of the groundwater quality data we used is from the last 30 years (for example, 85% of the chloride and 93% of the P measurements are from after 1980). In this study area, we do not expect that using some data from before 1980 creates a significant bias to the results of the study, because hydrogeochemical processes in the reactive subsurface such as sulfate reduction and methanogenesis have a stabilizing effect on the water composition in this area. Moreover, the overall flow patterns have not changed much in the past 30 to 100 years, because the flow systems are completely determined by the water levels maintained in the polder systems which have not changed much over the past 100 years. However, the interface between fresh and salt water is known to slowly move into the direction of a new equilibrium (Oude Essink et al., 2010), but the process is known to be very slow and to continue over the next 200 years.

To analyse the spatial pattern of groundwater quality, we averaged concentrations of all the monitoring wells located in the same polder (for more details, see Table S2.2). For 24 polders out of the polders without groundwater quality data, the concentrations were estimated by Inverse Distance Weighted interpolation, however using absolute elevation difference instead of distance. The greater the absolute elevation difference, the less influence the polder has on the output value. The equations are:

$$C_0 = \sum_{i=1}^{n} \lambda_i C_i \qquad (2.1)$$

$$\lambda_i = d_{i_o}^{-p} \Big/ \sum_{i=1}^{n} d_{i_o}^{-p}, \qquad \sum_{i=1}^{n} \lambda_i = 1 \qquad (2.2)$$

C_0, prediction of target polder; C_i, observed value of surrounding polders; n number of observations; p, power parameter (2 in this case); d_{i_0}, absolute elevation differences of target polder with surrounding polders. Subsequently, to interpret the groundwater quality patterns, the variation of concentrations in and between the 5 regions was visualized using boxplots (Helsel and Hirsch, 2002).

Because our dataset contains both fresh and brackish to saline water, we used the mass SO_4/Cl ratio of the samples as an indicator of sulfate reduction. SO_4/Cl ratios lower than the sea water ratio of 0.14 (Morris and Riley, 1966) point to the occurrence of sulfate reduction (Appelo and Postma, 2005; Griffioen et al., 2013). Ratios above 0.14 point to the addition of sulfate relative to diluted sea water through processes like pyrite (FeS_2) oxidation or through input via atmospheric inputs, fertilizers, manure, or leakage and overflow of sewer systems.

Average concentrations in groundwater for each polder were mapped to be compared with average annual surface water concentrations (See section 2.2.2.2). The potential relationship between the solute concentrations in groundwater (TN, NO_3, NH_4, SO_4, TP, Ca, HCO_3, and Cl), the N and P agricultural inputs, and the landscape variables (paved area percentage, elevation, seepage rate, surface water area percentage, lutum, humus and calcite percentages of top soil) were explored using the Spearman correlation, which reduces the influence of outliers and yields a robust correlation statistic (Helsel and Hirsch, 2002).

To further explore the statistical relations in our data set, scatter plots were made to evaluate HCO_3, SO_4, Cl, and nutrient (NO_3, NH_4 and PO_4) concentrations in groundwater. We also explored the links between alkalinity (over 99 % of our groundwater alkalinity was dominated by HCO_3, (Stuyfzand, 2006)), Cl concentration, SO_4/Cl ratio and nutrients (TN, NH_4 and TP) concentrations. For our interpretation, we also used the calculated amount of consumed or produced SO_4 in mg L^{-1} relative to the SO_4/Cl ratio of diluted seawater, using Eq. (2.3):

$$SO_4 consumed(-)\ or\ produced(+) = SO_4 measured - Cl\ measured \cdot \frac{SO_4 sea}{Cl} sea \tag{2.3}$$

In order to understand the impact of cation exchange processes involving Ca and Na exchange during salinization and/or freshening of aquifers (Griffioen, 2004; Stuyfzand, 2006) we defined the amount of exchange Na_{ex} as:

$$Na_{ex} = Na_{gw} - Cl_{gw}(Na_{gw}/Cl_{seaw}) \tag{2.4}$$

Where, Na_{ex} is the amount of Na exchange; gw, ground water; seaw, seawater. $Na_{ex} > 1$ points to freshening, $Na_{ex} < -1$ to salinizing conditions.

2.2.2.2 Surface water data

Loads represent the contribution of polders to surface water quality of the regional water system in weight per time unit. To eliminate the impact of the size of polders, we calculated daily load per area in kg ha^{-1} d^{-1}. This was calculated using the daily average loads of each solute divided by the polder areas using Eq. (2.5):

$$\text{Load per area} = \frac{L}{A} = \frac{1}{A} \cdot \frac{C \cdot Q}{1000} \tag{2.5}$$

Where L is daily load kg d^{-1}, A is polder area (ha), C is daily solute concentration in mg L^{-1} and Q is daily discharge in m^3 d^{-1}. Average daily loads for each year were multiplied by 365 to get average yearly loads per area. Monthly surface water quality measurements for the period 2006-2013 of 144 polders were extracted from the Waternet database. The measurements were converted to daily time series by stepwise interpolation between the monthly measurements. We assigned a concentration of zero to measurements below the detection limits. Discharge data Q are daily measurements over the same time period. An average over multiple pumps, when present, was taken for each polder. For further details about the data processing we refer to Table S2.2.

The pumping discharge is regulated to respond to water surplus or deficiency conditions in the polder catchments. Using the pumping frequency data, we proved that solute concentrations in pumped water are usually higher at the beginning of each pumping activity (Van der Grift et al., 2016). The pumping rates may also influence water quality in the polder. To eliminate differences caused by pumping rates, we used the normalized concentration calculated using Eq. (2.6):

$$C = \frac{\text{Load per area} \cdot A}{Q} \tag{2.6}$$

In this equation, C is the normalized concentration (mg L^{-1}), Load per area is from Eq. (1), Q is the pumping discharge (m^3 y^{-1}), and A is the polder area (m^2).The statistical methods that were used for groundwater quality (described in section 2.2.1) were also applied to the surface water normalized concentrations.

Based on a national assessment on ecosystem vulnerability, Environmental Quality Standards (EQSs) were set by the Water Boards (Heinis and Evers, 2007). For most ditches and channels in the clay and peat regions, EQSs of TN and TP are 2.4 mg L^{-1} and 0.15 mg L^{-1}, respectively (Rozemeijer, 2014). We used these most common EQSs as reference concentration values. For example, the EQSs of TN and TP were used for the legend classifications in our surface water quality maps and were added as reference lines in our concentration boxplots. Percentages of polders exceeded these standards were calculated in this paper.

2.2.2.3 Surface water compared with groundwater solute concentrations

We statistically analysed the groundwater and surface water quality data and landscape characteristic variables by (1) calculating the correlation coefficients between averaged groundwater solutes concentrations and normalized concentrations of surface water using the Spearman method, and (2) by selecting variables (based on the correlation matrix above) to be integrated into multiple linear regression models for predicting surface water solute concentrations. Again, the Spearman method was applied and linear regression was based on ranks in order to avoid outliers to determine the outcomes. The explaining variables for surface water concentrations include groundwater solute concentrations, N and P agricultural inputs, landscape characteristics, and the SO_4/Cl ratio in groundwater. We adopted the method described by Rozemeijer et al. (2010), who described a form of sequential multiple regression analysis, where variables were added to the regression depending on their effects on the coefficient of determination R^2. The regression analysis started with a singular regression using the explaining variable with the highest coefficient of determination (R^2) for explaining the surface water quality parameter under consideration. Subsequently, the best regression models were searched with

two and three explaining variables, where we accepted an additional variable only when the coefficient of determination R^2 increased with at least 0.03. In this method, dependent variables can still add to the resulting R^2 as the coefficient of determination R^2 of the individual dependent variable pair is seldom larger than 0.7, pointing to some explaining power may still be present in the uncorrelated part (0.3). For comparison purposes, we also used the surface water EQSs as reference concentration values in the groundwater quality maps and boxplots, although the EQS's have no administrative meaning for groundwater itself.

2.2.2.4 Solutes redistribution in surface water

Loads were used to assess the impact of different polders as sources of solutes for the boezems and the receiving water bodies further downstream. In general, the spatial patterns can be distinguished through maps of the surface water solute loads per area if there are no other influences. However, there are exceptions such as the seepage water which is pumped out of the two upconing polders Groot Mijdrecht and Horstermeer, which is discharged into the Boezem system and used as inlet water for the surrounding polders during summer. To show the impact of this inlet water on the receiving polders' water quality, we analysed the inlet solute loads and the resulting surface water concentrations for polder Botshol. Polder Botshol (part of polder # 104 Noorderpolder of Botshol (zuid and west)) with an area of 1.3 km^2 receives inlet water from the Amstel boezem system that has a significant contribution of seepage water that is pumped out of the polder Groot Mijdrecht.

Two models were applied for simple solute concentration calculations based on inlet water quality. Model 1 calculates the accumulation of solutes in the water body, with evaporation as the only output for water (leaving the solutes behind). Model 2 models the complete mixing and outlet of both water and solutes via other routes like the outlet weir, infiltration, and leakage. In reality, water leaves Polder Botshol partly via evaporation (Model 1) and partly via other routes (Model 2):

Model 1 (evaporation):

$$C_{i+1} = (C_i \cdot V_0 + C_{inlet} \cdot Q_{inlet})/V_0 \quad (2.7)$$

Model 2 (infiltration/outlet):

$$C_{i+1} = (C_i \cdot V_0 + C_{inlet} \cdot Q_{inlet})/(V_0 + Q_{inlet}) \quad (2.8)$$

where, C_{i+1} is the predicted solute concentration after getting inlet water at time i; C_i is the predicted solute concentration in the polder at time i, the outlet measurements in the beginning of wet period were taken as C_0; V_0 is the water volume in the polder (800.000 m^3), which is assumed to be constant as water levels are tightly controlled; C_{inlet} is the estimated Cl concentration in the inlet water (1000 mg L^{-1}); Q_{inlet} is estimated constant inlet water volume, 6000 m^3 d^{-1}. All parameters are shown in supplementary information Excel spread sheets. The models were applied in the year 2006, 2008, 2009, 2010, 2011 and 2012.

2.3 Results

2.3.1 Spatial pattern and statistical analysis of groundwater quality

Fig.2.5 and Fig.2.6 show the groundwater quality for the upper main aquifer under the 144 polders for Cl, Ca, HCO_3, SO_4, TN, NH_4, NO_3, and TP. The relations between groundwater solutes, landscape variables, and potential hydrochemical reactions in the subsurface were explored by correlation analysis of which the results are shown in Table 2.1 (yellow part) and Fig.2.7 and Fig.2.8.

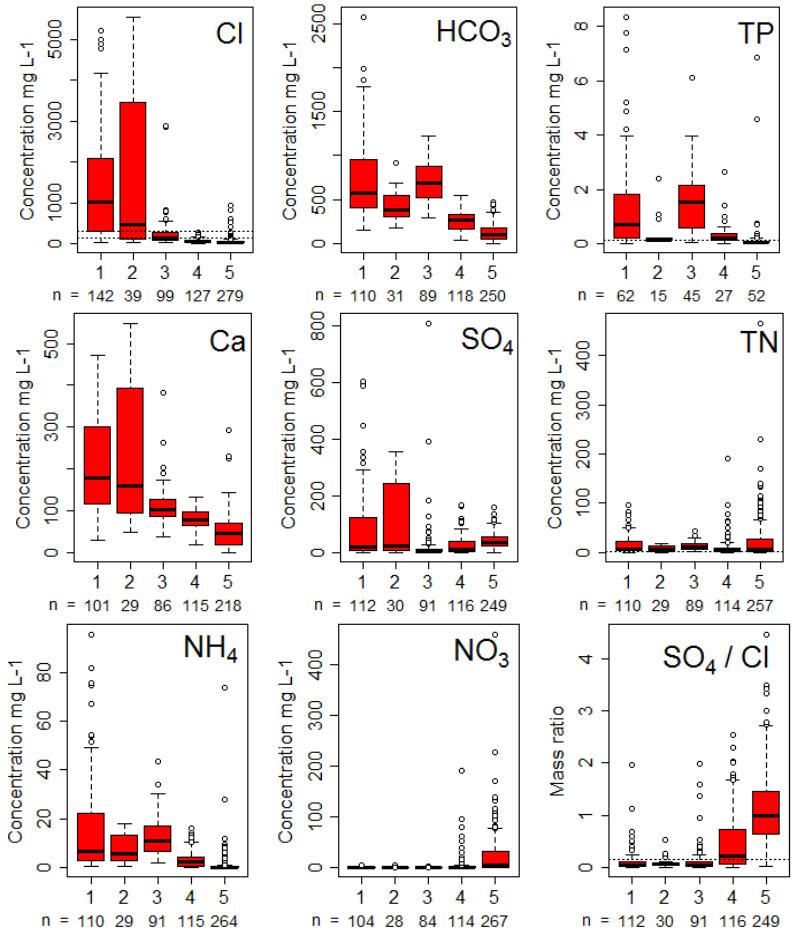

Figure 2.5 Spatial variation of groundwater quality. 1-Zuiderzee margin, 2-Upconing area (Groot Mijdrecht and Horstermeer), 3-Central Holland, 4-Vecht lakes, 5-Ice pushed ridge (see Fig. 4). n is the amount of available data of each group. Boxplots show the distribution of solutes in the five regions. The two horizontal dashed lines for Cl indicate fresh water (<150 mg L^{-1}) and brackish water (>300 mg L^{-1}), respectively. Dashed lines represent EQSs for TN (2.4 mg L^{-1}) and TP (0.15 mg L^{-1}). The dashed line in the SO_4/Cl plot indicates the mass ratio of 0.14 in seawater (<0.14 indicates sulfate reduction; >0.14 indicates additional sources of sulfate besides (diluted) seawater)

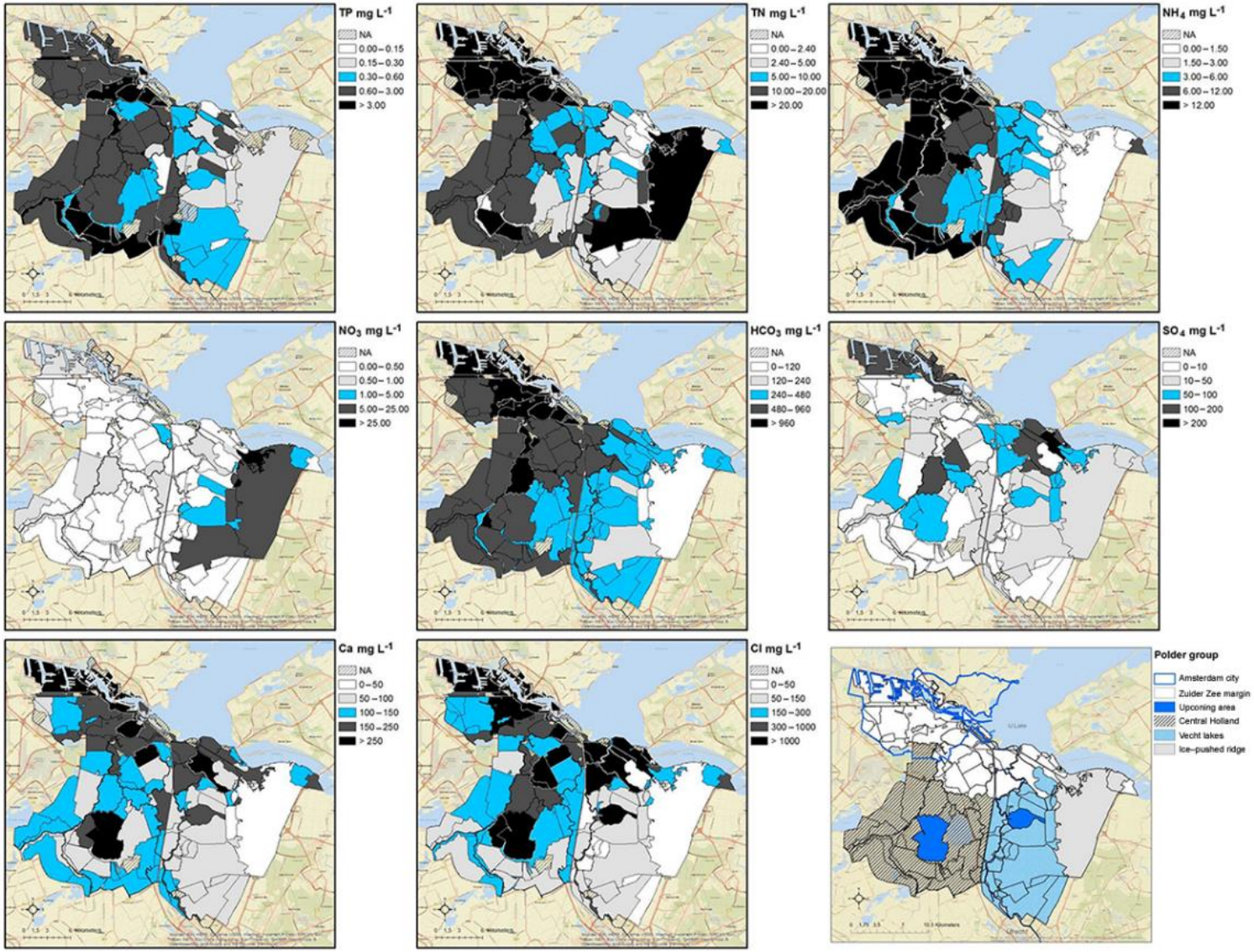

Figure 2.6 Average groundwater concentrations (mg L^{-1}) per polder.

Table 2.1 Coefficients of determination between groundwater quality and surface water quality

	TP GW	TN GW	NH_4 GW	NO_3 GW	HCO_3 GW	SO_4 GW	Ca GW	Cl GW	TP SW	TN SW	NH_4 SW	NO_3 SW	HCO_3 SW	SO_4 SW	Ca SW	Cl SW
TP $_{GW}$	1															
TN $_{GW}$	0.66	1														
NH_4 $_{GW}$	0.77	0.84	1													
NO_3 $_{GW}$				1												
HCO_3 $_{GW}$	0.68	0.63	0.82		1											
SO_4 $_{GW}$	-0.46			0.41		1										
Ca $_{GW}$					0.50		1									
Cl $_{GW}$					0.48	0.40	0.77	1								
TP $_{SW}$	0.49	0.51	0.60		0.64				1							
TN $_{SW}$	0.45		0.44		0.52				0.59	1						
NH_4 $_{SW}$			0.44		0.51				0.49	0.77	1					
NO_3 $_{SW}$										0.57		1				
HCO_3 $_{SW}$	0.57	0.55	0.64		0.68			0.41	0.63	0.47	0.67		1			
SO_4 $_{SW}$										0.57		0.50		1		
Ca $_{SW}$	0.59	0.54	0.63		0.71			0.41	0.55	0.56	0.64		0.88		1	
Cl $_{SW}$					0.47		0.47	0.69		0.47	0.51		0.52	0.49	0.55	1
N input kg ha^{-1} y^{-1}																
P input kg ha^{-1} y^{-1}																
Paved area %																
Elevation										-0.67	-0.59	-0.40	-0.48	-0.47	-0.57	
Seepage rate											0.48		0.45		0.46	
Surface water %																
Lutum %																
Humus %					0.50					0.46	0.40				0.41	0.48
Calcite %																

* Only absolute value of coefficients higher than or equal to 0.40 were shown in the table

TP sw: surface water TP concentration in mg L^{-1}

TP gw: groundwater TP concentration in mg L^{-1}

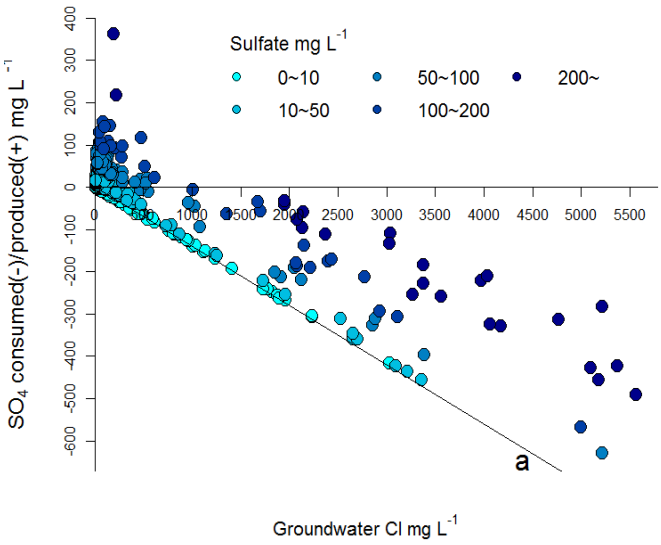

Figure 2.7 Calculated concentration of sulfate reacted versus groundwater chloride concentration. The black line indicates the fresh water – seawater mixing line where sulfate-reduction is complete.

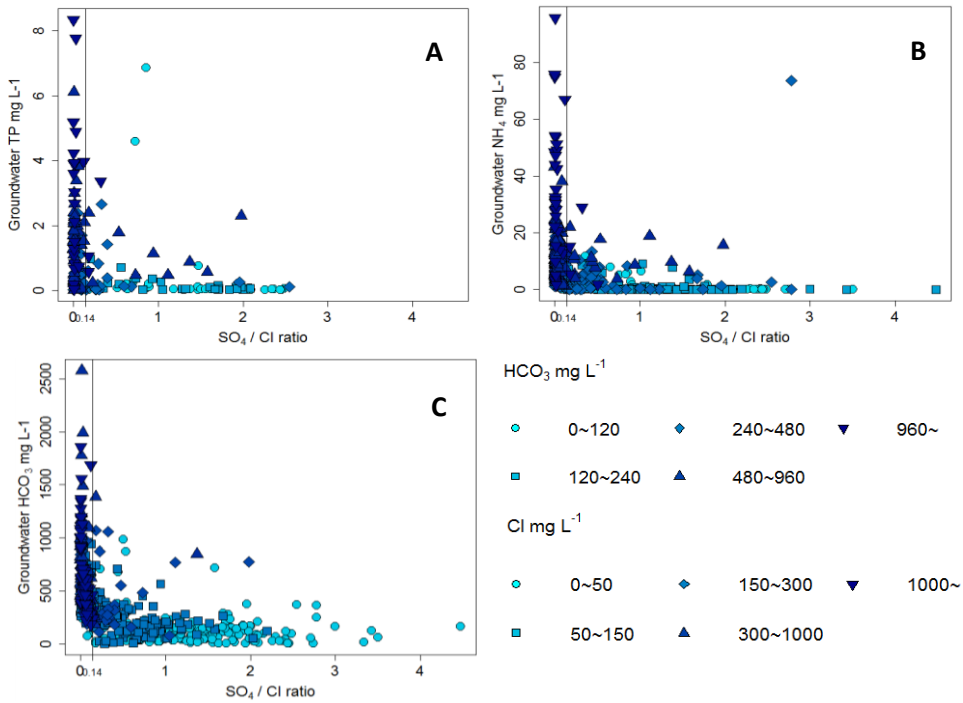

Figure 2.8 Groundwater nutrient (TP and NH_4) concentrations with sulfate reduction (mass ratio SO_4/Cl, samples with value below 0.14 are considered to be affected by sulfate reduction and above 0.14 indicates sulfate production by natural or artificial processes). The symbols in (A) and (B) are colored by HCO_3 concentration and in (C) by Cl concentration.

Cl, Ca, and HCO_3

In Fig.2.5, the Zuiderzee margin, where brackish groundwater is dominant, P25 and P75 of concentrations are between 290 and 2100 mg L^{-1} Cl, 100-300 mg L^{-1} Ca, and 400-1000 mg L^{-1} HCO_3. Relatively high concentrations of Cl, Ca and HCO_3 were also for the two deep polders Groot Mijdrecht (# 80) and Horstermeer (Upconing area) with known upconing of salt groundwater. The Central Holland area was dominated by fresh groundwater with low Cl and Ca concentrations, but with considerable amounts of HCO_3. Polders with relatively high chloride (>1000 mg L^{-1}) are distributed along the former Zuiderzee margin, plus the Upconing area which is two deep polders with known upconing of brackish water. Relative to the regions above, the Vecht lakes area and the Ice pushed ridge showed significantly less mineralized waters with lower HCO_3 and Cl concentrations. For example, the P75s of Cl in these two regions are below 150 mg L^{-1} and the P75s of HCO_3 below 350 mg L^{-1}. The groundwater HCO_3 concentrations (Fig.2.6) show an east-west increasing trend with highest concentrations in both the fresh and brackish areas west of the Amsterdam Rhine Canal.

SO_4 and SO_4/Cl

The Zuiderzee margin and the Upconing area showed large ranges of SO_4 concentrations (P25 and P75: 7-125 mg L^{-1} and 7-250 mg L^{-1}, respectively) with the SO_4/Cl mass ratios generally lower than the 0.14 ratio for diluted seawater. The polders in the eastern Zuiderzee margin showed the highest average SO_4 levels (Fig.2.6). The Central Holland area exhibited the lowest SO_4 concentrations with the smallest variability, with SO_4/Cl P75 typically lower than 0.14. However, some outliers in this region reached quite high sulfate concentration levels (>200 mg L^{-1}). The Vecht lakes and the Ice pushed ridge showed intermediate sulfate concentrations and typically have a SO_4/Cl ratio clearly above 0.14.

NH_4, TN, NO_3, and TP

The higher groundwater NH_4 and TP concentrations generally locate in the western part of the study area (Zuiderzee margin, Upconing area, and Central Holland regions). Median NH_4 concentrations in the Zuiderzee margin (6.4 mg L^{-1}) and Central Holland (10.6 mg L^{-1}) were far higher than in the Vecht lakes (2.1 mg L^{-1}) and Ice pushed ridge regions (0.07 mg L^{-1}). The same was observed for TP (0.7, 1.6, 0.2 and 0.06 mg P L^{-1}, respectively). Nutrient concentrations in the Upconing area (medians 5.7 mg NH_4 L^{-1} and 0.14 mg P L^{-1}) were relatively low compared with the groundwater in the Zuiderzee margin and Central Holland areas, although we consider the NH_4 concentration levels to be substantial given the surface water EQS of 2.4 mg N L^{-1}. TN showed the highest median concentration levels in the Zuiderzee margin and Central Holland regions, as well as in the Ice pushed ridge (7.3 mg N L^{-1}). The Ice pushed ridge region also showed the highest level of NO_3. In the latter region, nitrate is the main component of TN, while NH_4 is the main component in the other regions.

Groundwater quality varied from fresh, low mineralized in the eastern parts (Vecht lakes and Ice pushed ridge, Figure 2.4) towards brackish, highly mineralized and nutrient rich groundwater in the northwest (Zuiderzee margin and Central Holland, Fig.2.4). This relationship was further indicated by the strong correlations between Ca and Cl (Spearman R^2 0.77) and between HCO_3, TP and NH_4 (R^2 0.68-0.82) (Table 2.1, yellow part). The spatial Ca pattern corresponds largely with the Cl pattern (Fig.2.6), showing higher Ca concentrations in the brackish waters, which is related to the high Ca concentrations in (diluted) seawater (Section 2.4.1). The strong correlation between TN and NH_4 (R^2 0.81) showed the

dominance of NH_4 in TN, except in the suboxic groundwaters under the Ice pushed ridge where nitrate dominates TN. HCO_3, TP and NH_4 were all weakly negatively correlated with elevation, indicating that higher concentrations exist in the deeper polders which are more affected by brackish groundwater seepage. No significant correlation was found with agricultural N and P inputs, except for a negative correlation between groundwater TN concentrations and N input (Table S2.2, absolute value lower than 0.4). This suggests that non-agriculture sources of N dominate in most areas.

In the more mineralized groundwater systems, sulfate reduction is a potential cause of the significant relationship between HCO_3, TP, and NH_4. From using the SO_4/Cl ratio of the samples and comparing them with the SO_4/Cl ratio in seawater (Eq. 2.3), it appears that most of the brackish groundwater showed signs of sulfate reduction. Figure 2.7 shows that the amount of SO_4 consumed in the sulfate reduction process increased with the chloride concentration of the groundwater, and that sulfate reduction was complete only in part of the groundwaters. Note that groundwater below polders with excess SO_4 are all in water with Cl<1000 mg L^{-1}. It follows from Figure 2.8 that high HCO_3, TP, and NH_4 concentrations mostly occurred in groundwater with a SO_4/Cl ratio lower than 0.14, indicating sulfate reduction which induces the release of N and P from the mineralized organic matter in the subsurface and the production of alkalinity during that process. Therefore, these waters typically have increased HCO_3 concentrations above 480 mg L^{-1} (Fig.2.8A and 2.8B) and are often associated with brackish groundwater that once contained sulfate (Fig.2.8C: Cl>300 mg L^{-1}). The hypothetical chemical relation between sulfate reduction (SO_4 consumed) and HCO_3/NH_4/H_3PO_4 production from the mineralisation of organic matter can be found in the reaction equation below (Stuyfzand, 2006):

$$2SO_4^{2-} + 3.5CH_2O(NH_3)_x(H_3PO_4)_yI_zBr_a + Fe^{2+} \rightarrow FeS_2 + (2 + 3.5x)HCO_3^- + (1.5 - 3.5x)CO_2 + 3.5xNH_4^+ + 3.5yH_3PO_4 + zI^- + aBr^- \quad [1]$$

2.3.2 Spatial patterns and statistical analysis of surface water quality

Fig.2.9 and Fig.2.10 show the solute concentrations in the four regions: Zuiderzee margin, Upconing area, and Central Holland, and Vecht lakes. Due to insufficient surface water quality data, no results are shown for several polders in the Amsterdam city area (see Fig.2.4) and the Ice pushed ridge region. The first is related to the monitoring priorities of the Waternet water board, the latter is related to the almost absence of surface water in this region.

Cl, Ca, and HCO_3

Highest chloride levels (>300 mg L^{-1}) were found in the Upconing polders with brackish seepage and in a minority of the polders in the Zuiderzee margin and Central Holland regions (Fig.2.9 and 2.10). The high Ca and HCO_3 concentrations in these polders are also related to the occurrence of brackish water. However, most of the surface water in the Zuiderzee margin and the Central Holland area is fresh with relatively low Cl concentrations (Fig.2.10). The Vecht lakes area exhibits the most fresh and least mineralized surface water.

SO_4 and SO_4/Cl

The highest SO_4 concentration levels and SO_4/Cl mass ratios mostly occurred in the Central Holland area, especially the western part. The elevated SO_4 and SO_4/Cl ratios indicate the presence of sulfate sources other than (relict) seawater in this area, probably atmospheric deposition, agriculture and/or oxidation of pyrite exposed in the upper soils which developed in marine clay deposits and are denoted as "cat clays" (Wallenberg, 1975). In the Zuiderzee margin and the two upconing polders, the median SO_4 levels are 64 and 62 mg L^{-1}, respectively, and SO_4/Cl mass ratios of the two upconing polders are below 0.14. A generally lower SO_4 with SO_4/Cl ratios far exceeding the 0.14 were found in the Vecht lakes region.

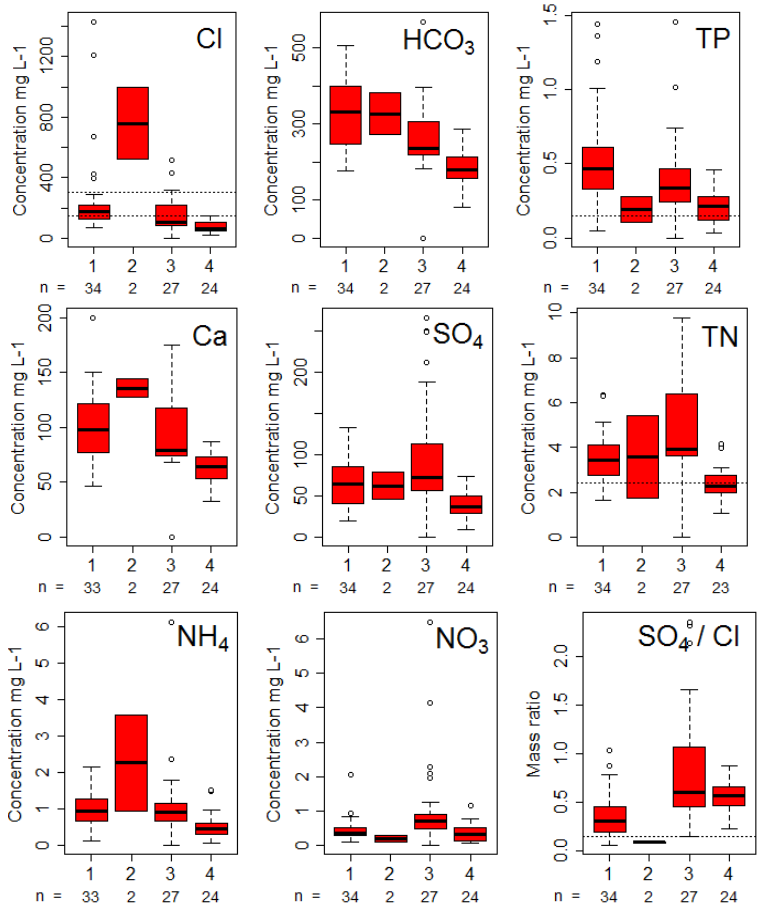

Figure 2.9 Spatial variation of surface water quality. 1-Zuiderzee margin, 2-Upconing area, 3-Central Holland, 4-Vecht lakes (5-Ice pushed ridge not shown due to insufficient data). n is the observation number of each group. The two horizontal dashed lines for Cl indicate fresh water (<150 mg L^{-1}) and brackish water (>300 mg L^{-1}), respectively. Dashed lines in TP and TN represent EQSs for TN (2.4 mg L^{-1}) and TP (0.15 mg L^{-1}). The dashed line in the SO_4/Cl plot indicates the mass ratio of 0.14 in seawater (<0.14 indicates sulfate reduction; >0.14 indicates additional sources of sulfate besides (diluted) seawater).

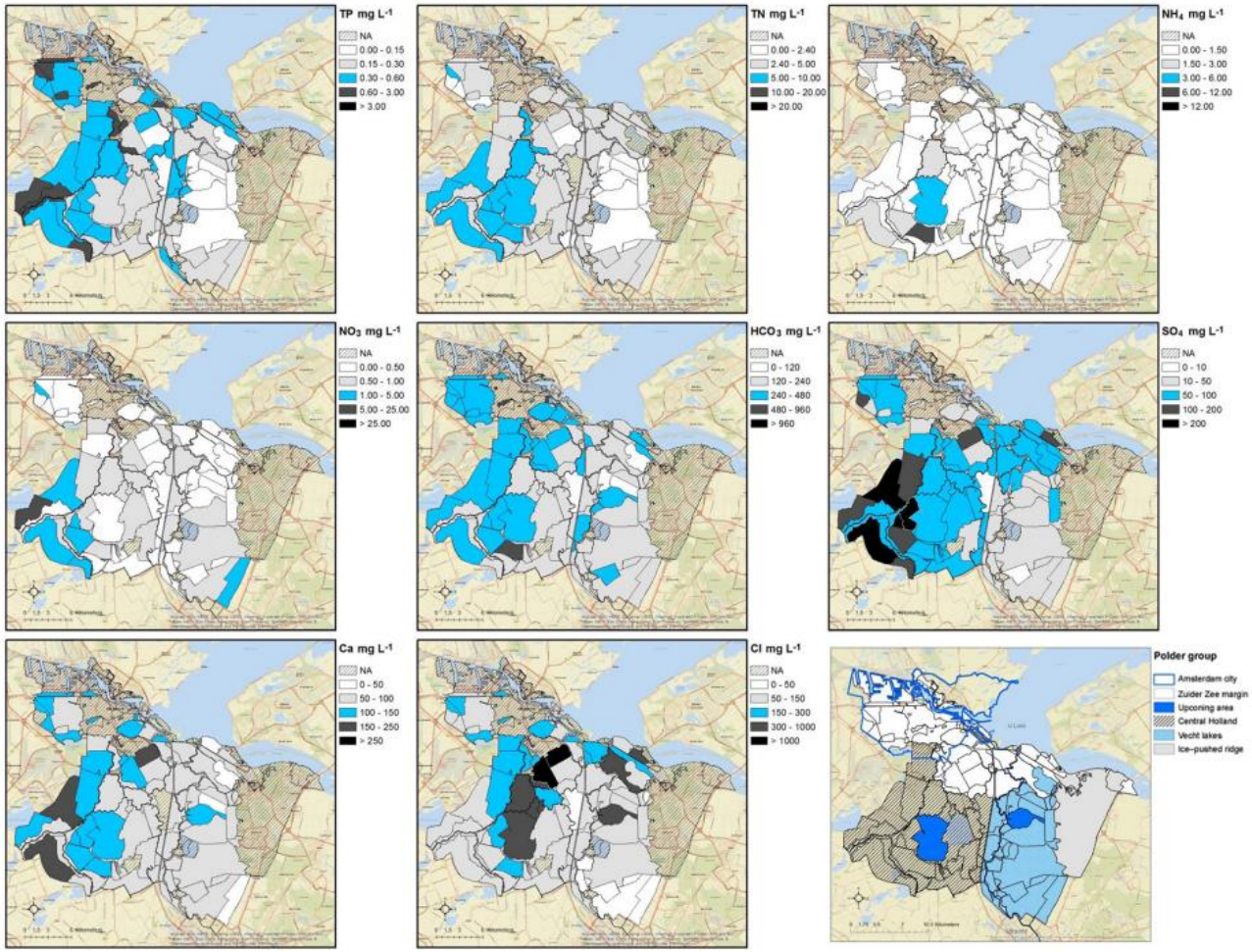

Figure 2.10 Discharge-normalized average concentrations (mg L^{-1}) per polder

TN, NH_4, NO_3, and TP

According to Fig.2.9 and Fig.2.10, surface water EQSs of TN (2.4 mg N L^{-1}) and TP (0.15 mg P L^{-1}) were exceeded in most polders of the study area. The outliers with even higher nutrient concentrations are mainly located in the west of the Central Holland region. P25 and P75 of TP and TN in the Zuiderzee margin and in Central Holland regions all significantly exceeded EQSs for surface water. In the two upconing polders, polder Groot Mijdrecht showed higher concentrations of TP and TN than polder Horstermeer (0.28 vs. 0.11 mg P L^{-1} and 5.4 vs. 1.8 mg N L^{-1}). Polders with concentrations below the EQSs were mainly situated in the Vecht lakes area where large open water areas exist. In this region, TP slightly exceeded the EQS with a median concentration of 0.22 mg L^{-1}, while the median TN concentration of 2.26 mg L^{-1} was just below the EQS. The concentrations of NO_3 and NH_4 in the Vecht lakes area were relatively low as well.

Similar to the results of groundwater, higher nutrient levels also exist in higher mineralized surface waters, which is also indicated by the correlation results (Table 2.1, blue part): Ca and HCO_3 are both correlated with NH_4 (Spearman R^2 are 0.64 and 0.67), TP (R^2 0.55, 0.62), and TN (R^2 0.57, 0.47). In surface water, Ca and HCO_3 had a significant correlation (R^2 0.88). This indicates that groundwater is the probable source of the water and nutrients in the surface water of the polders. This groundwater impact was further supported by the correlations between the following pairs of solutes in surface water: Cl with Ca (R^2 0.55), HCO_3 (R^2 0.52), SO_4 (R^2 0.49) and NH_4 (R^2 0.51), as well as SO_4 with TN (R^2 0.57) and NO_3 (R^2 0.50). A more direct indication for the groundwater impact is that NH_4, HCO_3 and Ca concentrations in surface water were positively related to the seepage rate. In a similar way, the groundwater impact is suggested by the negative correlations between elevation and the concentration levels of most surface water solutes (TN: R^2 -0.67, NH_4: R^2 -0.59, NO_3: R^2 -0.40, HCO_3: R^2 -0.48, SO_4: R^2 -0.47 and Ca: R^2 -0.57).

For the soil variables (lutum, humus and calcite), only humus showed correlations with TN, NH_4, Ca, and Cl in surface water (Table 2.1). Paved area percentage, surface water area percentage, calcite and clay percentages, and agricultural N and P inputs did not show absolute values of correlation coefficients above 0.4 with surface water quality, but a slight negative correlation was found between the agricultural N input and the normalized concentrations of HCO_3 in surface water (Table S2.2).

Surface water TN correlated more closely to NH_4 (0.77) than to NO_3 (0.57), which reflects that NH_4 is generally the main form of TN in the study area. This is especially true for the Zuiderzee margin, the Upconing area and the Central Holland area (Fig.2.9). The NO_3 and NH_4 contributions to TN are about equal in the Vecht lakes area. For the Ice pushed ridge (not shown in Fig.2.9 due to insufficient data), a dominance of NO_3 in surface water was expected as was the case in groundwater of this area. However, there is only limited amount of surface water that is draining the Ice pushed ridge directly.

2.3.3 Groundwater and surface water quality comparison

A common spatial pattern in surface and groundwater chemistry is that polders in the Zuiderzee margin area, the two upconing polders, and the Central Holland area suffer from a worse water quality situation than the polders in the Vecht lakes and Ice pushed ridge areas. However, compared with the underlying groundwater quality, surface water in the whole area has much lower chloride, bicarbonate, and nutrient

levels, but higher SO_4 concentrations (Fig.2.5 and Fig.2.9). The polders generally have much higher TP and TN concentrations in groundwater than in surface water. The groundwater nutrient concentrations exceeded the surface water EQSs in 93 % of the polders for TP, and in 91 % for TN. Polders with groundwater nutrient levels below the EQSs were mainly found near Lake IJssel. Especially the groundwater TN concentrations in the Ice pushed ridge severely exceeded surface water EQSs, which can be mainly attributed to the elevated NO_3 concentrations. For TP in groundwater, the Zuiderzee margin and Central Holland areas show more significant EQS exceedances compared to the Upconing area, Ice pushed ridge and the Vecht lakes area.

Table 2.1 shows that TP, NH_4, HCO_3, and Cl concentrations in groundwater correlate with the same components in surface water (R^2 0.49, 0.44, 0.68, and 0.69). In addition, HCO_3 in groundwater showed moderate correlations with nutrient concentrations in surface water (TP (R^2 0.64), TN (R^2 0.52), and NH_4 (R^2 0.51)). HCO_3 concentrations in surface water also correlated with nutrient concentrations in surface water (TP (R^2 0.62), TN (R^2 0.47), and NH_4 (R^2 0.67)). Based on these correlations, we selected groundwater parameters and landscape characteristics to be integrated in multiple linear regression models to predict concentrations of surface water components (Table 2.2). For most solutes (TP, NH_4, TN, HCO_3, and Cl, the R^2 of the regression models is around 0.5, which indicates that around 40 ~ 50% of the spatial variance in surface water can be explained by specific groundwater chemistry parameters, N agricultural input, seepage, and elevation and humus. For NO_3 and SO_4, the R^2 of the regression models (inverse with Elevation) are very low, 0.18 and 0.25, respectively. For all other parameters, the groundwater HCO_3 concentration was the best explaining variable for the surface water concentrations. The spatial variation in $HCO_{3\,SW}$ and Ca_{SW} were relatively well explained by only $HCO_{3\,GW}$ combined with Seepage/Elevation, respectively (Eq. 2.13 and Eq. 2.15).

The regression models were significantly improved by including groundwater concentrations of TP, NH_4, and Cl (Eq. 2.9, 11 and 2.16). For TN and NO_3, the R^2 also improved after adding N agricultural input. In regression models Eq. 2.10, 2.11, 2.12, 2.14, and 2.15, the elevation of the polders also explained part of the spatial variation in surface water concentrations. When only including polders with net groundwater seepage, the R^2 improved significantly for TP, NH_4 and HCO_3.

The results above strongly suggest that the groundwater composition puts limitations to the compliance of the receiving surface water towards the EQSs defined for N and P.

Table 2.2 Linear regression results of each surface water solute (Spearman)

	n_1	n_2	n_3	R^2	R^2 *with only seeping polders*	
TP_{SW}	+ $HCO_{3\,GW}$	+ NH_{4GW}		0.43	0.49	(2.9)
TN_{SW}	- Elevation	+ $HCO_{3\,GW}$	+ N_{input}	0.57	0.48	(2.10)
$NH_{4\,SW}$	- Elevation	+ $HCO_{3\,GW}$	+ Seepage	0.50	0.61	(2.11)
$NO_{3\,SW}$	- Elevation	+ N_{input}		0.18	0.23	(2.12)
$HCO_{3\,SW}$	+ $HCO_{3\,GW}$	+ Seepage	+ NH_{4GW}	0.57	0.70	(2.13)
$SO_{4\,SW}$	- Elevation	+ SO_{4GW}		0.25	0.22	(2.14)
Ca_{SW}	+ $HCO_{3\,GW}$	- Elevation	+ Seepage	0.65	0.63	(2.15)
Cl_{SW}	+ Cl_{GW}	+ $HCO_{3\,GW}$	+ P_{Humus}	0.57	0.51	(2.16)

* '+': positive relation, '-' negative relation
n_1: first variable, the most significant variable
$HCO_{3\,SW}$: surface water HCO_3 concentration in mg L^{-1}
Seepage: seepage rate in mm y^{-1}
$HCO_{3\,GW}$: groundwater HCO_3 concentration in mg L^{-1}
N_{input}: manure and fertilizer N input in kg ha^{-1} y^{-1}
Elevation: average polder elevation in m N.A.P
P_{Humus}: percentage of humus in the soil profile sample

2.3.4 Surface water solute redistribution

Figure 2.11 shows that the solute loads of polders to the boezem are relatively high in the Zuiderzee margin, the Upconing polders, and the Central Holland regions. The Vecht lakes area has large open water areas and showed the lowest loads to the boezem system. A clear similarity between the spatial patterns of the solute loads and the average seepage rate patterns was observed in Fig.2.3 and Fig.2.11. In general, polders with high seepage rates also discharge relatively high loads to the Boezem system. Some examples of polders with relatively high seepage rates are polder #119 (Bethunepolder, 13 mm d^{-1}), #79 (Horstermeer, 8.7 mm d^{-1}), #50 (Polder De Toekomst, 2.4 mm d^{-1}), #131 (Hilversumse Meent, 2.4 mm d^{-1}), #98 (Polder Wilnis-Veldzijde, 3.7 mm d^{-1}), #80 (Polder Groot Mijdrecht en Polder de Eerste Bedijking (oost), 5.0 mm d^{-1}), #74 (Polder de Nieuwe Bullewijk en Holendrechter- en Bullewijker Polder noord, 1.8 mm d^{-1}) and #75 (Bijlmer, 2.0 mm d^{-1}). The highest loads are discharged from the two upconing polders: Groot Mijdrecht (#80) and Horstermeer (#79).

The influence of the redistribution of the large water volumes and loads from deep polders was also observed in Fig.2.3 and Fig.2.11. Polders that receive inlet water from Groot Mijdrecht and Horstermeer (see section 2.2.1.1, Fig.2.3) showed relatively high solute loads, independent of their own seepage or infiltration fluxes. This especially holds for polders downstream of Groot Mijdrecht and Horstermeer, like polder #73 (Holendrechter- en Bullewijker Polder (zuid en west), -0.05), #74 (Polder de Nieuwe Bullewijk en Holendrechter- en Bullewijker Polder noord, 1.8 mm d^{-1}), #104 (Noorderpolder of Botshol (zuid en west), -1.4 mm d^{-1}), #105 (Noorderpolder of Botshol (Nellestein), -0.7 mm d^{-1}), #106 (Polder de Rondehoep, -1.1 mm d^{-1}), and polder #107 (Polder Waardassacker en Holendrecht, -0.15 mm d^{-1}).

The impact of this redistributed water on polder water chemistry is demonstrated by a simple water and solute mass balance calculation for the receiving polder Botshol (see paragraph 2.2.2.4). Fig.2.12 gives the chloride concentration results of both the 'evaporation' and the 'infiltration/outlet' models. Figure 2.12 shows that a very simple model can easily explain the peak Cl concentrations in the Polder Botshol to be the result of the inlet of water from the boezem and Groot Mijdrecht. The 'evaporation' model performs better in 2006 and 2008 and the 'infiltration/outlet' model in 2011 and 2012. Most of the time, the measured concentrations are between the calculated concentrations from both models. This aligns with the understanding that water leaves Botshol via a combination of evapotranspiration and other outflow routes, such as infiltration, leakage, and outlet.

2.4 Discussion

This study aimed at identifying the impact of groundwater on surface water quality in the polder catchments of the greater Amsterdam city area. According to the statistical analysis of data over five regions in the study area, a clear influence was identified. Solute concentrations in groundwater and surface water correlated well, although groundwater solute concentrations were generally much higher than normalized concentrations in surface water. The latter seems logical given the dilution of surface water by the precipitation surplus on an annual basis, with the annually discharged surface water being a mixture of seeping groundwater and precipitation. Moreover, similar spatial patterns in solute concentrations were found in groundwater and surface water. The findings on the dominance of groundwater inputs is also supported by the poor correlation with agricultural nutrients inputs, which are usually assumed to be a large source of N and P in surface water. Polders that are influenced by

groundwater seepage or by redistributed seepage water from nearby deep polders are at risk of non-compliance, as groundwater concentrations exceeded the TN and TP EQSs for surface water in more than 90% of the polders. Consequently, the groundwater nutrients input hinders achieving water quality targets in the surface water in those lowland landscapes.

2.4.1 Key hydro chemical processes

In general, the groundwater chemistry corresponds with the geological history of the study area. In the peat land polder catchments within the Dutch delta system of marine, peri-marine and fluvial unconsolidated deposits, abundant organic matter is present in the subsurface (e.g. Hijma, 2009). The presence of reactive organic matter in the shallow subsurface depletes the infiltrating groundwater from oxygen and nitrate, leading to an overall low redox potential in groundwater, which enables the further decomposition of organic matter downstream.

Our data strongly suggests that sulfate reduction, sometimes in combination with methanogenesis, is the main process releasing nutrients (N, P) and HCO_3 from the organic rich subsurface in the study area, especially in both the fresh and brackish groundwater of the Zuiderzee margin, the Upconing polders, and the Central Holland that are charactreized by low SO_4/Cl ratios (Table 2.1, Fig.2.8). The Holocene marine transgression undoubtedly influenced the chemistry of groundwater by salinizing processes that also increased sulfate availability derived from diluted sea water. Refreshing of the aquifers by infiltration of fresh water from rivers and rain in more elevated polders and lakes further influenced part of the groundwater. We examined the amount of freshening and salinization using the exchange Na (Na_{ex}) and investigated how this process may have influenced the release of P as was suggested by Griffioen et al. (2004). Figure S2.2 shows that high P (and HCO_3, not shown) does occur in both refreshing water (Na_{ex} > 1) and in salinizing water (Na_{ex} <-1), but mainly when the SO_4/Cl ratio is below 0.14. Therefore, we infer that sulfate reduction/organic matter decomposition is the prime process in releasing P, and is more discriminating high P than cation exchange processes. There is a high probability for sulfate reduction dominated polder catchments to have very high HCO_3 concentration in groundwater according to Eq. [1]. In our study area, high HCO_3 concentration levels in both groundwater and surface water were mainly present in areas with marine sediments that contain shell fragments and organic matter. The base level groundwater alkalinity from the dissolution of shell fragments and carbonate minerals is further increased by the organic matter decomposition in the subsurface. This observation confirms the earlier findings of Griffioen et al. (2013) who highlighted the relation between the nutrient concentrations and pCO_2 in these marine sediments. The main chemical reactions involved are listed in Table 2.3.

The seepage of the alkalized groundwater increases alkalinity of the surface water, which is indicated by the high correlation between groundwater and surface water HCO_3, and with Ca in surface water (Table 2.1). Subsurface organic matter mineralization by processes like sulfate reduction and methanogenesis (Chapelle et al., 1987; Griffioen et al., 2013) (Table 2.3 [2], [6]), is a probable major reason for enhanced surface water HCO_3 in polders with brackish groundwater, like the polders in the Zuiderzee margin and the Upconing polders (Fig.2.8).

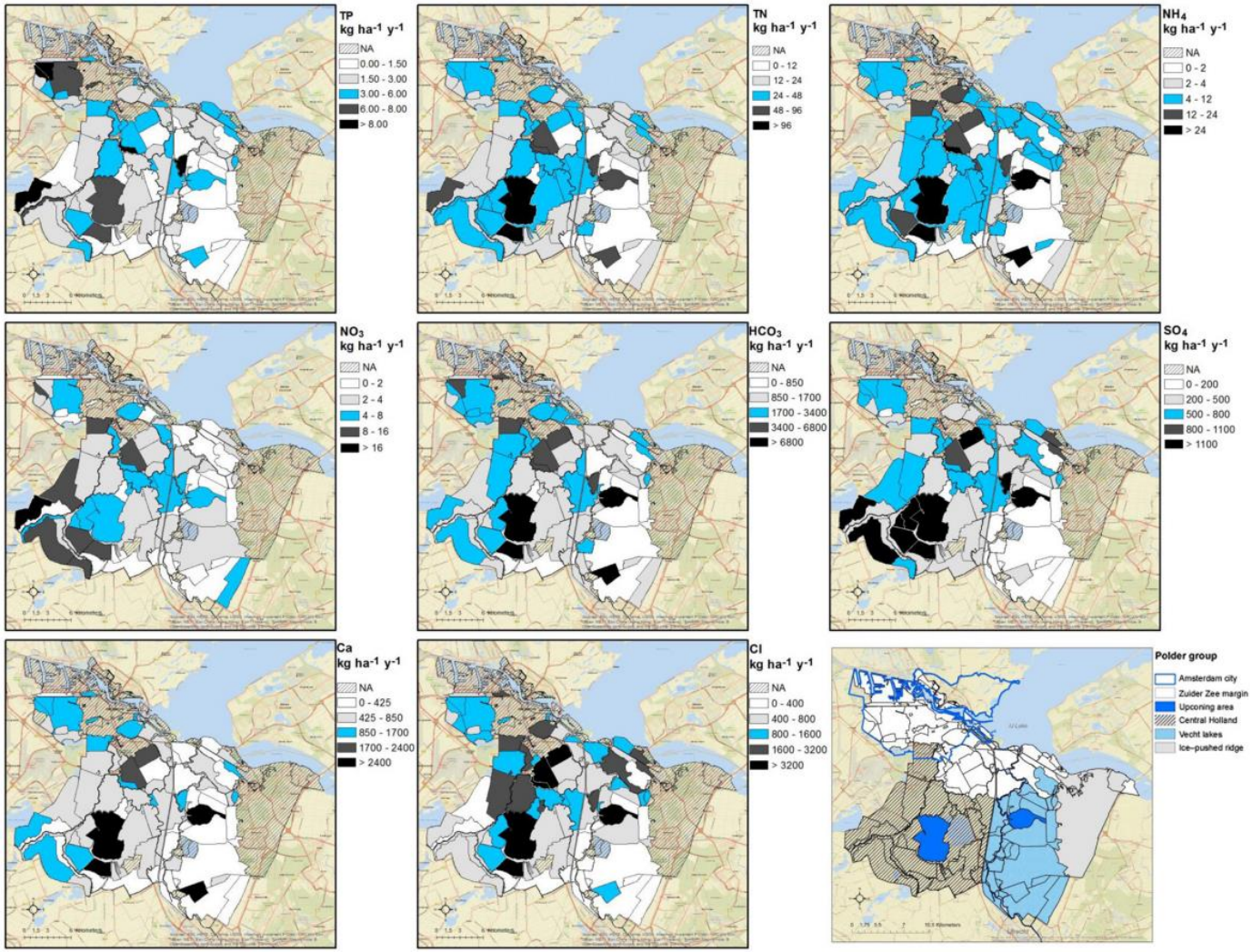

Figure 2.11 Surface water solute loads (average of 2010 to 2013) distribution maps in kg $ha^{-1}y^{-1}$

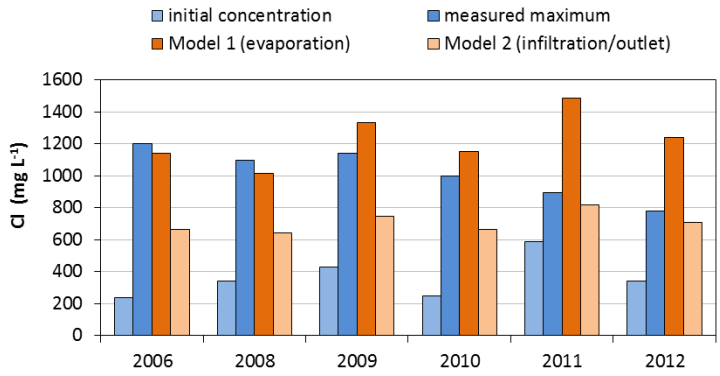

Figure 2.12 Summary of the water and chloride balance for polder Botshol; the graph shows (1) the initial Cl before the water inlet season (light blue), (2) the resulting Cl peak in Botshol after some months of inlet (dark blue), and (3) the results of the two models (model 1 dark orange, model 2 light orange).

Table 2.3 Main hydrogeochemical reactions in the study area

Process		Reactions	No
Organic matter decomposition		$CH_2O\ N_xP_y \rightarrow xN + yP + HCO_3^- +$ other components	[2]
		$CH_2O\ N_xP_y + O_2 \rightarrow CO_2 + H_2O + xN + yP$	[3]
		$5CH_2O\ N_xP_y + 4NO_3^- \rightarrow 2N_2 + CO_2 + 4HCO_3^- + 3H_2O + 5xN + 5yP$	[4]
		$2CH_2O\ N_xP_y + SO_4^{2-} \rightarrow H_2S + 2HCO_3^- + 2xN + 2yP$	[5]
Pyrite oxidation		$2CH_2O\ N_xP_y \rightarrow CH_4 + CO_2 + 2xN + 2yP$	[6]
		$2FeS_2 + 7O_2 + 2H_2O \rightarrow 2Fe^{2+} + 4SO_4^{2-} + 4H^+$	[7]
		$5FeS_2 + 14NO_3^- + 4H^+ \rightarrow 5Fe^{2+} + 10SO_4^{2-} + 7N_2 + 2H_2O$	[8]
Calcite dissolution	Closed system	$CaCO_3 + H_2O \leftrightarrow Ca^{2+} + HCO_3^- + OH^-$	[9]
	Open system	$CaCO_3 + CO_2 + H_2O \leftrightarrow Ca^{2+} + 2HCO_3^-$	[10]

In the urban area of Amsterdam sand suppletion, which varies greatly in thickness and chemical composition, is another source of alkalinity. Some of the sands contain shell fragments because of their marine origin. However, little is known about the distribution of these calcite-rich sands. The poorly registered spatial distribution and sources of the supplied calcite-rich sands might complicate the assessment of their impact on urban polder water quality.

Sulfate concentrations are higher in the receiving surface water than in the groundwater. We ascribe the sulfate surpluses (Fig.2.7) to additional sources affecting the surface water, including atmospheric deposition, agricultural inputs, sewer leakage (Ellis, et al., 2005), storm runoff, and/or the oxidation of pyrite (FeS_2). Pyrite is ubiquitously present in this area (Griffioen et al., 2013) and oxidizes in the topsoil, where either O_2 or NO_3 can act as electron acceptor (Wallenburg, 1975). We suggest that sulfate concentrations are especially high in polders where shallow groundwater flow is enhanced by the presence of tile drains in clay rich polders that needed this drainage system to prevent water tables rising into the root zone in wet periods. Tile drain flow can bring the released SO_4 to the surface water. For urban polders with high SO_4 concentrations, like the Zuiderzee margin region polders, sewer system leakage may be an additional source of SO_4. Aging and faulty connections of pipes may result in a leakage of water with high SO_4 and nutrient concentrations.

2.4.2 Groundwater contribution to surface water composition

The groundwater in the upper 50 m of the subsurface of the study area is an important source of nutrients in the study area's surface waters (Delsman, 2015). Brackish groundwater especially seeps up into the polders of the Zuiderzee margin region and into the Upconing area. The seepage of paleo-marine, brackish groundwater is driven by the low surface water levels after the lake reclamation and the drainage via pumping stations. De Louw et al. (2010) reported that this groundwater seepage predominantly takes place via concentrated boils through the clay and peat cover layer.

The excess water in the Upconing area is re-used as inlet water for several downstream polder catchments, which extends the impact of the brackish, alkaline, and nutrient rich groundwater to a larger scale. The water redistribution disturbs the 'natural' surface water quality patterns and local groundwater impact in the receiving polders, such as polder Botshol. The redistributed water largely infiltrates and returns with variable travel times via the groundwater system back towards the deep upconing polders.

Groundwater seepage in our study area leads to eutrophication and redistributing the discharge from some deep polders further spreads the nutrients into the whole water system. Similar patterns are expected to exist in other lowland areas, which are highly manipulated by human activities. Typical delta areas where subsurface processes are expected to release nutrients from reactive organic matter and peat in the subsurface are the Mekong delta (Minderhoud et al., 2017), the Mississippi delta (Törnqvist et al., 2008) and the Sacramento-San Joaquin delta (Drexler et al., 2009). In many of these areas the water management shows resemblance to the Dutch situation. However, the large amount of groundwater quality and surface water quality data that was available in our study area is unique. Still, signals of groundwater influence on nutrient concentrations were reported from eastern England (pers. comm. M.E. Stuart, British Geological Survey) and from the lowland parts of Denmark (Kronvang et al. 2013).

2.4.3 Other sources of nutrients

Besides the contribution from nutrient rich groundwater seepage, this study indicated that there are other possible sources of nutrients in the study area. In agricultural lands, a part of the applied nutrients is typically lost towards the surface water via drainage and runoff. The high groundwater NO_3 concentrations in the Ice pushed ridge are caused by the infiltration of agricultural water (Schot et al., 1992b). The high nitrate loads and concentrations in surface water and groundwater of the polders in the southeast (e.g. # 122 (Muyeveld), # 140 ('t Gooi)) originate from agricultural activities in surrounding polders.

In the urban polders within the Amsterdam city that have no significant seepage (average seepage $\leq$ 0), TP and TN EQSs are frequently exceeded because of intensive human activities such as application of fertilizer, feeding ducks and fish, and point emissions like sewer overflow leakage from the sewer system (pers. Comm. Waternet).

In the study area, the most intensively urbanized polders are mainly infiltrating and are more affected by inlet water containing high Cl and HCO_3 concentrations than by groundwater. For deep urban polders, the situation is different. In these polders, the influences of typical urbanization related water quality issues are masked by the large impact of brackish, nutrient rich groundwater exfiltration.

Although land use was incorporated in variables like paved area percentage and N and P inputs, (as well as agricultural land percentage, shown in Supplement Information), land use seems not be the dominant landscape characteristic that governs the spatial patterns in polder surface water quality. Urban water quality is determined by multiple factors, as was also concluded by several other studies (Göbel et al., 2007; Vermonden et al., 2009). However, a better measurement method or classification of paved area percentage may improve the explanatory power of this variable (Brabec et al., 2002).

The Vecht lakes polders with high surface water area percentages, representing lakes that are mainly used for recreation purposes, showed relatively low solute concentrations and loads in surface water (Fig.2.10 and Fig.2.11). In our study area, many lakes and polders with large surface water areas show large infiltration rates due to their elevation relative to other polders (Vermaat et al., 2010). Moreover, some of these lakes are replenished by inlet water that has passed a phosphate purification unit. In addition, the large open water area retains nutrient transport due to long residence times and ample opportunities for chemical and biological transformation processes like denitrification, adsorption, and plant uptake.

2.4.4 Uncertainties

Due to the disturbance of urban constructions, combined with redistribution of water through artificial drainage corridors, water flow in lowland urban areas is more complex than in rural or non-low-lying and freely draining catchments. Natural patterns of water chemistry might be significantly disturbed and hydrochemical processes are masked. The understanding of urban water quality patterns might improve if the monitoring program would be extended with tracers that are typical for specific sources, such as sewage leakage or urban runoff. Most solutes that are currently measured can originate from various anthropogenic and natural sources.

In the statistical analysis, for each pair of variables, only polders with complete data were taken into account, which could result in a loss of information. Seepage data was simulated by a group of models of which the results may deviate from the hard to measure actual seepage. We used averages of groundwater concentrations and soil properties, which caused a loss of information on the spatial variation within the polders. The interpolation of groundwater quality data also added uncertainty, for example hidden correlations for groundwater parameters. The calculation of the agricultural N and P inputs may also differ from the actual inputs due to errors in the nutrient book keeping and model uncertainties. In addition, differences in sampling methods and analytical procedures between groundwater and surface water quality monitoring programs may add uncertainties. These uncertainties may all have influenced the data characteristics apart from the uncertainties in the concentration measurements caused by the sampling, transport, and analytical procedures.

2.4.5 Perspectives

In future studies, urban lowland catchments with and without seepage could be studied separately and more detailed land use or paved area categories could be included. The drainage and/or leakage from sewage systems and the drainage via tube drains should be taken into consideration. Drainage systems can provide a short-cut for solute transport towards surface water (Rozemeijer and Broers, 2007), leading to higher solute concentrations in surface water. High groundwater levels may induce groundwater discharge via the sewage or drainage systems (Ellis, 2005). In addition, studying the

temporal variation of surface water quality will give more insights into how the groundwater impact on surface water quality functions, as well as on solutes transport and pathways in urban hydrological systems. A detailed monitoring network in several urban polder catchments, which is anticipated as further work, could yield a more complete insight into water and contaminant flow routes and their effects on surface water solute concentrations and loads.

To the water management scenarios, as our study showed that the groundwater nutrient loading towards surface water dominates, reducing the amounts of agricultural nutrient inputs might not contribute enough in improving the water quality. This certainly holds for urban areas where agricultural inputs are absent (see Fig.S2.3). Given the large loads of N and P that originate from one large polder with upconing brackish groundwater - the Groot Mijdrecht polder - one of the solutions proposed in The Netherlands was to turn this area back into a fresh water lake. By doing so, the seepage of nutrient rich groundwater would stop as the higher water levels would lead to neutral or even infiltrating conditions. However, this proposal led to a lot of protest among the municipalities and farming communities in the polder and was not considered feasible given the economic values that were involved. This example shows that the reclamation of swamps and lakes for urbanisation or agriculture can lead increased nutrient loads to surface waters in the surroundings which are hard to mitigate. This scenario has wider implications for water management in other urbanising lowland areas around the world.

2.5 Conclusion

In this paper, a clear groundwater impact on surface water quality was identified for the greater Amsterdam area. It was concluded that this groundwater seepage significantly impacts surface water quality in the polder catchments by introducing brackish, alkaline, and nutrient rich water. In general, nutrient concentrations in groundwater were much higher than in surface water and often exceeded surface water Environmental Quality Standards (EQSs) (in 93 % of the polders with available data for TP and in 91 % for TN) which indicates that groundwater is a large potential source of nutrients in surface water. Our results strongly suggest that organic matter mineralization is a major source of nutrients in lowland deltas where water levels are lowered to enable urbanisation and agricultural land use. High correlations (R^2 up to 0.88) between solutes in groundwater and surface water confirmed the effects of surface water-groundwater interaction on surface water quality. Especially in seepage polders, groundwater is a major source of Cl, HCO_3, Ca and the nutrients N and P, leading to general exceedances of EQSs for N and P in surface waters. The discharge and redistribution of nutrient rich water from reclaimed lakes and swamps enhances eutrophication in downstream water resources and is hard to mitigate. Surface water quality in the Amsterdam urban area is also influenced by groundwater seepage, but other anthropogenic sources, such as leaking and overflowing sewers might amplify the eutrophication problems.

Supplementary Information

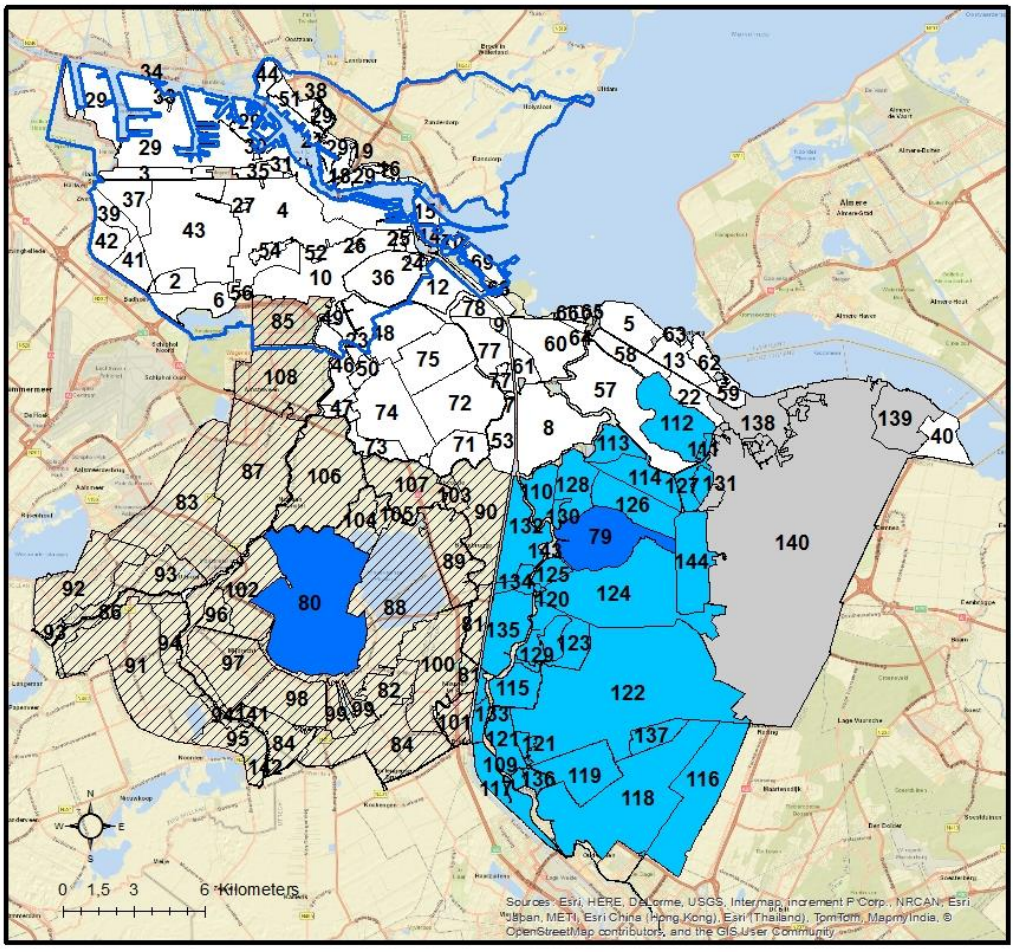

Figure S2.1 Polders, boezems of the research area and the groups they belong. The numbers given represent the numbers in Table S2.1, in which the full names of the polders are given. Polder amounts of each group are: Zuiderzee margin (78), Upconing area (2), Central Holland (28), Vecht lakes (30) and Ice pushed ridge (3).

Table S2.1 List of all polders and boezems in the study area. Numbers correspond to the numbers in Figure S1.

ID	Polder Names
1	Westerpark
2	Nieuw-Sloten
3	De Lange Bretten
4	Stadsboezem Amsterdam
5	Noordpolder beoosten Muiden
6	Riekerpolder
7	Aetsveldse Polder west (Driemond)
8	Aetsveldse Polder Oost
9	Gemeenschapspolder West (Betlem)
10	Boezem Amstelland-West
11	Atekpolder
12	Diemerpolder
13	B.O.B.M.-polder en Buitendijken tussen Muiderberg en Naarden
14	Eiland Zeeburg (oost)
15	Eiland Zeeburg
16	W.H. Vliegenbos
17	Polder Bernard
18	Florapark (zuid)
19	Forapark (noord)
20	Buiksloterdijk
21	Krasseurstraat
22	Keverdijkse Overscheense Polder
23	Venserpolder (volkstuinparken Nieuw Vredelust, Ons Lustoord en Dijkzicht)
24	Watergraafsmeer (Anna's Hoeve)
25	Flevopark
26	Oosterpark
27	Erasmuspark
28	Begraafplaats Vredenhof
29	Noordzeekanaal/IJ/Amsterdamrijnkanaalboezem
30	Sportpark Transformatorweg
31	Overbraker Binnenpolder (Zeeheldenbuurt)
32	Westelijk Havengebied (Hemspoorlijn)
33	Westelijk Havengebied (Sicilieweg/Capriweg)
34	Westelijk Havengebied (noord)
35	Overbraker Binnenpolder
36	Watergraafsmeer
37	Osdorperbinnenpolder
38	Sportpark Tuindorp Oostzaan
39	Osdorperbovenpolder
40	De Gooise Zomerkade
41	Middelveldse Akerpolder
42	Lutkemeerpolder
43	Sloterbinnen en Middelveldsepolder
44	Noorder IJ plas
45	Buiksloterweg
46	Duivendrechtsepolder noord en midden
47	Duivendrechtsepolder (zuid)

48	Venserpolder
49	Venserpolder (volkstuinpark Amstelglorie)
50	Polder De Toekomst
51	Noorder IJ Polder
52	Sarphatipark
53	Aetsveldse Polder west
54	Vondelpark
55	BP Huis Te Vraag
56	SP Zuid
57	Nieuwe Keverdijksche Polder en Hilversumse Bovenmeent
58	Zuidpolder beoosten Muiden
59	Buitendijken ten Noorden van Naarden
60	Bloemendalerpolder en Gemeenschapspolder Oost
61	Gemeenschapspolder zuid-oost
62	Buitendijksgebied Naarden en Muiderberg
63	Buitendijks gebied Muiderberg
64	Bloemendalerpolder
65	Noorder- of Rietpolder (oost)
66	Noorder- of Rietpolder (midden)
67	Noorder- of Rietpolder (west)
68	Over-Diemen
69	Haveneiland en Rieteiland
70	Steigereiland
71	Broekzijdse Polder
72	Zuid Bijlmer
73	Holendrechter- en Bullewijker Polder (zuid en west)
74	Polder de Nieuwe Bullewijk en Holendrechter- en Bullewijker Polder noord
75	Bijlmer
76	Gemeenschapspolder West (Tuincomplex Linnaeus)
77	Gemeenschapspolder West
78	Overdiemerpolder
79	Horstermeerpolder en Meeruiterdijksche Polder
80	Polder Groot Mijdrecht en Polder de Eerste Bedijking (oost)
81	Holland, Sticht, en Voorburg West en Polder het Honderd West
82	Veldhuiswetering
83	Noorder Legmeerpolder
84	Groot Wilnis-Vinkeveen (zuid) en Polder Groot en Klein Oud-Aa
85	Binnendijkse Buitenvelderse Polder
86	Buitendijkse Oosterpolder, Buitenwesterpolder en Blokland (noord)
87	Bovenkerkerpolder
88	Polder Groot Wilnis Vinkeveen
89	Baambrugge Westzijds
90	Baambrugge Oostzijds
91	Polder Zevenhoven
92	Zuider Legmeerpolder
93	Uithoornsche Polder
94	Blokland en Noordse Buurt (bovenland)
95	Noordse Buurt en Westveense Polder
96	Polder deTweede Bedijking

97	Polder de Derde Bedijking
98	Polder Wilnis-Veldzijde
99	Polder Groot Wilnis-Vinkeveen (midden)
100	Polder Oukoop en Polder Groot Wilnis-Vinkeveen (oost)
101	Polder Breukelerwaard West
102	Polder de Eerste Bedijking (west)
103	Baambrugge Oostzijds (west)
104	Noorderpolder of Botshol (zuid en west)
105	Noorderpolder of Botshol (Nellestein)
106	Polder de Rondehoep
107	Polder Waardassacker en Holendrecht
108	Middelpolder onder Amstelveen
109	Gansenhoef west
110	Horn- en Kuyerpolder
111	Meerlanden
112	Naardermeer
113	Heintjesrak- en Broekerpolder
114	Hollandsch Ankeveensche Polder
115	Polder Mijnden
116	Polder Achtienhoven
117	Polder Nijenrode
118	Polder Maarsseveen-Westbroek
119	Bethunepolder
120	Vreeland (oost)
121	Polder Breukelen-Proostdij
122	Muyeveld
123	Loenderveen
124	Polder Kortenhoef
125	Polder Dorssewaard
126	Stichtsch Ankeveensche Polder
127	Hilversumse Ondermeent
128	Spiegelpolder
129	Loenderveen (GWA)
130	Blijkpolder
131	Hilversumse Meent
132	Hoeker- en Garstenpolder
133	Breukelen Noord
134	Holland, Sticht, Voorburg oost (noord)
135	Holland, Sticht, Voorburg oost, Polder het Honderd oost en Polder Breukelerwaard oost
136	Gansenhoef oost
137	Oostelijke Binnenpolder van Tienhoven
138	`s-Gravelandsche vaartboezem
139	Huizen
140	't Gooi
141	Hoogwaterzone Amstelkade P1
142	Hoogwaterzone Amstelkade P2
143	Vechtboezem
144	's-Gravelandsche Polder

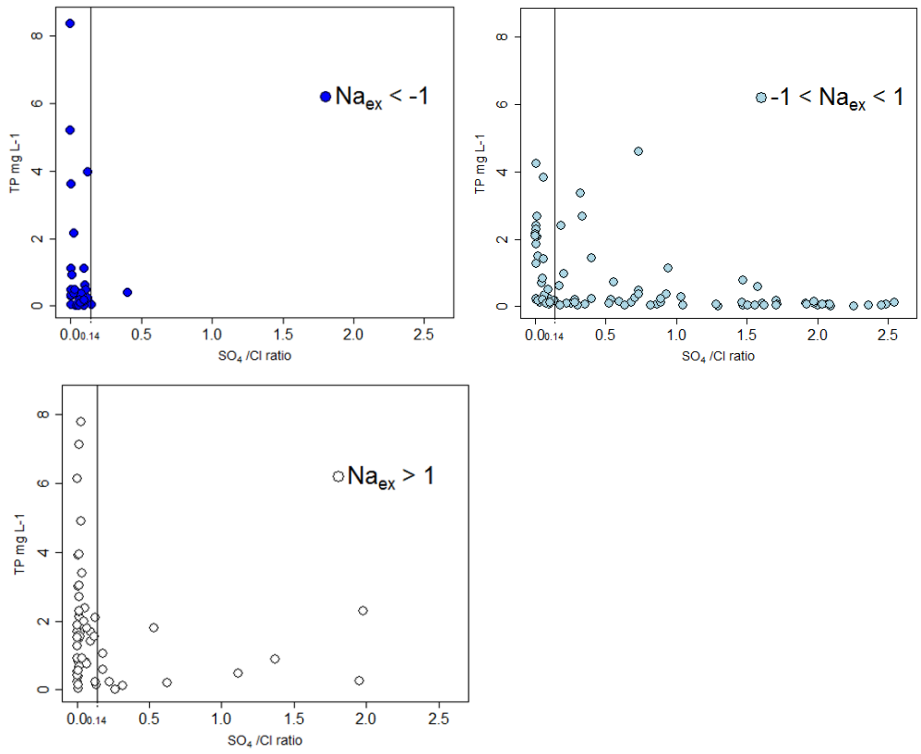

Figure S2.2 Total phosphorus (TP) concentration against SO_4:Cl, distinguished by Na exchange (freshening: Na_{ex} > 1, not defined: Na_{ex} between -1 and 1, and salinizing: Na_{ex} < -1)

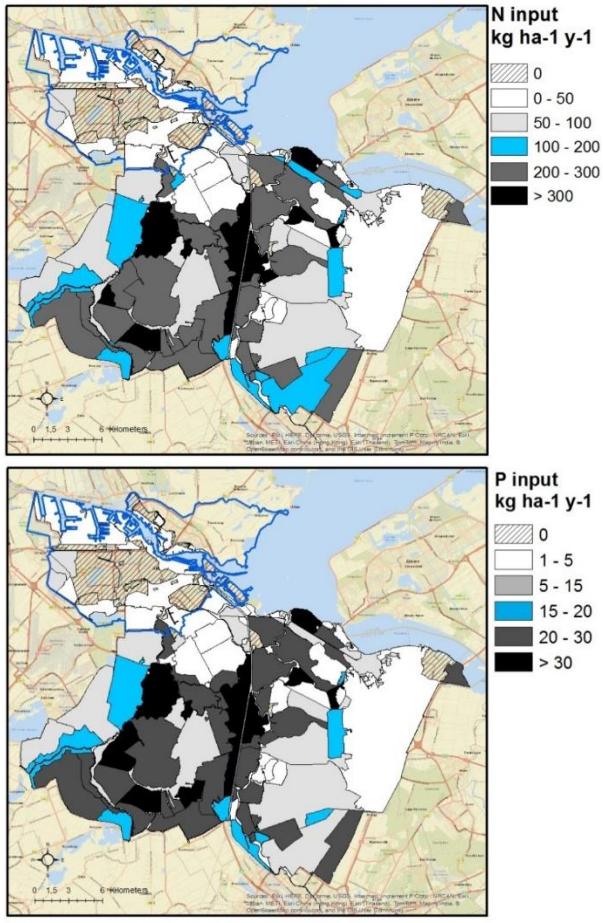

Figure S2.3 Spatial distribution of N and P inputs from agricultural land use (2011) in kg ha^{-1} y^{-1}.

Figure S2.3 shows the spatial distribution of N and P agricultural input (kg ha^{-1} y^{-1}) in the study area. Similar to the N and P agricultural input, agricultural land percentage shows no correlation with other variables (absolute values lower than 0.4) except with N and P inputs (0.99) (Table S2.2). This high correlation with agriculture land percentage suggests that the N and P inputs do not vary much between different types of agriculture, which may be caused by the maximum application rates as defined in the Dutch Manure Legislation. As shown in Fig.S2.3, nutrient inputs from agriculture mainly concentrate in the Central Holland and the Vecht lakes area. The values in most cases are much higher than the annual load per area in surface water (Fig.2.11) as most of the agricultural inputs are taken up by the crops and removed from the system. However, in the urban areas, especially the city of Amsterdam, high concentrations of N and P appear in groundwater and surface water whereas the agricultural inputs in those areas are minimal (Fig.S2.3). And their surface water N and P load per area are higher than agricultural N and P inputs as showed in Table S2.3.

Table S2.2 Coefficients of determination between N and P input with groundwater and surface water quality and landscape variables

	N input kg ha^{-1} y^{-1}	P input kg ha^{-1} y^{-1}		N input kg ha^{-1} y^{-1}	P input kg ha^{-1} y^{-1}		N input kg ha^{-1} y^{-1}	P input kg ha^{-1} y^{-1}
TP_{SW}	-0.12	-0.11	TP_{GW}	-0.15	-0.14	Paved area %	-0.22	-0.23
TN_{SW}	0.18	0.21	TN_{GW}	-0.33	-0.32	Elevation	-0.15	-0.18
$NH_{4\,SW}$	-0.03	0.00	$NH_{4\,GW}$	-0.24	-0.23	Seepage rate	0.02	0.03
$NO_{3\,SW}$	0.25	0.26	$NO_{3\,GW}$	-0.19	-0.20	Surface water %	-0.04	-0.04
$HCO_{3\,SW}$	-0.32	-0.31	$HCO_{3\,GW}$	-0.24	-0.23	Lutum %	0.24	0.23
$SO_{4\,SW}$	0.25	0.27	$SO_{4\,GW}$	0.10	0.09	Humus %	-0.18	-0.15
Ca_{SW}	-0.26	-0.25	Ca_{GW}	-0.10	-0.10	Calcite %	0.09	0.06
Cl_{SW}	-0.19	-0.18	Cl_{GW}	-0.15	-0.15	Agricultural land %	0.99	0.99

Table S2.3 Polders with surface water N and P load per area higher than agricultural N and P inputs

Polder ID	Group	Name	Landscape variables		P	N
			Paved area %	Agricultural land %		
2	1	Nieuw-Sloten	45	0	√	√
3	1	De Lange Bretten	8	11	√	√
6	1	Riekerpolder	36	7	√	
25	1	Flevopark	0	0	√	√
26	1	Oosterpark	0	0	√	√
27	1	Erasmuspark	0	0	√	√
35	1	Overbraker Binnenpolder	36	1	√	√
36	1	Watergraafsmeer	42	0	√	√
37	1	Osdorperbinnenpolder	12	24	√	
39	1	Osdorperbovenpolder	20	24	√	
41	1	Middelveldse Akerpolder	31	1	√	√
43	1	Sloterbinnen en Middelveldsepolder	44	0	√	√
52	1	Sarphatipark	0	0	√	√
54	1	Vondelpark	0	0	√	√
61	1	Gemeenschapspolder zuid-oost	65	0	√	√
74	1	Polder de Nieuwe Bullewijk en Holendrechter- en Bullewijker Polder noord	7	5	√	√
75	1	Bijlmer	37	1	√	√
85	3	Binnendijkse Buitenvelderse Polder	63	0	√	√
92	3	Zuider Legmeerpolder	38	25	√	√
130	4	Blijkpolder	51	0	√	√
131	4	Hilversumse Meent	45	10	√	

Table S2.4 Database description

Variables	Sources	Description	Processing
Discharge	Waternet database	Daily measurements of 2006-2013	Averages of all pumps in each polder
Surface water quality (TN, NO_3, NH_4, SO_4, TP, Ca, HCO_3, and Cl mg L^{-1})		Monthly measurement of 2006-2013; Measured upstream of the polder pumps.	Converted to daily time series by assuming daily values equalled to the monthly measurement in each month; Assigned zero to concentrations below detection limits; Took averages over 2006-2013.
Groundwater quality (TN. NO_3, NH_4, SO_4, TP, Ca, HCO_3, and Cl mg L^{-1})	TNO DINO database; Province of Noord-Holland database; "NH_ZH" database	Measurements from 1910 to 2013; Depth from -402.72 m to 40 m	Selected filters located higher than -50 m; Took averages of all screens at one position of all dates; Took averages of monitoring wells located in the same polder to represent the condition of the whole polder.
Agricultural N and P input kg $ha^{-1}y^{-1}$	Book keeping data for nutrient fate; transport model calculations using INITIATOR (De Vries, et al., 2003).	N and P input per area (kg $ha^{-1}y^{-1}$) from manure and fertilizer in each agriculture parcel (15242 parcels) in 2011;	Calculated the area of each parcel in ArcGIS; Calculated a total input (kg) of N and P to each agriculture parcel; Took a sum of all parcels in each polder; N and P input = total input from agriculture (*kg*)/ *total* polder area (*ha*).
Seepage rate mm d^{-1}	Waternet database	Modeling results from groundwater models	An average seepage rate was calculated and was assumed to be constant all the time.
Surface water area percent %	Waternet database	From GBKN database	25 polders out of polders without surface water area percentage data were estimated from Google maps
Elevation m N.A.P	Waternet database	Average elevation	
Paved area percentage %	Waternet database	From LGN6 database	24 polders out of polders without paved area percentage data were estimated from Google map
Soil data (clay, humus, and calcite content in %)	Deltares	Soil Map of The Netherlands (scale 1:50000)	Cover layer data of each polder.

Chapter 3

Urban hydrogeology: transport routes and mixing of water and solutes in a groundwater influenced urban lowland catchment*

Abstract: Urban areas in coastal lowlands host a significant part of the world's population. Here, cities have often expanded to unfavorable locations that have to be drained or where excess rain water and groundwater need to be pumped in order to maintain dry feet for its citizens. As a result, groundwater seepage influences surface water quality in many of such urban lowland catchments. This study aims at identifying the flow routes and mixing processes that control surface water quality in a groundwater-influenced urban catchment Polder Geuzenveld, which is part of the city of Amsterdam. Geuzenveld is a highly paved urban area with a subsurface rain water collection system, a groundwater drainage system, and a main surface water system that receive runoff from pavement and roofs, shallow groundwater and direct groundwater seepage, respectively. We conducted a field survey and systematic monitoring to identify the spatial and temporal variations in water quality in runoff, ditch water, drain water, and shallow and deep groundwater. We found that Geuzenveld receives a substantial inflow of deep, O2-depleted, nutrient-enriched groundwater. This groundwater is mixed in the ditches during wet periods with O2-rich runoff, and iron- and phosphate-rich drain water. Unlike natural catchments, the newly created, separated urban flow routes lead to mixing of water in the main surface water itself, shortcutting much of the soil and shallow subsurface. This leads to low O2 and high ammonia concentrations in dry periods, which might be mitigated by artificially increasing O2 levels by water inlet or bubbling air in the main water canals. Further research is necessary how to optimize such artificial urban systems to deliver ecological and chemical status of the surface water that is healthy for the residents globally that live in these lowland urban catchments.

* Based on: Liang Yu, Joachim Rozemeijer, Ype van der Velde, Boris M. van Breukelen, Maarten Ouboter, Hans Peter Broers. Urban hydrogeology: Transport routes and mixing of water and solutes in a groundwater influenced urban lowland catchment. *Science of the Total Environment*, 678: 288-300, 2019.

3.1 Introduction

As cities expand worldwide, the urban natural water resources are under stress of contamination, and ecological degradation by human activities (Leopold, 1968; McPherson, 1974; Paul & Meyer, 2001; Foster, 2001; Walsh, etc., 2005; Pataki, etc., 2011; Gumindoga, 2014). Meanwhile, urban waters are increasingly used for recreation such as boating, swimming, waterside picnics, etc. Urbanisation involves modifications in the natural water cycle by the introduction of impermeable surfaces and the installation of urban drainage systems. These modifications reduce infiltration, increase urban runoff and may shorten the hydrological travel times. In addition, urbanisation often involves the contamination of shallow groundwater and surface water with for example nutrients and heavy metals. The degeneration of urban water quality initiated interest in research on concentrations, sources, and sinks of pollutants in cities (e.g. Gobel, etc., 2007, Howard, 2007, Boogaard, 2014, Kojima, 2016, Zafra, etc., 2017). Typical urban pollutants include heavy metals, nutrients, and organic contaminants. In many cases the urban water systems are relatively simple: rain via runoff brings heavy metals generated by traffic, roofs, and other construction materials into the surface water system. Urban fertilizer application, waste water inflow, and atmospheric deposition introduce nutrients which are transported by superficial pathways (D.R. Oros, et al, 2007; Nyenje, 2010; Berndtsson, 2014). However, these pollutants may also infiltrate, causing groundwater pollution (Sorensen, etc., 2015; J. Bonneau, et al., 2017; Abdalla, 2018) and a delayed response of surface water quality. In many urban lowland catchments, surface water quality is also significantly influenced by upward groundwater seepage (Ellis & Rivett, 2007; Gabor, 2017). In a previous study (Yu, et al., 2018), upward seeping polders in the greater area of Amsterdam were shown to transport relatively high nutrients fluxes to the main water system, but these polders were never investigated in detail.

To create more space for residential areas, low-lying natural wetlands, lakes and excavated peat areas around Amsterdam have been reclaimed and urbanized. Large amounts of excessive water are being pumped out every day to maintain low surface and groundwater levels and prevent wet cellars or flooding of residential areas. The surface water levels, groundwater levels, and flow routes are regulated by pumping schemes. Factors like the electricity price, the choice of vegetation, maintenance frequencies, and city constructions including the drainage system design all influence the hydrology and water quality in such areas. Since the potentially eutrophicated and degraded surface waters gained more attention because of European legislation, such as the Water Framework Directive (EU, 2000), researchers and governments noticed that the urban routes of pollutants have not been enough considered, which creates a potential barrier for effective mitigation of urban water quality problem.

Little research has been done in lowland groundwater-fed urban catchments. Therefore, little is known about the flow routes of nutrients and other chemical variables from the subsurface of a city, which are an indirect consequence of the human manipulation of the hydrology. In addition, there is a lack of knowledge of the geochemical processes during the mixing of upwelling groundwater with rain water in the surface water system. Some studies addressed the mixing of water sources in urban settings in process-based models (e.g. Yan et al., 2018), but good measurement datasets for validation are lacking. As lowland cities are rapidly expanding worldwide, more wetlands will change into low-lying, groundwater-fed, artificial urban catchments. Understanding sources and flow routes of water and solutes and potential reaction processes is key to improve the water quality conditions in urban lowland settings.

The objectives of this study are to (1) identify the flow routes of nutrients, heavy metals, and major ions in a groundwater-influenced urban catchment, (2) to interpret the mixing of the runoff, drain water and groundwater in the surface water system through space and time, and (3) to formulate hypotheses on the effects of city infrastructure on urban water quality as a basis for further research. To address these goals, a spatial survey of the polder water system was performed and time series of water quality parameters and natural tracers (^{222}Rn and δ^{13}C-DIC) were collected for 8 locations during 2016-2017 at weekly and biweekly intervals, and a longer time series was collected at the pumping station during 2006-2016 at monthly intervals. We interpreted the time series data applying a temporal water quality separation based on APEI (Antecedent Precipitation and Evaporation Index), as the contribution of different flow routes depends on the meteorological and hydrological conditions (Rozemeijer & Broers, 2007). Empirical and statistical methods were applied to interpret the flow routes and mixing of water within the polder system.

3.2 Methods

Study site

The urban polder Geuzenveld is located in the western part of the city of Amsterdam (Fig.3.1). Its urban surface area covers 0.47 km^2, including a small park in the south. The area has a population of 2430 and its average elevation is 2.75 m below the Normaal Amsterdams Peil (NAP: Normalized Amsterdam Peil, a known standard conforming to mean sea level). The polder is the result of the excavation of peat in the early 20th century and the resulting lake was reclaimed between 1937 and 1941. Originally, the polder was in agricultural use, but between 1990 and 2000 the polder was converted to a residential area. The water levels in the urban polder and the park are maintained at 4.25 m below NAP, which is around 1.5 meter below the land surface. Open water area occupies 20% of the total area including the park. There are three ditches in North-South direction (called West ditch, Middle ditch, and East ditch) and two in West-East direction. The East ditch is the narrowest with less than 1 meter width and less than 0.5 meters in depth in general (Fig.3.1. E1 and E2), the other ditches have widths ranging from 2 to 5 meters and are about 1 to 1.5 meters deep. At least 50% of the polder is covered by houses and other impermeable or semi-permeable land surfaces such as concrete brick stones and asphalt streets. Around 25% of the area is unpaved, consisting of the park in the south, public and private gardens and small unpaved strips along the streets.

The subsurface deeper than 30 meters below NAP is made up of ice-pushed deposits of Pleistocene age formed by a Saalien land ice mass (Schokker et al., 2015, Fig.3.2). The coarse sand deposits of the covered ice-pushed ridge are overlain by fluvial sandy deposits of the Rhine river (Kreftenheye Formation; KRBXDE) and aeolian deposits of the Late Pleistocene (Boxtel Formation: BX). This sequence of Pleistocene deposits forms the main aquifer in this area. The aquifer is overlain by Holocene deposits of marine and peri-marine environments. The Holocene cover layer mainly consists of clays and clayey sands of the Wormer Member of the Naaldwijk Formation (green in Fig.3.2) that were deposited in a tidal flat environment. Two peat layers are prominent in the western part of the Netherlands. The basal peat (NIBA: Basisveen Bed of Nieuwkoop Formation) is typically at the basis of the Holocene sequence. This peat layer is typically strongly compacted and is known to represent a hydraulic barrier in the western part of the Netherlands (Stafleu et al., 2011). The second peat layer

rests on top of the Holocene clays of the Naaldwijk Formation (NIHO: Hollandveen Member of the Nieuwkoop Formation). This shallowest peat layer was excavated in the 20th century in this polder which was part of a larger polder called "The Eendracht" at that time. The peat is still existent in the urban area just east of the polder and in the North (see east side of Fig.3.2). This "Holland Peat" (NIHO) is also present directly east of the deep polder, where it forms the base of the waterway with the highest water levels in the residential area east of the polder and forms the dike between the two areas. In the southwest of the polder the clays of the Naaldwijk Formations were removed by erosion by a tidal channel from the Zuiderzee-IJ-estuary that deposited moderately fine to very fine sands (Fig.3.2: channel deposits in blue, Schokker et al., 2015).

On top of the geological deposits an artificial anthropogenic layer was created for developing the urban quarter (AAOP in Fig.3.2). It consists of an approximately one-meter thick sand layer that was supplied over the existing clayey polder surface. This artificial layer promotes the drainage of groundwater and rain water to a system of collection drains, thus keeping groundwater levels low enough to avoid water inconveniences in the urban settings. Figure 3.2 shows the position of these drains and the water levels that are maintained in the urban quarter. (detail refer to Fig.S3.1.1)

The average annual rainfall in the Amsterdam area is about 847 mm/year and the average annual evaporation (Makkink) is approximately 609 mm/year (2006-2017, 12 years average calculated from KNMI Schiphol meteo station in Amsterdam). In Geuzenveld, the excess rain water and groundwater is pumped out by the pumping station in the northeast corner (Fig.3.1). A negligible amount of water may leave the urban catchment through the park on the south side, but the water flow direction through the connecting 15 cm diameter pipe between the urban quarter and the park continuously changed during our study period, because water levels are maintained at the same level in the park and the urban quarter.

We estimated the average groundwater seepage rate to be around 0.6 mm/day, based on the pumping rates and the water level recovery after pumping events in winter periods without significant influence of precipitation and evapotranspiration. Because of the substantial groundwater seepage input to the Geuzenveld surface water system, water inlet during dry periods is not needed to maintain the water levels. Surplus water after precipitation is pumped towards waterways that have a higher water level, the so-called "Boezem-system" which is annotated with B and B' in Fig.3.1. (see also Yu et al. 2018).

Being a young urban polder built in 1990s (Fig.3.1), Geuzenveld has a relatively modern separated drainage system. The drainage system includes a rain water drainage system, a groundwater drainage system, and a sewer system (Fig.3.2, and Fig.S3.1.1-3.1.3). A rainwater collection system is installed on all the houses which either leads rain water towards manholes and further to the ditches, or directly to the ditches. The groundwater drainage system consists of perforated pipes mostly at a depth of approximately 2 meters below the surface. It collects both rainwater that infiltrates in the non-paved areas and shallow groundwater. The drains have a direct connection to the ditches. During low discharge periods a return flow from the ditches into the rain and drain pipes and manholes was observed. The sewer system separately transports household waste water towards a sewage treatment plant outside the polder and is disconnected from the polder water system. Potential leakage of sewerage into the subsurface cannot be completely excluded, but we found no evidence for this.

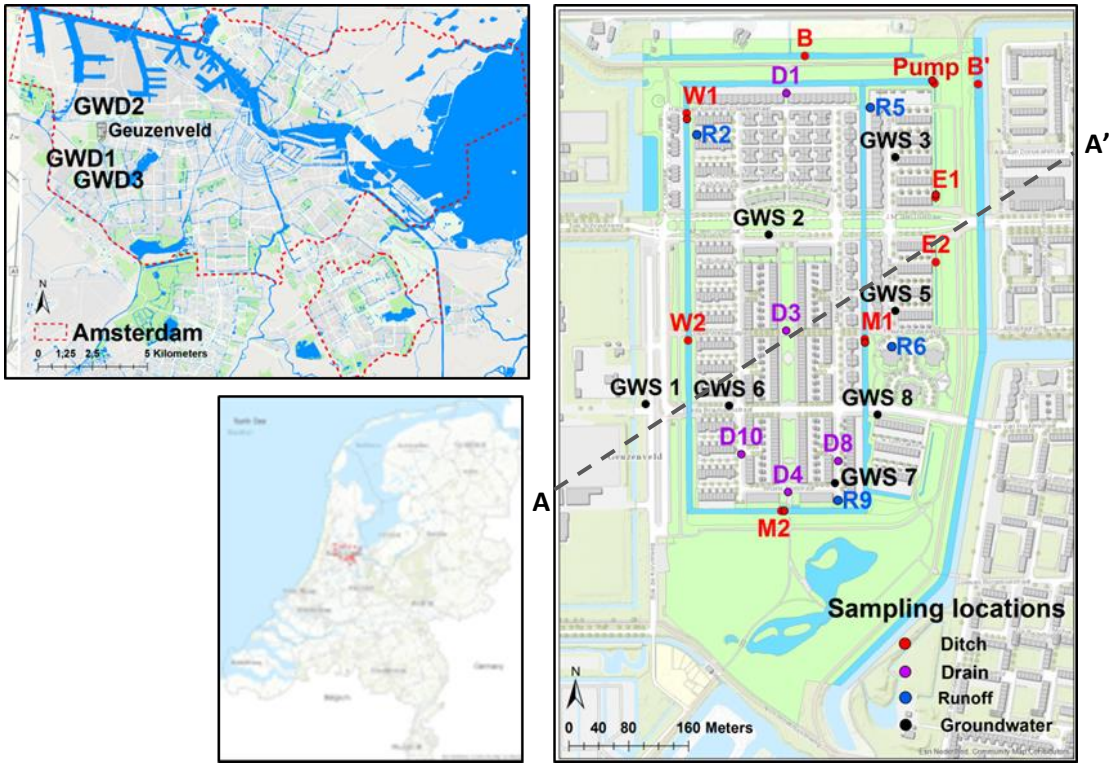

Figure 3.1 Location of polder Geuzenveld (52°23'01.3"N 4°47'37.7"E) in the Amsterdam area (left figure) and detailed map (right figure). Amsterdam map shows the location of polder Geuzenveld and the deep groundwater sampling locations (GWD1, GWD2 and GWD3). Geuzenveld map shows the sampling locations of the short term (2016-2017) grab sampling (W1, W2, M1, M2, E1, E2, B1, and B2), the water quality survey in 2017 of runoff (R2, R5, R6, and R9), ditch (W1, M1, M2, E1, and Pump) and drain water sampling manholes (D1, D3, D4, D8, D10) and shallow groundwater piezometers (GWS 1-3, GWS 5-8).

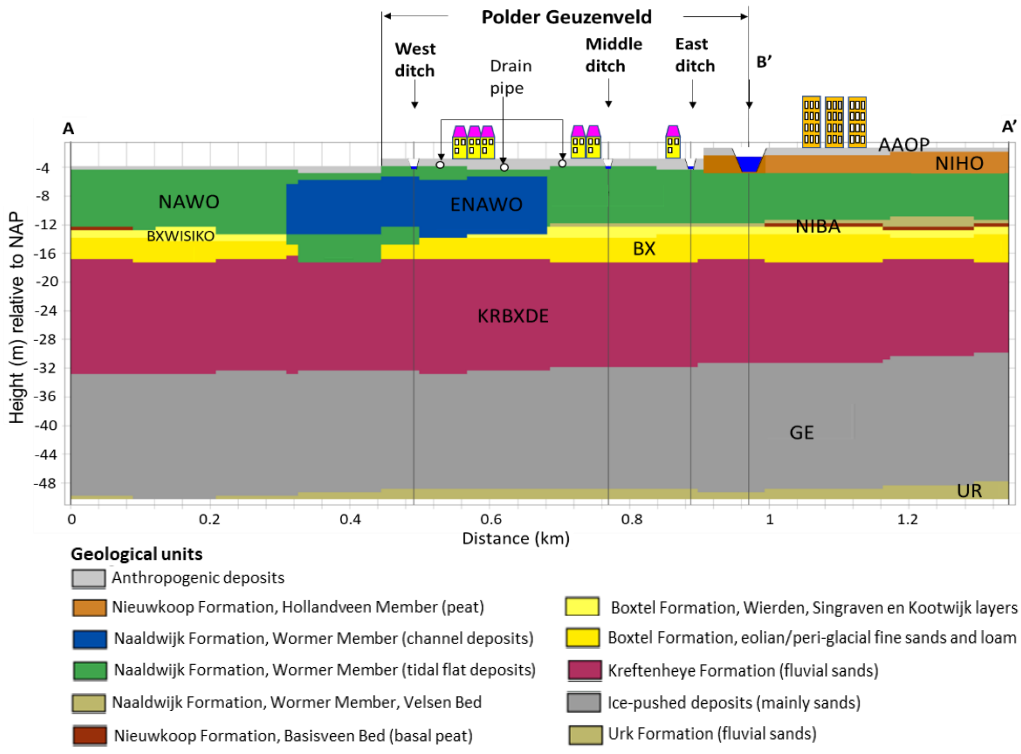

Figure 3.2 Geological Formations and their main lithology beneath the polder Geuzenveld with indicative positions of the main water courses and drains. A more detailed lithology bases on 100 x 100 x 0.5 m voxels (Schokker et al., 2015) for this cross-section is given in Fig.3.8. The cross-section A-A' is indicated in Fig. 3.1.

3.2.1 Data collection

To identify the flow routes of solutes and the mixing of different water sources within the polder system, water quality data were collected covering both the spatial patterns and temporal variations. We profited from the long-term time series of water quality monitoring by the Waternet water board covering the period 2006-2017. We intensified the monitoring through higher frequency grab sampling during 2016-2017, a groundwater water quality investigation from 2017-05-28 to 2017-05-30, spatial surveys of individual flow routes from 2017-11-28 to 2017-12-01, and groundwater tracer measurements (δ^{13}C-DIC and ^{222}Rn).

Runoff, ditch, drain, and groundwater water sampling

A first investigation of deep (GWD) and shallow (GWS) groundwater quality was conducted from 2017-05-28 to 2017-05-30, including 9 piezometers (GWS 1-3, GWS 5-8 and GWD 1-2, Fig.3.1). Groundwater sampling of the shallow piezometers with 1 meter length screens up to 5 meters depth (GWS) concentrated on the polder Geuzenveld itself, whereas the deeper groundwater was sampled for two piezometers at 10 to 25 meters depths with screen lengths of 1 meter at about 2 km distance from

our urban study polder Geuzenveld. The wells were purged removing at least three times of the stagnant water volume in the tubes using peristaltic pumps. The pump was connected to a flow through cell, and the pH, O_2, and EC were measured on-site until stabilization. Additionally, alkalinity as HCO_3 was measured on-site using an AL-DT HACH digital titration set. Parameters measured included pH, O_2, EC, HCO_3, Cl, ^{222}Rn, and $\delta^{13}C$-DIC.

Another survey was carried out from 2017-11-28 to 2017-12-01, in order to distinguish between the different flow routes that influence ditch water quality. The survey was carried out in a period with ample rain (cumulative 17.2 mm in the two days preceding the sampling from 2017-11-26 10:00 until 2017-11-28-10:00 (Fig.S3.8.1)) when drain and rain water systems discharged significant amounts of water. The survey included (Fig.3.1): (1) the sampling of runoff from the rain water system (Rain: R2, R5, R6 mix (runoff from the roof and the street), R6 street (runoff from the street), and R9), (2) the ditch water at locations West 1 (W1), Middle 1 (M1), Middle 2 (M2), East 1 (E1), and the pumping station (Pump), (3) the effluents of the artificial groundwater drainage system (Drains: D1, D3, D4, D8 and D10) and (4) the shallow and deep groundwater from piezometers (GWS 1-3, GWS 5-8 and GWD 1-3). Drain water and runoff samples were collected from manholes that allowed access to these water flow paths (Fig.S3.1.1-3.1.3). The sampling procedure of the ten existing piezometers for groundwater sampling were the same as described above.

Parameters measured in the latter survey included pH, O_2, EC, Temperature, HCO_3, Cl, SO_4, Na, Ca, K, Mg, Fe, Mn, NH_4, NO_3, TP, DOC, Ba, Sr, Ni, Al, Pb, As, Cd, Cr, Cu, and Zn. Five sample bottles were filled at each sampling point. Three samples were filtered through 0.45 µm filter for analysis at the joint TNO/University Utrecht Central Environmental Laboratory (Utrecht Castel). The samples that were pre-acidified with sulfuric acid were used for the analysis of ortho-PO_4, NH_4 (NEN-EN-ISO-11732 and NEN-EN-ISO-15681-2, respectively), and for Dissolved Organic Carbon(DOC) (NDIR). The samples that were pre-acidified with nitric acid was analyzed with ICP-MS for metals and TP. The non-acidified sample was used to measure NO_3, Cl, and SO_4, using IC. The additional two samples were treated as regularly done by the Waternet water board who do not typically filtrate the samples. TP was analyzed photometrically (NEN-EN-ISO 15681-2, 2005) and NH_4 using a discrete analyzer (NEN ISO 15923-1). Analysing TP and NH_4 in both labs was intended for quality control and for matching the long-term grab sampling time series from Waternet with the results of this spatial survey. In addition, comparing TP concentrations (filtered and unfiltered) and ortho-P concentrations helped to identify species of phosphorus among locations.

Long term surface water quality monitoring (2006-2017)

A low frequency (monthly) time series of water quality from grab sampling was collected by Waternet from 2006 to 2017 following the procedures used by the Dutch water boards. The monthly sampling was done at the location in front of the pumping station (“Pump” in Fig.3.1). The database contains results of EC, pH, and O_2, suspended solids (SS), Ca, Cl, HCO_3, SO_4, NH_4, and TP. The collected samples are preserved at site according to the standard NEN-EN-ISO 56667-3 (2012). Cl, NH_4, SO_4, and Ca are filtered at site. TP and Ca are acidified with respectively sulfuric acid and nitric acid. The field parameters EC, pH, and O_2 are measured with a Hanna HI9828 multi parameter probe and analyzed according to the standards NEN-ISO 7888 (EC), NEN-EN-ISO 10523 (pH) and in-house method (O_2). The following parameters are analyzed at the laboratory: SS is a filtration method and

analyzed according to standard NEN-EN 872; HCO_3 is a titration method and measured with a Metrohm titrator, according to an in house method; Cl, NH_4, and SO_4 are measured with a discrete Analyzer (DA) according to the standard NEN-ISO 15923-1; TP is measured with a continuous flow auto analyzer (AA) according to the standards NEN-EN-SIO 15681-2 and NEN 6645; Ca is measured with an ICP-MS according to the standard NEN-EN-ISO 17294-2.

Short term surface water quality monitoring (2016-2017)

A higher frequency (weekly and biweekly) grab sampling campaign was carried out between March 14th, 2016 and June 16th, 2017. Each sample was collected under random hydrological conditions following a systematic sampling design with fixed sampling moments. Samples were mostly taken at the middle of the canals in horizontal and vertical direction. Sampling at the pumping station (Pump) conformed with the low frequency sampling of the previous years but at higher (weekly and biweekly) frequency. Additional samples were collected from other 8 locations in the polder, West 1 (W1), West 2 (W2), Middle 1 (M1), Middle 2 (M2), East 1 (E1), East 2 (E2) and Boezem (B and B') (see Fig.3.1). The weekly and biweekly samples at the 8 new locations yielded values of EC, O_2, pH, HCO_3, and Cl that were measured on-site. Here, locations M1, M2, W1 and W2 represent the main ditches in the polder system that collect water from all the drainage systems present (runoff and drain water and groundwater seepage). Ditches E1 and E2 have smaller dimensions and mainly drain the foot of a dike at the east part of the polder, and do not receive water from runoff or drains.

δ^{13}C-DIC and ^{222}Rn sampling

δ^{13}C-DIC was measured as an additional parameter at three selected locations (M2, E2 and B'), as we hypothesized that the δ^{13}C-DIC values would differ between the end members of our mixed surface water samples. We expected δ^{13}C-DIC of groundwater to be mainly determined by organic matter mineralization (δ^{13}C-DIC = ± -25 ‰ of C3 plants) and the dissolution of subsurface calcite (δ^{13}C-DIC 0 ‰)) yielding values around -12‰ to be significantly different from runoff which is believed to be in equilibrium with atmospheric CO_2 (e.g. Mook 2006; δ^{13}C-DIC = ± -8 ‰)). δ^{13}C-DIC samples of the surface water at locations M2, E2, and B' were prepared in 100 mL brown glass bottles and stabilized with mercury chloride in the field. δ^{13}C-DIC samples for groundwater were taken from May 28th-30th 2016 with a similar sampling procedure. δ^{13}C in dissolved inorganic carbon was measured using mass spectrometry (Thermo Finnigan Isotope Ratio Mass Spectrometers). δ^{13}C-DIC is reported as δ^{13} (in ‰) using the universal δ notation with VPDB (Vienna Pee Dee Belemnite) as standard for marine carbonates.

To trace groundwater inflow, ^{222}Rn activity was additionally measured at all locations (Fig.3.3). ^{222}Rn is a radioactive gas that is produced by the decay of ^{226}Ra from the radioactive decay of uranium and is often used as a tracer for groundwater inflow into surface water (e.g. Cecil and Green, 2000; Dimova, 2013; Cartwright & Hofmann, 2016). Groundwater concentrations of ^{222}Rn are typically much higher than in receiving surface waters because of the continuous decay of ^{226}Ra which is present in minerals or adsorbed at reactive phases in the aquifer matrix. The radon gas is released continuously from subsurface minerals that contain ^{226}Ra and is mildly soluble in water. ^{222}Rn has a half-life of 3.8 days, which makes it suitable for tracing the very recent groundwater input into surface water bodies, although the method has drawbacks because the degassing of ^{222}Rn to the atmosphere is a process that is heavily dependent on the specific field and weather conditions (Cartwright & Hofmann, 2016). We

applied the RAD-H_2O (Durridge Company, 3D printed aerator cap) to analyze ^{222}Rn concentrations in water. ^{222}Rn samples were taken without filtration in 250 mL glass vials and were analyzed in the field. Before the measurement, the RAD-H_2O system had to be purged to remove potential ^{222}Rn residuals and to get the humidity of air lower than 10%. Then the glass vial was connected to the cap that formed a loop connection with the RAD 7 detector. Desiccant dehumidifier was used to keep the loop dry. Following the protocol, it first aerated the system for 5 minutes to achieve an equilibrium of ^{222}Rn in the water and air in the whole system. Subsequently, 4 measuring cycles of 5 minutes each were done. After this, we used the RAD 7 data processing software (Capture) to get an average ^{222}Rn concentration value corrected for humidity.

3.2.2 Data processing

The field sampling campaigns yielded three datasets for processing: (1) the 2017 spatial survey dataset consists of a single water quality survey for runoff, ditch water, drain water, and groundwater at 24 locations (with R6 separated into R6 runoff from street and R6 mix of runoff from streets and roofs); (2) the 2016-2017 time series at 8 locations with weekly/bi-weekly sampling; and (3) the 2006-2017 long time series with monthly data at the pumping station.

Runoff, ditch water, drain and groundwater flow route variation survey

For quality assurance, we checked the ion charge balance of this dataset using the following equation (Appelo, et al., 1996):

$$Ion\ balance\ error = \frac{\sum Anions - \sum Cations}{\sum Anions + \sum Cations} \quad (3.1)$$

The deviations between sum of anions and sum of cations were limited: 72% of the samples are below a deviation of 5%. The ion charge balances range between 1-16% for runoff, 3-15% for ditch water, 0-6% for drain water and 0-11% for groundwater.

The water quality data of runoff, ditch water, drain water, and groundwater were summarized in a group of boxplots. We applied Principal Component Analysis (PCA) to the 2017 Survey dataset, to identify solutes with similar behavior along the flow routes and the major controls on chemical composition of the waters within the polder. Because many of the water quality parameters were not normally distributed, and concentrations between parameters differ strongly, we normalized (via a box-cox transformation) and scaled all the variables. By plotting the first two principle components of the PCA, the water quality parameters were grouped into solutes with similar patterns along the flow routes.

Surface water quality: spatial and temporal variation

For the interpretation of the temporal variations in water chemistry, we applied an Antecedent Precipitation and Evaporation Index (APEI) based on meteorological data to distinguish between periods with wet and dry conditions in the catchment. We collected precipitation and potential evaporation (Makkink, 1957) data from the Schiphol Airport KNMI (The Royal Netherlands Meteorological Institute) weather station, which is located 9 km south from polder Geuzenveld. We divided the hydrological condition of the catchment for each day into 4 classes from driest (class 1) to

wettest (class 4) based on the calculated APEI values as below, following the procedure of Rozemeijer et al., 2010:

$$APEI_t = APEI_{t-1} \times Decay\ rate + (Precipitation - Evaporation)_t \quad (3.2)$$

$APEI_t$ is APEI (mm) at day t. Precipitation and evaporation are both daily records in mm (KNMI, http://www.knmi.nl). We chose a decay rate of 0.76 in this study area, based on the best fit between daily and weekly accumulated APEI values with known pumping volumes at the principal outlet of our polder system, and the recession line of the water levels (for details see Fig.S3.3.2).

The one-year surface water quality data (^{222}Rn, pCO_2, HCO_3, Cl, and Fe) of the 8 locations from 2016 to 2017 which fell in classes APEI = 1 (dry, see section 3.3.2) to APEI = 4 (wet), were plotted with the runoff, ditch, drain, and groundwater data from the survey in 2017. The survey was intentionally done during a wet period (APEI class 4) in order to have all transport routes contributing during the survey. In the paper we used the survey results as reference for interpreting the transport routes during a wet period, comparing it with the data from the longer time series.

In addition, the 2006-2017 and 2016-2017 time series of surface water concentrations measured at the pumping station were jointly summarized in boxplots for each of the 4 APEI classes. We separated the data into the periods 2006-2016 and 2016-2017 . The following parameters were analyzed: EC, Cl, HCO_3, Ca, TP, NH_4, SO_4/Cl (mass ratio), pCO_2, ^{222}Rn, and suspended solids (SS).

SO_4/Cl was calculated from the measured SO_4 and Cl concentration at the pumping station. This ratio is an indicator of sulfate reduction which commonly occurs in peat subsurface with abundant SO_4 sources like pyrite oxidation and salt/brackish water seepage in Amsterdam area (Yu et al., 2018). SO_4/Cl ratios lower than 0.14 indicate sulfate reduction, and SO_4/Cl ratios above 0.14 indicates influence of additional SO_4 sources (Appelo and Postma, 2005, Griffioen et al., 2013, Yu et al., 2018).

Partial CO_2 pressure (pCO_2) was calculated as (Appelo and Postma, 2005):

$$pCO_2 = 10\text{^}((log_{10}(HCO_3/1000) - pH + 7.73))\ (atm) \quad (3.3)$$

HCO_3 is in mmol/L and we assumed a temperature of 10°C for all samples, which is sufficiently distinguishing given the large differences in pCO_2 observed (the range of $K_H \cdot K_2$ = 7.69-7.8 between 3 and 22°C).

The patterns of pCO_2 and ^{222}Rn in relation to the hydrological conditions were studied by plotting them against APEI in boxplots. Scatter plots of ^{222}Rn, $\delta^{13}C$-DIC, and pCO_2 were made among the available locations. LOWESS trend lines (Cleveland, 1979) were used to identify patterns in the scatter plots.

3.3 Results & Discussion

3.3.1 Runoff, ditch water, drain water, and groundwater flow routes survey

The November 2017 survey yielded a dataset of 27 water quality parameters on 24 locations that span the dominant flow routes in our catchment: runoff (4 locations), drain water (5 locations), ditch water (5 locations), and shallow and deep groundwater (10 locations). A PCA on this dataset returned 2 principle components that explain 76% of the total variance (Fig.3.3). Based on these first 2 principle components, we grouped the 27 water quality parameters into 6 groups with similar flow route concentration patterns (Fig.3.3).

Groups 1-3 are the solutes that have the highest concentrations in the groundwater while the lowest concentrations are found in runoff (Fe, Temperature, pCO_2, TP, ^{222}Rn, Ba, Cr, NH_4, Ca, Sr, HCO_3, DOC, Mn, Cl, EC, K, Mg, and Na). Groups 4 and 5 have the highest concentrations in runoff (Al, Cd, Pb, Zn, Cu, NO_3, pH and O_2,). Group 6 contains three solutes that have the highest concentrations in drain and/or ditch (As, Ni, SO_4).

The solutes that were highest in groundwater (Groups 1-3) were further subdivided into three groups with each a characteristic flow route pattern (see Fig.3.3 boxplots):

- Group 1: concentration in ditch is significantly higher than in drains (Cl, EC, K, Mg, and Na),
- Group 2: concentration in ditch is similar to that of the drains (NH_4, Ca, Sr, HCO_3, DOC, and Mn),
- Group 3: concentration in drains is significantly higher than that of the ditch (Fe, Temperature, pCO_2, TP, ^{222}Rn, Ba, Cr).

Similarly, the solutes with highest concentrations in runoff were also divided into 2 groups:

- Group 4: ditch concentration clearly higher than the drain concentration (O_2, pH, NO_3, Cu),
- Group 5: both ditch and drain concentration are similar and much lower than in runoff (Pb, Zn, Cd, Al).

The median values of As, Ni, and SO_4 (Group 6) showed the highest level in the ditch and drain instead of groundwater or runoff which distinguishes these variables from the rest. Although Ni and As are attributed to this group, the patterns of Ni and As also conforms to some extent with group 2 (NH_4, Ca, Sr, HCO_3, DOC, and Mn).

Characteristic examples each of these groups are given in Fig.3.3, all solutes are presented in Figure S3.4.1.

The PCA confirms our hypothesis that groundwater and runoff are the two dominant sources for solutes in polder Geuzenveld (opposite directions of the G and R arrows along the principle component 1 (*x*-axis) representing the loadings of each of these flow routes, Fig.3.3 B). We derive the following conclusions from the PCA analyses:

- The groundwater is characterized by a neutral pH (6.8-7.0) resulting from carbonate dissolution (as indicated by Ca, HCO_3 and pCO_2) reduced conditions (low O_2 < 0.5 mg/L), enriched with nutrients (TP and NH_4) and a seawater influence (high Cl, Na, K and Mg). The low redox potential conditions allow Mn and Fe to be present in their reduced soluble form (Fe^{2+}, Mn^{2+}) (Appelo & Postma, 2010).

- The runoff is O_2-rich and contains heavy metals that are presumably desorbed and dissolved from roofs and paved areas (R arrows in Fig.3.3 B).
- Drains (arrows with D's in Fig.3.3 B) discharge the shallow groundwater, which consists of a mixture of groundwater and infiltration from rain in unpaved and partially paved terrains.
- In the main receiving ditches, waters from these three flow routes (groundwater, rain water and drain water) mix and react with each other (d arrows in Fig.3.3 B).

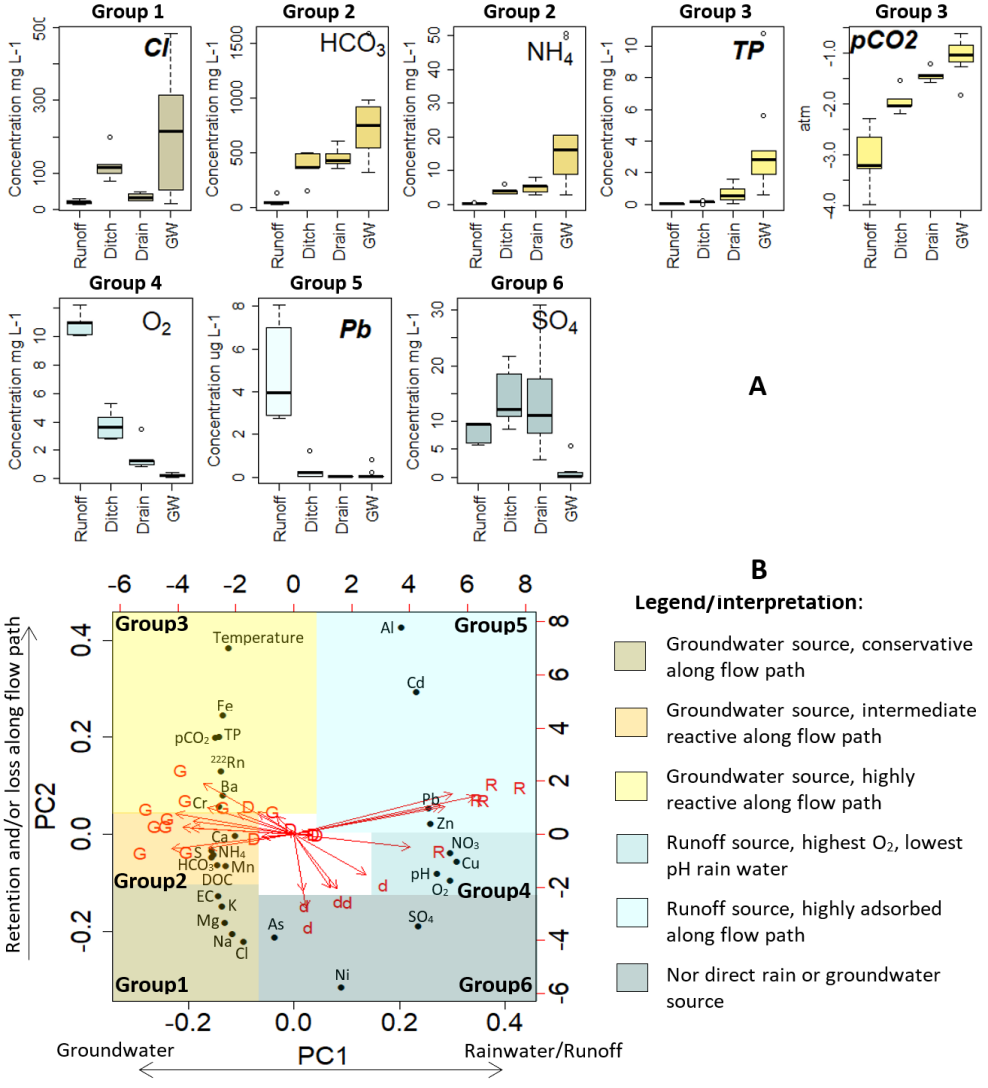

Figure 3.3 Results of the PCA analysis in graphical form. Fig.3.3(A): Boxplots the concentrations of flow route indicators based on the PCA analysis for as collected during the 2017 spatial survey. Boxplots for the complete set of solutes are given in Figure S3.4.1. At least one solute from each group in the PCA resullts of figure (B) is shown. Fig.3.3(B) shows the contributions of the first 2 principle components (PC1 and PC2) to explain the observed solute concentrations. The arrows in Fig.3.3(B) indicate the loadings of the flow routes sampled: runoff (R, observation number n = 5), ditch water (d, n = 5), drain water (D, n = 5), and groundwater (G, n = 10).

The first principle component (PC1) of the PCA analysis clearly reflects the mixing of groundwater with runoff, where solutes that originate from groundwater are plotted at the left side and solutes that originate from runoff on the right. The mixing process of these main origins is the major control on the solute composition of the water samples, explaining 66% of the total variance. We interpret the second principle component (PC2) of the PCA, which explains another 10% of the total variance, to reflect the reactivity of the solutes along the flow route from its source (groundwater or runoff) towards the ditch and further towards the pumping station. Here, Cl is being the least reactive (bottom part) and Fe and Al are the most reactive (upper part of the graph).

The groundwater derived solutes

Following this interpretation of PC2, the groups 1-3 represent solutes originating from groundwater that react along their flow route. Due to seawater influence, deep groundwater is relatively high in Cl, Na, Mg, and K and accordingly has an elevated EC (see also Yu et al. 2018 for a regional analysis of water types in the larger Amsterdam region). The higher concentrations of these stable solutes in the ditches compared with the drains point to the importance of direct flow paths of deep groundwater into the open water system. We interpret the similar concentration levels in the ditch and drains of solutes in group 2 to reflect moderate reactivity of these groundwater derived solutes under oxygenated conditions in drains and ditches. This reactivity intensifies going from drains to ditch due to both higher oxygen concentration and longer residence times in the ditch, which could explain the lower ditch concentration relative to drain concentration of group 2 compared to group 1. Strong reactivity under oxygenated conditions in the ditch is found for the solutes in group 3; the reactivity of Fe and TP is suggested to be related to the precipitation of Fe-hydroxides following oxygen inflush from runoff with subsequent sorption of phosphorus, and to the exchange with the atmosphere (pCO_2 and ^{222}Rn) combined with radioactive decay for ^{222}Rn (see section 3.3.3).

In a previous paper, (Yu et al., 2018), we argued that high TP and NH_4 concentrations of the groundwater around Amsterdam are related to SO_4-reducing or even methanogenic conditions in the principal aquifers. These conditions led to increased HCO_3 concentrations and enhanced mobilisation of N and P by mineralization of organic matter in the deeper subsurface of the region (Yu et al., 2018). This process could also explain the presence of NH_4, HCO_3, and DOC, in the same group, group 2. However, TP that also originates from these nutrient-rich groundwaters ends up in group 3 as it is much more reactive when the water is mixed with oxygenated water and Fe-hydroxides form that are able to sorb most of the phosphorus. This is illustrated in Fig.3.4 that shows that phosphorus in the ditches and the drains adjacent to the ditches (D1, D4), where oxygen from runoff is mixed with the groundwater and drain water, is mainly in the form of sorbed P (unfiltered P higher than filtered P). In contrast, phosphorus in groundwater and drain locations not affected by runoff (D3, D8, D10) is mainly in the form of dissolved ortho-P as this reduced water carries Fe(II) as main dissolved iron species under the low oxygen conditions encountered there. We suggest that the process of capturing of phosphorus in Fe-hydroxide particles in the transition zones between anoxic groundwater to oxic surface water, as was previously described by Van der Grift et al. (2014, 2018), determines the presence of Fe and TP in group 3 of the PCA analysis.

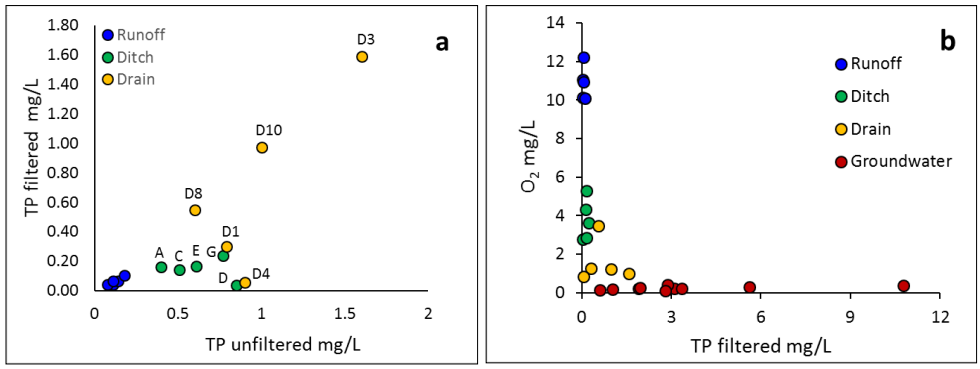

Figure 3.4 Comparison of TP from filtered and unfiltered samples (a) and TP variation with O_2 (b)

The runoff derived solutes

We interpret the difference between groups 4 and 5 as a result of a much higher retention of the heavy metals along the flow path from runoff, drain, to ditch compared to the reactions that O_2, pH and NO_3 undergo along this same flow path. The high pH of urban runoff initially was somewhat surprising given the low pH of urban rain water, but can be explained by buffering of street water in contact with concrete building and pavement materials (Galan et al., 2010, Van der Sloot et al., 2011, Van Mourik et al., 2003). The enrichment of urban runoff with metals is in accordance with previous studies in urban areas, for example Berndtsson (2014) who concluded that Pb, Zn, Cu, Ni, and Cd in storm runoff are mostly bound to particles. Zn is a known contaminant to be released from zinc applied in roofs and rain collection systems and a constituent of car tyres, and both Zn and Pb are known to be associated with urban traffic (Smolders & Degryse 2002, Göbel, 2007).

Group 6 grouped Ni, SO_4, and As. Especially Ni and sulfate stand out, as they showed the highest concentration in drain water and ditch water, meaning that direct groundwater seepage of sulfate and nickel does not occur in our polder. We hypothesize that oxygenated water that recharged under the parks, gardens, and other non-paved areas mixes with reduced shallow groundwater while converging towards the drain system. As the shallow subsoil of the polder catchment partly consist of a layer of supplied sand on top of a Holocene clay layer, we expect that the low groundwater levels and the oxygenated recharge water enable the oxidation of pyrite in the clay which mobilizes SO_4, Ni, and possibly As, which also has high concentration levels in groundwater (e.g. Dent & Pons, 1995, Zhang et al., 2009). As the groundwater is typically low in sulfate because of sulfate reduction (see Yu et al. 2018), we conclude that the drains are the main transport route for sulfate in our catchment.

3.3.2 Spatial and temporal variations in the urban catchment

For analyzing the surface water composition during different hydrological conditions, we divided the samples based on the APEI at the moment of sampling. We strived for a reasonable division of the periods with dry, intermediate, and wet conditions and used expert judgement to derive the following distribution of time over the 4 wetness classes: 12%, 13%, 50%, and 25% covering the period 2006-2017 (Fig.S3.3.1). The associated APEI values of each class were: APEI <= -10 for class 1, -10 < APEI <= -5 for class 2, -5 < APEI <= 9 for class 3, and APEI > 9 for class 4. The distribution of the wetness

classes gives a good fit between pumping rates and weekly APEI (see SI-APEI.xslx and Fig.S3.3.2) and yields an acceptable and credible distribution of the wetness classes over the seasons and in relation to periods with large precipitation events (Fig.3.5). The wettest period with accordingly higher classes are more found in autumn and winter and the driest are in spring and summer.

3.3.2.1 Spatial variations in ditch water quality over wet and dry conditions

We obtained time series of pH, O_2, EC, Cl, HCO_3, and ^{222}Rn for the monitoring period of March 2016 - June 2017 for 9 surface water locations (see Fig.3.1) and calculated the CO_2 partial pressures. The sampling moments were classified using the APEI approach into classes ranging from dry to wet catchment conditions. Figure 3.6 summarizes the March 2016 - June 2017 time series data for the wetness classes dry (APEI 1) and wet (APEI 4) and compares the monitoring data with the spatial survey data that were described in the previous section. The samples of the West (W), Middle (M), and East (E) were taken from the main ditches that collect the water in the urban polder, combining the W1 and W2, M1 and M2 and E1 and E2 measurements in order thus avoiding redundancy in the data. A mixture of water from those locations W, M and E is eventually pumped out at the main outlet (Pump) and pumped into the regional channel system (called "Boezem"), where location Boezem B' was sampled. Because location B' appeared to be directly influenced by the discharge from the pump, we chose Location B for "Boezem" water, using it as an independent reference to the measurement points in the polder itself.

The water quality variables in the polder ditches W, M and E all reveal relatively low variability under *dry conditions* (APEI=1) which is reflected in the low variability of the water composition that is pumped out of the polder at location P under these conditions. The anions HCO_3 (600-700 mg/L) and Cl (150-200 mg/L) dominate over SO_4 (< 40 mg/L) and NO_3 (< 5 mg/L). During these dry conditions, the water is characterized by high partial CO_2 pressure (~10^{-2} atm) and low, but constant O_2 concentrations (< 3 mg/L). Relative to the locations W, M and P, the shallow ditches that drain the of the eastern dike (E) exhibit lower Cl concentrations (100-150 mg/L), higher ^{222}Rn (600-800 Bq/m^3) and higher pCO_2 ($10^{-1.7}$-$10^{-1.2}$). The higher O_2 concentrations measured in these shallower ditches are considered to be an artefact, as the east ditches could not be sampled deep enough to avoid entrance of air during sampling. The boezem water at B, which is not connected to the polder, have widely different chemistry, with much lower HCO_3 (300-400 mg/L), and partial CO_2 pressure ($10^{-2.8}$-$10^{-3,5}$ atm) and much higher O_2 (~10 mg/L).

Variability increases for all variables under wet conditions (APEI=4). Lower concentrations of Cl and HCO_3 are more typical, and the overall concentrations pumped out at location P decrease relatively to dry conditions. On the contrary, O_2 concentrations are much higher and range between 3 and 9 mg/L at most locations in the polder under wet conditions. The patterns for ^{222}Rn and pCO_2 do not change much, except that the variability tend to increase relative to dry conditions.

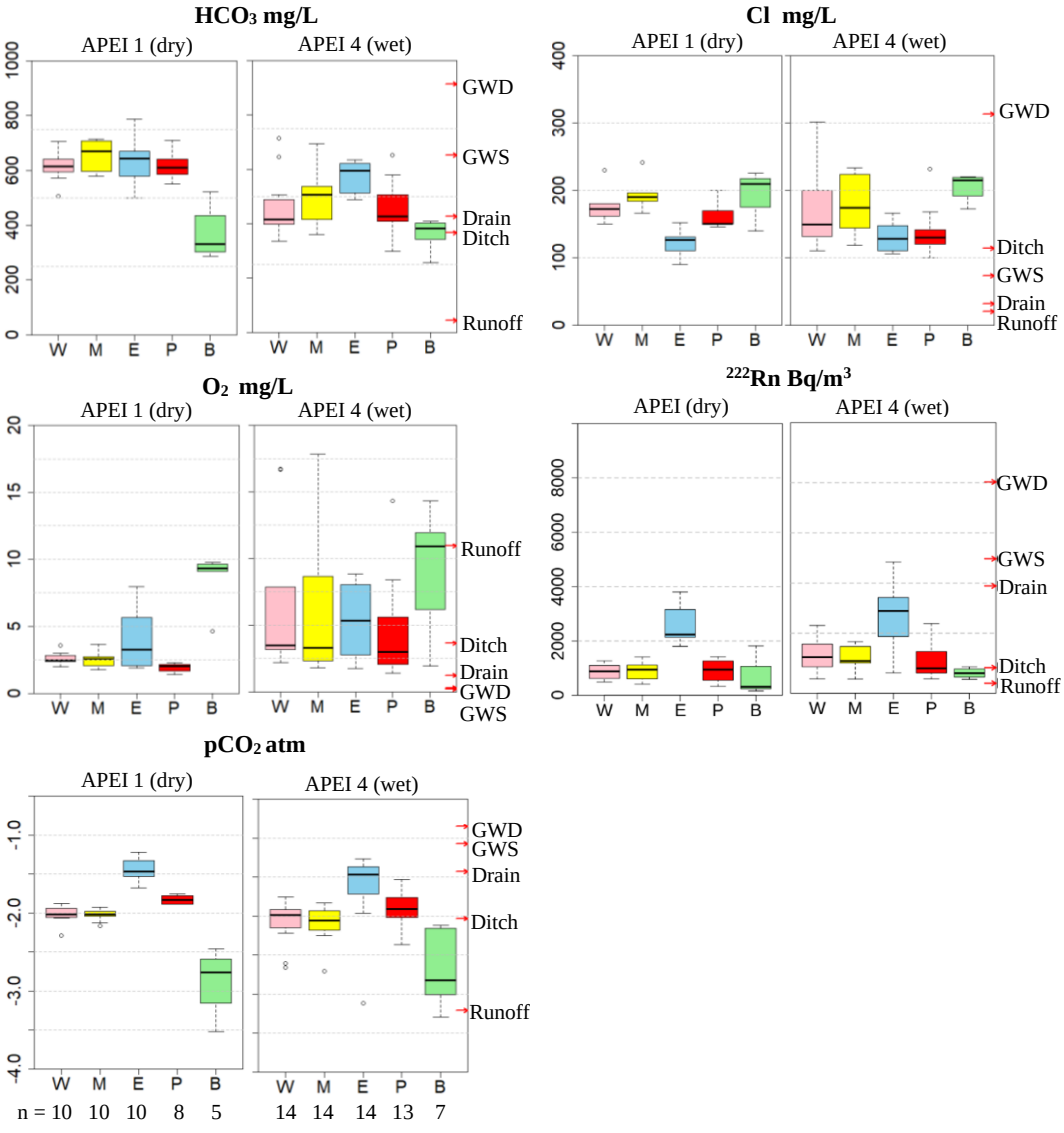

Figure 3.6 Summary of the measured HCO_3, Cl, O_2, ^{222}Rn, and pCO_2 concentrations in the surface water aggregating the 2016-2017 data for dry periods (APEI class = 1) and wet periods (APEI class = 4) The locations of W, M, E, and B represent the total of measurements in the West ditch, the Middle ditch, the East ditch and boezem water north of Geuzenveld, respectively. "P" represents the measurements at the pumping station. Red arrows are used to illustrate the median concentrations that were observed in the 2017 spatial survey (see section 3.3.1 and Fig. 3.3).

We attribute the increase in variability, the increase of O_2 concentrations and the apparent dilution of Cl and HCO_3 at location P, where all water is pumped out of the polder, to be the result of the activation of the separate runoff collecting system in the polder during wet conditions. During the runoff events, the water that resided in the ditches is diluted by the runoff flux, which is high in O_2 (see section 3.3.1).

Under dry conditions the concentrations tend to be less variable and to be specifically enriched in Cl and HCO_3, reflecting the seepage of groundwater (groups 1 and 2, in section 3.3.1). This overall pattern is visible in the west and middle ditches and the pumping station, but not apparent from the E ditches at the foot of the dike. These exhibit higher pCO_2 and ^{222}Rn, and lower Cl, which points to another origin of the seeping groundwater. As these shallow ditches do not receive water from the runoff or drain system, they do not show the variability that is introduced by these systems under wet conditions. Especially the high ^{222}Rn is an indication that the seeping water at the foot of the dike was in direct contact with the subsurface and is replaced before concentrations are lowered by atmospheric exchange and the radioactive decay of the radon gas.

Relatively to the polder water, the water in the boezem water system, which has higher water levels, showed less variability, higher O_2 concentrations and lower partial CO_2 pressure. Both O_2 (~10 mg/L) and CO_2 (pCO_2 $10^{-2.8}$-$10^{-3.5}$ atm) seem to have been equilibrated with the atmosphere (Appelo & Postma 2010), which points to a larger contact time with the atmosphere and more stagnant conditions, as the water is not replenished by groundwater or drain inputs. Moreover, these boezem waters show an abundance of water plants and oxygen producing submerged plants (Fig.S3.6, photos Location B and Location B').

3.3.2.2 Spatial variations in the groundwater composition affecting the surface water

The previous section highlighted the apparent differences between the east ditches at the foot of the dike and the overall chemistry of the main water collecting ditches in the polder. Table 3.2 indicates that differences in groundwater composition are also apparent in the polder.

Table 3.2 Groundwater sampling results of two campaigns in May and November 2017

	Campaign 28-05-2017				**Campaign 28-11-2017**			
	Cl mg/L	EC µS/cm	δ^{13}C-DIC ‰ VDPB	pCO_2 atm	Cl mg/L	EC µS/cm	NH_4 mg/L	pCO_2 atm
Shallow groundwater								
GWS1	496	2610	3.82	-1.36	483	2640	17.4	-1.27
GWS2	203	1660	-7.50	-0.97	187	1608	14.4	-0.99
GWS3		692	-8.00	-1.17	31	733	6.5	-1.07
GWS5	73	1338	-1.34	-0.90	55	1090	15.0	-0.85
GWS6	270	2180	3.09	-0.92	255	2138	19.5	-0.86
GWS7	211	2092	5.75	-1.06	15	516	2.8	-1.83
GWS8	285	2520	-3.66	-0.77	73	989	8.9	-1.18
Deeper groundwater								
GWD1	793	2515	8.17	-1.33	313	2048	20.5	-1.18
GWD2		3470			365	3300	49.6	-0.62
GWD3					243	2400	50.6	-0.85

Groundwater in the polder (GWS, shallow piezometers) and around the polder (GWD1 and GWD2, deeper groundwater at ~1 km distance) was sampled twice during the monitoring campaign. Once in the dry season (May 2017) and once in the wet season (November 2017). Groundwater composition is rather constant in time, except for the shallow piezometers GWS7 and GWS8 that show lower Cl concentrations, EC and partial CO_2 pressure during the wet season when infiltrating rain water may have affected the concentrations. It is clear that both the shallow and deep groundwater contain

significant concentrations of Cl, especially in the southern (GWS 1, 6, 7 and 8) and middle (GWS2) parts of the polder. Contrary, the piezometers GWS 3 and 5 which are in the northeastern part show much lower Cl, closer to the east ditches (E) that were characterized by lower Cl concentrations as well.

Our data suggests that the hydrogeological build-up of the area is responsible for these spatial variations in both groundwater and surface water chemistry over the polder. Figure 3.7 illustrates this hypothesis and provides a conceptual model for the differences observed. Our model suggests that the east ditches are fed by groundwater that has infiltrated in the adjacent boezem and in the upstream urban area east of the polder where a higher water level is maintained (right side of the cross-section). This dike seepage and shallow groundwater seepage would explain the lower Cl concentrations as the water is not replenished by the deeper groundwater in the first aquifer but follows a shallower flow path through the Holocene deposits, presumably at a level above the basal peat layer (see Fig.3.7). The relatively high pCO_2, HCO_3, and high ^{222}Rn of the water that seeps on the base of the dike at locations E1 and E2 implies a recent contact with the subsurface sediments and a typical groundwater origin.

However, especially the surface water in the SW corner of the polder catchment is affected by upward seepage of deeper groundwater with higher Cl concentrations. As the deeper groundwater has a higher hydraulic head than the water level that is sustained in the main ditches M and W, an upward flow is maintained, that profits from the connection between the deeper aquifers and the shallow subsurface that once was established by the sandy tidal channel. The fine sands that distinguish this channel have created a low resistance flow path (Fig.3.7) that allows seepage from the deeper subsurface to enter the ditches. This mechanism is suggested to be the main cause of the high and temporally constant concentrations in the main ditches under dry conditions (see Fig.3.6).

Interestingly, also the δ^{13}C-DIC signature shows a trend over the shallow groundwater in the polder, showing very high δ^{13}C-DIC values in the wells GWS 1, 6 and 7 (all above 0) which corresponds with the high δ^{13}C-DIC of the deeper groundwater (GWD 1: δ^{13}C-DIC = 8.2 ‰ VDPB). This confirms the connection between the deeper groundwater and the shallow groundwater in this part of the polder (see Fig.3.7). A similar finding is recorded for the NH_4 concentrations. The shallower wells of GWS 1, 2 and 6 show high NH_4, resembling the 20 mg/L found in the deeper groundwater. Together, the high δ^{13}C-DIC, pCO_2 and NH_4 concentrations indicate that the process of methanogenesis has occurred in the deeper subsurface, which tends to enrich the remaining δ^{13}C of Dissolved Inorganic Carbon (e.g Han et al. 2002), to increase the CO_2 partial pressure and to mobilize nutrients N and P (see also Yu et al. 2018 who describe this for the larger Amsterdam region). In contrast, the shallow wells GWS 2, 3, 5 in the middle and northeast part of the polder show negative δ^{13}C-DIC, which excludes deeper groundwater feeding into the shallow groundwater in these parts of the polder (Fig.3.7).

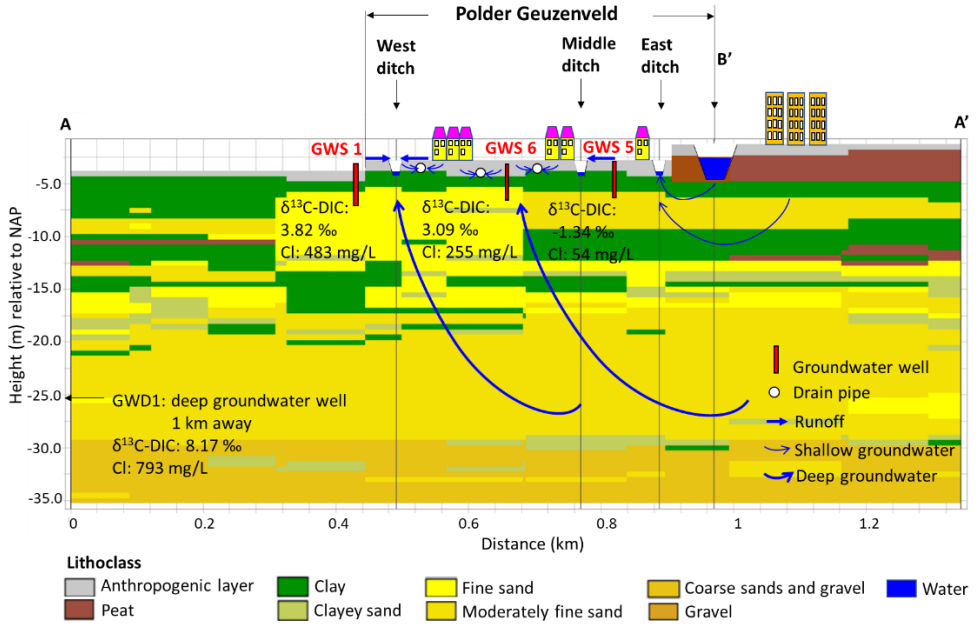

Figure 3.8 Interpreted flow routes along the SW-NE cross-section showing the most probable lithology as provided by geostatistical characterization in GeoTOP (Schokker et al., 2015) and the water levels that are maintained in the waterways. Cl and δ^{13}C-DIC data are shown for a number of shallow groundwater observation wells and the deeper groundwater sampled 1 km SW of the polder.

3.3.2.3 Indications for degassing: ^{222}Rn, pCO_2 and δ^{13}C-DIC

The PCA analysis (section 3.3.1) indicates that the groundwater seepage controls a range of solutes, some of which mix without any reactive pattern (groups 1 and 2) but other groundwater derived solutes tend to have lower concentrations in the ditches than might have been expected from the concentrations in the seeping groundwater (group 3, including pCO_2, ^{222}Rn, Fe and TP). As shown in section 3.3.1, indications exist that Fe and TP have been fixated by redox reactions involving O_2 and subsequent mineral precipitation and sorption. For pCO_2 and ^{222}Rn, the mechanism might be related to atmospheric exchange of CO_2 and radon gas, thus equilibrating with the concentrations and isotope ratios in the atmosphere. Indications for degassing of CO_2 and radon are indeed present in our polder system. Figure 3.9 shows how ^{222}Rn and pCO_2 are related for different APEI wetness classes, combining all the collected data for the 2016-2017 period. In general, there is a clear relation between the two variables with decreasing ^{222}Rn coupled to decreasing partial CO_2 pressure, for all 4 APEI classes. Here, pCO_2 values of $10^{-1.5}$ atm point to typical groundwater pressures and $10^{-3.5}$ atm is representative for complete equilibrium with atmospheric CO_2 (Appelo and Postma, 2005; Mook, 2006). The data suggest that both ^{222}Rn and pCO_2 equilibrate with the atmosphere through gas exchange, which points to a significant residence time of water in the polder. Equilibration of CO_2 and degassing and decay of ^{222}Rn seem to go hand-in-hand. Because the pattern exists for all APEI classes, we believe that the residence time of the water in the polder is such that there is ample time for degassing of CO_2 and radon and decay of radon in the surface water system under almost all weather conditions.

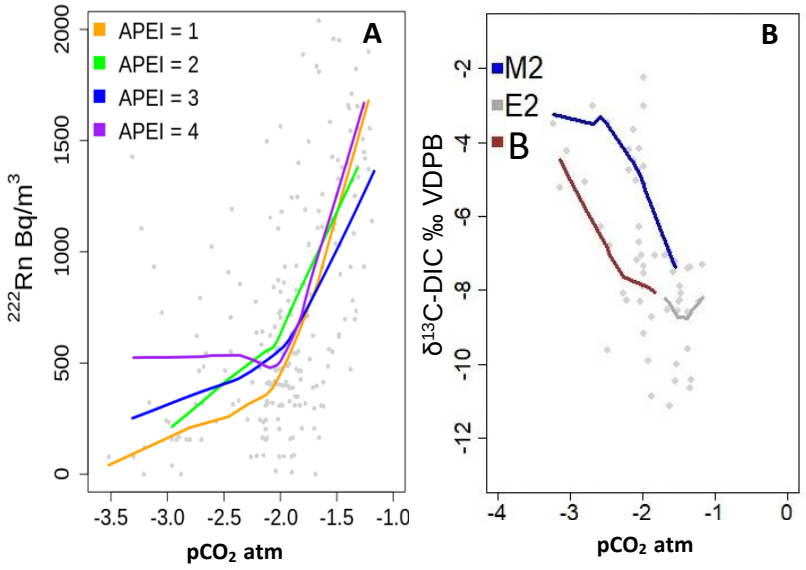

Figure 3.9 Relations between ^{222}Rn, $\delta^{13}C$-DIC and pCO_2 during the 2016-2017 monitoring campaign. A: ^{222}Rn versus pCO_2 for all 9 locations and divided over 4 APEI classes (1 = dry, 4 = most wet, LOWESS smooth represent the central tendency in the scatter), B: $\delta^{13}C$-DIC versus pCO_2 for the location B, M2 and E2.

The small amount of $\delta^{13}C$-DIC data available give extra clues for this hypothesis (Fig.3.9 B). The $\delta^{13}C$-DIC values measured at three locations in and outside the polder follow an inverse relation with the partial CO_2 pressure for locations B and M2. The $\delta^{13}C$-DIC values are highest under conditions of CO_2 equilibrium with the atmosphere (pCO_2 ~$10^{-3.5}$) and lowest when typical groundwater partial CO_2 pressures are measured ($10^{-1.5}$ atm). This suggests that $\delta^{13}C$ fractionates during exchange with the atmosphere, leaving the remaining water in the ditch enriched in $\delta^{13}C$ following a Rayleigh type process (Mook 2006). We relate the absence of such an exchange pattern in the shallow ditch E to the short residence time of water, which is confirmed by the high ^{222}Rn and partial CO_2 pressures in this ditch and the observation that the water flows significantly in this shallow ditch. For this interpretation, we need to assume that biological processes, such as primary production, play no role, which seems reasonable given the mere absence of water plants in the polder, combined with the low O_2 concentrations that were measured under dry conditions. These low O_2 conditions, that result from the continuous seepage of low-oxygen water to the polder water system, are assumed to be the prime reason for this lack of vegetation.

3.3.3 Temporal variations at the polder's main outlet

Further information about the functioning of the polder system was derived from studying the temporal patterns of the main solutes concentrations at the pumping location P, which covers the longest monitoring record. Figure 3.10 shows the concentration ranges of the measured variables at location P in relation to the wetness classes from the APEI analysis (very dry (class 1), dry (2), wet (3) and very wet (4) as done previously by Rozemeijer & Broers (2007). The graphs of Fig.3.10 combine the data of the long time series (2006-2016) and the March 2016 - June 2017 monitoring campaign.

In general, the 2016-2017 weekly/biweekly dataset aligns well with the longer time series covering the monthly data of 2006-2017. A clear decreasing trend in concentrations from dry to wet conditions was observed for Cl, EC, HCO_3, and Ca, reflecting groups 1 and 2 of the PCA analysis (see section 3.3.1). The opposite is true for the O_2 concentrations and the SO_4/Cl ratio (groups 4 and 6). Less distinct patterns occur for pH and pCO_2 (small decrease towards wetter conditions) and NH_4 (small decrease towards wet conditions but large variation). No significant pattern was observed for TP and turbidity (Suspended Matter ZS). The pattern for ^{222}Rn is deviant, showing the highest concentrations under intermediate wetness, and lower concentrations at very dry and very wet conditions.

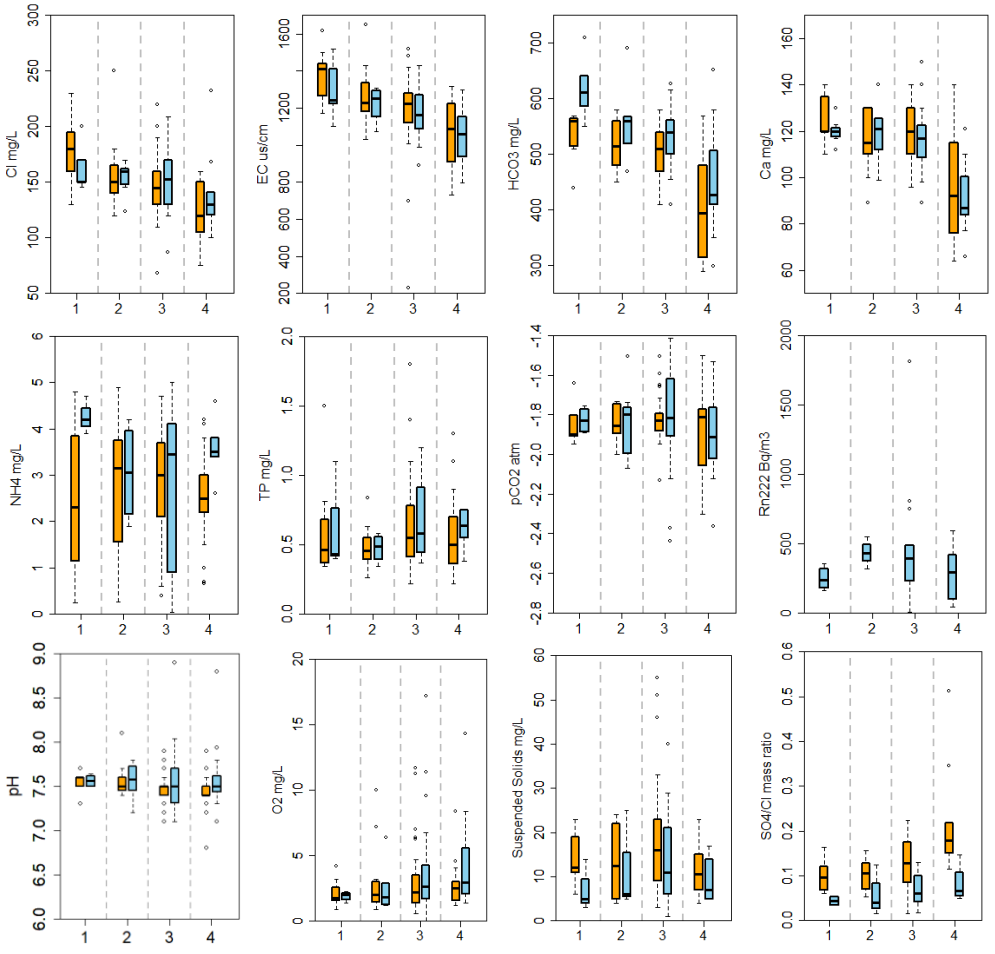

Figure 3.10 Water quality at the main outlet as a function of catchment wetness (APEI classes 1 to 4, very dry to very wet). Orange: 2006-2016 long time series, blue: monitoring campaign 2016-2017.

The general trend observed for the main constituents of the water (Cl, HCO_3, Ca and EC, groups 1 and 2 of the PCA analysis) is a concentration decrease towards wetter conditions. This trend should be regarded as a dilution process, as runoff water is transported to the main water courses draining the polder and pumped out at the monitoring location. The increase in O_2 concentrations towards wetter

conditions confirms this hypothesis, as the runoff was high in O_2 during the spatial survey under wet conditions as well (see section 3.3.1). The smaller, less distinct decrease in NH_4 and TN (not shown) is probably also related to this dilution pattern. However, the temporal patterns of these nutrients may be obscured by the increased flow through the drain system which brings a mixture of rain water and shallow groundwater towards the main ditches. This drain water is now known to transport 3-5 mg/L of NH_4 which might effectively buffer the variability in NH_4 concentrations at the pumping station where all water is collected. This process might also be responsible for the decreasing trend in pH and the buffering of the partial CO_2 pressure going from dry to wet conditions. Both drain flow and runoff may add to the increasing SO_4/Cl ratio, which indicates that sulfate-reduced water with a SO_4/Cl ratio < 0.14 that originated from groundwater seepage is replaced and diluted with runoff and drain water that both carry SO_4 towards the main waterways in the polder (see Fig.3.4, and group 6 in Fig.3.3). It is no surprise that TP, pCO_2 and ^{222}Rn do not show the overall dilution patterns, as these variables were grouped together in the reactive group 3; solutes and gases that are supplied by groundwater, but react or exchange within the polder system itself.

Here, the ^{222}Rn pattern of Fig.3.10 seems most complicated. As a tracer of groundwater, the emanated ^{222}Rn is taken up by the groundwater when passing through soils and sediments (Grolander, 2009). We observed that ^{222}Rn was high in both shallow and deep groundwater (1500-4000 Bq/m^3, see Fig.3.4). At first sight, one would expect base flow to be traced by high ^{222}Rn concentrations from groundwater seepage, and therefore expect the highest ^{222}Rn at dry conditions. However, the residence time of ^{222}Rn in the surface water system is probably the longest under dry conditions with low surface water flows. Given the short half life time of dissolved ^{222}Rn of 3.8 days, ^{222}Rn in water that is no longer in contact with sediments will decrease relatively fast by both decay and exchange with the atmosphere which apparently led to concentrations less than 350 Bq/m^3 in the ditch water under dry conditions. The highest ^{222}Rn concentrations at the pumping station were found at intermediate conditions between dry and wet (APEI classes 2 and 3, Fig.3.10) where an optimum is obtained between the groundwater seepage and drain water fluxes (see Fig.3.4) that supply ^{222}Rn and the loss of ^{222}Rn through radioactive decay and atmospheric exchange. Under very wet conditions, the ^{222}Rn concentrations seem to be diluted by the influx of ^{222}Rn free runoff water, which explains the deviant ^{222}Rn pattern shown in Fig.3.10.

3.3.4 The effects of urbanization on polder hydrogeochemistry

In the Netherlands and other lowland areas, expanding cities rely on areas that are not automatically optimal for urban development. Reclamation of wet areas, creating polder systems, requires the lowering of water levels and drainage of the areas. These polder systems demand a system for continuously pumping the surplus of seeping groundwater to higher grounds. The low water levels that are maintained enhance the oxidation of peat and compaction of clay, which may release nutrients and heavy metals into shallow groundwater and the seepage of deeper nutrient-rich groundwater may amplify that problem as we disclosed in the paper. This study shows the strong effect that city infrastructure has on the reactive interfaces between O_2-rich rainwater and reduced deep groundwater. Our polder Geuzenveld is a lowland urban polder fed by a large amount of groundwater through four seasons. It has a separated drainage system that collects O_2-rich rain water and transports this into the ditches. The groundwater drainage system and the system of ditches effectively drain the area and a pumping station controls the surface water level in the polder. These infrastructures cause faster and

shorter transport routes of groundwater into the open water system. The O_2-rich and heavy metals loaded runoff mixes with the anoxic, nutrient- and Fe-rich groundwater in the open ditch water system, leading to a number of subsequent hydrochemical processes in the polder, such as the precipitation of Fe-hydroxides, the sorption of phosphorus and exchange of gases with the atmosphere.

In lowland cities, the construction of separate drainage systems for runoff and shallow groundwater effectively changes the natural reactive interface between anoxic groundwater and oxic infiltrating water, bypassing the soil system that normally plays an attenuating role. Without a drainage system, part of the mixing and reactions are likely to take place in the redox transition zone within the soil or shallow subsurface and fluxes of Fe, As, P, and heavy metals may never reach the surface water system. By separating the flow routes, both the nutrient-rich groundwater and the heavy metal rich runoff bypass the natural redox transition zone and directly enter the surface water system. The binding of P and heavy metals may then take place within the surface water system, but a larger proportion of the contaminants and metals may be able to affect downstream water resources.

In our urban system, the nutrient-rich groundwater and the oxygen- and metal-rich runoff bypass the soil system and mix only within the receiving ditch system, which yields a relatively dynamic water quality pattern with oxygen-low and oxygen-high phases alternating with time. Therefore, a side-effect of the separated flow routes is that the continuous supply of low-oxygen groundwater in dry periods seems to prevent the growth of water plants, leaving runoff and exchange of O_2 with the atmosphere as primary sources of O_2, thus determining the ecological status of the water system. Further research is necessary how to optimize such artificial urban systems to deliver ecological and chemical status of the surface water that is healthy for the residents globally that live in these lowland urban catchments. Remediation techniques might involve to artificially increase O_2 concentrations in dry periods, by the inlet of water from the oxygen-rich boezem, of by enhancing the oxygen-mixing by promoting gas exchange with the atmosphere by bubbling of air and the creation of fountains.

3.4 Conclusions

In this study, we identified the major flow routes of nutrients, heavy metals and major ions in a groundwater-influenced urban catchment and interpreted the mixing of the runoff, drain water and groundwater in the surface water system through space and time. For this goal, we conducted a spatial and temporal analysis of water quality and isotope data using a 10-year dataset with monthly data and a monitoring campaign with a (bi)weekly frequency during the years 2016-2017.

In our urban lowland polder catchment, groundwater seepage constantly determines the surface water quality, being the main source of solutes in the water system. A Holocene tidal channel with sandy deposits in the SW of the polder hydraulically connects the deeper aquifer system with the shallow groundwater, thus providing a pathway for seepage of the high DIC and nutrient-rich waters present at 30 m depth. The resulting groundwater seepage is low in O_2 and high in Cl and the nutrients N and P. Runoff from the paved areas and roofs under wet weather conditions supplies the surface water system with O_2 and the trace metals Al, Cu, Pb, Zn and Cd, and dilutes the water for all other components under wet weather conditions. PCA analysis reveals that mixing between these two flow components with contrasting chemistry is determining the composition of the water that is pumped from the

catchment. An artificial groundwater drainage system provides a third flow route that captures a mixture of shallow groundwater and recently infiltrated rain water and adds to the sulfate concentrations and nutrients under intermediate and wet conditions. The PCA analysis helped to distinguish 6 subgroups of water quality variables that are indicative of the retention and reactivity of the different solutes in the open water system.

The concentrations that are pumped out at the polder outlet are a mixture of these transport routes and feed the receiving boezem water system with a time changing pattern of solutes. For the major groundwater derived solutes such as Cl, HCO_3, Ca and Na, a clear dilution pattern in periods with low-mineralized runoff is obvious at the pump location. Other solutes, including Fe, TP, NH_4, pCO_2 and ^{222}Rn undergo retention and/or reactive processes. The data suggests that TP is sorbed and fixated to Fe-hydroxides in the ditch sediments due to the mixing of oxygen-rich runoff with seeping groundwater, that NH_4 is partly released from the shallow subsurface and that CO_2 and ^{222}Rn undergo atmospheric exchange and/or radioactive decay, suggesting that the residence times of the water in the polder suffices to equilibrate the concentrations with the atmosphere, except under very wet conditions.

The regular low O_2 conditions in the water system of the polder, that result from the continuous supply of low-oxygen groundwater, seem to prevent aquatic plants growing there and leaves runoff and exchange of O_2 with the atmosphere as primary source of O_2, thus determining the ecological status of the water system. The separation of flow routes that is artificially created during the building of the residential area distinguishes the water quality processes from natural or agriculture dominated catchments. In our urban system, the nutrient-rich groundwater and the oxygen- and metal-rich runoff bypass the soil system and mix only within the receiving ditch system, which yields a relatively dynamic water quality pattern with oxygen-low and oxygen-high phases alternating with time. Further research is imperative for optimizing such artificial urban systems to deliver ecological and chemical status of the surface water that is healthy for the residents globally that live in these lowland urban catchments.

Supplementary Information

S3.1 Information over the rain water collection system, the groundwater drainage system and the sewage system in the study area

Polder Geuzenveld has a separated system of sewer and rain drainage system. Groundwater drainage system is also planted to drain excessive groundwater into surface water. Figure S3.1.1 and Figure S3.1.2 show the groundwater (purple line) drainage and rain water drainage (blue lines) systems. The red line is the main sewer system that transport municipal water to the treatment plant.

The precipitation on the roofs is collected by the pipes installed on the buildings, and transported to the rain water manhole, that is connected to the ditches. Precipitation on the street is considered as runoff that flows into the drainage system which also ends up in the manhole then flow into the ditches.

The outlets are the places where the pipes end. At the locations of the outlets, water qualities are influenced depends on it is rain water drainage outlet or groundwater drainage outlet. There are rain water outlets in the west and middle ditches, especially location W1 and M1 (where A and G for survey sampling, rain water influenced water sample were collected). The groundwater drainage system only placed in the middle of the polder with the outlets open in the north (1 outlet) and south ditches (3 outlets). The two outlets in the west and middle ditch are hidden. There are no outlets open in the East ditch, which leave location E1 and E2 out of influences from runoff and drain water.

The manholes accordingly belong to rain water, groundwater drainage and sewer water. Each of them has their elevations refer to N.A.P and codes recorded in Waternet's water system. The outlook of the manholes is shown in Fig.S3.1.3.

S3.2 Data collection and data treatment

Groundwater sampling

Groundwater in the polder (GWS, shallow piezometers) and around the polder (GWD1 and GWD2, deeper groundwater at ~1 km distance) was sampled twice during the monitoring campaign. Once in the dry season (May 2017) and once in the wet season (November 2017). Groundwater wells were purged removing at least three times of the stagnant water volume in the tubes using peristaltic pumps. The pump was connected to a flow through cell, and the pH, O_2, and EC were measured on-site until stabilization. Additionally, alkalinity as HCO_3 was measured on-site using an AL-DT HACH digital titration set. Parameters measured included pH, O_2, EC, HCO_3, Cl, ^{222}Rn, and $\delta^{13}C$-DIC.

Figure S3.1.1 Groundwater drainage system and the sewer system

Figure S3.1.2 Rain water drainage system and the sewer system

Figure S3.1.3 Example of a manhole of the groundwater drainage system (the dead fish indicates the possible back flow from the ditch to the drain manhole)

Sampling the flow routes during a spatial survey

Five sample bottles were filled at each sampling point. Three samples were filtered through 0.45 µm filter for analysis at the joint TNO/University Utrecht Central Environmental Laboratory (Utrecht Castel). The samples that were pre-acidified with sulfuric acid were used for the analysis of ortho-PO_4, NH_4 (NEN-EN-ISO-11732 and NEN-EN-ISO-15681-2, respectively), and for Dissolved Organic Carbon(DOC) (NDIR). The samples that were pre-acidified with nitric acid was analyzed by ICP-MS for metals and TP. The non-acidified sample was used to measure NO_3, Cl, and SO_4, using IC. The additional two samples were treated as regularly done by the Waternet water board who do not typically filter the samples. TP was analyzed photometrically (NEN-EN-ISO 15681-2, 2005) and NH_4 using a discrete analyzer (NEN ISO 15923-1). Analysing TP and NH_4 in both labs was intended for quality control and for matching the long-term grab sampling time series from Waternet with the results of this spatial survey. In addition, comparing TP concentrations (filtrated and non-filtrated) and ortho-P concentrations helped to identify species of phosphorus among locations. 72% of the samples had an ion balance error of < 5%. Large deviations were only found for the samples that contained low-mineralized runoff water, where measurement errors easily lead to deviations > 5%.

Short and long term water quality monitoring

During the monitoring campaigns, each sample was collected under random hydrological conditions following a systematic sampling design with fixed sampling moments in time. The weekly and biweekly samples at the 8 new locations yielded values of EC, O_2, pH, HCO_3, and Cl that were measured on-site. The database contains results of EC, pH, and O_2, suspended solids (SS), Ca, Cl, HCO_3, SO_4, NH_4, and TP. The collected samples were preserved onsite according to the standard NEN-EN-ISO 56667-3 (2012). Cl, NH_4, SO_4, and Ca were filtered at site. TP and Ca were acidified with respectively sulfuric acid and nitric acid. The field parameters EC, pH, and O_2 were measured with a Hanna HI9828 multi parameter probe and analyzed according to the standards NEN-ISO 7888 (EC), NEN-EN-ISO 10523 (pH) and in-house method (O_2). The following parameters were analyzed at the laboratory: SS is a filtration method and analyzed according to standard NEN-EN 872; HCO_3 is a titration method and measured with a Metrohm titrator, according to an in house method; Cl, NH_4, and SO_4 were measured with a discrete Analyzer (DA) according to the standard NEN-ISO 15923-1; TP

was measured with a continuous flow auto analyzer (AA) according to the standards NEN-EN-SIO 15681-2 and NEN 6645; Ca was measured with an ICP-MS according to the standard NEN-EN-ISO 17294-2. For quality assurance, we checked the ion charge balance of this dataset using following Appelo, et al. (2010).

δ^{13}C-DIC and ^{222}Rn sampling

δ^{13}C-DIC samples of the surface water at locations M2, E2, and B' were prepared in 100 mL brown glass bottles and stabilized with mercury chloride in the field. δ^{13}C-DIC samples for groundwater were taken from May 28th-30th 2016 with a similar sampling procedure. δ^{13}C in dissolved inorganic carbon was measured using mass spectrometry (Thermo Finnigan Isotope Ratio Mass Spectrometers). δ^{13}C-DIC is reported as δ^{13} (in ‰) using the universal δ notation with VPDB (Vienna Pee Dee Belemnite) as standard for marine carbonates. We applied the RAD-H2O (Durridge Company, 3D printed aerator cap) to analyze ^{222}Rn concentrations in water. ^{222}Rn samples were taken without filtration in 250 mL glass vials and were analyzed in the field. Before the measurement, the RAD-H2O system had to be purged to remove potential ^{222}Rn residuals and to get the humidity of air lower than 10%. Then the glass vial was connected to the cap that formed a loop connection with the RAD 7 detector. Desiccant dehumidifier was used to keep the loop dry. Following the protocol, it first aerated the system for 5 minutes to achieve an equilibrium of 222Rn in the water and air in the whole system. Subsequently, 4 measuring cycles of 5 minutes each were done. After this, we used the RAD 7 data processing software (Capture) to get an average ^{222}Rn concentration value corrected for humidity.

S3.3 Calculating the Antecedent Precipitation-Evaporation Index

For analyzing the surface water composition during different hydrological conditions, we divided the samples based on the APEI at the moment of sampling. We collected precipitation and potential evaporation (Makkink, 1957) data from the Schiphol Airport KNMI (The Royal Netherlands Meteorological Institute) weather station, which is located 9 km south from polder Geuzenveld. We divided the hydrological condition of the catchment for each day into 4 classes from driest (class 1) to wettest (class 4) based on the calculated APEI values as below, following the procedure of Rozemeijer et al., 2010:

$$APEI_t = APEI_{t-1} \times Decay\ rate + (Precipitation - Evaporation)_t \quad \text{(S3.1)}$$

APEIt is APEI (mm) at day t. Precipitation and evaporation are both daily records in mm (KNMI, http://www.knmi.nl). We chose a decay rate of 0.76 in this study area, based on the best fit between daily and weekly accumulated APEI values with known pumping volumes at the principal outlet of our polder system, and the recession line of the water levels.

We strived for a reasonable division of the periods with dry, intermediate, and wet conditions and used expert judgement to derive the following distribution of time over the 4 wetness classes: 12%, 13%, 50%, and 25% covering the period 2006-2017 (Fig.S3.3.1). The associated APEI values of each class were: APEI <= -10 for class 1, -10 < APEI <= -5 for class 2, -5 < APEI <= 9 for class 3, and APEI > 9 for class 4. The distribution of the wetness classes gives a good fit between pumping rates and weekly APEI (Fig.S3.3.2) and yields an acceptable and credible distribution of the wetness classes over the

seasons and in relation to periods with large precipitation events. The wettest period with accordingly higher classes are more found in autumn and winter and the driest are in spring and summer.

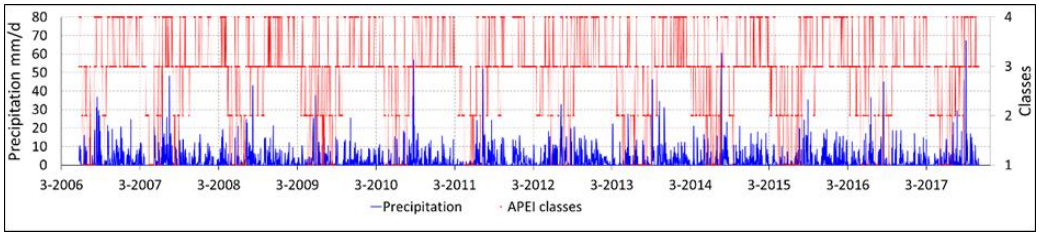

Figure S3.3.1 APEI wetness classes with precipitation from 2006 to 2017, left y-axis is precipitation in mm/d (blue color), right y-axis is APEI classes (red color).

We tested the APEI indicator against the weekly pumping rate for the 2006-2017 period. A small number of values of Q (weekly discharge rate) > 30000 m^3/week were considered improbable given the total capacity of the pumps in the pumping house, and the known pumping schedule of the water board, were distracted from the analysis. The graph indicates that pumping is much less in dry periods with negative weekly APEI than in wet periods with positive weekly APEI.

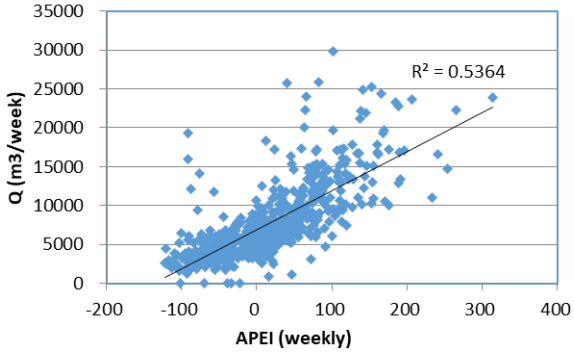

Figure S3.3.2 weekly cumulative pumping rates with weekly cumulative APEI of polder Geuzenveld

S3.4 Boxplots of the 2017 survey and the results of the principle component analysis

Table S3.4.1 Cumulative explained variance of the principle components

	PC1	PC2	PC3	PC4
Scaled (original value-mean)/SD	0.57	0.72	0.79	0.85
Scaled & normalized (box-cox in R program)	0.66	0.76	0.83	0.89

The correlation of the variables to each component is not shown, as they are almost all correlated to the first component.

Group 1:

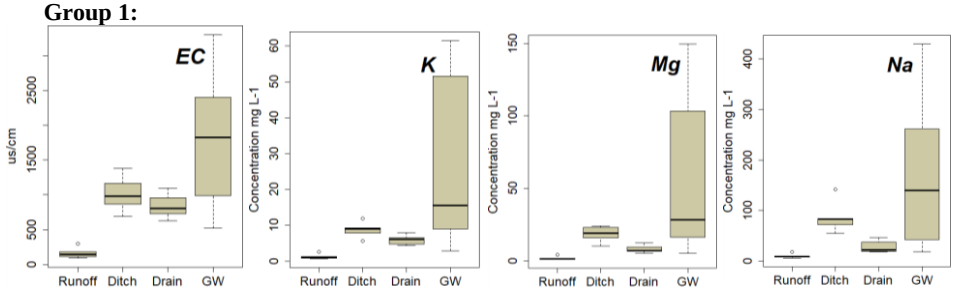

Group 2:

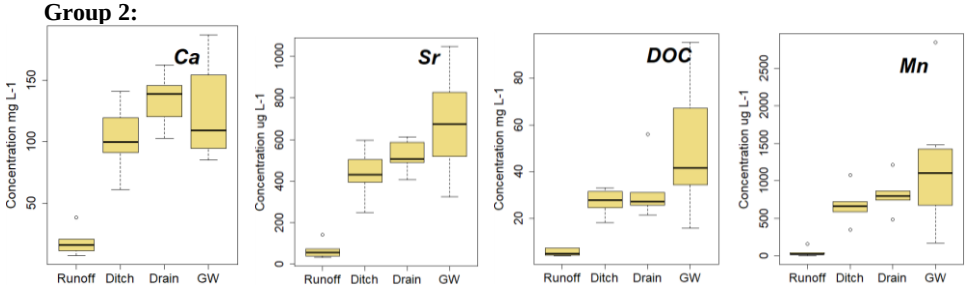

Group 3:

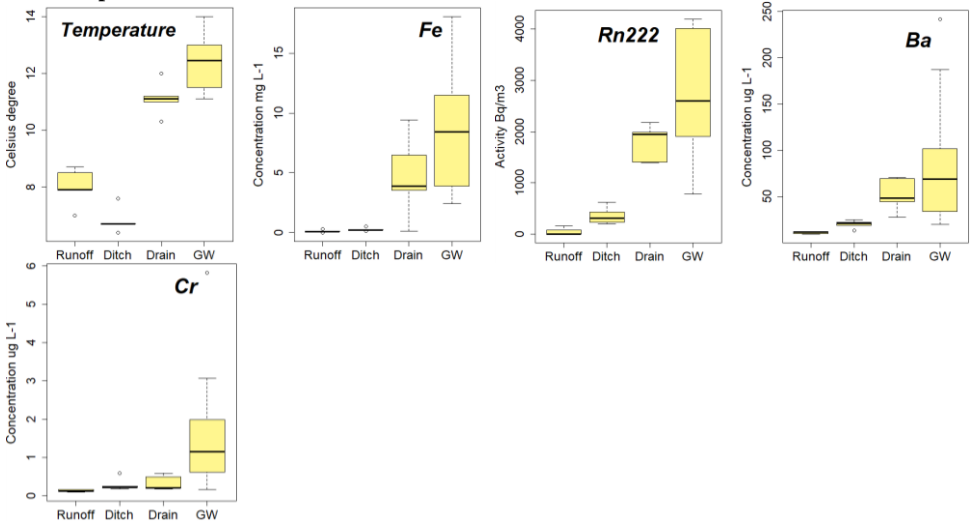

Group 4:

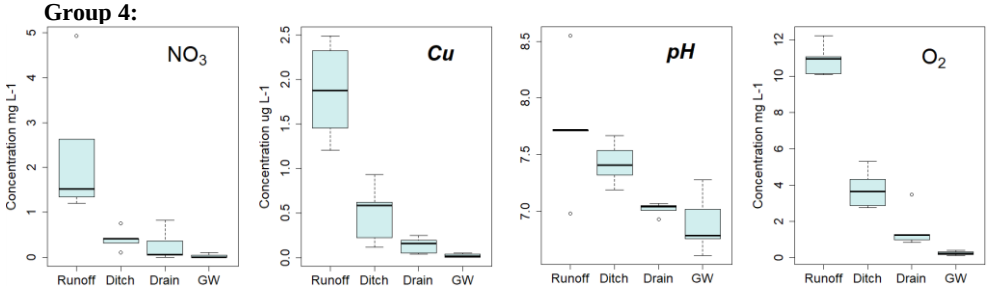

Group 5:

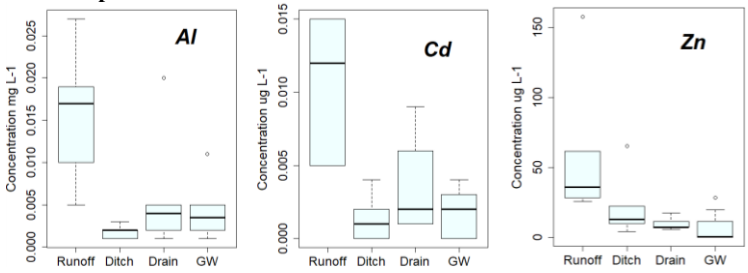

Group 6:

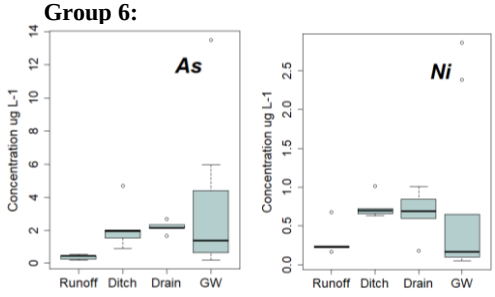

Figure S3.4.1 Concentrations of the water quality variables collected during the 2017 survey, ordered using the groups from the PCA resullts below as a function of the flow routes sampled: runoff (observation number n = 5), ditch water (n = 5), drain water (n = 5), and groundwater (n = 10).

S3.5 Mixing processes using a Piper diagram

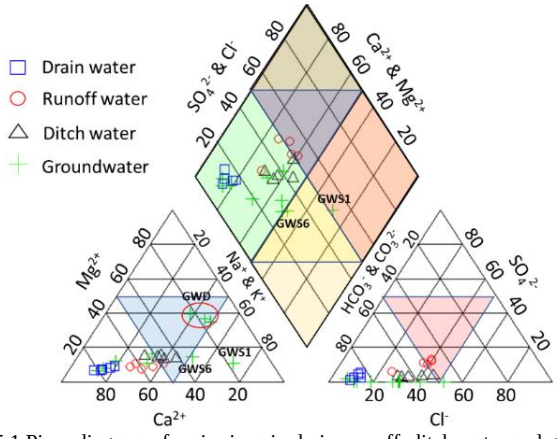

Figure S3.5.1 Piper diagram of major ions in drain, runoff, ditch water and groundwater

We primarily used a PCA approach to unravel the mixing processes in our urban catchment, but add a Piper diagram here which confirms the main mixing processes that we identified in the main text. Ditch water is centered in the diagram and is a mixture between the 3 main flow routes: seepage of groundwater, and inflow of drain and rain water. The Piper diagram also confirms our finding the shallow groundwater at locations GWS 1 and GWS 6 in the southwest polder show some similarity

with the deeper groundwater and reveals a slightly brackish signature in this shallow water with higher Na and Cl. In the main text, we argue this to be the result of seepage through the connection between the deep and shallow groundwater in the southwest part of the polder where the tidal channel is located. The other shallow wells show large similarity to the drain water, and mainly fresh infiltrated water is transported by this shallow system of groundwater and drains.

S3.6 Pictures of the setting of the locations where water from the canals was sampled during the 2016-2017 water quality surveys

Location W1

Location W2

Location M1

Location M2

Location E1

Location E2

Location B’

Location B

Location Pump

The park

S3.7 Iron-hydroxides precipitation

The following pictures show the iron-hydroxides precipitation phenomenon, during dry and wet period. Iron-hydroxides are indicated by the brown color in the water bodies. In the dry period, the water bodies had brownish color and low transparence. In the wet period (which just after ample rain), the appearance of the water was still brownish while only the upper part is more transparent made the iron precipitant in the deeper water or on the bottom visible. Iron precipitants also clearly visible in the aeration sampling plate in the water, which bubbles water to repel dirt, that brought O_2 into water and caused dissolved iron precipitated on the plate.

Figure S3.7.1 Iron precipitation on an aeration sampling plate

S3.8 Information about the precipitation pattern during the November 2017 spatial water quality survey

Ample rainfall happened before and during the survey (2017-11-28 to 2017-12-01) of ditch, drain, rain and groundwater. Ditch, drain and rain water were sampled between 11-28 and 11-29, and groundwater were mostly sampled on 11-30 and 12-01. The ample rainfall events may cause the shallow groundwaterquality dilution.

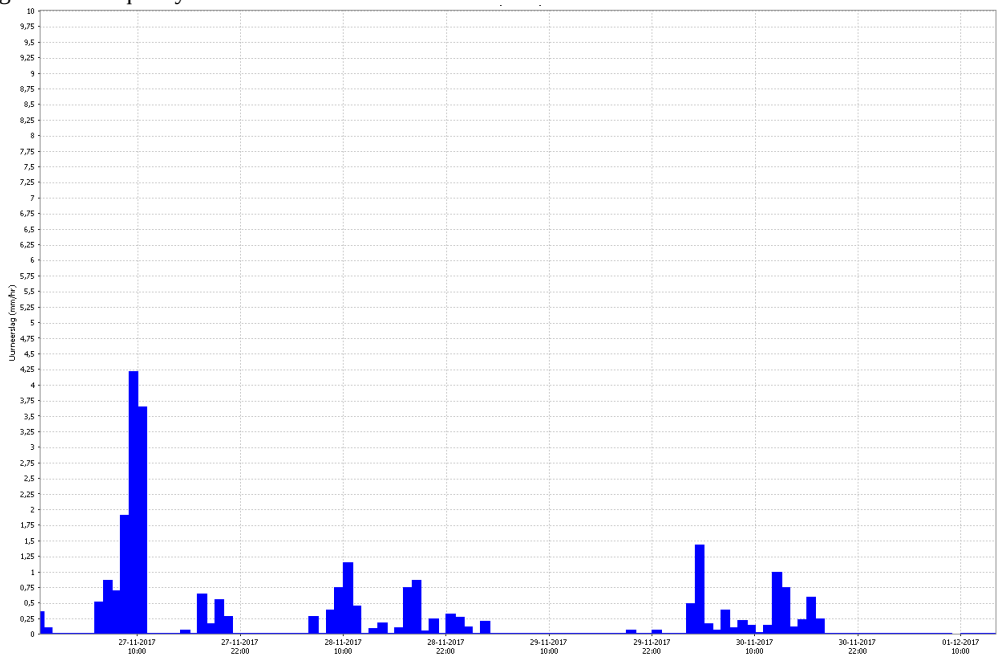

Figure S3.8.1 Precipitation around the survey sampling

Chapter 4

Drivers of nitrogen and phosphorus dynamics in a groundwater-fed urban catchment revealed by high frequency monitoring*

Abstract: Eutrophication of water bodies has been a problem causing severe degradation of water quality in cities. To gain mechanistic understanding of the temporal dynamics of nitrogen (N) and phosphorus (P) in a groundwater fed low-lying urban polder, we applied high frequency monitoring in Geuzenveld, a polder in the city of Amsterdam. The high frequency monitoring equipment was installed at the pumping station where water leaves the polder. From March 2016 to June 2017, total phosphorus (TP), ammonium (NH_4), turbidity, electrical conductivity (EC), and water temperature were measured at intervals smaller than 20 minutes. This paper discussed the results at three time scales: annual scale, rain event scale, and single pumping event scale. Mixing of upwelling groundwater (main source of N and P) and runoff from precipitation on pavements and roofs was the dominant hydrological process governing the temporal pattern of the EC, while N and P fluxes from the polder were also regulated by primary production and iron transformations. In our groundwater-seepage controlled catchment, NH_4 appeared to be the dominant form of N with surface water concentrations in the range of 2-6 mg N L^{-1}, which stems from production in an organic-rich subsurface. The concentrations of NH_4 in the surface water were governed by the mixing process in autumn and winter and were reduced down to 0.1 mg N L^{-1} during the algal growing season in spring. The depletion of dissolved NH_4 in spring suggests uptake by primary producers, consistent with high concentrations of chlorophyll-a, O_2, and suspended solids during this period. Total P and turbidity were high during winter (range 0.5-2.5 mg P L^{-1} and 200-1800 FNU, respectively) due to the release of P and reduced iron from anoxic sediment to the water column, where Fe^{2+} was rapidly oxidised and precipitated as iron oxides which contributed to turbidity. In the other seasons, P is retained in the sediment by sorption to precipitated iron oxides. Nitrogen is exported from the polder to the receiving waters throughout the whole year, mostly in the form of NH_4, but in the form of organic N in spring. P leaves the polder mainly during winter, primarily associated with $Fe(OH)_3$ colloids and as dissolved P. Based on this new understanding of the dynamics of N and P in

* Based on: Liang Yu, Joachim Rozemeijer, Hans Peter Broers, Jack J. Middelburg, Boris M. van Breukelen, Maarten Ouboter, Ype van der Velde. Drivers of nitrogen and phosphorus dynamics in a groundwater-fed urban catchment revealed by high frequency monitoring. *Hydrology and Earth System Sciences*, 2020 (Accepted).

this low lying urban catchment, we suggested management strategies that may effectively control and reduce eutrophication in urban polders and receiving downstream waters.

4.1 Introduction

Eutrophication is one of the most notorious phenomena of water quality impairment in cities, caused by excess inputs of N and P. The identified sources of nutrients are from wastewater treatment plants, storm runoff, overflow of sewage systems, manure and fertilizer application in urban green areas and atmospheric deposition (Walsh et al., 2005; Kabenge et al., 2016; Toor et al., 2017; Yang & Toor, 2018; Putt et al., 2019). Recently, groundwater has been identified as another important source of N and P in cities situated in low-lying deltas, where dissolved NH_4 and PO_4 in groundwater seep up into urban surface water (Yu et al, 2018 & 2019). The upwelling nutrients in groundwater, originating from the organic rich delta subsurface, reaching the surface water of cities and are transferred to downstream waters and eventually reach the coastal zones, where they may induce harmful algal blooms or cause hypoxia along coastlines (He and Xu, 2015; Beusen et al., 2016; Le Moal et al., 2019). Hence, it is of pivotal importance to understand N and P dynamics in the urban freshwater bodies in order to mitigate the input of nutrients into the oceans (e.g. Nyenje, et al., 2010; Toor et al., Paerl et al., 2016; 2017; Le Moal et al., 2019).

Nutrients dynamics are governed by biological, chemical and physical processes and their interactions. Assimilation by primary producers is a major biological factor regulating N and P concentrations in the aquatic environment. Aquatic micro- and macro-organisms assimilate P as PO_4 and N mainly in fixed forms such as nitrate (NO_3) and ammonium (NH_4), but for some specific organisms also in the form of N_2. In estuaries, NH_4 is the preferred N-form for microbes (Middelburg and Nieuwenhuize, 2000), but the uptake rate for both NH_4 and NO_3 can achieve maximum rates under sustained exposure of NH_4 or NO_3 (Bunch and Bernot, 2012). Moreover, the nitrogen species are also involved in redox transformations (Soetaert and Herman, 1995). Under anaerobic conditions, NO_3 can be reduced to NH_4, in particular with high organic matter contents. It may also be denitrified to N_2 and N_2O under such condition (Mulder et al., 1995), the latter is a climate-active gas. Under aerobic conditions, NH_4 can be oxidized to NO_3 through nitrification by nitrifying microbes, which is an O_2 consuming and acid generating process. Nitrification even occurs under cold conditions (below 10 °C) (Painter, 1970; Wilczak et al., 1996; Cavaliere and Baulch, 2019).

The mixing of water from different flow routes is an important hydrological process that controls nutrient dynamics (Rozemeijer and Broers, 2007; Rozemeijer et al., 2010a; Van der Grift et al., 2014; Yu et al., 2019). As nutrient concentrations and speciation differ among different flow routes (Wriedt et al., 2007; Rozemeijer et al., 2010a; Yu et al., 2019; Yang and Toor, 2019), the mixing process results in dilution or enrichment of nutrients in surface water bodies during precipitation events (Wang et al., 2016).

Retention is another factor that determines nutrient concentrations and transport (McGlathery et al., 2001; Zhu et al., 2004; Henry and Fisher, 2003), especially for phosphorus most of which is retained in inland water bodies sediment (Audet et al., 2019). The retained P are either being permanently buried in the sediment or temporarily stored and acting later on as internal nutrient source (Kleeberg et al., 2007; Filippelli, 2008; Zhang et al., 2018). Multiple researchers have highlighted the influence of iron chemistry on the dynamics of P in pH neutral environments (Chen et al., 2018; Van der Grift et al., 2018). This is especially relevant when iron-rich groundwater interacts with surface water (Griffioen, 2006; Rozemeijer et al., 2010a; Van der Grift, 2014; Yu et al., 2019), in which P is immobilized by the

formation of iron(oxy)hydroxides during groundwater aeration. However, changes in chemistry or temperature may lead to the release of P and reduced iron. For instance, under anaerobic conditions, Fe and P can be mobilized by sulfate reduction, but this can be counteracted by the presence of NO_3 as electron acceptor (Smolders et al., 2006).

Most studies of eutrophication are based on discrete sampling events which can give a general pattern of nutrient dynamics, but can easily miss important nutrient transport and processing phenomena (Rozemeijer et al., 2010; Rode et al., 2016; Toor et al., 2017). The countermeasures to control eutrophication have been hampered because of limited knowledge of N and P dynamics, for instance their response to changing weather conditions and land use (van Geer et al., 2016). In the past few years, the development of new sensors and sampling technologies allow us to obtain data with substantially shorter intervals. In this paper, the high frequency monitoring technology is referred to as an automatic monitoring program with sampling and analyzing frequencies that are sufficient for obtaining detailed water quality variation information. High frequency technology has proved to be a way to understand nutrient dynamics (Rode et al., 2016; Van Geer et al., 2016; Bieroza et al., 2018). Due to the abundant information offered by this technology, combined methodologies have been developed to quantitatively understand the in stream hydrochemistry of nutrients (Miller et al., 2016, Van der Grift et al., 2016, Duncan et al., 2017).

In our previous study on the water quality of Amsterdam (Yu et al, 2019), the transport routes of N and P from groundwater to surface water through seepage and drains were identified. In addition, spatial and temporal concentration patterns from discrete sampling campaigns showed a clear dilution pattern of other water quality parameters such as EC. However, the temporal patterns of N and P were still poorly understood, probably due to their reactive nature and more complex biogeochemistry. In order to obtain insight into the controlling mechanisms of N and P transport and fate in urban delta catchments affected by groundwater, we performed a year-round high-resolution N and P concentration monitoring campaign. A deep understanding of the water quality dynamic drivers would be a great asset for controlling eutrophication and improving aquatic ecological status (Fletcher et al., 2015; Díaz et al., 2016; Eggimann et al., 2017; Nizzoli et al., 2020). We conducted a one-year high frequency monitoring campaign in 2016-2017. Measured parameters were EC, NH_4, TP, turbidity and water temperature. The temporal patterns of these parameters were studied at three time scales: the annual scale, rain event scale, and pumping event scale.

4.2 Methods

4.2.1 Study site

The Geuzenveld study site is part of an urban lowland polder catchment, which is characterized by groundwater seepage that constantly determines the surface water quality, being the main source of solutes in the water system. The groundwater seepage is a continuous source of slightly brackish, anoxic, and iron and nutrient rich water. Yu et al. (2019) presented the results of a 10 year monitoring program describing the main processes determining the water quality in the catchment, which is dominated by mixing of runoff water and seepage water. A high-frequency monitoring campaign was set-up to further unravel the temporal patterns of the nutrient N and P, of which N is typically present in the form of NH_4 from groundwater.

Geuzenveld is a newly built urban polder on the west of the city of Amsterdam (Fig.4.1). Since the 1990s, when it was converted from agricultural to urban land, it has developed into a highly paved area. Similar to other new neighborhoods, Geuzenveld is equipped with a separated drainage system. A rain harvesting system was installed on all the buildings and houses in the polder, leading rain water from the roof and the street directly to the ditches, which results in fast and large amounts of runoff during storm events. Geuzenveld is a groundwater fed catchment due to the constantly higher groundwater head (-2.5 ~ -3 m NAP, NAP: Normalized Amsterdam Peil) in the main aquifer relative to the surface water level in the polder ditches (~ -4.25 m NAP) (Fig.4.2). To keep the foundations of the building dry, there is a groundwater drainage system placed under an artificial sandy layer, right on top of a natural clay layer. The drain elevations range from -4.84 to -4.61 m NAP , which is below the phreatic groundwater level throughout the year, making sure that groundwater seepage either discharges through the drains or the ditches.

The water system of Geuzenveld is connected to the secondary water channel to its east, then connected to the adjacent primary channel, called boezem, the Boezem Haarlemmerweg. The boezem water level is -2.10 m NAP. It is much higher than the target surface water level of Geuzenveld, -4.25 m NAP. The surface water level in polder Geuzenveld is controlled by a pump station, which is the main outlet of this polder, situated in the northeastern corner.

There are two pumps (Pump 1 and Pump 2) in the pumping station, and they have different start and end pumping threshold points (Table 4.1).

Table 4.1 Pumping scheme of polder Geuzenveld

Time	Settings	Pump 1	Pump 2
05:00:00-19:00:00	Start point (m NAP)	-4.20	-4.16
	End point (m NAP)	-4.26	-4.24
19:00:00-05:00:00	Start point (m NAP)	-4.23	-4.18
	End point (m NAP)	-4.31	-4.29

The two pumps are activated when the surface water level exceeds the triggering level which are furthermore separated as day and night triggering levels (Table 4.1). The capacity of each pump is 3.6 m^3 per minute. Most of the time, only one of the two pumps works and the surface water level is maintained between -4.31 m NAP and -4.23 m NAP, which are the night inactive and active pumping levels respectively. Normally, the surface water level drops immediately when the pump(s) start(s) working. Once the pump(s) stop(s), the surface water level will steadily rise due to the continuous inflow of groundwater seepage. During rainfall events, the surface water level rises faster (Fig.4.2A).

4.2.2 Monitoring network setup

4.2.2.1 High frequency monitoring

A high frequency monitoring network was built on a temporary floating platform in front of the pumping station. The water flowed around and underneath this platform to the pumping station when the pumps started working. One year time series of NH_4-N (mg L^{-1}), TP (and ortho-P) (mg L^{-1}), turbidity (Formazin Nephelometric Unit, FNU), electrical conductivity (EC, µS/cm) and water temperature (°C) were collected by the following equipment: a Sigmatax sampler combined with a Phosphax sigma auto analyser for total phosphorus (TP), Amtax for NH_4-N combined with a Filtrax automatic sampler, a Solitax-tline sc for turbidity (manufactured by: Hach Lange GmbH Düsseldorf, Germany), and CTD-Diver for electrical conductivity (EC) and water temperature (manufactured by: Van Essen Instruments,

Delft, The Netherlands). The monitoring frequencies were set to 20 mins, 10 mins, 5 mins, 5 mins and 5 mins interval for TP, NH_4-N, turbidity, EC and water temperature, respectively.

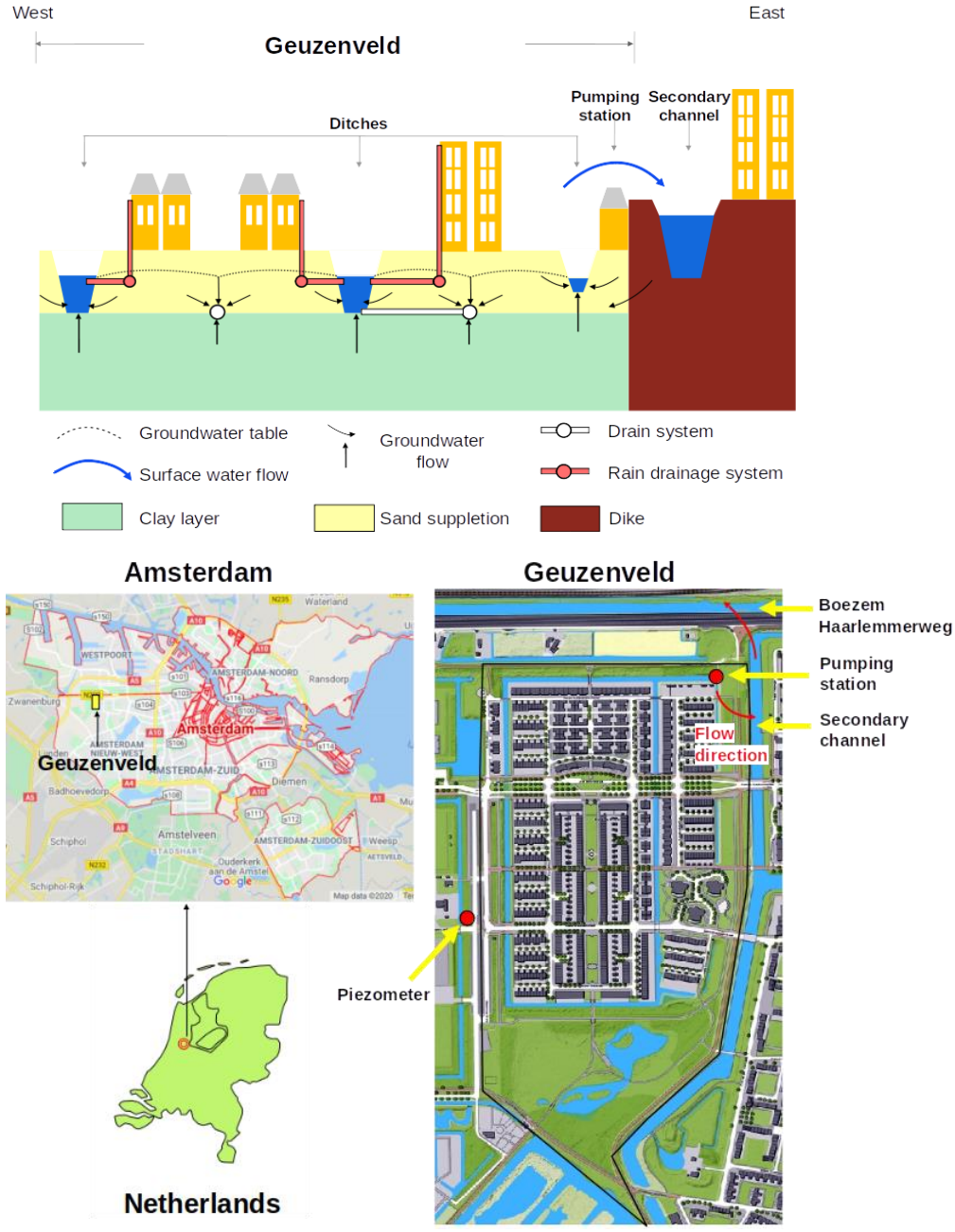

Figure 4.1 Location of polder Geuzenveld (source: © Google Maps) and its landscape cross section and rain water and groundwater drainage system

The Phosphax sigma is an analogue analyser for the high precision determination of total phosphorus concentration in accordance with EN 1189 Phosphormolybdenum Blue method. Samples are automatically taken through a Sigmatax sampling probe and include suspended solids. Subsequently, the sample is ultrasonic homogenized before delivery to the Phosphax sigma. It is digested by the sulphuric acid-persulphate method (APHAAWWA-WPCF, 1989), and analysed with a LED photometer (at 880 nm) (Hach, user manual of Phosphax sigma, 2016).

Samples for NH_4 are prepared by a filtration system, Filtrax. It continuously extracts samples through two ultra-filtration membranes (0.15 µm) plates. Particles get dispersed by a continuous aeration system near the surface of the membranes (The aeration caused severe build-up iron precipitants on the plates). The samples are then delivered to Amtax sc for analysis. The ammonium in the sample is first converted to gaseous ammonia. Only the NH_3 gas passes through the gas-permeable membrane of the electrode and is detected. This method guarantees a wide measuring range and is less sensitive to other compounds compared to methods that make use of an ion-selective electrode (ISE). The Amtax sc in our study was calibrated automatically at 22:00 every 24 hours before September 2016, every 48 hours thereafter. Maintenance work was conducted weekly as the tubes were easily blocked by iron precipitates (Hach, user manual of Amtax sc, 2013).

The Solitax-tline sc sensor is a turbidity sensor with dual-beam optics and added backscatter. The measuring principle is based on a combined infrared absorption scattered light technique that measures the lowest turbidity values in accordance with DIN EN 27027 just as precisely and continuously as high sludge contents. Using this method, the light scattered sideways by the turbidity particles is measured over an angle of 90° (Hach, User manual of Solitax sc, 2009).

The monitoring period of NH_4 and turbidity is from 2016-05-10 to 2017-06-16. Time series of phosphorus were obtained from 2016-05-23 to 2017-06-16. Electrical conductivity and temperature data are from 2016-06-10 to 2017-06-15. The NO_3 analyser, Nitratax, time series consistently showed an artificial drift and proved to be unreliable in our field setting, possibly due to biofilm accumulation in combination with iron oxides precipitation (see discussion). All the equipment outputs were integrated into one wireless station. The monitoring station was shut down several times by lightning, so an electricity restart program was also applied in this network. It worked for all equipment except for the Phosphax, which had to be restarted manually after a black out.

Precipitation (hourly) and Evapotranspiration (daily) data were downloaded from the Schiphol KNMI station which is about 2 km away from Geuzenveld. Hourly pumping activity and surface water level data were obtained from Waternet, the water authority of Amsterdam.

4.2.2.2 Low frequency monitoring

Since 2006, Waternet has monitored the water quality with a frequency of 12 times per year by sampling at the pumping station of Geuzenveld. Between 2016 and 2017, the sampling frequency was increased to twice per month. We selected the following parameters from the routine monitoring campaign: (1) EC, NH_4-N and TP to fill in the gaps in the continuous time series, and to verify and monitor the potential drift and offset of the high frequency data and (2) pH, O_2, HCO_3, NO_3, TN, Kjeldahl-N, suspended solids (detail of methods are described by Yu et al, 2019), chlorophyll-a, and transparency

for further understanding the biogeochemical processes. Organic-N was estimated by subtracting NH_4-N from Kjeldahl-N.

Bi-weekly total iron in the water column was analysed separately using ICP-AES (inductively coupled plasma-atomic emission spectrometry). Total Fe was analysed from samples to which $HgCl_2$ was added for preservation and that were stored in a dark and cool environment. To release all Fe that may have sorbed or precipitated during storage, we added 1 or 0.5 ml HCl in the water samples to dissolve eventual flocks. Then the samples were homogenized in an ultrasonic bath for 24h, mixed again to break down all the flocks. For extraction of all the Fe, we transferred 10 mL of the homogenized sample into a Teflon bottle, added 3.2 mL HCl : HNO_3 3:1 , and stored in a stove at 90 °C for 24 hours. The final solutions were analysed by ICP-AES. Blanks were included and treated identical to samples.

4.2.3 Data processing and analysis

A correlation analysis between the high frequency and discrete monitoring data was applied to illustrate the reliability of the high frequency time series. Furthermore, the time series data were analysed at 3 time scales: annual scale, rainfall events (several days) and single pumping events (several hours). The relationships among the monitored parameters was explored by testing their correlations at each time scale. At the annual scale, a correlation analysis was applied to the complete time period and the wet and dry periods (definition in section 4.3.1.1). To discern the hydrological and chemical/biological attributes to the observed dynamics, a linear mixing model was introduced at the annual scale, assuming precipitation and groundwater seepage are the only water inputs, pumping and evapotranspiration are the only outputs, and pumping activity is the only way solutes leave the water system. In this model, we assumed a constant seepage rate. Accordingly, surface water level was calculated from:

$$\frac{dV}{dt} = \big(P(t) + S - E(t)\big) * A_{polder} - Pump(t) \tag{4.1}$$

$$L(t) = V\,(t)/A_{ditch} \tag{4.2}$$

$\boldsymbol{V}$ is total water volume in the ditches, $\boldsymbol{P}$ is precipitation, $\boldsymbol{S}$ is a constant seepage, $\boldsymbol{E}$ is potential evapotranspiration, $\boldsymbol{A_{polder}}$ is area of the polder, $\boldsymbol{Pump(t)}$ is water volume being pumped out with maximum capacity 216 $m^3\ h^{-1}$, $\boldsymbol{A_{ditch}}$ the area of the ditches in the polder. $\boldsymbol{L}$ is surface water level in the ditches. Water level $\boldsymbol{L}$ determines the activation of pumping activity. Once $\boldsymbol{L(t)}$ exceeds the upper ranges of water level (start point, section 4.2.1), the pumps will start to pump until $\boldsymbol{L}$ goes below the stopping end (section 4.2.1) in the pumping scheme. Given the year-round seepage conditions throughout the polder, combined with an artificially drained subsurface, we assumed that the potential evapotranspiration was close to the actual evapotranspiration as no water shortages occur in our situation. In this study, we used the difference between groundwater head in the first aquifer and the surface water level (Fig.4.2A) to estimate a range of the seepage. The actual number of 2 mm per day was chosen based on the behavior of the mixing model and calibrated using the measured surface water levels (Fig.S4.1).

A complete mixing of solutes was assumed in the model, which means that seepage, ditch water and precipitation mix instantaneously when they enter the surface water. A delay from precipitation to run-off/drainage and to ditches was not specifically considered.

$$\frac{d(VC)}{dt} = S * A_{polder} * C_{gw} + P(t) * A_{polder} * C_P - Pump(t) * C(t) \tag{4.3}$$

$\boldsymbol{V}$ is the ditch water volume given by equation (1), $\boldsymbol{C(t)}$ is solute concentration at time t, $\boldsymbol{C_{gw}}$ is the average groundwater concentration, $\boldsymbol{C_p}$ is the average concentration in runoff.

In our study area, the EC is a useful water quality parameter for describing the mixing processes between groundwater and runoff water, as the EC represents the end members of the mixing: groundwater with an high EC (1750 µS/cm) and runoff water (100 µS/cm) with a low EC (see also Yu et al., 2019). Moreover, we assume that EC behaving as a conservative tracer as the EC is highly correlated with the Cl concentration ($R^2 = 0.71$, *p*-value < 0.05) and the temporal patterns of EC and Cl are very similar (see supplement Fig.S4.2). In the model, seepage rate was adapted to get the best fit between the modeled and the measured EC. The calibrated seepage rate was 2.0 mm d^{-1}. Compared to EC, nutrients are highly reactive solutes and thus can vary a lot along their flow routes due to biogeochemical processes. The model provided a tool to simulate hourly concentration dynamics under the assumption that EC, NH_4 and TP were conservative. The simulated EC, NH_4-N and TP were plotted together with the high frequency time series and the grab sampling data in Fig.4.3. Same as in Fig.4.2, the high frequency measurements were aggregated from 5 min (EC), 10 min (NH_4), and 20 min (TP) intervals into an hourly interval. The grab sampling results were all set to be measured at 10:00 AM as that coincides with the usual grab sampling times. Additionally, a comparison between the modeled and the measured results at the annual scale was performed by using correlation analysis, aggregating the model, the high-frequency and the grab sampling results at an 4-days average.

The average concentration of EC in groundwater was set equal to the average of the sampling survey, which was 1750 µS/cm (including both deep and shallow groundwater, Yu et al., 2019). For the NH_4 and TP concentration data, we chose the measurement from a drain sampling point (Drain 3, Yu et al., 2019) in the middle of the polder as the non-disturbed groundwater collected by the drains in this area of the polder. They were 8.1 mg N L^{-1} and 1.6 mg L^{-1} respectively. The starting (01-06-2015) concentrations were 1200 µS/cm, 4 mg L^{-1}, and 2 mg L^{-1} for EC, NH_4, and TP respectively. The model was not sensitive to the selected end-member values.

The time series data were further analysed at shorter scales: rain event scale and pumping event scale. Four rain events were selected according to the dilution extent of EC, defined as an EC value reduced by over 35%, they were: 10-06-2016 ~ 15-07-2016, 15-08-2016 ~ 26-09-2016, 10-11-2016 ~ 05-01-2017, and 20-02-2017 ~ 10-04-2017. These four events covered both EC dilution during rainfall and the recovery afterwards in different seasons. We selected 4 representative pumping events to present the response of EC, NH_4, TP, and turbidity to the pumping activities. Those events were in 15-07-2016 ~ 17-07-2016, 27-10-2016 ~ 29-10-2016, 20-12-2016 ~ 22-12-2016, and 05-05-2017 ~ 07-05-2017. Correlation analysis was as well applied to each event at the corresponding two time scales, averaging over whole days for precipitation events and over hours for pumping events. Data processing and analyzing were performed using Rstudio (R version 4.0.2) and time series package “xts”.

4.3 Results

4.3.1 Annual pattern of meteorological, hydrological, and water quality time series

4.3.1.1 Meteorological and hydrological conditions in polder Geuzenveld

To explain the time series (Fig.4.2), we distinguish between dry/wet periods and dry/wet seasons. The wet and dry periods (days to weeks) are represented by a water surplus (light blue color in Fig.4.2B, daily evapotranspiration < daily precipitation) or a water deficiency (dark blue in Fig.4.2B, daily evapotranspiration > daily precipitation). We defined the wet and dry seasons based on water surplus and deficit. The average net rainfall (the water surplus/deficit in Fig.4.2) is 1.4 mm d^{-1} for the period of 01-10-2016~15-03-2017, and -0.8 mm d^{-1} for the rest. Subsequently, we statistically analysed the difference between these two periods for multiple parameters. Table 4.2 shows the mean of each parameter for the wet and dry seasons and their significance test results. The wet and dry seasons means are significantly different for all parameters, but the EC.

Table 4.2 The mean of each parameter, and the significance for the wet and dry seasons

	Net rainfall* mm d^{-1}	Pump volume* $m^3 d^{-1}$	Water temperature* °C	EC µs cm^{-1}	NH_4* mg N L^{-1}	TP * mg P L^{-1}	Turbidity* FNU	Fe* mg L^{-1}	O_2* mg L^{-1}
Wet	1.4	1050	6.7	1212	3.7	0.8	197	3.4	4.3
dry	-0.8	712	17	1252	3.0	0.5	15	1.5	3.3

* $p < 0.05$*

Over the whole monitoring period, the water temperature ranged between 2 to 26 °C. From June to mid-September 2016, the temperature remained above 18 °C, then declined to become lower than 10 °C at the end of October. The following four months (November to February) were the coldest. Especially in January and February 2017, during which the water temperature dropped to below 3 °C. By the end of February temperatures started to rise again to reach 10 °C by the end of March 2017.

The surface water level in Geuzenveld has been maintained between -4.31 and -4.1 m NAP, strictly regulated by pumping (Fig.4.2A). After the pumps stopped, the surface water level recovered faster during the wet season (between October 2016 and March 2017) than during the dry season. Similarly, the shallow groundwater level positively corresponded to the precipitation and negatively to the daily accumulative pumping volume. The phreatic groundwater level in Fig.4.2A (light blue) was from one of the piezometers, which lies right outside of the polder (Fig.4.1, 52°22'46.0"N 4°47'15.6"E). In contrast to the constant surface water levels (Fig.4.2A, dark blue), the shallow groundwater had relatively low levels in the wet season compared to the dry season. This is related to the water level regulation of the boezem Haarlemmerweg with higher levels in summer than in winter (https://www.rijnland.net/actueel/water-en-weer/waterpeil). Phreatic water levels were consistently 20-40 cm higher than the surface water level in the polder, which confirms the continuous groundwater seepage into the surface water system.

* Wilcoxon rank-sum test. The tests were performed in Rstudio (version 4.0.2), wilcox.text() in package “stats”.

4.3.1.2 Annual water quality patterns

The Pearson's coefficients of determination (R^2)between the high frequency data and the routine discrete sampling data from the water authority are 0.88 for EC (*p*-value < 0.05), 0.92 for NH_4 (*p*-value < 0.05), and 0.97 for TP (*p*-value < 0.05). The scatter plots between the high and low frequency measurements are shown in Fig.S4.7.

During a rainfall event, rain and runoff from pavements and roofs, which were collected by a separate drainage system, directly fed the surface water (Fig.4.1). Distinct rainfall events cause a strong dilution pattern of both EC and NH_4 (in Fig.4.2C). The EC ranged from 600 to 1500 µS/cm. In general, during rainfall events, the EC declined because of dilution, while, after the events, EC gradually rose back up to around 1500 µS/cm. The duration of this process, i.e. *recovery time,* was longer in the wet season than in the dry season. A similar pattern of dilution and recovery is also visible for NH_4, especially for the period August 2016 – March 2017, where NH_4 shows a very similar response as EC (Table S4.2, wet season, $R^2 = 0.73$), although with somewhat larger day to day fluctuations. However, a contrasting pattern without NH_4 recovery occurred twice: from the middle of June to the end of August 2016 and from the middle of March to the middle of May 2017. During these periods, concentrations of NH_4 were considerably lower and deviated from the slope of the EC pattern. NH_4 decreased from around 4 mg L^{-1} to around 2 mg L^{-1} between the middle of June to the end of August 2016, but the continuous NH_4 measurements are not supported by the discrete samples which follow the EC pattern more closely. During the second period from March to the middle of May the deviation from the recovery pattern is more pronounced, and NH_4 concentrations dropped to almost 0 mg L^{-1} and started recovering from the beginning of May. This pattern is fully supported by the available discrete samples. During the same period in 2016 the high-frequency monitoring had not yet started, a single NH_4 discrete measurement is available for the 2nd of May, that seems to reveal a similar pattern in the spring of 2016.

Both TP and turbidity showed contrasting patterns during the wet and dry seasons (Fig.4.2D). Turbidity stayed below 60 FNU during the dry season until October and rapidly increased after a first rain event to 500 FNU (more details refer to Fig.S4.3 in supplementary information). A drop to about 200 FNU occurred right after this first peak, which seemed to correspond to excessive precipitation and a large pumping volume (Fig.4.2B). Soon after, turbidity went up again and peaked at 1800 FNU. Turbidity leveled off towards values around 200 FNU for the rest of the wet season and dropped below 60 FNU from April 2017 onwards.

TP concentrations were significantly higher during the period between 15-11-2016 and 01-03-2017 than the rest of the time (p-value < 0.001, Fig.S4.5), during which TP fluctuated around 0.5 mg L^{-1}, but always below 1 mg L^{-1}. During the wet season with the low temperatures (Table S4.2, $R^2 = -0.68$), TP almost constantly stayed above 1 mg L^{-1} and even reached values of about 3 mg L^{-1} in December. Although there were large gaps in the TP time series during this period, the high TP concentrations appear to have been diluted by rain events, for example the event at around January 10th, 2017. Most discrete samples measurements of TP matched well with values from the high frequency time series (Fig.4.2D, Table S4.1, $R^2 = 0.88$).

Total-Fe concentrations were most of time lower than 2 mg L^{-1} (Fig.4.2E), but for the wet season concentrations were higher and reached up to about 6 mg L^{-1}. The initiation of Fe increases at the beginning of the wet season coincided with that of turbidity (Fig.4.2D and Table S4.2, $R^2 = 0.72$). Upon

the increasing temperature in March 2017, total Fe concentrations dropped back to below 2 mg L^{-1} (a negative correlation between temperature and Fe is shown in Table S4.1). Dissolved O_2 concentrations were generally low in the water column; i.e. usually below 5 mg L^{-1}. Concentrations of over 3 mg L^{-1} were only found in March, April and May.

4.3.2 Model of water quality time series based on water balance

A simple fixed-end-member mixing model was used to reconstruct the conservative mixing of EC, NH_4, and TP. The simulated and the measured EC, NH_4, and TP are plotted in Fig.4.3. The correlations between the modeled and measured results are shown in the supplementary information (Table S4.4-S4.6). Potential processes that might deprive or enrich nutrients relative to the conservative mixing process along the flow routes were inferred from the discrepancies between the modeled and the measured data. Fig.4.3(A) and Table S4.5 show that the predicted and observed EC dynamics agree reasonably well from May to November 20th, 2016 (R^2 = 0.91). After that, the conservative mixing approach underestimated the EC but the main dynamics and the amplitudes were still reproduced (Table S4.6, R^2 = 0.82); as groundwater is the only contributor to the high EC due to the seepage of quite mineralized, slightly brackish water, the model must underestimate the seepage flux from November 20th, 2016 on. Overall, the observed dynamics of EC are consistent with mixing of high EC seepage water with low EC runoff water (coefficient of determination between the modeled and measured EC is 0.65 over the complete period, Table S4.4).

The dynamics of measured NH_4 concentrations show close resemblance to the model results, especially during the wet season (01-10-2016~15-03-2017). Clearly, NH_4 is diluted during the rain events and a gradual increase of NH_4 starts after each rain event during the wet season showing slopes that resemble the model reconstruction. Over the whole period, measured NH_4 concentrations were overestimated by the model, indicating that some NH_4 is probably lost due to non-conservative processes. This is especially true for the spring season of 2017, where NH_4 concentrations must be controlled by additional processes. Concentrations of TP are generally far below the conservative model reconstruction, except between the end of November and the beginning of March. During this particular period the minimum measured TP concentrations are captured nicely by the conservative model, but the distinct peaks up to 3 mg L^{-1} are not .

4.3.3 Water quality responses to single events analysis

To elucidate the response pattern of water quality to precipitation and pumping activity, we selected four major events (Fig.4.2 (4 pink shades) and Fig.4.4) and four pumping events (Fig.4.5). The former events were chosen according to their clear dilution pattern of EC (Fig.4.4), while the latter were pumping events without occurrence of rainfall (Fig.4.5). All seasons were covered, including some of the wet and dry periods.

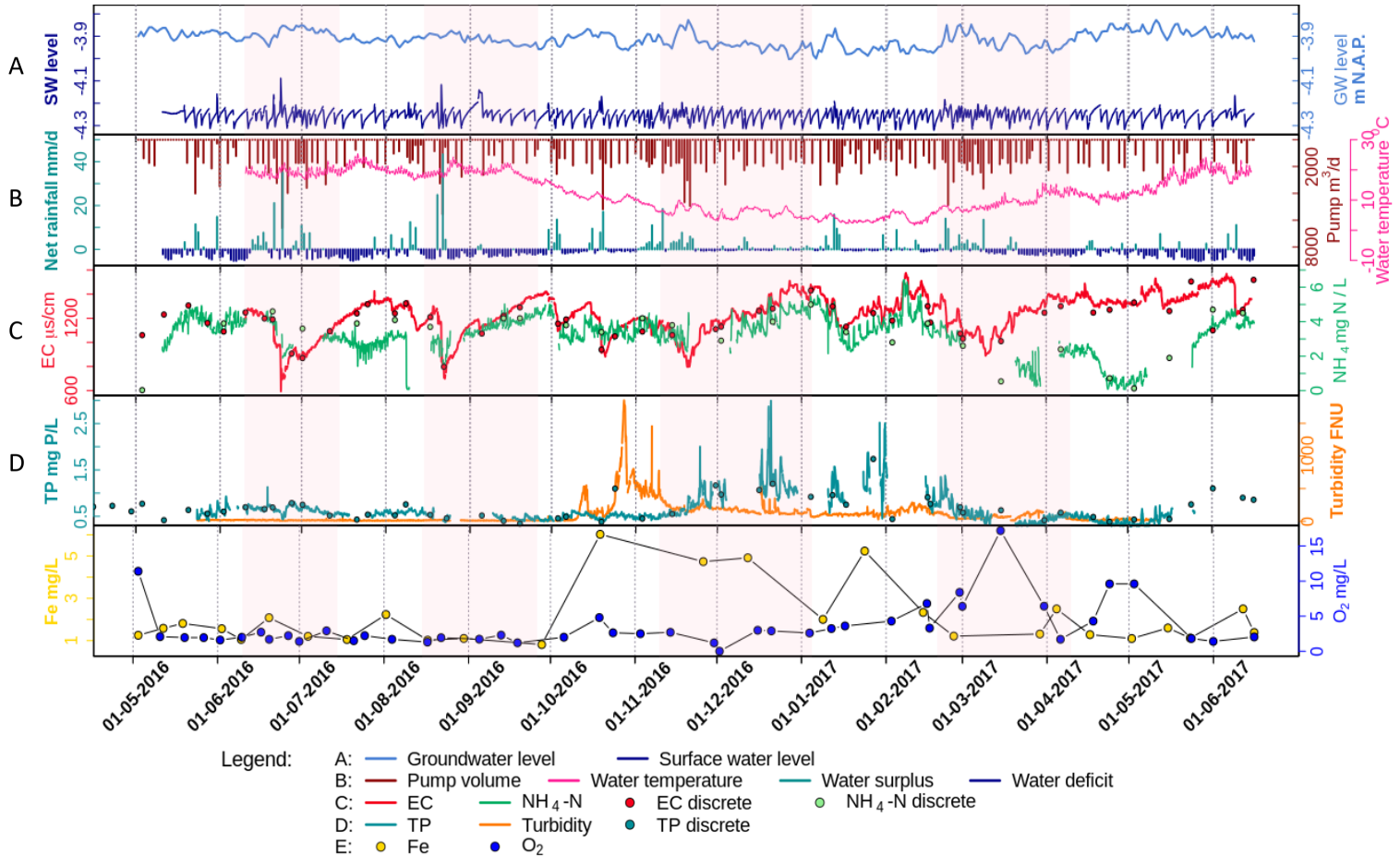

Figure 4.2 Time series of (A) surface water level (SW level) and groundwater level (m NAP), (B) net rainfall (daily water surplus (+) (lightblue) and deficit (-) (darkblue), mm d-1) and daily pumping volume (Pump m3 d-1), (C) hourly time series of EC (µS/cm) and NH4 -N (mg N L -1), and (D) hourly TP, turbidity, (E) discrete samples of Fe (total iron in water column) and O2 concentrations (mg L -1). The dots in (C) and (D) are the corresponding discrete sampling data, which are plotted to show their close match to the continuous time series data, as well as to fill in the gaps. All data were monitored at the pump station. The transparent pink blocks are the selected rain events for further analysis in section 3.3. See Table S4.1-S4.3 for the correlation tests performed on the dataset.

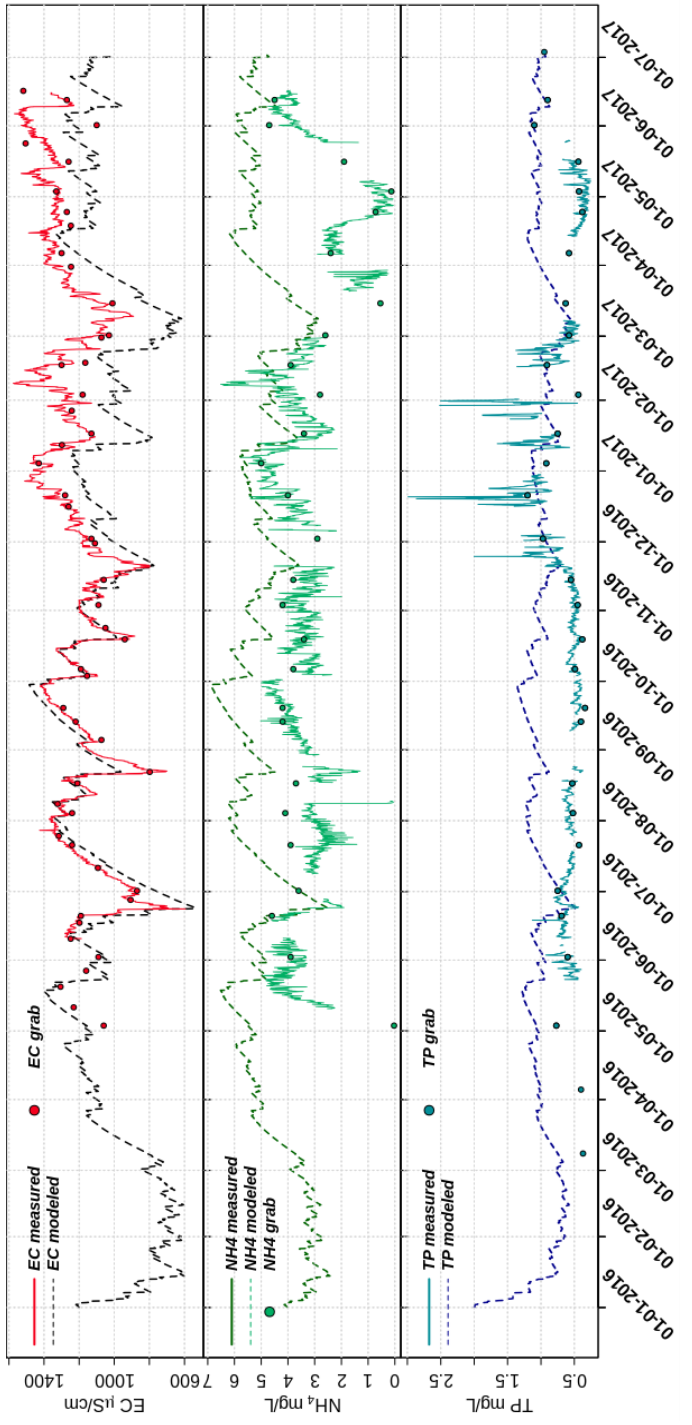

Figure 4.3 Plots of fixed-end-member mixing model predicted (A) EC, (B) NH_4 and (C) TP with their measured time series data and the discrete sampling results. See Table S4.4-S4.6 for the correlation tests performed on the dataset.

4.3.3.1 Rainfall events

EC and NH_4 showed clear dilution and recovery patterns during all events, while the pattern was not clear for TP and turbidity (Fig.4.4). The extent of dilution of EC appears to depend on the precipitation intensity. Rainfall during the recovery period determined how long it took to recover back to the highest level. The short but intensive rainfall during dry season events 1 and 2 reduced EC rapidly from around 1300 to around 700 µS/cm, while the recovery took about 1 month. Events 3 and 4 had less rainfall and dilution of EC was less (from about 1300 to about 800 µS/cm) and recovery took more than one and a half month in event 3, during which multiple small events occurred. The dilution patterns of the NH_4 in events 1 and 2 were similar to those of EC (R^2 = 0.86 and 0.83, respectively, Table S4.7 & S4.8) and show resemblance for event 3 (R^2 = 0.75, Table S4.10). Moreover, a direct negative correlation between NH_4 and rain intensity supports this dilution effect for event 2. Due to the data gaps of NH_4 in event 4 we cannot completely describe the pattern of NH_4 for this one, but it corresponds with that start of reduced NH_4 which was described in sections 4.3.1 and 4.3.2.

The response of TP was generally not related to the intensity of rainfall and pumping, except for event 3 during the wet period. Dilution effects, as were observed for NH_4, were not observed for TP for events 1, 2 and 4. During the wet season event 3, TP concentrations show negative correlations with precipitation and pumping intensity (R^2 = -0.79 and -0.59, respectively, Table S4.9) and correspond with decreasing turbidity. Event 4 marks the transition between the wet and dry season and the drop in TP coincides with the drop in NH_4, independently from individual rain storms during the dry season.

During the dry season (with event 1 and 2 included) turbidity always stayed below 50 FNU. Turbidity sometimes showed single peaks which are likely related to disturbances of the floating platform by wind and should probably be treated as false signals. Turbidity is more variable and has higher variance for wet season events 3 and 4, which corresponds with the findings of the annual scale analysis (section 4.3.1.2). During event 3, turbidity varied between 100 and 500 FNU. Although clear relations exist between Fe, TP and turbidity, all higher during the wet season (Fig.4.2, Table S4.2), these are not clearly reflected at the scale of individual precipitation events. Simultaneous peaks of TP and turbidity occur that are not easily related to the weather conditions in November and December but TP and turbidity show contrasting signals at the start of the event. The turbidity clearly decreases during rain storm event 3 and at the start of event 4. This change is not reflected by the correlation at the total event scale (Tables S4.9 and S4.10) but obvious when studying only the time scale of the decreasing limb of the EC dilution. Event 4 coincides with the transition to the spring season in 2017, showing decreasing EC, TP and turbidity in the last rains of the wet season and a strong decrease of NH_4 and increase of turbidity when conditions dried up and temperatures rose.

4.3.3.2 Pumping events and day and night pattern

The selected pumping events covered four seasons: summer (2016 July, event 1), autumn (2016 October, late autumn, event 2), winter (2016 December, event 3) and spring (2017 May, event 4) (Fig.4.5). While the effects of pumping on EC are rather small, TP, NH_4 and turbidity are all affected by pumping. The effects of pumping appear to be different for events in different seasons; turbidity for example increases during pumping in July and December but decreases in May. The increase during the December pumping is especially marked (R^2 Pumping intensity versus Turbidity = 0.77, Table S4.13). TP

decreases during pumping in July (R^2 = -0.67) and October and increases in May (R^2 = 0.6). Event 2 seems to have started a major drop in turbidity (more than 1000 FNU) that continued for some time after pumping.

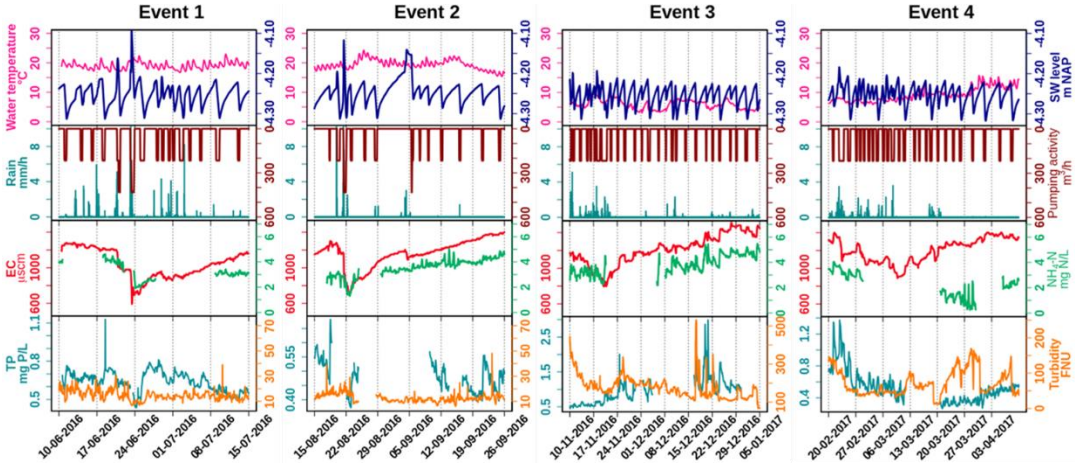

Figure 4.4 Selected events showing dilution and peaks of water quality parameters, with hourly precipitation (mm h^{-1}) and hourly pumping activity (m^3 h^{-1}). Note that between events different scales of TP and turbidity were used to reveal the dynamics. See Table S4.7-S4.10 for the correlation tests performed on the dataset.

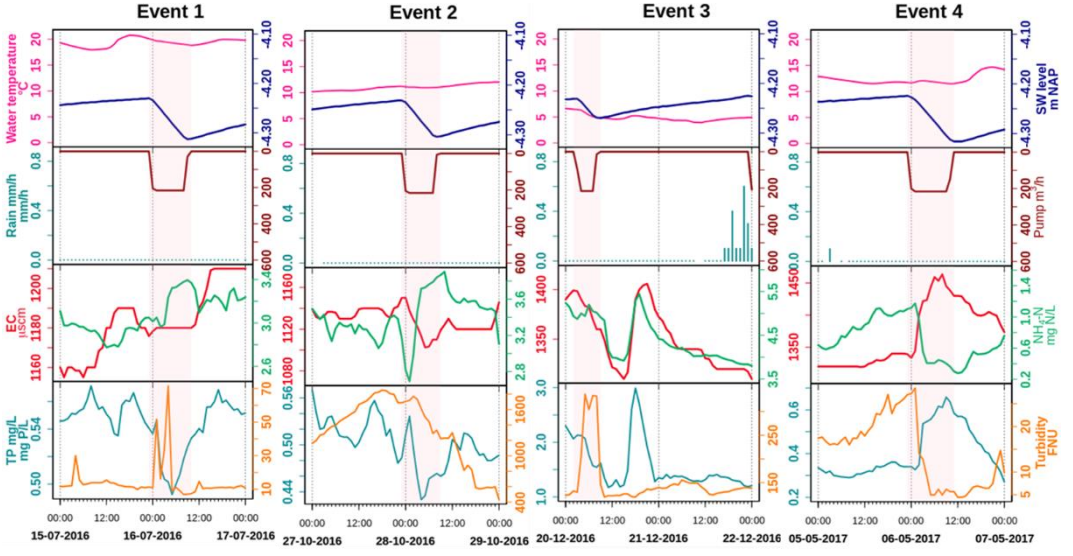

Figure 4.5 Pumping and pumping effect patterns on water quality, blue blocks represent the pumping duration. See Table S4.11-S4.14 for the correlation tests performed on the dataset.

4.4 Discussion

This study aimed at understanding the dynamics of N and P fluxes from the low-lying urban polder of Geuzenveld to downstream surface waters in order to eventually support water managers to mitigate eutrophication. Based on our high-resolution water quality measurements, we found that the surface-water chemistry at the polder outlet pumping station is governed by a complex combination of hydrological mixing and biogeochemical processing. In the following discussion, we start with the presentation of the relatively straightforward dilution behavior of EC, followed by adding the impact of primary production (i.e. algae growth) for understanding the NH_4 concentration patterns, and benthic primary producer and iron chemistry for understanding the turbidity and TP concentration patterns.

4.4.1 Hydrological mixing between groundwater and rainfall

In a highly manipulated low-lying urban catchment like Geuzenveld, mixing between rainwater and groundwater in the ditches is fast due to the high fraction of impervious area and the installation of both a rainwater and a groundwater drainage system that transport these contrasting water types efficiently to the ditches (Yu et al., 2019; Walsh et al., 2005). Runoff in Geuzenveld has EC of about 166 µS/cm (Yu et al., 2019), which is lower than the groundwater EC (1746 µS/cm on average). As a relatively conservative water quality parameter (Fig.S4.2), mixing between rainwater and groundwater should be the main process for EC. This presumption is supported by the agreement between the modelled and the measured EC dynamics for the period between May to November 2016. Precipitation events diluted the EC values at the pumping station, and the magnitude of dilution depended on the intensity of precipitation; heavy rainfall resulted in low EC values (Fig.4.2D and Fig.4.4). In periods with the absence of rainfall, the EC values follow a recovery curve that resembles a linearly mixed reservoir with concentrations increasing to values that approach the EC of the continuous groundwater supply of around 1500 µS/cm. After November 2016, EC was underestimated by the model. The sudden increase of the measured EC around Nov 20th coincides with an intensive pumping event after the first intensive rainfall that happened after a prolonged period of cumulative water deficit. This may be related with a first flush from the drain system that starts to be activated more strongly, thus removing clogged material and lowering the overall resistance of the drain system for shallow and deep groundwater inflow (van der Velde et al., 2010). It suggests that this triggered the inflow of somewhat more mineralized groundwater relative to the period before, creating a shift in the EC towards ~250 µS/cm higher values that continued during the remainder of the monitoring campaign. It appeared that it raised the EC, but did not change its amplitude or dynamics during the remainder of that period (Fig.4.2 and 4.3, Table S4.6). The elevated EC may alternatively due to the application of road salts in winter which starts from November. But we did not find any evidence for the prolonged effects of road salts, as the chloride concentrations in the grab samples only showed two higher measurements, one in December 2016 and one in January 2017 (see Supplement, Fig.S4.2).

The mixing process can explain part of the dynamics of NH_4 and TP in the wet season, but insufficient for explaining the dynamics during the dry season due to the presence of biological and chemical processes. Compared with groundwater, which carries around 8 mg L^{-1} NH_4 and 1.6 mg L^{-1} TP, rain and runoff have much lower nutrient concentrations, which makes groundwater the main nutrients source (Yu et al., 2019). Nutrients derived from groundwater mix with rainwater in the ditches through direct seepage and the efficient groundwater drainage systems. Clearly, NH_4 is diluted during the rain

events and a gradual increase of NH_4 starts after each rain event during the wet season showing slopes that resemble the model reconstruction. The overestimation of the modeled NH_4 in general indicates a probable lost to transformation processes, especially in the spring of 2017. Concentrations of TP are also generally far below the conservative model reconstruction. The distinct peaks up to 3 mg L^{-1} are not captured by the model and must be determined by different physical or chemical processes.

4.4.2 Primary production and nutrients

NH_4 dynamics during winter can be explained by mixing. However, biological processes are overruling the mixing process during spring and summer. It resulted in lower measured NH_4 concentrations than modeled during this period. Studies have shown that benthic and planktonic primary producers (e.g. phytoplankton) assimilate nutrients and are an important factor controlling nutrient dynamics in rivers, lakes, and streams (Hansson, 1988; Jäger et al., 2017). In polder Geuzenveld, the biological nutrient uptake is not only reflected in the time series data (Fig.4.2 and 4.3, Table S4.3) but is also evident in the monthly measurements from the water authority for the period 2007-2018, as summarized in Fig.4.6 and Table S4.15-S4.19.

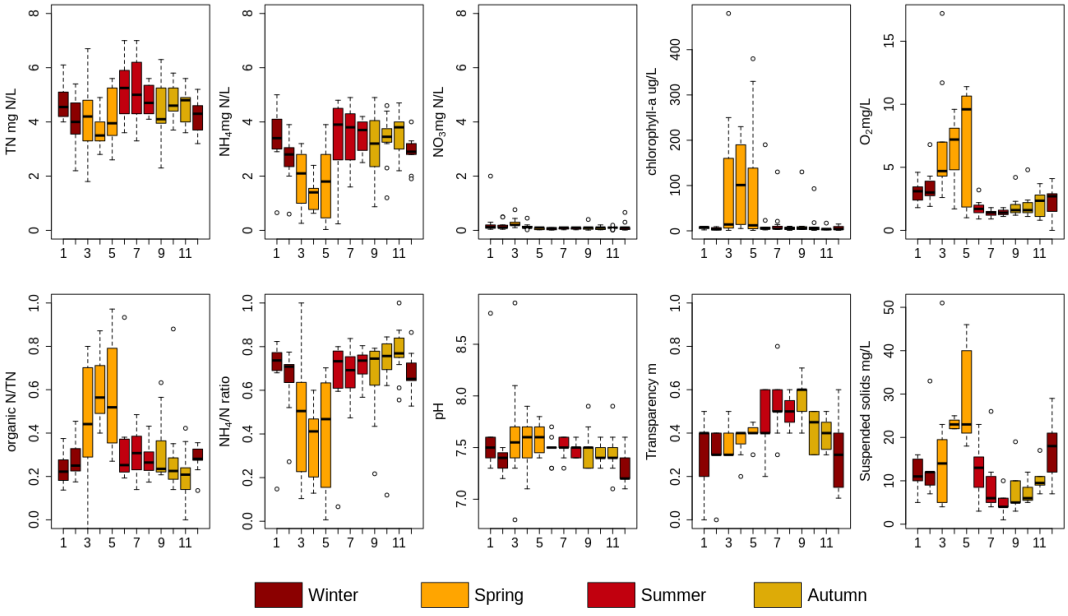

Figure 4.6 Monthly measurements of TN, NH_4-N, NO_3- N, chlorophyll-a, O_2 organic N/ TN and NH_4-N /TN (NH_4/N) mass ratio, *pH* , water transparency, and suspended solids in Geuzenveld from 2007 to 2018. X axis is month. See Table S15-S19 for the correlation tests performed on the dataset.

The increasing availability of light (and temperature increase) during spring (Fig.S4.6), induces growth of primary producers. Growth of primary producers results in consumption of ammonium, phosphate and a production of organic-N, chlorophyll-a, oxygen, and suspended solids, and led to a relatively higher pH because of the uptake of CO_2 (Fig.4.6, Table S4.16). These patterns are also clearly reflected in the shift in the NH_4/TN and organic-N/TN ratios during spring (Fig.4.6). Primary production occurs

both in the water column by phytoplankton as well as by benthic algae. Macrophytes could in principle also contribute, but they were absent in Geuzenveld. One of the structuring factors governing the relative importance of benthic and planktonic primary producers is light availability: benthic algae and macrophytes tend to dominate in shallow and clear waters, while phytoplankton is more likely to dominate in deeper and more turbid waters (Hartwig, 1978; Jäger and Borchardt, 2018; Petranich et al., 2018; Middelburg, 2019). Although our data do not allow conclusive determination whether benthic or pelagic primary producers dominate, it appears that their relative importance varies with season.

These primary producers also compete for nutrients. Benthic primary producers have direct (macrophytes) or first (benthic algae) access to nutrients that seep up from the subsurface, while planktonic primary producers depend on nutrient supply from surface runoff and nutrients remaining after consumption by benthic primary producers. For example, Henry and Fisher (2003) found that benthic algae can remove up to 80% of nitrogen from an upwelling water source. As we stated above, nutrient-rich groundwater is the major source of N and P to surface waters in polder Geuzenveld. In addition, due to the shallow depth of the ditches, light reaches the bottom with the consequence that benthic algae can proliferate in this polder. These benthic primary producers might utilize the up-flowing nutrients from groundwater and intercept the nutrients from seeping further into the water column (Hansson, 1988; Pasternak et al., 2009). The increasing light availability and thus primary production during spring led to the nearly complete deprivation of NH_4 in the water column (Fig.4.2C).

Following the spring bloom, concentrations of chlorophyll-a (proxy for phytoplankton biomass) and O_2 dropped substantially, while NH_4 concentrations rapidly recovered to around 4 mg L^{-1} in both the time series (Fig.4.2C) and the long-term monthly sampling results (Fig.4.6). Dissolved O_2 remained low (close to hypoxia) during the whole summer (below 2 mg L^{-1}) (Fig.4.2E and Fig.4.6), indicating that oxygen consumption by organic matter degradation and re-oxidation of reduced components from groundwater seepage outcompeted oxygen production from primary production. During summer, suspended solid and chlorophyll-a concentrations were low (Fig.4.6), indicating low biomass of plankton algae. Suspended solid and phytoplankton dominate light attenuation (Scheffer, 1998; Middelburg, 2019). Consequently, during this period, we observed an abrupt shift of the water regime from a turbid state to completely clear, as reflected in the high transparency from June to September (Fig.4.6). The low biomass of phytoplankton might be due to N limitation as nutrients are intercepted by benthic algae at the sediment interface. An alternative explanation is that zooplankton grazing maintained phytoplankton biomass low (Strayer et al., 2008; Genkai-Kato et al., 2012).

Temperature and light reaching the sediment started to fall from September onwards (Fig.S4.6), thereby reducing the intensity of biological activity, including NH_4 assimilation. Consequently, NH_4 started to behave conservatively again like EC (Fig.4.2 & Fig.4.3). The best fit between the modeled and measured NH_4 was from the end of November to the beginning of March, i.e during the winter period with lower light levels and shorter day lengths and very low primary production. The absence of primary production during winter, leads to conservative behavior of NH_4 governed by the mixing between groundwater and rain water.

4.4.3 P binding and turbidity

Iron chemistry is considered the dominant process governing the P dynamics in shallow groundwater fed ditches (Lijklema, 1994; Smolders et al., 2006; van der Grift et al., 2018). However, primary producers take up P for growth and at the same time release O_2 that regulates iron chemistry in lake water column (Table S4.1-S4.3, Spear et al., 2007; Zhang and Mei, 2015; Lu et al., 2016). This web of interactions likely controls P dynamics in these ditches.

From spring to autumn, TP concentrations were fluctuating around 0.5 mg L^{-1}, and the water had low turbidity (<50 FNU), thus high transparency allowing the growth of benthic algae that produce oxygen. Consequently, when P and Fe rich anoxic groundwater reaches the surface water-sediment interface, Fe oxidized into iron hydroxides in a short time (Van der Grift et al., 2014). P is then sorbed onto those Fe-hydroxides and retained in the sediments. Oxidation of reduced iron consumes O_2, contributing to the low O_2 conditions of the water column (Fig.4.2E). Moreover, it leads to the formation of a reddish-brown film of ferric iron (hydrous ferric oxide, Baken et al., 2013; van der Grift et al., 2018) on the bottom of the ditches, which can be seen in summer when the water was transparent. This slimy layer comprising iron hydroxides and benthic microbes can easily be resuspended and therefore act as a source of turbidity following perturbations by pumping, wind, rain or foraging fish, e.g. event 1 (Fig.4.5). Lu et al (2016) showed that co-precipitation of P with metal oxides was stimulated by periphytic biofilm activity that increased the water pH. Consistently, a relatively higher pH was also observed in our spring monthly samples (Fig.4.6).

From the late autumn onwards, turbidity and total Fe concentrations substantially increased compared to the rest of the time (Fig.4.2, p value < 0.001 for turbidity and = 0.02 for Fe). Turbidity peaked first at 1800 FNU and stayed at a plateau of ~200 NFU during the rest of the cold and wet season. Total Fe in the water column reached to 6 mg L^{-1} from below 1 mg L^{-1}. During this period the water turned brownish and transparency declined (Fig.4.6). Iron-rich particles are the most likely source of turbidity in freshwater (Lyvén et al., 2003; Gunnars et al., 2002; and Lofts et al, 2008). The suspension of these brownish iron colloids was likely stabilised by the presence of the dissolved organic matter (Mosley et al., 2003; Van der Grift et al., 2014), which (DOC) increased up to 18~33 mg L^{-1} during events (Supplementary information Fig.S4.4). In the late autumn, the anoxic/oxic interface shifts from the sediment into the water column and so does the locus of colloid formation. The ditch sediment, which had benthic algae activity releasing O_2 during spring and summer, became anoxic in the fall by the upwelling of the anoxic groundwater. The anoxic seepage occurs year-round, but the production of oxygen by the benthic algae creates an anoxic-oxic transition at the water-sediment interface, which leads to iron hydroxides precipitation in the slimy layer at the bottom that disappears after the algae die off. As a consequence, Fe oxidation moved into the water column where the conditions were relatively oxic (Van der Grift et al., 2014). Nevertheless, there was probably still enough Fe or other mineral oxides, such as aluminum hydroxide (Kopáček et al., 2005), binding capacity in the sediment for the fixation of P, as P concentrations remained low during this first turbidity peak. We suggest that the turbidity peak of 1800 FNU is caused by the mineralisation of the benthic algae once they die off when light and temperature conditions decrease, combined with the shift of ironhydroxide formation from the sediment-water interface to the water column. The latter process continues through the whole winter season, until primary production restarts in spring (Fig.4.7).

During winter, temperatures were below 5°C, pH values were relatively lowered, and TP achieved its peak concentrations (Fig.4.2D). During this period, iron reduction in the sediments continued, P bounded to iron oxides gradually got released along with reduced iron (Li et al., 2016). In the water column, reduced iron was oxidized but much slower than during spring-autumn due to the lower temperatures (Van der Grift et al., 2014), and dissolved P was incorporated in iron flocs with the result that particulate P concentrations and turbidity became high (Table S4.1, R^2 for Fe~turbidity 0.81, TP~Fe 0.65; Table S4.2, Fe~turbidity: R^2 = 0.72, , TP grab~Fe 0.79; Yu et al., 2019).

4.4.4 Process synthesis

With the presence of benthic algae, abundant organic matter and bacteria, the sediment functions as an active environment for biotic processes (such as primary production and nitrification-denitrification-anammox) and abiotic processes (such as iron oxidation). Figure 4.7 shows a conceptual diagram for the N and P dynamics in this lowland urban catchment during the four seasons which summarizes our hypotheses about the functioning of the system.

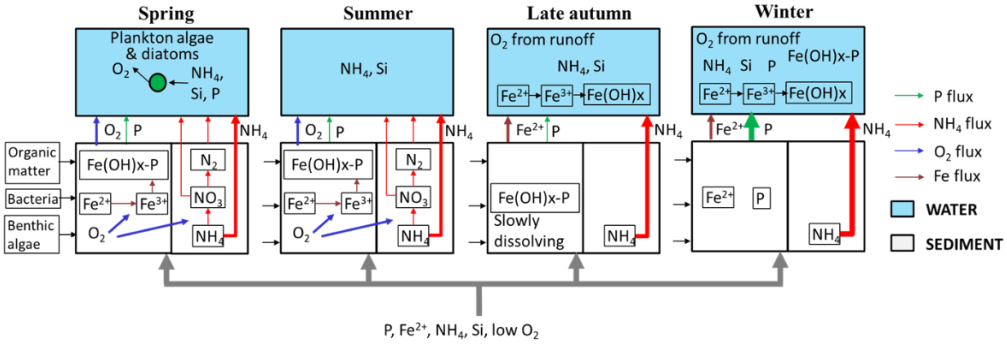

Figure 4.7 Schematic representation of N and P dynamics in spring, summer, later autumn and winter. The thickness of the flow lines represents the concentration magnitudes, the thicker the line, the higher the concentrations.

Spring: The improved light (and temperature) conditions stimulated primary production and nutrient uptake (N, P, Si) by phytoplankton and benthic algae. The resulting oxygen production caused oxidation of reduced iron from groundwater and the formation of iron oxides at the sediment surface. P was mostly bounded to this particulate iron instead of being released into the upper water layer. In this period turbidity was relatively low, but suspended solids reached a high concentration due to the phytoplankton.

Summer: N and P were still being removed by biological processing, in particular by benthic algae. Phytoplankton biomass decreased because of competition for N or grazing activity. Benthic algae produced O_2, which in turn was used to oxidize all reduced iron reaching the sediment-water interface and P was still retained by iron hydroxides in the sediment. The water column was transparent (low TP and phytoplankton biomass) and relatively low in oxygen due to the continuous supply of anoxic groundwater, the mere absence of O_2-rich runoff, the oxidation process of Fe(II) and possibly by microbial organic matter decomposition during warm periods with relatively stagnant water.

Late autumn: Biological activity declined (colder and less light), and more NH_4 reached the water column. Moreover, the redox zone moved from the sediment-water interface into the water column (Van der Grift et al. 2014, 2016); the oxidation of Fe in the water column caused a peak of turbidity. P was still sequestered to minerals in the sediment.

Winter: During winter, NH_4 and TP showed the highest concentrations because of low biological activity. Iron oxides in the sediment dissolved under reductive and organic matter abundant conditions and released Fe^{2+} and P into the water column increasing P concentrations therein. NH_4 and EC dynamics were primarily governed by the conservative mixing between groundwater and precipitation/runoff.

4.4.5 Event scale N and P dynamics

At the event scales, NH_4 and EC were reduced by dilution from precipitation/runoff. For P and turbidity there was no clear relation to precipitation events, except for events in late autumn and winter (e.g. Fig.4.4, event 3). The responses to precipitation and pumping events were different from those reported in the literature. Rozemeijer et al. (2010b) studied an agricultural catchment and found that rainfall events led to NO_3 decreases and P increases. Miller et al. (2016) observed NO_3 decreases during large discharges in an urban catchment. The lowering of turbidity in our urban catchment during the dilution periods that was associated with the winter events 3 differs from the observations in literature (van der Grift et al., 2014, Rozemeijer et al., 2010b). In agriculture areas, turbidity usually peaks in response to rainfall events due to erosion and remobilization of sediments. In an urban, paved environment erosion may be limited and runoff water has a low turbidity. Moreover, in the case of turbid pre-event conditions, fresh precipitation water flushes away this turbid water. In addition, Yu et al. (2019) showed that precipitation runoff delivers particles and O_2 to the ditches. We suggest that this accelerates the further aggregation of the iron complexes; the resulting larger particles more readily settle to the bottom, causing a reduction of turbidity during the events itself (Fig.4.4, EC dilution part of events 3 and 4).

In artificial lowland catchments, water systems are intensively regulated by pumping activity to prevent flood and drought. However, there is a substantial lack of knowledge about the possible consequences of such regulation on aquatic ecology and water quality. Peaks in P and turbidity by the activation of pumps was observed by Van der Grift et al. in their high frequency monitoring campaign in an agriculture lowland polder (Van der Grift et al., 2014 & 2016). This type of event scale dynamics would be easily missed in a daily or lower frequency sampling schedule, especially because pumping occurs almost solely overnight in our regulated catchments. As such, only a sampling schedule with 7 hours intervals (e.g. Neal et al. 2011) or high-frequency monitoring is able to catch the short-term dynamics (Van Geer et al. 2016).

Contrary to the findings of Van der Grift et al. (2014, 2016), the effects of pumping activity on N, P and turbidity dynamics were variable, depending on the season. During the phytoplankton bloom in spring, activation of pumps resulted in flushing and as a result reduced turbidity during the event (Fig.4.5 event 4). Consequently, phytoplankton was transferred to the downstream channel and added to the total N pool in that system. In summer (Fig.4.5 event 1), the dead detritus and the layer of iron compounds at the sediment surface were easily resuspended and contributed to turbidity peaks at the beginning of the pumping, but the materials also re-sedimented almost immediately once the flow reached stability. Resuspension also resulted in an increase of NH_4 in the water column which then was

being pumped out (Fig.4.5 event 1). During late autumn, we observed that the water was highly turbid (see also Yu et al. 2019) which we suggest to be caused by the formation of iron hydroxide colloids in the water column, which is supported by correlations between Fe-grab and Turbidity (R^2= 0.72, Table S4.2). We explain the reduced turbidity after a precipitation event as a result of the activation of the pumps which caused the export of the turbid water towards the receiving boezem in combination with aggregation of iron hydroxides in the water column and subsequent settling of the aggregates due to the supply of new O_2-rich water (Fig.4.5 event 2, see also Van der Grift, et al., 2014). Moreover, NH_4 increased again by the pumping activity and was transferred downstream (Fig.4.5 event 2). The eventual impact of regulation of the Geuzenveld water system turns the pumping discharge into a point source for nutrients to downstream water bodies as shown in Fig.4.8.

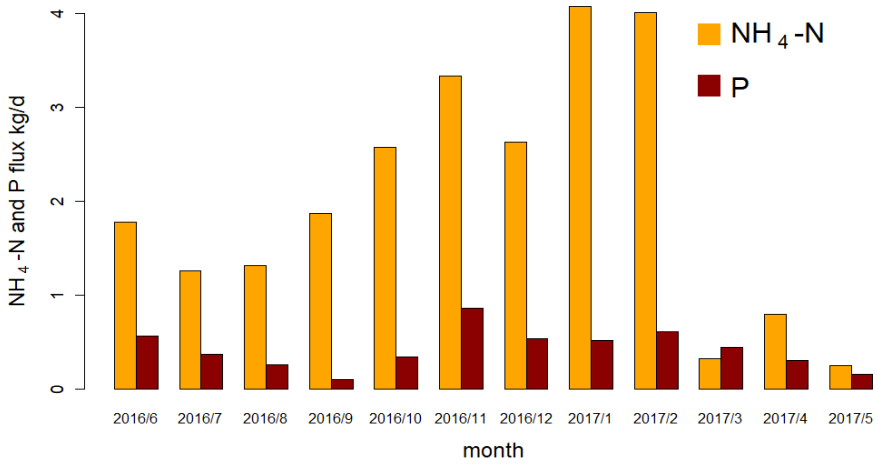

Figure 4.8 Average daily NH_4-N and P flux (kg per day) in each month in the discharge (calculated from the continuous measurements) of polder Geuzenveld from June 2016 to May 2017.

Fluxes of N and P were highest during winter (Fig.4.6). These high fluxes are caused not only by the more frequent pumping activity, but also by the higher concentration of N and P in the water column in winter. In the time series data, NH_4 (the major form of N), had concentrations above 2.4 mg N L^{-1} (the local environmental quality standard (EQS) for N-total), in all seasons except spring. NH_4 concentrations even reached up to 6.5 mg L^{-1}. TP concentrations were constantly higher than 0.15 mg P L^{-1} (the local EQS); during winter it was always over 1 mg P L^{-1}. Although the NH_4 flux in the discharge was very low in spring (Fig.4.8), the actual total N flux might have been much higher, as organic N (phytoplankton) was the major form of TN instead of NH_4 during this period (Fig.4.6 NH_4/N and organic-N/TN). Therefore, even though water authority measures have been effective in controlling the water quantities in the polder, it had unanticipated impact on nutrients export to the downstream water bodies. In order to prevent eutrophication in the urban waters, nutrient rich discharge from these areas is exported directly to the North-Sea Canal and to the North Sea.

4.4.6 Implications for urban water management in low lying catchments

This study demonstrated high frequency monitoring technology to be an effective tool for understanding the complex water quality dynamics. Investment in high frequency monitoring would greatly benefit the management of urban lowlands with substantial groundwater seepage by elucidating the principle biogeochemical processes and nutrient temporal patterns for realizing efficient mitigation and control of eutrophication. For example, redirecting the drain water effluent into constructed wetlands could be considered as a mitigation measure in low lying areas with artificial water systems that resemble the Amsterdam region, e.g. in cities such as New Orleans, Shanghai and Dhaka (Li et al., 2009; Nahar et al., 2014; Jones et al., 2016; Stahl, 2019). Centralizing the treatment of discharge water is also recommended, for instance by harvesting N as phytoplankton from the discharge during spring, or filtrating P at the pumping station during winter. Measures that artificially increase oxygen concentrations in the waters, such as the inlet of oxygen rich water, aeration by fountains or the artificial introduction of grazers or macrophytes may be considered to improve the ecological status of these urban waters. Moreover, aeration of the water in summer and autumn would possibly enhance processes such as coupled-nitrification-denitrification and anammox, eventually converting NH_4 to N_2, before the water is discharged to downstream waters. Importantly, before the application of any measures or maintenance in urban low-lying catchments, managers should evaluate the potential effects on the biological and chemical resilience, e.g. dredging of a layer with abundant benthic activity might destroy an important buffer to nutrients in growing seasons, especially P.

In this study, we focused on the analysis of the temporal patterns of water composition and on the deduction of the potential biogeochemical processes. Detailed studies about these processes and the biotic communities at the sediment-water interface were outside of the scope of this paper. A comprehensive study on the sediment-water interface would be necessary to further increase our knowledge on the role of the benthic zone in attenuating N and P seeping up from groundwater. Besides, further research would need to consider the optimal physical dimensions of water courses and drain configurations, as to benefit the ecological status of urban waters that are prone to nutrient-rich groundwater seepage.

4.5 Conclusions

This study aimed at improving our understanding of the mechanisms that control the temporal patterns of nutrients and other water quality parameters in an urban catchment. Time series of EC, NH_4, TP, and turbidity were obtained by applying a high frequency monitoring technology for one year (May 2016 to July 2016). Observed EC, NH_4 and TP could only partly be explained by conservative mixing of groundwater and precipitation components. In particular, N and P fluxes in the shallow ditches were also impacted by biogeochemical processes, such as primary production and iron redox transformations.

(1) NH_4, the dominant form of N in surface water, originates primarily from groundwater seepage, and concentrations are lowered by primary producers (phytoplankton and benthic algae) in the growing season. High algal biomass was also clear from high chlorophyll-a and suspended solids in the water column.

(2) TP showed high concentrations in winter, but relatively low concentrations in other seasons. Iron redox chemistry was the principle process controlling the P dynamics in shallow groundwater fed ditches. P dynamics may also have been partly influenced by primary production which consumes P for growth and at the same time produces O_2 influencing the redox status in the sediments and in the water column.

(3) High turbidity levels occurred in the late autumn and winter, mostly in the form of iron hydroxides. It resulted from a shift of the anoxic/oxic interface where the formation of iron hydroxides moves from the sediment towards the water column.

(4) Water pumped from the polder to downstream water bodies was rich in NH_4 from summer to winter, but rich in organic N in the form of algae during spring. P leaves the polder mainly during the winter season when it is released from the sediment and exported mostly in the form of P sorbed to $Fe(OH)_3$ colloids and as dissolved P.

(5) Precipitation diluted concentrations of most water quality parameters, but delivered O_2 to the water column, and in that way indirectly affected P and turbidity by intensifying iron oxidation and precipitation.

(6) Unlike many other natural and artificial catchments, rainfall and pumping events did not increase turbidity or TP concentrations at the short time scale, rather reduced turbidity and TP because of enhanced iron hydroxide precipitation due to oxygen inputs by runoff.

Our understanding of the N and P dynamics in this low-lying urban catchment may contribute to the development of effective water management strategies that reduce eutrophication conditions in both the urban polders and the downstream waters. Drainage of very low-lying areas (for use as residential and/or agricultural areas) not only increases pumping costs, but can also result in difficult to manage water quality conditions. Controlling the source, redirecting and utilizing the drainage water might be strategies to reduce the input of N and P from groundwater into surface water. In addition, we showed that in lowland urban areas with high seepage rates the reactivity of the stream bed sediments largely controls water quality of surface waters and thus should be managed with care when cleaning the surface water systems.

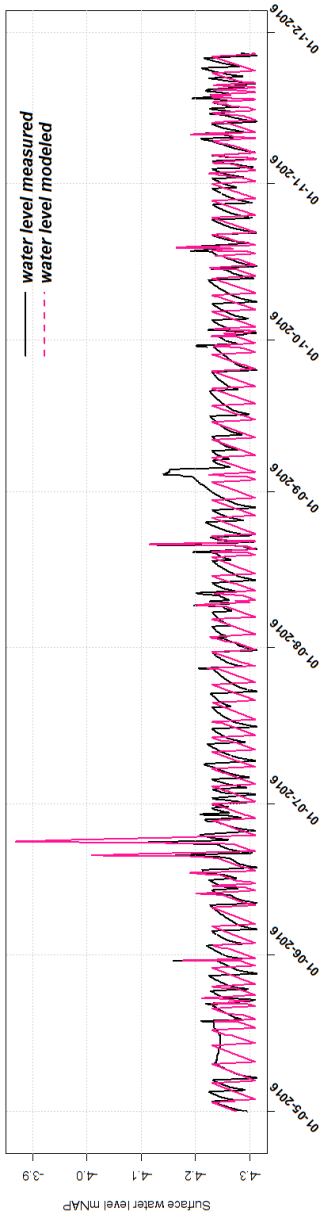

Figure S4.1 modelled versus measured water level

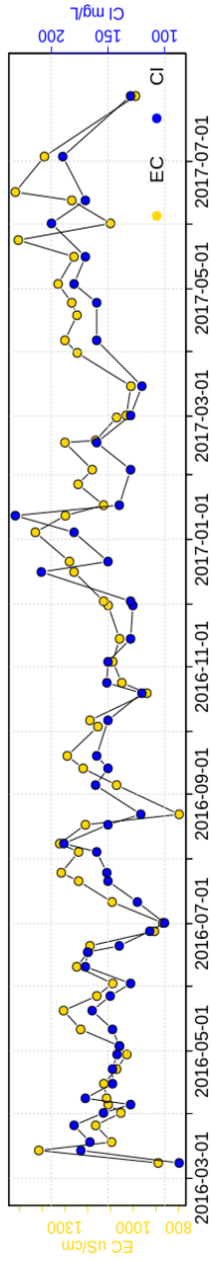

Figure S4.2 Discrete sampling of Cl concentration and EC from 2016 to 2017 at the pumping station

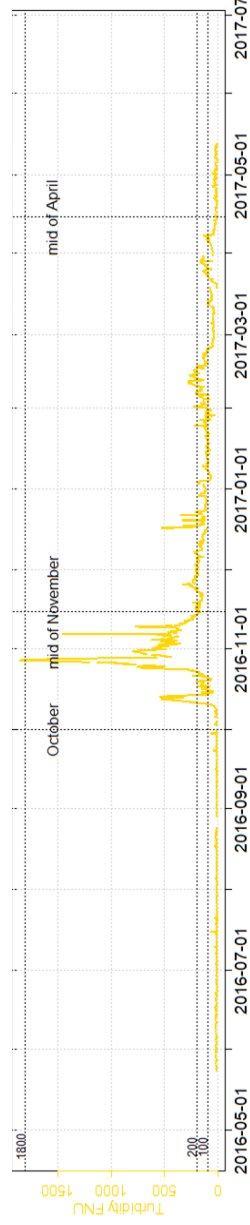

Figure S4.3 Hourly time series of turbidity, with the horizontal dashed lines indicating the 100, 200 and 1800 FNU levels, and vertical event lines for October, 2016, mid of November, 2016 and mid of April, 2017

Cl is a conservative parameter and a commonly used tracer in hydrology. A good match between EC and Cl ($R^2 = 0.71$, p-value < 0.05) indicates the conservative nature of EC and validates its use as conservative parameter for the mixing concept calculations in this paper.

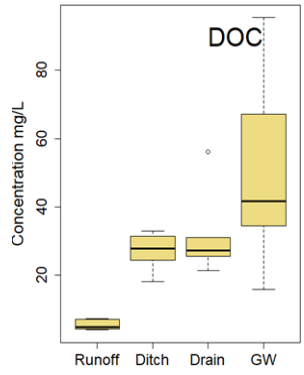

Figure S4.4 Dissolved organic carbon (DOC) in the runoff, ditch water, drain water and groundwater.

Samples are from a water quality survey during an event between 2017-11-28 to 2017-12-01 (Yu et al., 2019)[4]. The bar of "Ditch", being referred in this paper, represents the samples from the surface water in polder Geuzenveld. They were sampled from the ditches in the east, west, and middle, and the pumping station. The DOC concentration at the pumping station during this event is 24 mg/L.

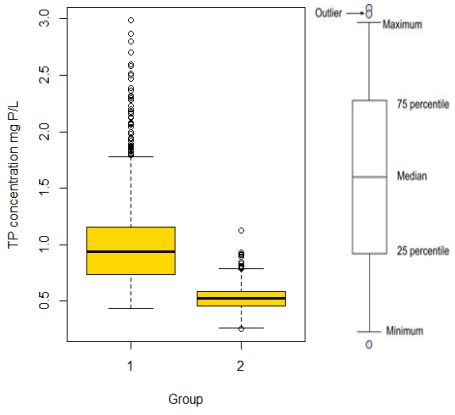

Figure S4.5 Statistics of TP concentrations in two periods (group 1: before 15-11-2016 and after 01-03-2017, group 2: the TP value between 15-11-2016 and 01-03-2017). The boxplots include the medians, 25% and 75% percentiles and outliers.

[4]Yu L., Rozemeijer J.C., van der Velde Y., van Breukelen B.M., Ouboter M., and Broers H.P.. Urban hydrogeology: Transport routes and mixing of water and solutes in a groundwater influenced urban lowland catchment. Science of the Total Environment, 678: 288-300, 2019.

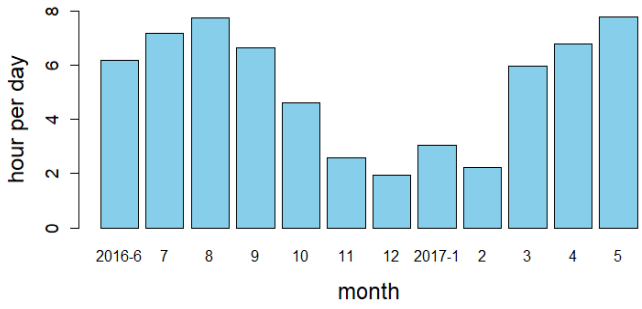

Figure S4.6 Sunshine duration (hours per day in each month)

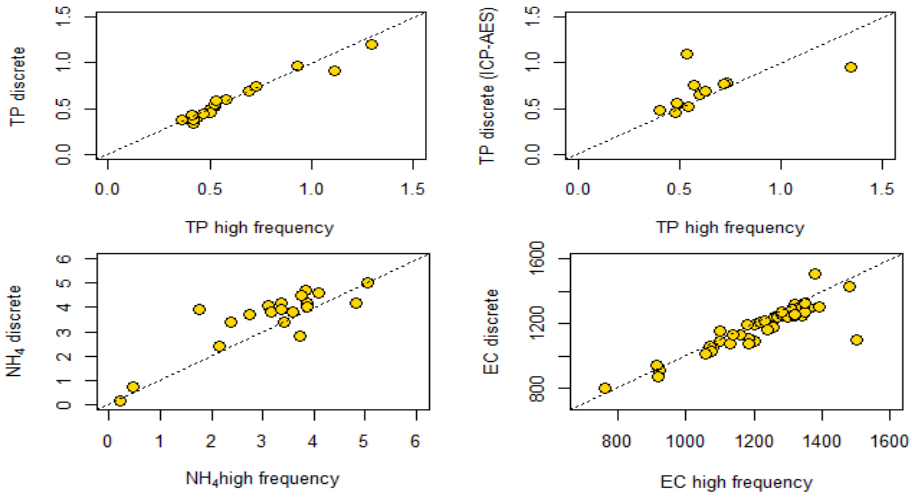

Figure S4.7 Scatter plots of the high frequency measurement vs. the discrete sampling results for TP, NH_4, and EC. "TP discrete (ICP-AES)" are the discrete samples preserved by mercury chloride. The dashed line is the 1:1 line.

Correlation tables

(only R^2 values > 0.55 are shown)

Table S4.1 Coefficient of determinations for Figure 4.2 (complete year)

	GL	SL	PV	WT	NR	EC	ECd	NH_4	NH_4d	TP	TPd	Turb	O_2d	Fed
GL	1													-0.59
SL		1												
PV			1		0.69	-0.57	-0.61							
WT				1						-0.57				-0.63
NR					1									
EC						1	0.85							
ECd							1							
NH_4								1	0.88					
NH_4d									1				-0.82	
TP										1	0.88			0.65
TPd											1			0.82
Turb												1		0.81
O_2d													1	
Fed														1

GL: groundwater level SL: surface water level PV: pumping volume
WT: water temperature NR: net rainfall EC: electrical conductivity high frequency
ECd: electrical conductivity discrete sample NH_4: ammonium high frequency
NH_4d: ammonium discrete sample TP: total phosphorus high frequency
TPd: total phosphorus discrete sample Turb: Turbidity high frequency
O_2d: oxygen discrete sample Fed: iron discrete sample

Table S4.2 Correlation of determinations for Figure 4.2 (wet: 01-10-2016 ~ 15-03-2017)

	GL	SL	PV	WT	NR	EC	ECd	NH_4	NH_4d	TP	TPd	Turb	O_2d	Fed
GL	1		0.56		0.56	-0.57				-0.57				-0.65
SL		1												-0.6
PV			1		0.67									
WT				1						-0.68				
NR					1									-0.56
EC						1	0.93	0.73						
ECd							1	0.67	0.61	0.78				
NH_4								1	0.62					
NH_4d									1					
TP										1	0.83			
TPd											1			0.79
Turb												1		0.72
O_2d													1	
Fed														1

Table S4.3 Correlation of determinations for Figure 4.2 (dry: ~ 30-09-2016 and 16-03-2017 ~)

	GL	SL	PV	WT	NR	EC	ECd	NH_4	NH_4d	TP	TPd	Turb	O_2d	Fed
GL	1													
SL		1												
PV			1		0.67	-0.58	-0.64							
WT				1				0.66	0.89	0.6		-0.69	-0.76	
NR					1									
EC						1	0.82							
ECd							1							
NH_4								1	0.95				-0.73	
NH_4d									1	0.69			-0.87	
TP										1	0.87		-0.62	
TPd											1			
Turb												1	0.64	
O_2d													1	
Fed														1

Table S4.4 Correlation of determinations for Figure 4.3 (complete period)

	EC	ECm	ECd	NH_4	NH_4m	NH_4d	TP	TPm	TPd
EC	1	0.65	0.88		0.65			0.65	
ECm		1			1			1	
ECd			1						
NH_4				1		0.89			
NH_4m					1			1	
NH_4d						1			
TP							1		0.86
TPm								1	
TPd									1

* ECm: electrical conductivity modeled result
NH_4m: ammonium modeled result
TPm: total phosphorus modeled result

Table S4.5 Correlation of determinations for Figure 4.3 (before 20-11-2016)

	EC	ECm	ECd	NH_4	NH_4m	NH_4d	TP	TPm	TPd
EC	1	0.91	0.97		0.91	0.58		0.91	
ECm		1	0.67		1			1	
ECd			1		0.67			0.67	
NH_4				1		0.89			
NH_4m					1			1	
NH_4d						1			
TP							1		0.69
TPm								1	
TPd									1

Table S4.6 Correlation of determinations for Figure 4.3 (after 20-11-2016)

	EC	ECm	ECd	NH_4	NH_4m	NH_4d	TP	TPm	TPd
EC	1	0.82	0.72		0.82			0.82	
ECm		1	0.69		1			1	
ECd			1		0.69			0.69	
NH_4				1		0.94	0.84		0.62
NH_4m					1			1	
NH_4d						1	0.87		0.78
TP							1		0.96
TPm								1	
TPd									1

Table S4.7 Correlation of determinations for Figure 4.4 (Event 1)

	EC	TP	NH_4	Turb	Rain(h)	PV(h)	SL	WT
EC	1		0.86	0.84		-0.75		
TP		1						-0.56
NH_4			1	0.84				
Turb				1		-0.6		
Rain(h)					1	0.66	0.66	-0.57
PV(h)						1		
SL							1	
WT								1

* Rain(h): hourly rainfall PV(h): hourly pumping volume

Table S4.8 Correlation of determinations for Figure 4.4 (Event 2)

	EC	TP	NH_4	Turb	Rain(h)	PV(h)	SL	WT
EC	1		0.83					
TP		1						
NH_4			1		-0.72			
Turb				1	0.76			-0.56
Rain(h)					1	0.73		
PV(h)						1		
SL							1	
WT								1

Table S4.9 Correlation of determinations for Figure 4.4 (Event 3)

	EC	TP	NH_4	Turb	Rain(h)	PV(h)	SL	WT
EC	1	0.66	0.75		-0.56	-0.69		-0.59
TP		1		-0.56	-0.79	-0.59		
NH_4			1					
Turb				1	0.63			
Rain(h)					1	0.62		
PV(h)						1		0.72
SL							1	
WT								1

Table S4.10 Correlation of determinations for Figure 4.4 (Event 4)

	EC	TP	NH_4	Turb	Rain(h)	PV(h)	SL	WT
EC	1	0.81		0.88		-0.61		0.64
TP		1	0.76	0.8				
NH_4			1	0.99				
Turb				1			-0.64	-0.61
Rain(h)					1	0.84	0.58	-0.59
PV(h)						1	0.68	-0.71
SL							1	
WT								1

Table S4.11 Correlation of determinations for Figure 4.5 (Event 1)

	EC	TP	NH_4	Turb	Rain(h)	PV(h)	SL	WT
EC	1							0.72
TP		1				-0.67		
NH_4			1				-0.78	
Turb				1				
Rain(h)					1			
PV(h)						1		
SL							1	
WT								1

Table S4.12 Correlation of determinations for Figure 4.5 (Event 2), $R^2 \geqslant 0.5$are shown

	EC	TP	NH_4	Turb	Rain(h)	PV(h)	SL	WT
EC	1	0.5	-0.78	-0.49				
TP		1	-0.52					
NH_4			1				-0.55	
Turb				1				-0.66
Rain(h)					1			
PV(h)						1		
SL							1	-0.52
WT								1

Table S4.13 Correlation of determinations for Figure 4.5 (Event 3)

	EC	TP	NH_4	Turb	Rain(h)	PV(h)	SL	WT
EC	1	0.75	0.88					
TP		1	0.81					
NH_4			1					0.55
Turb				1		0.77		
Rain(h)					1			
PV(h)						1		
SL							1	
WT								1

Table S4.14 Correlation of determinations for Figure 4.5 (Event 4)

	EC	TP	NH_4	Turb	Rain(h)	PV(h)	SL	WT
EC	1	0.71	-0.57			0.58	-0.69	
TP		1	-0.74	-0.58		0.6		
NH_4			1	0.59				
Turb				1			0.65	
Rain(h)					1			
PV(h)						1		
SL							1	
WT								1

Table S4.15 Correlation of determinations for Figure 4.6 (complete)

	TN	NH_4	NO_3	chlor	O_2	pH	Trans	Suspended Solids	OrgN/TN	NH_4/TN
TN	1	0.6								
NH_4		1			-0.64				-0.74	0.88
NO_3			1							
chlor				1	0.63			0.85		-0.6
O_2					1				0.67	-0.72
pH						1				
Trans							1			
Suspended Solids								1	0.67	-0.64
OrgN/TN									1	-0.87
NH_4/TN										1

* chlor: chlorophyll-a
Trans: Transparency
OrgN/TN: organicN/TN

Table S4.16 Correlation of determinations for Figure 4.6 (spring)

	TN	NH_4	NO_3	chlor	O_2	pH	Trans	Suspended Solids	OrgN/TN	NH_4/TN
TN	1							0.71		
NH_4		1			-0.7				-0.87	0.91
NO_3			1							
chlor				1				0.88		
O_2					1				0.63	-0.73
pH						1				
Trans							1			
Suspended Solids								1	0.58	
OrgN/TN									1	-0.98
NH_4/TN										1

Table S4.17 Correlation of determinations for Figure 4.6 (summer)

	TN	NH_4	NO_3	chlor	O_2	pH	Trans	Suspended Solids	OrgN/TN	NH_4/TN
TN	1	0.87								
NH_4		1							-0.75	0.79
NO_3			1							
chlor				1					0.65	-0.62
O_2					1				0.6	-0.58
pH						1				
Trans							1			
Suspended Solids								1		
OrgN/TN									1	-0.99
NH_4/TN										1

Table S4.18 Correlation of determinations for Figure 4.6 (autumn)

	TN	NH_4	NO_3	chlor	O_2	pH	Trans	Suspended Solids	OrgN/TN	NH_4/TN
TN	1									
NH_4		1	-0.58	-0.62						0.85
NO_3			1	0.84	0.56			0.76		-0.65
chlor				1	0.85			0.83		-0.81
O_2					1					
pH						1				
Trans							1			
Suspended Solids								1	0.59	-0.65
OrgN/TN									1	-0.63
NH_4/TN										1

Table S4.19 Correlation of determinations for Figure 4.6 (winter)

	TN	NH_4	NO_3	chlor	O_2	pH	Trans	Suspended Solids	OrgN/TN	NH_4/TN
TN	1	0.79								
NH_4		1	-0.62						-0.57	0.81
NO_3			1							-0.8
chlor				1						
O_2					1					
pH						1				
Trans							1			
Suspended Solids								1	0.56	
OrgN/TN									1	-0.77
NH_4/TN										1

Chapter 5

Synthesis

5.1 Summary

Urban water eutrophication is a worldwide issue causing significant societal, economic and environmental losses. However, effective water quality management in the urban systems is seriously hampered by a lack of knowledge of the water quality dynamics. The research described in this thesis was performed in the west of The Netherlands where lands consist of low-lying polders, a form of artificial catchments which are actively pumped to maintain water levels. The polders in the western part of the Netherlands often suffer from excessive nutrient concentrations, often leading to the exceedance of surface water environmental quality standards (Rozemeijer et al., 2014). The aims of the current research were to identify the sources and flow routes of nutrients in the greater Amsterdam region and to explore their spatial and temporal patterns at different scales from a multidisciplinary perspective. Field experiments and statistical analyses were conducted, which demonstrated the importance of groundwater for the surface water quality, especially for nitrogen and phosphorus. The answers to the research questions raised in Chapter 1 are as below:

(1) What is the impact of groundwater on the surface water quality in the polder catchments of the greater Amsterdam city area?

Concentrations of major elements in the surface water in and around Amsterdam appears to be highly correlated to the concentrations in the underlying groundwater. High nutrient concentrations in the surface water are caused by both the hydrogeological conditions of the catchment (Chapter 2) and by human alterations to the groundwater flow paths at the catchment and regional scales (Chapters 2&3).

We concluded that subsurface organic matter acts as the most important source of nutrients in groundwater and affects surface water composition by groundwater seepage. Organic matter is in ample presence in the subsurface around the world, especially in delta settings (Dai et al., 2019). The Dutch subsurface is known to contain abundant reactive organic matter, such as peat formed during the Holocene marine transgression, or organic detritus incorporated in fluvial and marine sediments (Griffioen et al., 2013). Human activities, such as the excavation of peat and the extended pumping for dry land, caused a drop in groundwater levels and resulted in peat oxidation, which is a process that potentially releases nutrients into the pore water. Moreover, groundwater sulfate in the relict brackish

waters that resulted from periods with sea water intrusion provided an electron acceptor needed for microbial decomposition of organic matter in the subsurface. Our study suggests that the processes of sulfate reduction induced organic matter oxidation released nutrients into the groundwater. The nutrient-rich groundwater seeps into the surface water system, eventually leading to the exceedance of the environmental quality standards for nutrients.

The installation of groundwater drainage systems in the urban and agricultural areas (tile drains and urban drainage systems, Rozemeijer et al., 2010) may further accelerate the flow of groundwater into open water bodies, thus enhancing the nutrient inputs or changing the dynamics (Chapter 3). Redistribution of the excess nutrient-rich seepage water occurred when this water was channeled towards the surroundings, thus influencing the regional water system as a whole. Therefore, the nutrient rich groundwater seepage and the subsequent redistribution of this water via surface waters became the dominant factors for the high nutrient (TN, NH_4, and TP) concentrations in both the urban and agricultural polders in the greater Amsterdam region. Inputs of N and P from fertilizer and manure seem less significant in the majority of the artificial polder catchments in this part of the Netherlands. While in the arable areas, and in regions with few water courses and no seepage (ice pushed ridge) agricultural activity is the major source exporting nutrients.

(2) What are the flow routes and mixing processes that control surface water quality in the groundwater influenced urban catchment?

The mixing between nutrient- and iron-rich anoxic groundwater and oxic runoff is the key hydrological process that determines the water quality dynamics in the urban study catchment. It was notably illustrated by the temporal pattern of relatively conservative parameters such as EC and Cl, in both a long-term monthly discrete monitoring (Chapter 3) and short-term high frequency monitoring campaign (Chapter 4). The increase of impervious area and the installation of drainage system in the process of urbanization reduces the infiltration of rain water and changes the hydrological mixing process of natural catchments by creating shortcuts bypassing the soil and shallow subsurface for the groundwater and rain water to the surface water. As a result, water mixes preferentially in the surface water system itself, instead of somewhere underway between recharge and discharge locations in a natural catchment.

The brackish groundwater found mainly in the southwest part of the urban polder was the main source for Cl and total dissolved solutes for which the EC serves as a proxy. Correspondingly, the major cations (Na, K, Ca, Mg, Fe) mainly stem from groundwater but direct precipitation and runoff were the main sources of oxygen and heavy metals (Cu, Zu, Pb, and Cd) were mainly carried by the runoff in the study catchment. In the study catchment, NO_3 is only significant in runoff that passes through public and private gardens. SO_4 might come from deep peri-marine waters and/or pyrite oxidation occurring in the artificial top soil that was dug up from nearby deep pits.

The solute concentrations measured at the polder outlet represented a mixture of these end members and fed the receiving water system (boezem) with a time changing pattern of solutes. For the major groundwater derived solutes such as Cl, HCO_3, and Ca a clear dilution pattern in periods with low-mineralized runoff was obvious at the pumping station(Chapter 3). Other parameters, including TP, NH_4, pCO_2, and ^{222}Rn underwent retention and/or reactive processes (Chapter 3). The discrete

sampling results in Chapter 3 suggested that TP might be sorbed and fixated to Fe-hydroxides during the mixing of the oxygen-rich runoff with the seeping groundwater, that NH_4 might be more controlled by other factors than the mixing, and that CO_2 and ^{222}Rn underwent atmospheric exchange and/or radioactive decay, suggesting that the residence times of the water in the polder suffices to equilibrate the concentrations with the atmosphere, except under very wet conditions. However, the patterns of the nutrients N and P were not very clear, indicating that a number of processes, including biogeochemical ones, might be impacting the temporal dynamics.

(3) What are the mechanisms controlling the dynamics of N and P in urban delta catchments affected by groundwater? (i.e. hydrological and biogeochemical processes that are controlling solutes dynamics along their pathways)(Chapter 4)

The driving mechanisms of nutrient dynamics in the selected low-lying urban catchment were discussed at three time scales: annual scale, rain event and pumping event scale.

As the key hydrological process that determines the water quality dynamics, the mixing and dilution pattern that was recognized from the discrete sampling data (Chapter 3) was confirmed by the high temporal resolution time series of the electrical conductivity (EC). And it was further proved by the simple mixing model that reproduces the mixing process well ($R^2 = 0.65$) at the annual time scale. On top of the physical mixing process, biogeochemical processes, such as primary production and iron redox transformations were also strongly suggested by the continuous and discrete sampling data to be the drivers of N and P dynamics in the shallow ditches. As a preferable form of nitrogen by plants and microbes, NH_4 concentrations in our study area were drastically lowered by primary producers (presumably both phytoplankton and benthic algae) during the growing season, which was deduced from the monthly distribution of chlorophyll-a (high in summer) and silica (lower in spring and summer). Primary production produces O_2, which subsequently influenced the redox status in the sediments and in the water column, directly regulated the pattern of P in the ditches. I deduced that the iron redox chemistry is the dominant process controlling the P dynamics in the shallow groundwater fed ditches and suggested that the high turbidity levels which occurred in the late autumn and winter were the result of iron hydroxides formation in the water column. The turbidity time series and Fe grab sampling data suggested a shift of the anoxic/oxic interface where the formation of iron hydroxides moves from the sediment in summer towards the water column in autumn and winter.

In the rain event scale, EC, NH_4, TP, and turbidity all decreased during events. The decline of EC and NH_4 may mainly be due to dilution. While chemical reactions might be more of importance for TP and turbidity as the O_2 and particles were brought by rain water/runoff.

Water pumped from the polder towards the downstream water bodies was rich in NH_4 from summer to winter but rich in organic N in the form of algae during spring. TP concentrations stayed very low during most time of the year but showed significant peaks in the late autumn and winter. Thus, the annual P load towards downstream catchments is determined by winter and autumn fluxes. Phosphorus leaves the polder mainly during the winter season when it is released from the sediment and exported mostly in the form of P sorbed to $Fe(OH)_3$ colloids and as dissolved P.

5.2 Main conclusions

This thesis concludes that, in low-lying urban catchments in near shore river deltas, groundwater is likely to outcompete other traditionally considered urban factors as an important source of nutrients. The role of groundwater in surface water eutrophication highly depends on the hydrogeological and hydrogeochemical conditions of the subsurface. An aquifer with the presence of organic matter that contributes to significant seepage calls for extra attention to the groundwater - surface water interaction which may be relevant for similar sedimentological and densely populated delta settings all around the world, such as the Mississippi and Ganges deltas (e.g. Naus et al., 2019). In our case, the groundwater - surface water interaction determines the surface water quality dynamics in an artificial polder catchment above such an aquifer. For conservatively transported solutes, such as chloride and EC as proxy for total dissolved solutes, these dynamics were controlled by the physical end member mixing between the anoxic, highly mineralized groundwater and the oxic, less mineralized runoff in the receiving surface water system of the polder. In the urban polder setting, the installation of rain and groundwater drainage systems leads to flow shortcuts where rain water and groundwater bypass large parts of the shallow subsurface and soil system. Thus, the mixing zone is transferred from the upper soil layer to the open water systems, such as ditches, ponds and shallow reservoirs. On top of the physical mixing process, the high frequency monitoring set-up helped to capture the impacts of hydrogeochemical and biogeochemical processes on the dynamics of the considered non-conservative parameters of N and P. The obtained data suggest that water temperature and light condition might be limiting factors for the biogeochemical processes, especially for shallow ditches. In the shallow water courses, the sediment-water interface is of importance where O_2 is released from primary production fixating P in ironhydroxides in growing seasons and releasing P when temperature drops and benthic algae die off in the late autumn and winter. N from groundwater ammonium is assimilated by primary production of benthic algae and phytoplankton in spring and summer, but sustains almost year-round fluxes being pumped towards downstream catchments with whether organic N or NH_4 as the dominant form. The novel high-frequency monitoring technology proved to be crucial to capture the temporal patterns and helped to frame a conceptual model that may be explored by water managers for creating more effective eutrophication mitigation strategies.

5.3 Implications

5.3.1 Implications for urban water management in low lying areas

The implications of this study for urban water management in low lying catchments are explained in the aspects of groundwater, runoff and discharge management from the perspective of reducing eutrophication to improve surface water quality status. The aquatic environment management section describes the implications for increasing biodiversity in shallow low-lying catchments for the goal of achieving substantial ecological improvement.

Groundwater management

Large amounts of excess brackish and nutrient rich water have to be pumped away from the seeping polders in order to keep the land dry for agricultural or residential uses. The redistribution of this water further spreads the groundwater influences towards the receiving regional water bodies (Chapter 2).

Groundwater drainage in the residential areas of an urban catchment as discussed in Chapter 3 and 4, shortens the flow routes of iron and nutrients to surface water by bypassing the soil layer and the reactive sediment layer in the ditches, enhancing the impacts of groundwater on surface water chemistry. Treatment of the drain water could be an option for water managers to mitigate excess nutrient loads exported to polders and downstream, but would require lots of local equipment and local maintenance. Instead, treatment of water pumped out at the main pumping station could be considered, centralizing the treatment and preventing high nutrient fluxes towards downstream waters. Alternatively, constructed wetlands could be designed halfway between seepage polders and the main pumping stations that pass the water towards the downstream boezem water. These constructed wetlands would act as biofilters, removing nutrients from the water by natural processes such as the growth of reeds (Tanner et al., 2005; Díaz, et al., 2012; Davies et al., 2017). For instance, constructed wetlands might be applicable for removing the excess nutrients from Geuzenveld drain water before being transported to the receiving water body. The excess nutrient rich groundwater might also be considered to be transported to the water treatment plant but very careful assessment of the applicability must be performed first.

Urban runoff management

Runoff carries the highest heavy metal concentrations of all flow routes in the study catchment. In the water quality survey, most runoff samples exceeded the Maximum Permissible Concentrations (MPCs) for Cu (MPC: 1.5 µg/l dissolved fraction, Geuzenveld runoff samples: 1.2-2.5 µg/l) and Zn (MPC: 9.4 µg/l dissolved fraction, Geuzenveld runoff samples: 25-157 µg/l). And heavy metals are able to accumulate in the sediment causing a potential risk for the aquatic organisms. However, apart from diluting solute concentrations, flushing catchments, and recharging aquifers (Putro et al., 2016; McGrane et al., 2017), in this study, urban runoff was found delivering oxygen into the surface water system and enhancing the chemical processes such as the oxidation of the Fe(II) that was supplied by the anoxic groundwater (chapter 3 and 4). Oxygen-rich runoff helped to fix P in the sediment layer for most of the year. From this point of view, letting runoff enter the surface water system should be encouraged in those areas with nutrients- and iron-rich groundwater seepage, which would prevent P and other metals being transported to downstream waters. The oxygen enrichment strategies below were partly inspired by this phenomenon.

Discharge management based on N and P dynamics

Mitigation measures for nutrient discharge to downstream should be based on the dynamics of N and P. The current study improved the understanding of the water quality dynamics by using high frequency monitoring technology, and exemplifies the necessity for developing new N and P controlling strategies to achieve an effective management.

Chapter 4 showed that N exists mainly as NH_4 in the study area and is being pumped downstream during most of the year, except for spring and early summer when primary production consumes most of the supply. To reduce the N flux from the polder, N could be harvested as phytoplankton which were abundant in the water column in spring. Further reduction of ammonium fluxes might be accomplished through artificial aeration of the water in summer and autumn, for example by using fountains, in order to enhance processes such as nitrification, denitrification and anammox, eventually converting NH_4 to N_2, before the water is discharged to downstream waters.

The study indicates that phosphorus from groundwater is further transported in the surface water system in either a dissolved form or in a sorbed form associated with suspended matter. The latter process seems to dominate P transport in our study catchment, especially contributing to P loads to downstream in winter. Groundwater in The Netherlands contains high concentrations of Fe(II), the hydroxides of which efficiently fix P in the sediment when Fe^{2+} reacts with oxygen at the sediment-water interface. In Chapter 4, this process is the main driver fixating P in the sediment in spring, summer and autumn. For such cases, dredging the sediment before the winter could remove P from the water system before it is transported further. In winter, the oxidation zone tends to shift towards the water column, resulting in a winter discharge with high P flux. As P is mainly in the form of particles (Fe(OH)x-P) during this period, filtrating P away from the discharge at the pumping station might be a good way to reduce P load to the downstream water system.

An engineering measure that potentially increases P retention in the sediment is to re-direct the flow of drain water. Such as, to relocate the outlets of the drains towards locations that further away from the pumping station. It extends the flow distance from the outlet to the pumping station, gives more time for iron oxidation and precipitation and adsorption of P. However, this measure might create a problem in spring and summer, as the higher retention time might increase the probability for cyanobacteria blooms. Importantly, before the application of any measures or maintenance in urban low lying catchments, managers should consider about the potential effects on the biological and chemical resilience of the ecosystem communities, e.g. dredging of a layer with abundant benthic activity might destroy an important buffer to nutrients in growing seasons, especially P. Due to the significant correlation between P and Fe, the water manager should add Fe into the routine monitoring list, which will further improve the understanding of the dynamics of P in surface water then to format effective measures to reduce eutrophication.

Aquatic environment management

High water transparency and high biodiversity are often the management targets of water authorities. To achieve such good ecological status, water dimensions such as water depth should be considered as an important factor in the future design of groundwater fed urban water systems, as these features largely determine which ecosystem and hydrogeochemical system evolves under conditions with high seepage rates of nutrient-rich groundwaters. In the shallow groundwater-fed ditches as I observed in my study area, the proliferation of the benthic community might inhibit the growth of macrophytes in the ditches, resulting in a turbid water appearance. As plankton and benthic communities compete for nutrients and light, measures such as shading the water surface by the planting of trees could be a way to reduce the benthic activity and to increase the growth of macro plants on and submerged in water. Deepening the ditches is an alternative way to shift the ecosystem by reducing radiation to the sediments at bottom of the ditches, thus reducing benthic community growth. Possibly, this would destruct the ecosystem balance in the benthic zone, consequently causing increase loads of N and P to the downstream waters as less oxygen is produced at the sediment - water interface.

In Chapter 3, it was discussed that runoff from pavements and roofs oxygenates the ditch water in wet periods, yielding enhanced water transparency during and after precipitation events. Measures that artificially increase the oxygen concentrations in these waters, such as the inlet of oxygen rich water,

aeration by fountains or similar or the artificial introduction of grazers or macrophytes may be considered to improve the ecological status of these urban waters.

5.3.2 Implications for urban water quality monitoring

The data in this thesis were collected by routine biweekly and monthly discrete systematic monitoring by the water board and a year-long high resolution monitoring campaign complemented by intensified weekly discrete sampling. The pros and cons of these two monitoring methodologies are compared in Table 5.1.

Table 5.1 Comparison between discrete routine monitoring and high frequency monitoring

	Pros	Cons
Discrete routine monitoring	• Required by Dutch law • larger amount of parameters, including ecological ones • not limited by number of locations • No need for maintenance of equipment • Relatively robust	• Only sample during the day, not during the night • Most parameters are not in-situ results • Results may differ among labs • Inefficient data transmission • Significant costs involved over long periods • Inaccurate for load estimation
High frequency monitoring	• 24 hours automatic monitoring, day and night • Options for real time water management • Easy data transmission • More sensors will be available in future • Data quality is sensitive to events and incidents • Reveals more information at a range of time scales • Supplies abundant data for modelling of biogeochemical processes	• Limited parameters • Need space and electricity • Pricy equipment and maintenance • Heavy maintenance • Need grab samples to calibrate in case of drift

Both discrete and continuous monitoring show pros and cons (Table 5.1) and their application depends on the monitoring purposes. They should be regarded complementary in water quality management. For example, monthly or weekly grab sampling appears to be insufficient in order to understand the governing mechanisms of N (NH_4) and P transport in urban catchments fed by groundwater (Chapter 3). Information is incomplete in the routine discrete sampling campaign, such as missing the peak of TP observed in winter in the high frequency time series (Chapter 4). It is likely that the samples were taken after rainfall events (and not during) when TP was already diluted or adsorbed to newly formed iron oxides. High frequency monitoring time series significantly improves our understanding of the complex nutrient dynamics (Chapter 4) by giving more insights into the temporal heterogeneity (McGrane et al., 2017). Investment in high frequency monitoring is a prerequisite for incorporating the determining biogeochemical processes into the management of urban lowlands with substantial groundwater seepage. With the assistance of this technology, we can monitor the real time changes of water quality once measures are applied to improve the water quality and ecosystem, and serve as a decision making tool (Briciu-Burghina et al., 2014; Di et al., 2019). The deployment of a high frequency

monitoring platform along pipe systems and at the hotspots of sewer leakage and faulty connection in the cities can detect possible water pollution (McGrane, 2016; Revitt and Ellis, 2016). Those strengths makes high frequency monitoring technology an asset for smart city management (e.g. Kirchner et al., 2004; Rozemeijer et al., 2010; Heffernan and Cohen, 2010; Macintosh et al., 2011; Halliday et al., 2013; Chen and Han, 2018). But to guarantee a robust performance of the high frequency monitoring equipment, we need to combine with regular discrete sampling activities. Sufficiently utilizing the obtained data from discrete sampling to some extent can give insights into the general water quality features in a catchment. In combination with high frequency monitoring, it will help to identify the periods with the highest ecological risk exposure (Halliday et al., 2015). For purpose such as giving a general environment assessment or water quality evaluation, testing compliance against set environmental quality standards, discrete sampling is more suitable than high frequency monitoring. But the sampling time should be considered to obtain representative samples, as a bias may be introduced by only measuring during day time or sampling during pumping period in some case (Halliday et al., 2015; Neal, et al., 2011; Van der Grift et al., 2016).

5.4 Recommendations for future research

5.4.1 Collect information of the subsurface in surface water quality management in coastal cities

This thesis demonstrated that groundwater is a generally unnoticed provider of nutrients to surface water in seepage areas with abundant organic matter in the subsurface which impacts the chemistry and vegetation composition in in the receiving waters (Vermonden et al., 2009; van Dijk et al., 2019a; van Dijk et al., 2019b). Investigations for gathering information on the subsurface, thus will give hints for identifying the sources and sinks of certain pollutants in urban surface water system (Wang et al., 2019). In The Netherlands, the subsurface has been intensively studied and the sufficient groundwater and surface water quality data are an asset. With this knowledge of the geology, geochemistry and lithology (e.g. Griffioen et al., 2013; Schokker et al., 2015;), we were able to identify the source of the excess nutrients in the surface water and groundwater. For example, in the urban polder Geuzenveld we were able to link the flow path of the deep nutrient rich groundwater to the presence of a paleo-tidal channel. It is recommended to identify other regions worldwide where high nutrient concentrations in groundwater may depreciate surface waters as that these high concentrations may occur in other densely populated coastal aquifers in river deltas or estuarine sedimentological settings where salt water intrusion and/or marine transgressions have supplied sulfate or created sulfate reducing conditions, such as the Ganges delta region of Bangladesh and India (Halim et al., 2009), Mississippi detla (Törnqvist et al., 2008; Borrok et al., 2018), and Yangtze estuary (Wen et al., 2020).

5.4.2 A comprehensive study on the sediment-water interface --- benthic zone and nutrients dynamics

In urban catchments fed by nutrient rich groundwater, nutrient loads to the water column and downstream are strongly influenced by the sediment-water interface (i.e., benthic zone and hyporheic zone) (Chapter 4). Understanding the roles of these zones in the nutrient cycle is essential for controlling eutrophication. The benthic zone is the layer between water column and the upper surface of sediment.

It is only a small part of the hyporheic zone but is habituated by abundant organism communities. The biological processes affecting the zones are controlled by temperature and radiation; as demonstrated in polder Geuzenveld, N and P were significantly retained in spring and summer due to primary production and coupled iron oxidation, but N and P got released into the water column in winter after temperatures dropped and light got reduced. For N, there are also pathways like denitrification, nitrification, microbial ammonification, ammonium oxidation, and anammox, which might also be important processes happening in the benthic zone (Nizzoli et al., 2020). Utilizing the functions of these zones may provide for an effective water quality management strategy once it is thoroughly understood (Robinson, 2015). A thorough investigation of the ecosystem, the physicochemical characterisitics of the hyporheic zone and the microbial community structure (Risse-Buhl et al., 2017) are appealing topics. For instance, in this thesis, I hypothezised that the seasonal behaviour of phytoplankton and benthic algae affects the N and P dynamics. In this process, the benthic zone especially plays a crucial role in the P dynamics by releasing O_2 into pore water, regulating the redox status at the water-sediment interface. However, these discussions were only based on a limited dataset of mostly water quality data. To test these hypotheses, dedicated lab and field experiments are needed to understand:

- Ecosystem: the state and dynamics of the benthic community over time and space, and further characterizing the phytoplankton biomass dynamics;
- Physicochemical status: depths of the hyporheic and benthic zone, oxygen, ammonium, phosphorus and redox profiles from the subsurface to the sediment layer and to the water column; the relation of iron transformation with the changes of the redox status in the stream bed and the water column year-round;
- Microbial community: microbial community structure that may significantly influence nutrient dynamics such as the bacteria communities that inducing the transformation and loss of N by nitrification, denitrification and anammox (e.g.Nizzoli et al., 2020).

5.4.3 Study on the limiting factors for ecological status

To achieve a good ecological status, it is important to assess and understand the factors that are retaining nutrients and affecting ecological communities (Nizzoli et al., 2020). I recommend a systematic study of the relationship of ecological status with the following potential limiting factors proposed in this study:

Nutrient sources: Geuzenveld is a specific/typical polder catchment with significant amount of groundwater (large seepage rate >1 mm/d) seeping into the water system and being the main source of nutrients. Rain water and seepage water mix in the shallow ditches, in which large water plants are absent in most locations and where the benthic community prevails in the growing season, as it encounters the seepage water before it enters the water column (Fig.5.1a). Possibly, the benthic community is less important in polder without substantial nutrient seepage, as other sources might supply the nutrients, such as inlet water or agriculture inputs. I hypothesized that communities that have fast access to the supplied nutrients might become the dominant species in those kind of systems. For example, Figure 5.1b shows a completely different ecosystem in the downstream secondary channel (water level: 0.25 mNAP) to the east of Geuzenveld (Fig.5.1b) compared with the ditches within the polder Geuzenveld. The secondary channel receives the nutrient rich headwaters from the upstream

polder – Geuzenveld, but it developed into an ecosystem dominated by emergent aquatic plants that produce ample oxygen and lead to high water transparency. It would be recommended to study the benthic, phytoplankton and macrofauna in a number of well-characterized polder systems to get a better grip of the dominant species in relation to the main sources of nutrients.

Figure 5.1 (a) Ditch in polder Geuzenveld and (b) the downstream polder to its east, connects to the primary channel Haarlemmerweg (water level: 0.25 mNAP) in the north (August, 2018)

Physical dimension of water courses: In lowland pit lakes, shaping the form of the lakes was reported to some extent increasing N retention and its permanent removal (Nizzoli et al., 2020). Literature has as well reported that small water bodies, especially shallow fresh surface water systems, such as wetlands, shallow lakes and reservoirs, and drainage ditches showing disproportionately larger capability of retaining nutrients than larger water bodies (Alexander et al., 2000; Harrison et al., 2009; Brainard and Fairchild, 2012; Cheng and Basu, 2017). The capability of shallow ditches for retaining N and P by biogeochemical processes was demonstrated in Chapter 4. In Geuzenveld, the shallowness of the ditches favors the growth of benthic algae as light can penetrate easily to the bottom. In other polders, vast growth of phytoplankton could be the dominant community under conditions favoring plankton organisms (deeper water, downward nutrients flow, lack of a NH_4 source from groundwater seepage).

To achieve a shift of the water regime from turbid (possible benthic dominant) to clear state (large aquatic plants), a potential measure is to deepen the ditches. However, changing the dimensions of ditches in real-world setting should be tested carefully first, because deeper ditches would reduce the hydraulic resistance of the subsurface and may cause increased groundwater seepage rates. Moreover, deepening might also disturb the retention of P in the sediment due to the destruction of the benthic communities. Studies show that the nutrient retention rates decrease with the increase of depth of water bodies (Olli et al., 2009; Cheng and Basu, 2017). Stability of the side of the ditches is also an important factor such as more gradual slopes may enhance nutrient processing from surface runoff by the riparian vegetations (Valkama et al., 2019). Research is recommended to focus on establishing favourable dimensions for water courses, finding a balance that optimizes the ecological status as a function of seepage rate, nutrient concentrations and water depth. Eventually, optimizing the dimensions of ditches and drains may benefit water management as it aims to reduce nutrient loads, increases nutrient retention and eventually controlling eutrophication.

5.4.4 Upscaling from catchment scale to regional scale ---- Integrated model for artificial urban water systems

Sustainable and effective urban water management requires an integrated and holistic perspective (Fletcher et al., 2015; Díaz et al., 2016; Eggimann et al., 2017). To achieve integrated regional water management, scaling up the specific hydro-biogeochemical processes at the catchment scale to the regional scale is a requisite but also difficult (McGrane, 2016). However, modeling is an effective tool for improved quantitative understanding of the water system at large scales. Integrated modeling is playing an important role as a support system supplying comprehensive information for decision makers. Adoption of integrated modeling in activities like urban infrastructure design, flood risk management (Bach et al., 2014), water quality management (Raja Segaran et al., 2014), etc, is progressing worldwide. For water quality management, it meets the urgent requirement of being able to predict and prevent eutrophication and harmful algae blooms (Smith and Schindler, 2009; Beusen et al., 2016). However, the development of such models is facing a variety of obstacles, such as limited data availability and accuracy (Hill et al., 2014; Fletcher et al., 2015; Tscheikner-Gratl et al., 2019), and especially lack of full understanding of the hydrological system, solute pathways and the biogeochemical processes involved.

In this thesis, I collected a large amount of data which could be used to validate a model that integrates hydrology, hydrochemistry, and biochemistry in the future. To supply a foundation for such a water quality and biochemistry model, a water balance or water dynamics module should be built first. The pumping discharge and meteorological data are available as inputs, and water level were previously used as boundary conditions in the very much simplified model in Chapter 4 can also be used for validation/calibration. As discussed in this thesis, EC is a relatively conservative parameter mainly controlled by the mixing process between groundwater and rainwater. Thus, we can use the high frequency EC data to calibrate the fractions of the drain, rain infiltration, and deep groundwater seepage. The water quality module should at least consist of three sub-modules: a mixing, chemistry and a biology module. The water quality parameters would involve N (NH_4, NO_3, organic N), P(PO4 and particle P), Fe, and O_2. The mixing sub-module is the base for the other two sub-modules, requiring detailed information on the stores of water (subsurface, soils and surface waters) within the catchment. Furthermore, N is mainly involved in biological processes, but P requires both the chemistry and biology modules, same as O_2. The benthic zone should be considered as an important compartment in an integrated water quality model, regulating the water quality composition of the discharge from groundwater to surface water (Robinson, 2015). The proposed model could be applied to simulate the dynamics and interactions of water quality parameters and their responses to precipitation and pumping events and could play a role in exploring potential measures that aim to improve the ecological status. For example, it can be used for testing the hypothesis about the kinetics of the processes of $Fe(OH)_3$ precipitation under different temperature regimes, for evaluating measures like dredging the ditches, changing the flow directions, installing fountains to aerate the ditches and introducing microbes and grazers to improve ecological status.

5.5 Final messages

Nutrient loads reduction has been set as a target for abating eutrophication in natural and artificial water bodies. This thesis highlighted an important source of nutrients which has been impeding the reduction

of nutrient loads – groundwater in coastal low-lying areas. Like many other coastal cities, Amsterdam is in a key spot along the land-sea continuum. Nutrient loads from this region are partly determining the ecosystem downstream in the North Sea. The findings in this thesis are not limited to artificial catchments, or nutrients or coastal areas. Artificial catchments might deviate from natural systems, but due to their possibilities for manipulating the key boundary conditions, such as water levels, pumping regimes and connections between different parts of their water systems, they are a valuable field laboratory for understanding the complexity of urban catchments and for testing management options. These catchments can help improve our understanding of biogeochemical processes in both artificially altered systems and natural systems.

The water system that I studied in the greater Amsterdam region is unique in the sense that the artificial polders were established early on since the 17th century and intensive water management is historically a Dutch asset. However, river deltas and low-lying areas are facing increased urbanization worldwide, creating artificial water systems that resemble the Amsterdam region in cities such as New Orleans, Shanghai and Dhaka. We recommend to study the interaction between groundwater and surface water in these urban landscapes, expecting that groundwater may have an overriding impact on the water quality and nutrient cycling in the low-lying cities worldwide.

Acknowledgements

I would like to acknowledge China Schloarship Council for awarding me the scholarship to perform this study, and Waternet, TNO, Deltares, and TU Delft for funding the research. I also would like to thank Waternet, TNO and VU Amsterdam for the financial support during the extension. This PhD means so much more than a diploma to me. It is a wonderful and profound journey of my academic and personal development, which was surrounded by world best scientists, genuine colleagues and friends.

First and foremost, I would like to thank my supervision team for all those years consistent support and guidance. Hans Peter, for everything you have done for me, I probably can write an entire chapter about it. I really wouldn't have come so far without your consistent care and selfless guidance through each difficult stage in the past 7 years. Your immense knowledge and profound expertise were invaluable in formatting this dissertation and the three high quality papers. From you, I greatly benefited from your rigorous scientific approach, and your valuable attitude and integrity towards science. Most important, you are so good at stimulating my research interests and infusing me with enthusiasms for science. People say that I have grown a lot in the past a few years. I know it came from the accumulation of your great patience and efforts, step by step, day by day. Having you as my mentor is one of the luckiest things in my life. Joachim, I am profoundly grateful for your intelligent work and your substantial contribution in improving my academic writing. You were always being able to keep the positiveness when I had lost mine. Thank you for always being there when I needed the most and for constantly checking my well being during the corona crisis. I am deeply grateful to have you as my supervisor and my friend. Our countless positive and delightful discussions within and beyond science really lighted up my PhD journey. Boris, your insightful comments always deepened my thinking and enormously improved the first two papers. I am deeply grateful that you have always been giving me suggestions and guiding me. It was very unfortunate that the re-organization broke our team and our plan. But I am very glad that we made it to the end. Ype, with you joining my supervision team is a wonderful touch for the end of my PhD. It was a period full of stress, but I really appreciate that you gave me a lot of freedom to incubate my own ideas, which enormously built up my confidence as a professional. Your valuable and to the point suggestions profoundly enlightened me which I am more than grateful.

My sincere thanks also goes to my promoters professor Jack Middelburg and professor Han Dolman, for your support in the accomplishment of this research. I would like to specially thank Jack for your insightful comments and encouragement. Your brilliant idea about benthic algae lead me solved the complex puzzle and formatted the third paper, the one I am proud of the most.

I would like to specially thank those who made this PhD journey possible. Peter, thank you for recruiting me from Beijing 7 years ago and your constant confidence in me. Without you this amazing adventure would have not begun. professor Sampurno Bruijnzeel and professor Pieter Stufyzand, thank you for helping me successfully applied the CSC scholarship. Sampurno, I am more than grateful for your continuous spiritual support for the rest of my PhD.

I would like to thank my outstanding reading committee members: professor Eddy Moors, professor Jeroen Aerts, professor Britta Schmalz, professor Brian Kronvang and dr. Bas Van der Grift, for your valuable time in assessing my thesis, and for your insightful comments and your nice words.

My deepest gratitude goes to my dear colleagues at Waternet, without whom this research would not have been accomplished. Maarten, I don't think I can ever thank you enough for everything you have done for me. Without your confidence and your essential support, there would not be this thesis. You were instrumental in making this research happen and in bringing it to the perfect end. Thank you for all the inspiring discussions and the insightful feedbacks. We undoubtedly greatly benefited from your sharp eyes and your vast knowledge of the whole research area. In addition, I am very lucky to have you as a colleague, a guide and a friend. I am deeply grateful that you gave me an opportunity to keep pursuing my interests at Waternet after my PhD. I am in great debt to your trust and your confidence in me. Eelco, there would not be these wonderful results in this thesis without your unbelievably efficient help in the field. You were so responsive which made the endless problems in the field less troubling, and guaranteed my work running smoothly. Working with you was super efficient and joyful. Frank, thank you for generously sharing your knowledge and teaching me very cool hydrogeometry skills. Discussion with you was always inspiring, you are so good at tutoring. Henk, thank you for your great and kind help with my field work in Geuzenveld, and bringing me along with you to let me get to know more about my research area in vision. The old and newly built dikes, the burst pipe line, the Groot Mijdrecth polder, and the Amstel River tour were all valuable field experiences for me. Laura, it was always delightful with your presence in the group meetings and hearing your enlighting opinions. Especially when there were a lot of discussions happening, you would always listen to what I said which I am deeply grateful. Sonja, we would not have got such nice data set without your efficient help with the perfect sampling arrangement. Now I understand it was not as simple as I thought to arrange those. Ruth, thank you for checking my well being and teaching me FEWS during my internship, and having the empathy ear to listen to my "horror" stories in the field. Laura, Sonja and Ruth, I would like to give my sincere thanks to you for accepting me in the team. It has been such a joy working with you. My special thank also goes to Marc, Jan Willem, Rob, Jos, Marcel, Ben, for generous sharing your data and your expertise, and to Frank, Mark, George, and all colleagues from floor A8, for your caring and kindness during my stay. Especially Peter, congratulations to your retirement. I would miss a lot our lunch talk from which I always learned something new either in water science or in art. I would like to wish you the best for your new journey.

I would also like to thank Corne, for the wonderful collaboration we had at the very beginning of my PhD. It was already such a long time ago, but I remember it would had been difficult to kick off without your hard work and your help. My thanks also go to my colleague Tano from TNO, for your greatly help with the water quality survey; and Vince from Deltares, for the fun field work we had in Geuzenveld and Twente. A special thank also goes to the previous hydrology group: Maarten, Henk, Iliya, and Micheal. Maarten, thank you for all the chats within and outside of the office, and for introducing me to a wonderful art teacher. Henk, thank you for your confirmation after my presentation at Deltares, it was a big encouragement for me.

I have been fortunate to be surrounded by lovely and inspiring colleagues and friends from VU (names are listed in alphabetical order): Artem, Alex, Aniee, Anouk, Bret, Dirk, Enirco, Katyon, Katherina, Katrin, Kanayim, Lintao, Mellissa, Nick, Oscar, Ove, Qirui, Roland, Stefane, Srijana, Thanos, Tom, Thomas, Thomas, Youserf, Yanjiao. Thank you for the countless enjoyable coffee breaks, all the fun nights out, and generously sharing your experiences and information with me. They are all precious memories that I cherish a lot. Particularly, I would like to thank Fenny, for all your essential and kind

help during my PhD, you made things a lot more easier for me. Tanya, I am deep grateful for sharing an office with you, thank you for being such a thoughtful and supportive officemate, cheering me up when I was really down. I am going to miss our fun office chat so much! Dave, you are a great friend. Thank you for helping me carefully prepare my Dutch summary, you are the best! Dear Rebacca, it was always so comfortable around you. Thank you for laughing and voting every joke I made, you really made me feel that I had a great sense of humor. Srijana, our countless long and fun conversations are something that I am really going to miss, and of course your amazing Nepal cuisine! Jim, you are the sweetest. Conversations with you were always so at ease. Thank you for inviting me to the field and good luck with your PhD. You are going to do it so well. Heloise, it was a lot easier of having you understanding how unpredictable a PhD journey can be. I am also so grateful of having you and Sjoerd encouraging my art pursuing journey. Looking forward to seeing the result of your art project. Alexa, my dearest friend, thank you and Vito for always being there firmly whenever I needed during the most difficult time of my PhD. With you beside me, I feel completely safe. We have had so much fun together, your brilliant jokes can always make me laugh so hard and refresh my mind with positiveness. In addition, I couldn't be more grateful that you helped me improved my English so much.

My sincere thanks also go to my Chinese friends that I have met in The Netherlands (names are listed in alphabetical order): Bochao, Bao Yue, Chao, Chunhai, Fei, Gang, Huirong, Hong, Jin, Junhui, Li, Li Han, Lihui, Mei, Meichen, Na Zhao, Qing, Rujun, Shanliang, Siqiao, Shu, Ting, Tingting, Wanhai, Wenna, Wenjing, Xiaobo, Xiaolong, Xilin, Xiaoxia, Xinying, Yuanfang, Yongmei, Yuan Shang, Yongjie, Yumei, Yurui, Zhi, Zhiqing, Zongliang, for the lovely conversations and fun time we had together. Wish you all success in the way you want, no matter where you are. Particularly thank to Huan and Yuan Shang, you can always bring sunshine wherever you go, I am truly a big fan of you. I must express my sincere gratitude to Kai, it would be much more difficult without your genuine conversations during the lockdown. Your positiveness and fun point of view towards life are the most inspiring. I would also like to give my deepest gratitude to Jina, thank you for your thoughtful company and strong support during the most difficult time of my PhD. Conversations with you can always clear up my mind and induce more profound understandings of life. Particular thank also goes to friends who freed my mind completely from my study during the countless lovely conversations, wonderful trainings, parties, dinners, museum tours, and festival openings: Sylvia, Zoe, Jun, Jeanette, and Jane. Your valuable encouragement and inspirations worth a great deal to me.

I would also like to thank my previous supervisors and friends back in China. Professor Xia and professor Ren, thank you for bringing me to the field of hydrology, and constantly being such strong support in the past 11 years. I wouldn't have gone so far without you believing and guiding me. Songjie, Yaping, and Jing, thank you for keeping me always being 19 years old. We are everywhere in this world, but I am so glad that distance did not weaken our friendship, instead, it is growing stronger. Thank you for always being there whenever I am in need, laughing with me, crying with me, and no matter what happened always trusting me deeply. My journey would be so much less colorful without you.

最后，我要感谢我的家人，谢谢你们那么坚强，那么有力量。你们无条件的爱是我不竭力量的源泉。尤其是外公，在您身上， 我明白了什么是终身学习。我的爸爸妈妈，谢谢你们为我付出和改变的一切，谢谢你们与我一起成长，谢谢你们用你们无比强大的爱和智慧助我完成博士学习，我爱你们。

References

Armendáriz L.C., Cortese B., Rodriguez M., and Capítulo A.R.. ArmenEcosystem services of runoff marshes in urban lowland basins: proposals for their management and conservation. Knowl. Manag. Aquat. Ecosyst, 418, 32, 2017.

Abdalla, F. and Khalil R.. Potential effects of groundwater and surface water contamination in an urban area, Qus City, Upper Egypt. Journal of African Earth Sciences, 141: 164-178, 2018.

Appelo, C. A. J. and Postma, D.. Geochemistry, groundwater and pollution, Second Edition, A.A. Balkema Publishers, Leiden, The Netherlands, 2005.

Appelo, C.A.J. and Postma, D.. Geochemistry, groundwater and pollution (2nd edition). CRC Press, UK, 2010.

Alexander R. B., Smith R. A., and Schwarz G. E.. Effect of stream channel size on the delivery of nitrogen to the Gulf of Mexico. Nature, 403(6771): 758–761, 2000. doi:10.1038/35001562.

Audet J., Zak D., Bidstrup J., and Hoffmann C.C.. Nitrogen and phosphorus retention in Danish restored wetlands. Royal Swedish Academy of Sciences, 1-13, 2019. https://doi.org/10.1007/s13280-019-01181-2

Berndtsson, J.C.. Storm water quality of first flush urban runoff in relation to different traffic characteristics. Urban Water Journal, 11 (4): 284-296, 2014.

Bunch N.D. and Bermot M.J.. Nitrate and ammonium uptake by natural stream sediment microbial communities in response to nutrient enrichment. Research in Microbiology. 163(2): 137-141, 2012.

Bouwman A.F., Bierkens M.F.P., Griffioen J., Hefting M.M., Middelburg J.J., Middelkoop H., and Slomp C.P.. Nutrient dynamics, transfer and retention along the aquatic continuum from land to ocean: towards integration of ecological and biogeochemical models. Biogosciences, 10: 1-22, 2013.

Boesch D.F., Brinsfield R.B., and Magnien R.E.. Chesapeake Bay Eutrophication: Scientific Understanding, Ecosystem Restoration, and Challenges for Agriculture. Journal of Environmental Quality, 30(2): 303-320, 2001.

Beusen A.H.W., Bouwman A.F., Van Beek L.P.H., Mogollón J.M., and Middelburg J.J.. Global riverine N and P transport to ocean increased during the 20th century despite increased retention along the aquatic continuum. Biogeosciences. 13: 2441-2451, 2016.

Brainard, A. S., and Fairchild G. W.. Sediment characteristics and accumulation rates in constructed ponds. Journal of Soil and Water Conservation, 67(5): 425–432, 2012. doi:10.2489/jswc.67.5.425.

Bieroza M.Z., Heathwaite A.L., Bechmann M., Kyllmar K., and Jordan P.. The concentration-discharge slope as a tool for water quality management. Science of the Total Environment, 630: 738-749, 2018.

Borrok D.M., Lenz R.M., Jennings J.E., Gentry M.L., Steensma J., Vinson D.S.. The origins of high concentrations of iron sodium, bicarbonate, and arsenic in the Lower Mississippi River Alluvial Aquifer. Applied Geochemistry, 98: 383-392, 2018.

Briciu-Burghina C., Sullivan T., Chapman J., and Regan F.. Continuous high-frequency monitoring of estuarine water quality as a decision support tool: a Dublin Port case study. Environ Monit Assess, 186: 5561-5580, 2014.

Baken S., Sjostedt C., Gustafsson J.P., Seuntjens P., Desmet N.. Characterisation of hydrous ferric oxides derived from iron-rich groundwaters and their contribution to use suspended sediment of streams. Applied Geochemistry, 39: 59-68, 2013.

Bonneau, J., Fletcher T.D., Costelloe J.F., Burns M.J.: Stromwater infiltration and the 'urban karst' A review. Journal of Hydrology, 552: 141-150, 2017.

Bouraoui F. and Grizzetti B.. Long term change of nutrient concentrations of rivers discharging in European seas. Science of the Total Environment. 409: 4899-4916, 2011.

Borst B., Mahmoud N.J., van der Steen N.P., and Lens P.N.L.. A case study of urban water balancing in the partly sewered city of Nablus-East (Palestine) to study wastewater pollution loads and groundwater pollution. Urban Water Journal, 10(6): 434-446, 2013.

Bach, P. M.; Rauch, W.; Mikkelsen, P. S.; McCarthy, D. T.; Deletic, A. A critical review of integrated urban water modelling − Urban drainage and beyond. Environmental Modelling & Software, 54, 88−107, 2014.

Brabec, E., Schulte, S., Richards, P. L.: Impervious Surfaces and Water Quality: A Review of Current Literature and Its Implications for Watershed Planning, Journal of Planning Literature, 16, 499-513, 2002.

Boogaard, F.C., Van de Ven, F., Langeveld, J.G., and Van de Giesen, N.. Stormwater quality characteristics in (Dutch) urban area and performance of settlement basins. Challenges, 5, 112-122, 2014.

Cleveland, W.S.: Robust Locally Weighted Regression and Smoothing Scatterplots. Journal of the American Statistical Association, 74 (368): 829–836, 1979. doi:10.2307/2286407.

Charette M.A. and Buesseler K.O.. Submarine groundwater discharge of nutrients and copper to an urban subestuary of Chesapeake Bay (Elizabeth River). Limnol. Oceanogr., 49(2): 376-385, 2004.

Cheng, F. Y., and Basu N. B.. Biogeochemical hotspots: Role of small water bodies in landscape nutrient processing. Water Resources Research, 53: 5038–5056, 2017. doi:10.1002/ 2016WR020102.

Cavaliere E. and Baulch H.M.. Winter nitrification in ice-covered lakes. PLoS ONE, 14(11): e0224864, 2019. https://doi.org/10.1371/journal.pone.0224864

Chen Y., Cebrian J., Lehrter J., Christiaen B., Stutes J., and Goff J.. Storms do not alter long-term watershed development influences on coastal water quality. Marine Pollution Bulletin, 122(1-2): 207-216, 2017.

Chen M., Ding S., Chen X., Sun Q., Fan X., Lin J., Ren M., Yang L., and Zhang C.. Mechanisms driving phosphorus release during algal blooms based on hourly changes in iron and phosphorus concentrations in sediments. Water Research, 133: 153-164, 2018.

Cecil, L. D. and Green, J. R.: Radon-222, in: Environmental tracers in subsurface hydrology, edited by: Cook, P. G. and Herczeg, A. L., Kluwer, Boston, USA, 175-194, 2000.

Cartwright, I. and Hofmann H.: Using radon to understand parafluvial flows and the changing locations of groundwater inflows in the Avon River, southeast Australia. Hydrology and Earth System Sciences, 20, 3581-3600, 2016.

Chen Y. and Han D.. Water quality monitoring in smart city: A pilot project. *Automation in Construction* **2018,** *89*, 307-316. DOI: 10.1016/j.autcon.2018.02.008.

Chapelle, F. H., Zelibor, J. L., Grimes, D. J., Knobel, L. L.: Bacteria in deep coastal plain sediments of Maryland: a possible source of CO2 to groundwater. Water Resour Res, 23, 1625-1632, 1987.

Dinoloket: https://www.dinoloket.nl/, last access: date October, 14, 2016.

Delsman, J. R.: Saline Groundwater - Surface Water Interaction in Coastal Lowlands. Ph. D. thesis, VU University Amsterdam, Amsterdam, The Netherlands, 2015.

Dimova, N.T., Burnett W.C., Chanton J.P., Corbett J.E.. Application of Radon-222 to investigate groundwater discharge into small shallow lake. Journal of Hydrology, 486: 112-122, 2013.

Di Z., Chang M., and Guo P.. Water quality evaluation of the Yangtze River in China using machine learning techniques and data monitoring on different time scale. Water, 11(339): 1-23, 2019.

Drexler J. Z., De Fontaine C. S., Deverel S. J.: The legacy of wetland drainage on the remaining peat in the Sacramento San Joaquin Delta, California, USA, Wetlands, 29,1, 372-386, 2009.

Delsman, J. R., Huang, K. R. M., Vos, P. C., De Louw, P. G. B., Oude Essink, G. H. P., Stuyfzand, P. J., Bierkens, M. F. P.: Paleo-modeling of coastal saltwater intrusion during the Holocene: an application to the Netherlands, Hydrol Earth Syst Sc, 18, 10, 3891-3905, 2014.

Destouni G., Fischer I., and Prieto C.. Water quality and ecosystem management: Data-driven reality check of effects in streams and lakes. Water Resources Research, 53, 6395–6404, 2017.

Destouni G. and Jarsjö J.. Zones of untreatable water pollution call for better appreciation of mitigation limits and opportunities. WIREs Water, 5:e1312, 2018.

De Vries, W., Kros J., Oenema, O., De Klein, J.: Uncertainties in the fate of nitrogen II: A quantitative assessment of the uncertainties in major nitrogen fluxes in the Netherlands, NUTR CYCL AGROECOSYS, 66, 71-102, 2003.

Díaz F.J., O'Geen A.T., and Dahlgren R.A.. Agricultural pollutant removal by constructed wetlands: Implications for water management and design. Agricultural Water Management, 104: 171-183, 2012.

De Louw, P. G. B., Oude Essink, G. H. P., Stuyfzand, P. J., van der Zee, S. E. A. T. M.: Upward groundwater flow in boils as the dominant mechanism of salinization in deep polders, The Netherlands. J Hydrol, 394, 494-506, 2010.

Dent, D.L. and Pons, L.J.. A world perspective on acid sulphate soils, Geoderma, 67: 263-276, 1995.

Díaz P., Stanek P., Frantzeskaki N., and Yeh D.H.. Shifting paradigms, changing waters: Transitioning to integrated urban water management in the coastal city of Dunedin, USA. Sustainable Cities and Society. 26: 555-567, 2016.

Dai Y., Shangguan W., Wei N., Xin Q., Yuan H., Zhang S., Liu S., Lu X., Wang D., and Yan F.. A review of the global soil property maps for Earth system models. SOIL, 5: 137-158, 2019.

Davies C.G., Vogwill R., and Oldham C.. Urban subsurface drainage as an alternative water source in a drying climate. Australasian Journal of Water Resources, 20(2): 148-159, 2017.

Duncan J.M., Welty C., Kemper J.T., Groffman P.M., and Band L.E.. Dynamics of nitrate concentation-discharge patterns in an urban watershed. Water Resources Research, 53: 7349-7365, 2017. doi: 10.1002/2017WR020500

Ellis, P.A. and Rivett, M.O.. Assessing the impact of VOC-contaminated groundwater on surface water at the city scale. Journal of Contaminant Hydrology, 91: 107-127, 2007.

European Commission (2012). Commission Staff Working Document, European Overview (1/2) Accompanying the Document: “Report From the Commission to the European Parliament and the Council on the Implementation of the Water Framework Directive (2000/60/EC) River Basin Management Plans.

European Commission (2003). Common Implementation Strategy for the Water Framework Directive. Guidance Document No. 2, Identification of Water Bodies. Produced by Working Group on Water Bodies Directorate General Environment of the European Commission, Brussels.

EU (2017). Commission Staff Working Document; the EU Environmental Implementation Review. Country Report – The Netherlands. The EU Environmental Implementation Review: Common Challenges and how to combine efforts to deliver better results. COM(2017) 63 final, http://ec.europa.eu/environment/eir/pdf/report_nl_en.pdf

Ellis, J. B., Marsalek, J., Chocat, B.: Encyclopedia of Hydrological Sciences, Urban Water Quality, 1st edition, M G Anderson, John Wiley & Sons, Ltd, United States, 8, 97, 2005.

Eggimann S., Mutzner L., Wani O., Schneider M.Y., Spuhler D., de Vitry M.M., Beutler P., and Maurer M.. The Potential of Knowing More: A Review of Data-Driven Urban Water Management. Environmental Science & Technology, 51: 2538-2553, 2017.

Foster, S.S.D.. The interdependence of groundwater and urbanization in rapidly developing cities. Urban Water, 185-192, 2001.

Filippelli M.G.. The global phosphorus cycle: Past, present, and future. Elements, 4(2): 89-95, 2008.

Fletcher T.D., Shuster W., Hunt W.F., Ashley R., Butler D., Arther S., Trowsdale S., Barraud S., Semadeni-Davies A., Bertrand-Krajewski J.L., Mikkelsen P.S., Rivard G., Uhl M., Dagenais D., and Viklander M.. SUDS, LID, BMPs, WSUD and more – The evolution and application of terminology surrounding urban drainage. Urban Water Journal, 12(7): 525-542, 2015.

Griffioen, J.: Uptake of phosphate by iron hydroxides during seepage in relation to development of groundwater composition in coastal areas. Environmental Science & Technology, 28, 675-681, 1994.

Griffioen J.. Extent of immobilisation of phosphate during aeration of nutrient-rich, anoxic groundwater. Journal of Hydrology, 320 (3-4): 359-369, 2006.

Grolander S.: Radon as a groundwater tracer in Forsmark and Laxemar. SKB Rapport R-09-47, ISSN 1402-3091.

Galan, I., Andrade C., Mora P., and Sanjuan M.A.: Sequestration of CO_2 by concrete carbonation. Environmental Science & Technology, 44: 3181-3186, 2010.

Gunnars A., Blomqvist S., Johansson P., and Andersson C.. Formation of Fe (III) oxyhydroxide colloids in freshwater and brackish seawater, with incorporation of phosphate and calcium. Geochim. Cosmochim. Acta, 66 :745-758, 2002.

Göbel, P., Dierkes C., Coldewey W.G.: Storm water runoff concentration matrix for urban areas. Journal of Contaminant Hydrology, 91: 26-42, 2007.

Gabor, R.S., Hall S.J., Eiriksson D.P., Jameel Y., Millington M., Stout T., Barnes M.L., Gelderloos A., Tennant H., Bowen G.J., Neilson B.T., and Brooks P.D.: Persistent Urban Influence on Surface Water Quality via Impacted Groundwater. Environmental Science & Technology, 51, 9477-9487, 2017.

Griffioen, J., Notenboom, J., Schraa, G., Stuurman, R. J., Runhaar, J., and Van Wirdum, G.. Systeemgericht grondwaterbeheer. Groningen: Wolters-Noordhoff, 2003.

Gumindoga W., Rientjes T., Shekede M.D., Rwasoka D.T.,. Nhapi I., Haile A.T.: Hydrological impacts of urbanization of two catchments in Harare, Zimbabwe. Remote Sensing, 6(12), 12544-12574, 2014.

Gustafsson B.G., Schenk F., Blenckner T., Eilola K., Markus Meler H.E., Müller-Karulis B., Neumann T., Ruoho-Airola T., Savchuk O.P., and Zorita E.. Reconstructing the Development of Baltic Sea Eutrophication 1850-2006. Ambio. 41(6): 534–548, 2012.

Garrett, C. G., Vulava, V. M., Callahan, T. J., Jones, M. L.: Groundwater-surface water interactions in a lowland watershed: source contribution to stream flow. Hydrol Process, 26, 3195-3206, 2012.

Genkai-Kato M., Vadeboncoeur, Liboriussen L., and Jeppesen E.. Benthic-planktonic coupling, regime shifts, and whole-lake primary production in shallow lakes. Ecology, 93(3): 619-631, 2012.

Griffioen J., Vermooten S., and Janssen G.: Geochemical and palaeohydrological controls on the composition of shallow groundwater in the Netherlands. Applied Geochemistry, 39, 129-149, 2013.

Hartwig E.O.. Factors affecting respiration and photosynthesis by the benthic community of a subtidal siliceous sediment. Marine Biology, 46: 283-293, 1978.

Hansson L.A.. Effects of competitive interactions on the biomass development of planktonic and periphytic algae in lakes. Limnology and Oceanography, 33(1): 121-128, 1988.

Hijma, M. P.: From river valley to estuary: the early-mid Holocence transgression of the Rhine-Meuse valley, Ph. D. thesis, Utrecht University, Utrecht, The Netherlands, 2009.

Huisman, P., Cramer, W., van Ee, G., Hooghart, J. C., Salz, H. Zuidema, F. C.: Water in the Netherlands. Netherlands Hydrological Society, Rotterdam, the Netherlands, 1998.

Heinis, F. and Evers, C. H. M.. Toelichting op ecologische doelen voor nutrienten in oppervlaktewateren. STOWA-report (in Dutch), Utrecht, The Netherlands, 2007.

Henry J.C. and Fisher S.G.. Spatial segregation of periphyton communities in a desert stream: causes and consequences for N cycling. Journal of The North American Benthological Society, 22 (4): 511-527, 2003.

Hobbie S.E., Finlay J.C., Janke B.D., Nidzgorski D.A., Millet D.B., and Baker L.A.. Contrasting nitrogen and phosphorus budgets in urban watersheds and implications for managing urban water pollution. PNAS, 114(6): 4177-4182, 2017.

Helsel, D. R. and Hirsch, R. M.: Statistical Methods in Water Resources, Techniques of Water Resources Investigations, 2nd edition, U. S. Geological Survery, U. S. A, Book 4, chapter A3, 2002.

Hill D., Kerkez, B., Rasekh, A.; Ostfeld, A.; Minsker, B.; Banks, M. K. Sensing and Cyberinfrastructure for Smarter Water Management: The Promise and Challenge of Ubiquity. Journal of Water Resources Planning and Management, 140 (7), 01814002, 2014.

Howard K.W.F., Maier H.: Road de-icing salt as a potential constraint on urban growth in the Greater Toronto Area, Canada. Journal of Contaminant Hydrology, 91(Issues 1-2): 146-170, 2007.

Harrison, J.A., Maranger R.J., Alexander R.B., Giblin A.E., Jacinthe P.A., Mayorga E., Seitzinger S.P., Sobota D.J., and Wollheim W.M.. The regional and global significance of nitrogen removal in lakes and reservoirs.Biogeochemistry,93(1–2):143–157, 2009. doi:10.1007/s10533-008-9272-x.

Halim MA., Majumder RK., Nessa SA., Hiroshiro Y., Uddin MJ., Shimada J., and Jinno K.. Hydrogeochemistry and arsenic contamination of groundwater in the Ganges Delta Plain, Bangladesh. Journal of Hazardous Materials, 164(2-3): 1335-1345.

Han, L.F., Plummer L.N., Aggarwal P.: A graphical method to evaluate predominant geochemical processes occurring in groundwater systems for radiocarbon dating. Chemical Geology, 318-319: 88-112, 2012. doi.org/10.1016/j.chemgeo.2012.05.004.

Halliday S.J., Skeffington R.A., Wade A.J., Bowes M.J., Gozzard E., Newman J.R., Loewenthal M., Palmer-Felgate E.J., and Jarvie H.P.. High-frequency water quality monitoring in an urban catchment: hydrochemical dynamics, primary production and implications for the Water Framework Directive. HYDROLOGICAL PROCESSES, 29: 3388-3407, 2015.

Hellmann, F. and Vermaat, J. E.: Impact of climate change on water management in Dutch peat polders. Ecol Model, 240, 74-83, 2012.

Holman, I. P., Whelan, M. J., Howden, N. J. K., Bellamy, P. H., Willby, N. J., Rivas-Casado, M., McConvey, P.: Phosphorus in groundwater - an overlooked contributor to eutrophication, HYDROL PROCESS, 22, 5121-5127, 2008.

He S. and Xu Y.J.. Three decadal inputs of nitrogen and phosphorus from four major coastal rivers to the summer hypoxic zone of the northern Gulf of Mexico. Water, Air, and Soil Pollution, 226: 311, 2015. DOI 10.1007/s11270-015-2580-6

Jäger C.G. and Borchardt D.. Longitudinal patterns and response lengths of algae in riverine ecosystems: A model analysis emphasizing benthic-pelagic interactions. Journal of Theoretical Biology, 442: 66-78, 2018.

Jäger C.G., Hagemann J., and Borchardt D.. Can nutrient pathways and biotic interactions control eutrophication in riverine ecosystems? Evidence from a model driven mesocosm experiment. Water Research, 115: 162-171, 2017.

Jenny J.P., Normandeau A., Francus P., Taranu Z.E., Gregory-Eaves I., Lapointe F., Jautzy J., Ojala A.E.K., Dorioz J.M., Schimmelmann A., and Zolitschka B.. Urban point sources of nutrients were the leading cause for the historical spread of hypoxia across European lakes. PNAS, 113(45): 12655-12660, 2016.

Kuenen J.. Anammox bacteria: from discovery to application. Nature Reviews Microbiology, 6: 320-326, 2008. doi:10.1038/nrmicro1857

Kopáček J., Borovec J., Hejzlar J., Ulrich K., Norton S.A., and Amirbahman A.. Aluminum control of phosphorus sorption by lake sediments. Environmental Science & Technology, 39 (22): 8784-8789, 2005. DOI: 10.1021/es050916b

Kleeberg A., Hupfer M., and Gust G.. Phosphorus entrainment due to resuspension in a lowland river, Spree, NE Germany-A laboratory microcosm study. Water, Air, and Soil Pollution, 183(1-4): 129-142, 2007.

Kronvang B., Køgestrand J., Windolf J., Ovesen N., Troldborg L.: Background phosphorus concentrations in Danish groundwater and surface water bodies, EGU General Assembly 2013, 7-12 April, 2013, Vienna, Austria, id. EGU2013-2249.

Kojima, K., Sano S., Kurisu F., Furumai H.: Estimation of source contribution to nitrate loading in road runoff using stable isotope analysis. Urban Water Journal, 14: 337-342, 2017.

Kabenge M., Wang H., and Li F.. Urban eutrophication and its spurring conditions in the Murchison Bay of Lake Victoria. Environmental Science and Pollution Research, 23: 234-241, 2016. DOI 10.1007/s11356-015-5675-0

Leopold, L.B.: Hydrology for urban land planning-a guidebook on the hydrologic effects of urban land use. U.S. Geological Survey, Washington, D. C., 1968.

Lijklema L.. Nutrient dynamics in shallow lakes: effects of changes in loading and role of sediment-water interactions. Hydrobiologia, 275/276: 335-348, 1994.

Le Moal M., Gascuel-Odoux C., Ménesguen A., Souchon Y., Étrillard C., Levain A., Moatar F., Pannard A., Souchu P., Lefebvre A., and Pinay G.. Eutrophication: A new wine in an old bottle. Science of the Total Environment, 651: 1-11, 2019.

Lyvén B., Hassellöv M., Turner D.R., Haraldsson C., and Andersson K. Competition between iron- and carbon-based colloidal carries for trace metals in a freshwater assessed using flow field-flow fractionation coupled to ICPMS. Geochimica et Cosmochimica Acta, 67(20): 3791-3802, 2003.

Li H., Song C.L., Cao X.Y., and Zhou Y.Y.. The phosphorus release pathways and their mechanisms driven by organic carbon and nitrogen in sediments of eutrophic shallow lakes. Science of the Total Environment, 572: 280-288, 2016.

Lofts S., Tipping E., Hamilton-Taylor J.. The Chemical Speciation of Fe(III) in Freshwaters. Aquatic Geochemistry, 14(4): 337-358, 2008.

Lu H., Wang J., Li J., Shao H., and Wu Y.. Periphytic biofilm: A buffer for phosphorus precipitation and release between sediments and water. Chemosphere, 144: 2058-2064, 2016.

Makkink, G.F.: Testing the Penman formula by means of lysimeters. Journal of the Institution of Water Engineers and Scientists, 11, 277-288, 1957.

McPherson, M.B.: Hydrological effects of urbanization. Report of the sub-group on the Effects of Urbanization on the Hydrological Environment, of the Co-ordinating Council of the International Hydrological Decade, The Unesco Press, Paris, 1974.

Mook, W.G.: Introduction to isotope hydrology: stable and radioactive isotopes of hydrogen, oxygen and carbon, IAH International Contributions to Hydrogeology 25. Taylor & Francis, London New York, ISBN: 9780415381970, p.226, 2006.

McGrane S.J.. Impacts of urbanisation on hydrological and water quality dynamics, and urban water management: a review. Hydrological Sciences Journal, 61(13): 2295-2311, 2016. DOI: 10.1080/02626667.2015.1128084

Middelburg J.J.. Marine Carbon Biogeochemistry - A Primer for Earth System Scientists. Springer Briefs in Earth System Sciences. Switzerland, 2019.

McGlathery K.J., Anderson I.C., and Tyler A.C.. Magnitude and variability of benthic and pelagic metabolism in a temperate coastal lagoon. Marine Ecology Progress Series, 216: 1-15, 2001.

Minderhoud P. S. J., Erkens G., Pham V. H., Bui V. T., Erban L., Kooi H., Stouthamer E.: Impacts of 25 years of groundwater extraction on subsidence in the Mekong delta, Vietnam, Environ Res Lett., 12, 2017.

Mosley L. M., Hunter K. A., and Ducker W. A.. Forces between Colloid Particles in Natural Waters. Environmental Science & Technology, 37 (15): 3303-3308, 2003. DOI: 10.1021/es026216d

Meinikmann, K., Hupfer, M., Lewandowski, J.: Phosphorus in groundwater discharge - A potential source for lake eutrophication, J Hydrol, 524, 214 - 226, 2015.

McGrane S.J., Hutchins M.G., Miller J.D., Bussi G., Kjeldsen T.R., Loewenthal M.. During a winter of storms in a small UK catchment, hydrology and water quality responses follow a clear rural-urban gradient. Journal of Hydrology, 545: 463-477, 2017.

Middleburg J.J. and Nieuwenhuize J.. Uptake of dissolved inorganic nitrogen in turbid, tidal estuaries. Marine Ecology Progress Series, 192: 79-88, 2000.

Morris, A. W. and Riley, J. P.: The bromide/chlorinity and sulphate/chlorinity ratio in sea water, Deep Sea Research and Oceanographic Abstracts, http://dx.doi.org/10.1016/0011-7471(66)90601-2, 13, 699-705, 1966.

Miller M.P., Tesoriero A.J., Capel P.D., Pellerin B.A., Hyer K.E., and Burns D.A.. Quantifying watershed-scale groundwater loading and instream fate of nitrate using high-frequency water quality data. Water Resources Research, 52: 330-347, 2016.

Mourad, D. S. J. and Van der Perk, M.: Spatio-temporal patterns of nutrient concentrations and export in a north-eastern European lowland catchment. Hydrol. Process, 23: 1821- 1833, 2009.

Mulder A., Van de Graaf A.A., Robertson L.A., and Kuenen J.G.. Anaerobic ammonium oxidation discovered in a denitrifying fluidized bed reactor. FEMS Microbiology Ecology, 1(16): 177-184, 1995.

NAP (https://nl.wikipedia.org/wiki/Normaal_Amsterdams_Peil), 2019-02-12.

Nyenje, P.M. Foppen J.W., Uhlenbrook S., Kulabako R.N., Muwanga A.: Eutrophication and nutrient release in urban areas of sub-Saharan Africa-A review. Science of the Total Environment, 408 (3): 447-455, 2010.

Neal, C., Reynolds, B., Norris, D., Kirchner, J. W., Neal, M., Rowland, P., Wickham H., Harman S., Armstrong L., Sleep D., Lawlor, A., Woods C., Williams B., Fry M., Newton G., Wright D.. Three decades of water quality measurements from the Upper Severn experimental catchments at Plynlimon, Wales: an openly accessible data resource for research, modelling, environmental management and education. Hydrological Processes, 25(24), 3818-3830, 2011.

Neal C. and Robson A.J.. A summary of river water quality data collected within the Land-Ocean Interaction Study: core data for eastern UK rivers draining to the North Sea. Science of The Total Environment, 251-252: 585-665, 2000.

Naus, F. L., Schot, P. P., Ahmed, K., and Griffioen J.. Groundwater salinity variation in Upazila Assasuni (southwestern Bangladesh), as steered by surface clay layer thickness, relative elevation and present-day land use. Hydrology and Earth System Sciences, 23(3): 1431-1451, 2019.

Neumann B., Vafeidis A.T., Zimmermann J., Nicholls R. J.: Future Coastal Population Growth and Exposure to Sea-Level Rise and Coastal Flooding - A Global Assessment, Plos One, 10, 3, 2015. e0118571. doi:10.1371/journal.pone.0118571.

Nizzoli D., Welsh D.T., and Viaroli P.. Denitrification and benthic metabolism in lowland pit lakes: The role of trophic conditions. Science of the Total Environment, 703: 134804, 2020.

OECD. Water Governance in the Netherlands: Fit for the Future?, OECD Studies on Water, OECD Publishing, 2014. http://dx.doi.org/10.1787/9789264102637-en

Olli, G., Darracq A., and Destouni G.. Field study of phosphorous transport and retention in drainage reaches. Journal of Hydrology, 365(1–2):46–55, 2009. doi:10.1016/j.jhydrol.2008.11.039.

Oude Essink., G. H. P., Houtman, H., Goes, B. J. M.: Chloride concentration at the bottom of the Holocene aquitard in the Netherlands (in Dutch), Rep. NITG 05-056-A, 17 pp., TNO, Utrecht, Netherlands, 2005.

Oros D.R., Ross J.R.M., Spies R.B., Mumley T.E.: Polycyclic aromatic hydrocarbon (PAH) contamination in San Francisco Bay: A 10-year retrospective of monitoring in an urbanized estuary. Environmental Research, 105: 101-118, 2007.

Oude Essink, G. H. P., Van Baaren, E. S., De Louw, P. G. B.: Effects of climate change on coastal groundwater systems: a modeling study in the Netherlands, Water Resour Res, 46, 10, 2010.

Painter H.A.. A review of literature on inorganic nitrogen metabolism in microorganisms. Water Research, 4: 393-450, 1970.

Pataki, D.E., Boone C.G., Hogue T.S., Jenerette G.D., McFadden J.P., Pincetl S.: Ecohydrology bearings-Invited commentary: socio-ecohydrology and the urban water challenge. Ecohydrology, 4: 341-347, 2011. https://doi.org/10.1002/eco.209

Pasterank A., Hillebrand H., and Flöder S.. Competition between benthic and pelagic microalgae for phosphorus and light-long-term experiments using artificial substrates. Aquatic Sciences, 71: 238-249, 2009.

Putro B., Kjeldsen T.T., Hutchins M.G., and Miller J.. An empirical investigation of climate and land-use effects on water quantity and quality in two urbanising catchments in the southern United Kingdom. Science of the Total Environment, 548-549: 164-172, 2016.

Poikane S., Kelly M.G., Herrero F.S., Pitt J., Jarvie H.P., Claussen U., Leujak W., Solheim A.L., Teixeira H., and Phillips G.. Nutrient criteria for surface waters under the European Water Framework Directive: Current state-of-the-art, challenges and future outlook. Science of The Total Environment, 695: 133888, 2019.

Paul, M.J. and Meyer J. L.: Streams in the urban landscape. Annual Review of Ecology and Systematics, 32: 333-365, 2001.

Putt A.E., MacIsaac E.A., Herunter H.E., Cooper A.B., and Selbie D.T.. Eutrophication forcings on a peri-urban lake ecosystem: Context for integrated watershed to airshed management. PLoS ONE, 4(7): e0219241, 2019. https://doi.org/ 10.1371/journal.pone.0219241

Paerl, H.W., Scott, J.T., McCarthy, M.J., Newell, S.E., Gardner, W.S., Havens, K.E., Hoffman, D.K., Wilhelm, S.W., Wurtsbaugh, W.A. It Takes Two to Tango: When and Where Dual Nutrient (N & P) Reductions Are Needed to Protect Lakes and Downstream Ecosystems. Environmental Science and Technology, 50: 10805-10813, 2016. https://doi.org/10.1021/acs.est.6b02575

Robinson C.. Review on groundwater as a source of nutrients to the Great Lakes and their tributaries. Journal of Great Lakes Research, 41(4): 941-950, 2015.

RIVM Report 2017-0050, 2017: Water quality in the Netherlands; status (2012-2015) and trend (1992-2015) Addendum to report 2016-0019

Rozemeijer J.C.. Dynamics in groundwater and surface water quality-from field-scale processes to catchment-scale monitoring. Utrecht University, Utrecht, The Netherlands, 2010.

Rozemeijer, J.C. and Broers H.P.: The groundwater contribution to surface water contamination in a region with intensive agricultural land use (Noor-Brabant, The Netherlands). Environmental Pollution, 148: 695-706, 2007.

Revitt D.M. and Ellis J.B.. Urban surface water pollution problems arising from misconnections. Science of the Total Environment, 551-552: 163-174, 2016.

Rozemeijder J.C., Klein J., Broers H.P., van Tol-Leenders T.P., and van der Grift B.. Water quality status and trends in agriculture-dominated headwaters; a national monitoring network for assessing the effectiveness of national and European manure legislation in The Netherlands. Environ Monit Assess, 186: 8981-8995, 2014.

Rozemeijer J.C., Klein J., Hendriks D., Borren W., Ouboter M., and Rip W.. Groundwater-surface water relations in regulated lowland catchments; hydrological and hydrochemical effects of a major change in surface water level management. Science of The Total Environment, 660: 1317-1326, 2019.

Raja Segaran R., Lewis M., andOstendorf B.. Stormwater quality improvement potential of an urbanised catchment using water sensitive retrofits into public parks. Urban Forestry and Urban Greening, 13(2), 315-324, 2014.

Risse-Buhl U., Mendoza-Lera C., Norf H., Pérez J., Pozo J., and Schlief J.. Contrasting habitats but comparable microbial decomposition in the benthic and hyporheic zone. Science of The Total Environment, 605-606: 683-691, 2017.

Rozemeijer, J. C., Van der Velde, Y., Van Geer, F. C., Bierkens, M. F. P., Broers, H. P.: Direct measurements of the tile drain and groundwater flow route contributions to surface water contamination: From field-scale concentration patterns in groundwater to catchment-scale surface water quality, Environmental Pollution, 158, 3571-3579, 2010a.

Rozemeijer J. C., Van der Velde Y., Van Geer F., de Rooij G.H., Torfs P. J. J. F., Broers H. P.: Improving load estimates of N and P in surface waters by characterizing the concentration response to rainfall events, Environmental Science & Technology, 44, 6305-6312, 2010b.

Rode M., Wade A.J., Cohen M.J., Hensley R.T., Michael J. Bowes, Kirchner J.W., Arhonditsis G.B., Jordan P., Kronvang B., Halliday S.J., Skeffington R., Rozemeijer J., Aubert A.H., Rinke K., and Jomaa S.. Sensors in the stream: the high-frequency wave of the present. Environmental Science & Technology, 50: 10297-10307, 2016.

Scheffer, M.. Ecology of shallow lakes, 1st edition. London: Chapman & Hall, 1998.

Sorensen, J.P.R., Lapworth D.J., Nkhuwa D.C.W., Stuart M.E., Gooddy D.C., Bell R.A., Chirwa M., Kabika J., Liemisa M., Chibesa M., Pedley S.: Emerging contaminants in urban groundwater sources in Africa, Water Research, 72: 51-63, 2015.

Schokker, J., Bakker M.A.J., Dubelaar C.W., Dambrink R.M., and Harting R.: 3D subsurface modelling reveals the shallow geology of Amsterdam, Netherlands Journal of Geosciences, 94(4): 399-417, 2015. doi:10.1017/njg.2015.22.

Spears B.M., Carvalho L.., Perkins R., Kirika A., and Paterson D.M.. Sediment phosphorus cycling in a large shallow lake: spatio-temporal variation in phosphorus pools and release. Hydrobiologia, 584: 37-48, 2007. https://doi.org/10.1007/s10750-007-0610-0

Smolders, E. and Degryse F.: Fate and Effect of Zinc from Tire Debris in Soil. Environmental Science & Technology, 36(17), 3706-3710, 2002.

Schot, P. P. and Molenaar, A.: Regional changes in groundwater flow patterns and effects on groundwater composition, J Hydrol, 130, 151-170, 1992 a.

Stafleu, J., Maljers D., Gunnink J.L., Menkovic A., Busschers F.S.: 3D modelling of the shallow subsurface of Zeeland, the Netherlands. Netherlands Journal of Geosciences, 90(4): 293-310, 2011.

Smolders A. J. P., Lamers L. P. M., Lucassen E. C. H. E. T., Van Der Velde G. and Roelofs J. G. M.. Internal eutrophication: How it works and what to do about it—a review. Chemistry and Ecology, 22(2): 93-111, 2006. DOI: 10.1080/02757540600579730

Strayer D.L., Pace M.L., Caraco N.F., Cole J.J., and Findlay S.E.G.. Hydrology and grazing jointly control a large-river food web. Ecology, 89(1): 12-18, 2008.

Stuyfzand, P. J. and Stuurman, R. J.: Origin, distribution and chemical mass balances of non-anthropogenic, brackish and (hyper) saline groundwaters in the Netherlands, 1st SWIM-SWICA Joint Saltwater Intrusion Conference, Cagliari-Chia Laguna, Italy, 2006.

Smith V.H. and Schindler D.W.. Eutrophication science: where do we go from here? Trends in Ecology & Evolution. 24(4): 201-207, 2009.

Schot, P. P. and Van der Wal, J.: Human impact on regional groundwater composition through intervention in natural flow patterns and changes in landuse. J Hydrol, 134, 297-313, 1992 b.

Strokal M., Yang H., Zhang Y., Kroeze C., Li L., Luan S., Wang H., Yang S., and Zhang Y.. Increasing eutrophication in the coastal seas of China from 1970 to 2050, Marine Pollution Bulletin, 85(1): 123-140, 2014.

Tscheikner-Gratl F., Bellos V., Schellart A., Moreno-Rodenas A., Muthusamy M., Langeveld J., Clemens F., Benedetti L., Shucksmith J., Heuvelink G.B.M., and Tait S.. Recent insights on uncertainties present in integrated catchment water quality modelling. Water Research, 150: 368-379, 2019.

Thamdrup B. and Dalsgaard T.. Production of N2 through anaerobic ammonium oxidation coupled to nitrate reduction in marine sediments. Applied and Environmental Microbiology, 68(3): 1312-1318, 2002.

Timoshkin O.A., Moore M.V., Kulikova N.N., Tomberg I.V., Malnik V.V., Shimaraev M.N., Troitskaya E.S., Shirokaya A.A., Sinyukovich V.N., Zaitseva E.P., Domysheva V.M., Yamamuro M., Poberezhnaya A.E., Timoshkina E.M.. Groundwater contamination by sewage causes benthic algal outbreaks in the littoral zone of Lake Baikal (East Siberia). Journal of Great Lakes Research, 44(2): 230-244, 2018.

Tanner C.C., Nguyen M.L., and Sukias J.P.S.. Nutrient removal by a constructed wetland treating subsurface drainage from grazed dairy pasture. Agriculture, Ecosystems & Environment, 105 (1-2): 145-162, 2005.

Toor G.S., Occhipinti M.L., Yang Y.Y., Majcherek T., Haver D., and Oki L.. Managing urban runoff in residential neighbourhoods: Nitrogen and phosphorus in lawn irrigation driven runoff. PLoS ONE, 12(6): e0179151, 2017. https://doi.org/ 10.1371/journal.pone.0179151

Törnqvist T. E., Wallac D. J., Storms J. E. A., Wallinga J., Van Dam R. L., Blaauw M., Derksen M. S., Klerks C. J. W., Meijneken C., Snijders E. M. A.: Mississippi Delta subsidence primarily caused by compaction of Holocene strata. Nat Geosci, 1, 3, 173-176, 2008.

Van Wallenburg, C.: Kattekleigronden en potentiele katteklei in droogmakerijen in het Westen van Nederland. Boor en Spade: verspreide bijdragen tot de kennis van de bodem van Nederland, 19, 116-133, 1975.

Van Loon, A. H.: Unravelling hydrological mechanisms behind fen deterioration in order to design restoration strategies, Ph. D. thesis, Utrecht University, Utrecht, The Netherlands, 2010.

Van der Sloot et al.: Enviromental criteria for cement based products. ECRICEM, ECN report ECN-E-11-020, Petten, The Netherlands, 2011.

Vos, P.: Origin of the dutch coastal landscape: long-term landscape evolution of the Netherlands during the Holocene, described and visualized in national, regional and local palaeogeographical map series, Ph. D. thesis, Utrecht University, Utrecht, The Netherlands, 2015.

Van der Grift, B., Broers, H. P., Berendrecht, W., Rozemeijer, J. R., Osté, L., and Griffioen, J.: High-frequency monitoring reveals nutrient sources and transport processes in an agriculture-dominated lowland water system, Hydrol. Earth Syst. Sci., 20, 1851-1868, doi:10.5194/hess-20-1851-2016, 2016.

Van Beek, C. L., Droogers, P., van Hardeveld, H. A., van den Eertwegh, G. A. P. H., Velthof, G. L., Oenema, O.: Leaching of solutes from an intensively managed peat soil to surface water, Water Air Soil Poll, 182, 291-301, 2007.

Vadas P.A., Fiorellino N.M., Coale F.J., Kratochvil R., Mulkey A.S., and McGrath J.M.. Estimating legacy soil phosphorus impacts on phosphorus loss in the Chesapeake Bay watershed. Journal of Environmental Quality, 47: 480-486, 2018.

Vermaat, J. E., Hellmann, F.: Covariance in water- and nutrient budgets of Dutch peat polders: what governs nutrient retention? Biogeochemistry, 99, 109-126, 2010.

Vermonden K., Hermus M.A.A., van Weperen M., Leuven R.S.E.W., van der Velde G., Smolders A.J.P., Roelofs J.G.M., and Hendriks A.J.. Does upward seepage of river water and storm water runoff determine water quality of urban drainage systems in lowland areas? A case study for the Rhine-Meuse delta. Hydrological Processes, 23(21): 3110-3120, 2009.

Van Geer F.C., Kronvang B., and Broers H.P.. High-resolution monitoring of nutrients in groundwater and surface waters: process understanding, quantification of loads and concentrations, and management applications. Hydrology and Earth System Sciences, 20: 3619-3629, 2016.

Van Dijk G., Lamers L.P.M., Loeb R., Westendorp P.J., Kuiperij R., van Kleef H.H., Klinge M., Smolders A.J.P.. Salinization lowers nutrient avaliability in formerly brackish freshwater wetlands; unexpected results from a long-term field experiment. Biogeochemistry, 143:67-83, 2019.

Van der Grift B., Osté L., Schot P., Kratz A., van Popta E., Wassen M., Griffioen J.: Forms of phosphorus in suspended particulate matter in agriculture-dominated lowland catchments: Iron as phosphorus carrier. Science of the Total Environment, 631-632, 115-129, 2018.

Van der Velde Y., Rozemeijer J.C., de Rooij G.H., van Geer F.C., Broers H.P.. Field-scale measurements for separation of catchment discharge into flow route contribution. Vadose Zone Journal, 9(1): 25-35, 2010.

Van der Grift B., Rozemeijer J.C., Griffioen J., van der Velde Y.: Iron oxidation kinetics and phosphate immobilization along the flow-path from groundwater into surface water. Hydrology and Earth System Sciences, 18, 4687-4702, 2014.

Vadas P.A., Srinivasan M.S., Kleinman P.J.A., Schmidt J.P., and Allen A.L.. Hydrology and groundwater nutrient concentrations in a ditch-drained agroecosystem. Journal of Soil and Water Conservation, 62(4): 178-188, 2007.

Valkama E., Usva K., Saarinen M., and Uusi Kämppä J.. A Meta-Analysis on Nitrogen Retention by Buffer Zones. Journal of Environmental Quality, 48(2): 270-279, 2019.

Van Mourik, W., Van der Mijle Meijer H.J., van Tilborg W.J.M., and Teunissen R.J.M.: Emissies van bouwmaterialen, RIZA report 2003.027. ISBN 9036956412 (in Dutch). DOI: 10.1021/es025567p.

Van Dijk G., Wolters J., Fritz C., de Mars H., van Duinen G.J., Ettwig K.F., Straathof N., Grootjans A.P., and Smolders A.J.P.. Effects of Groundwater Nitriate and Sulphate Enrichment on Groundwater-Fed Mires: a Case Study. Water Air Soil Pollut, 230(122): 1-18, 2019.

Walsh,C.J., Fletcher T.D. and Ladson A.R.: Stream restoration in urban catchments through redesigning stormwater systems: looking to the catchment to save the stream. Journal of the North American Benthological Society, 24(3): 690-705, 2005.

Wilczak A., Jacangelo, J.G., Marcinko J.P., Odell L.H., Kirmeyer G.J.. Occurrence of nitrification in chloraminated distribution systems. Journal AWWA, 88(7):74-85, 1996.

Wang T., Liu G., Gao L., Zhu L., Fu Q., and Li D.. Biological and Nutrient Responses to a Typhoon in the Yangtze Estuary and the Adjacent Sea. Journal of Coastal Research, 32(2): 323-332.

Wu J. and Malmstrom M. E.: Nutrient loadings from urban catchments under climate change scenarios: Case studies in Stockholm, Sweden, Sci Total Environ, 518-519, 393-406, 2015.

Wen Y., Qiu J., Cheng S., Xu C., Gao X.. Hydrochemical Evolution Mechanisms of Shallow Groundwater and Its Quality Assessment in the Estuarine Coastal Zone: A Case Study of Qidong, China. Environmental Research and Public Health, 17(10): 3382, 2020.

Walsh C.J., Roy J.W., Feminella J.W., Cottingham P.D., Groffman P.M., and Morgan II R.P.. The urban stream syndrome: current knowledge and the search for a cure. Journal of The North American Benthological Society, 24(3): 706-732, 2005.

Wriedt, G., Spindler J., Neef T., Meißner R., and Rode M.. Groundwater dynamics and channel activity as major controls of in-stream nitrate concentrations in a lowland catchment system? Journal of Hydrology, 343: 154–168, 2007.

Wade, A. J., Palmer-Felgate, E. J., Halliday, S. J., Skeffington, R. A., Loewenthal, M., Jarvie, H. P., Bowes, M. J., Greenway, G. M., Haswell, S. J., Bell, I. M., Joly, E., Fallatah, A., Neal, C., Williams, R. J., Gozzard, E., Newman, J. R.: Hydrochemical processes in lowland rivers: insights from in situ, high-resolution monitoring, Hydrol Earth Syst Sc, 16, 4323-4342, 2012.

Wang B., Xin M., Wei Q., and Xie L.. A historical overview of coastal eutrophication in the China Seas. Marine Pollution Bulletin, 136: 394-400, 2018.

Wang, S., Zhu, G., Zhuang, L. Li Y., Lavik G., Berg M., Liu S., Long X.E., Guo J., Jetten M.S.M., Kuypers M.M.M., Li F., Schwark L., and Yin C.. Anaerobic ammonium oxidation is a major N-sink in aquifer systems around the world. The *ISME Journal Multidisciplinary Journal of Microbial Ecology,* 14, 151–163, 2020. https://doi.org/10.1038/s41396-019-0513-x

Yan R., Huang J., Li L., Gao J.: Hydrology and phosphorus transport simulation in a lowland polder by a coupled modeling system, Environmental Pollution, 227, 613-625, 2017.

Yan, R., Li L. and Gao J.: Modeling the regulation effects of lowland polder with pumping station on hydrological processes and phosphorus loads. Science of the Total Environment, 637-638: 200-207, 2018.

Yu, L., Rozemeijer J., van Breukelen B.M., Ouboter M., van der Vlugt C., and Broers H.P.: Groundwater impacts on surface water quality and nutrient loads in lowland polder catchments: monitoring the greater Amsterdam area. Hydrology & Earth System Sciences, 22: 487-508, 2018.

Yu L., Rozemeijer J.C., van der Velde Y., van Breukelen B.M., Ouboter M., and Broers H.P.. Urban hydrogeology: Transport routes and mixing of water and solutes in a groundwater influenced urban lowland catchment. Science of the Total Environment, 678: 288-300, 2019.

Yang Y.Y. and Toor G.S.. Stormwater runoff driven phosphorus transport in an urban residential catchment: Implications for protecting water quality in urban watersheds. Scientific Reports, 8, 11681, 2018. doi:10.1038/s41598-018-29857-x

Zhu W.X., Dillard N.D., and Grimm N.B.. Urban nitrogen biogeochemistry: status and processes in green retention basins. Biogeochemistry, 71: 177-196, 2004.

Zhang X. and Mei X.. Effects of benthic algae on release of soluble reactive phosphorus from sediments: a radioisotope tracing study. Water Science and Engineering, 8(2): 127-131, 2015.

Zhang W., Jin X., Meng X., Tang W., and Shan B.. Phosphorus transformations at the sediment-water interface in shallow freshwater ecosystems caused by decomposition of plant debris. Chemosphere, 201: 328-334, 2018.

Zhang, Y.C., Slomp, C. P., Broers H. P., Passier H. F., Böttcher M.E., van Cappellen P.: Sources and fate of nitrate and sulfate in a sandy aquifer: A multi-isotope study. Geochimica et Cosmochimica Acta (Supplement), 73, p.A1513, 2009.

Zafra, C., Temprano J. and Tejero I.: The physical factors affecting heavy metals accumulated in the sediment deposited on road surfaces in dry weather: a review. Urban Water Journal, 14 (6): 639-649, 2017.

Zhou L., Wang S., Zou Y., Xia C., and Zhu G.. Species, abundance and function of ammonia-oxidizing Archaea in inland waters across China. Scientific Reports, 5: 15969, 2015. DOI: 10.1038/srep15969